Interconversion Between Ni and Pd Bound N-Heterocyclic Carbenes and Azolium Salts: Fundamental Reactivity and Applications to Catalysis

By

Adrien Normand

Submitted in partial fulfilment of the requirements for the Degree of

Doctor of Philosophy

School of Chemistry

Cardiff University

Wales, United Kingdom

ProQuest LLC
789 East Eisenhower Parkway
P.O. Box 1346
Ann Arbor, MI 48106-1346

DECLARATION

This work has not previously been accepted in substance for any degree and is not being concurrently submitted in candidature for any degree.

Signed.....(candidate)

Date.....18/02/2008.....

STATEMENT 1

This thesis is being submitted in partial fulfilment of the requirements for the Degree of PhD.

Signed.....(candidate)

Date.....18/02/2008.....

STATEMENT 2

This thesis is the result of my own investigations, except where otherwise stated. Other sources are acknowledged by footnotes giving explicit references. A bibliography is appended.

Signed.....(candidate)

Date.....18/02/2008.....

STATEMENT 3

I hereby give consent for my thesis, if accepted, to be available for photocopying and for inter-library loan, and for the title and summary to be made available to outside organisations.

Signed.....(candidate)

Date.....18/02/2008.....

ABSTRACT

This thesis focuses on different aspects of the relationship between N-heterocyclic carbene (NHC) complexes of Ni and Pd and azolium salts, particularly imidazolium salts.

Chapter one introduces the reader to the field of organometallic chemistry and homogeneous catalysis. General aspects of the chemistry of NHCs are then discussed.

Chapter two describes studies aimed at optimising the recently discovered direct intermolecular coupling (*via* C-H activation and formation of an NHC hydride Ni(II) intermediate) of azolium salts with olefins. An extensive experimental study (in conjunction with DFT calculations conducted by Kirsty J. Hawkes and Brian F. Yates at the University of Tasmania) of the Ni(0)-catalysed reaction of 1-propyl-3-methylimidazolium bromide ([pmim]Br) with ethylene revealed that the mechanism of this reaction changes with the size of the ancillary ligand. This reaction was further developed into an intramolecular version, allowing for the synthesis of fused-ring imidazolium salts bearing a chiral carbon atom. Extension of this chemistry to Lewis acid activated neutral azoles is also described, as well as the development of a Pd-catalysed version of the intermolecular coupling.

In chapter three, the synthesis, solid-state (X-Ray) and solution phase (gs-NOESY) characterisation of a new family of cationic mixed phosphine/NHC Pd(II) π-allyl complexes of general formula $[Pd(\pi\text{-allyl})(NHC)PR_3]BF_4$ are described. This family of compounds was designed to generate monoligated Pd-PR_3 fragments upon thermal, solvent or olefin-mediated activation. For example, complex $[Pd(\eta^3\text{-}C_3H_5)(tmiy)PCy_3]BF_4$ (**1b**) was expected to generate an efficient catalyst for the Pd-catalysed coupling of olefins with azolium salts described in chapter two.

Chapter four describes the catalytic activity of **1b** and studies of its activation mechanism. The serendipitous discovery of the reaction of **1b** with phenyl iodide, yielding a 2-phenylimidazolium salt and $[Pd(\eta^3\text{-}C_3H_5)(I)PCy_3)]$ is reported as well as subsequent studies aimed at elucidating the scope and mechanism of this reaction.

ACKNOWLEDGEMENTS

First and foremost, I would like to thank my PhD supervisor Prof. Kingsley J. Cavell for his guidance and support throughout the duration of this study. I do hope the work we have accomplished will lead to many more years of fruitful scientific collaboration.

Some of the work described in this thesis has been conducted in collaboration with computational chemists. I would like to thank Prof. Brian F. Yates and Dr Kirsty J. Hawkes from the University of Tasmania, and Dr Dave J. Willock from Cardiff University, for all their hard work, and for insightful discussions.

My thanks also go to Dr Dave J. Nielsen and Dirk J. Beetstra for their precious help in many aspects of my work, including (but not limited to) the redaction of this thesis. I also thank them for all the good times we had in the lab, at home and in the pub.

I thank Dr Andreas Stasch and Dr Li-Ling Ooi for collecting and solving most of the crystal structures discussed in this thesis.

Technical members of staff in Cardiff University have made this work possible. Their vital help is duly acknowledged. Mr Robert Jenkins deserves a special mention for his help in the kinetic experiments described in chapter 4.

I would like to express my endless gratitude to my friends in the UK and abroad (they know who they are), to my family (particularly my parents) and to Joëlle for their support. Without you guys I would never have made it. I love you all.

Finally, I dedicate this thesis to the memory of my grandfather, André Normand (1911-2005).

GLOSSARY

Bu	butyl
Bz	benzyl
COD	1,5-cyclooctadiene
Cy	cyclohexyl
dba	dibenzylideneacetone
DCM	dichloromethane
DEPT	Distortionless Enhancement by Polarization Transfer
dipdmiy	N,N'-diisopropyldimethylimidazol-2-ylidene
DMF	N,N-dimethylformamide
Dmim	dimethylimidazolium
dmiy	dimethylimidazol-2-ylidene
DMSO	dimethylsulfoxide
ESI/MS	electrospray mass spectrometry
Et	ethyl
Et_2O	diethylether
HSQC	Heteronuclear Single Quantum Coherence
IMes	1,3-bis(2,4,6-trimethylphenyl)imidazol-2-ylidene
IPr	1,3-bis(2,6-diisopropylphenyl)imidazol-2-ylidene
^{i}Pr	*iso*-propyl
I^{t}Bu	N,N'-di-*tert*-butylimidazol-2-ylidene
M	metal
Me	methyl
MeCN	acetonitrile
NHC	N-heterocyclic carbene

NMP	N-methylpyrrolidinone
NMR	nuclear magnetic resonance
NOESY	Nuclear Overhauser Enhancement Spectroscopy
OAc	acetate
Ph	phenyl
pmim	1-propyl-3-methylimidazolium
R	alkyl or aryl
r.d.s.	rate-determining step
r.t.	room temperature
S	solvent
SMes	1,3-bis(2,4,6-trimethylphenyl)imidazolin-2-ylidene
SPr	1,3-bis(2,6-diisopropylphenyl)imidazolin-2-ylidene
^{t}Bu	*tert*-butyl
tmiy	tetramethylimidazol-2-ylidene
THF	tetrahydrofuran
TON	turnover number
TOF	turnover frequency
X	halogen

TABLE OF CONTENTS

1 Chapter one: Introduction

1.1 Homogeneous catalysis and organometallic chemistry

1.1.1 Definitions and background

Organometallic chemistry: a field of chemistry dealing with the synthesis, characterisation and reactivity of compounds containing at least one carbon-metal bond.

The first characterised organometallic complex (1827) is thought to be Zeise's salt **1**, a Pt(II) complex of ethylene obtained by dehydration of EtOH (***Figure 1***).[1]

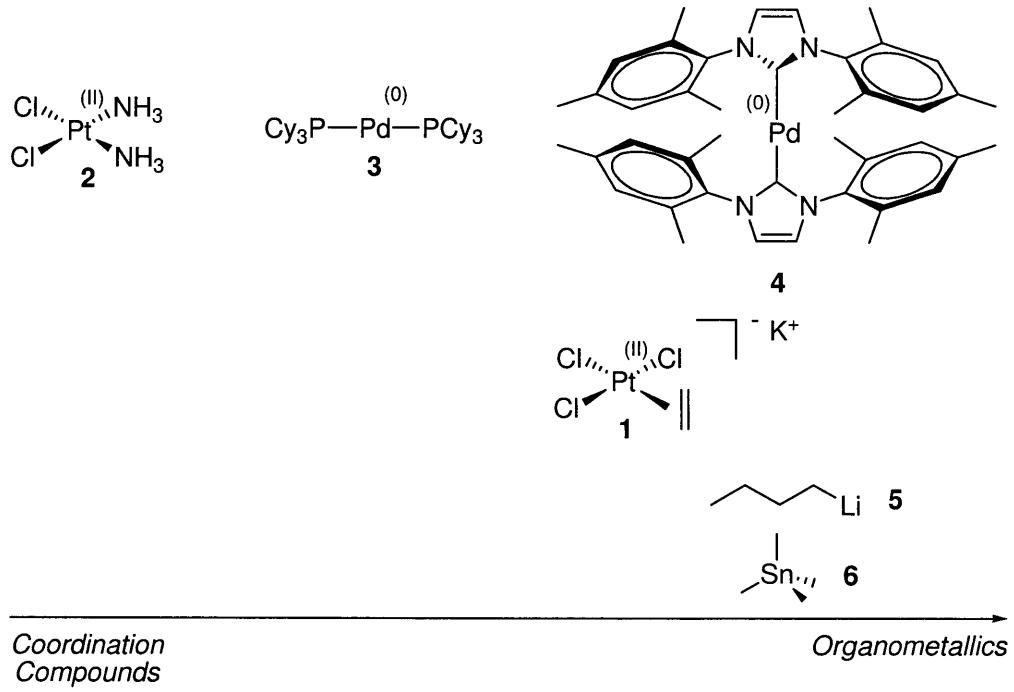

Figure 1: *coordination compounds/organometallics continuum*

This *stricto sensu* definition excludes typical coordination compounds such as cisplatin **2**, but it may be extended to metallic compounds containing organic ligands (*e.g.* tertiary phosphines). Thus, bis(tricyclohexylphosphine) palladium(0) **3** might be regarded as an organometallic compound, especially for comparison purposes with bis(N,N'-bis(2,4,6-trimethylphenyl)imidazol-2-ylidene)palladium(0) **4**, which fits perfectly with the above definition. Due to the ever-growing number and complexity of metallic compounds, it is useful to place them on a continuum going from pure coordination compounds to pure organometallics (***Figure 1***). Compounds **1-4** are all transition metal complexes but alkali and alkaline earth metals compounds such as *n*-butyllithium **5**, or main group compounds such tetramethyltin **6** are also organometallics (***Figure 1***).

Homogeneous catalysis: "the use of a soluble additive (the catalyst) in substoichimetric amount to bring about a reaction at a temperature below that required for the uncatalysed reaction".[2]

Figure 2 illustrate how a catalyst enables a reaction by lowering the activation energy (EA) of the uncatalysed sequence.

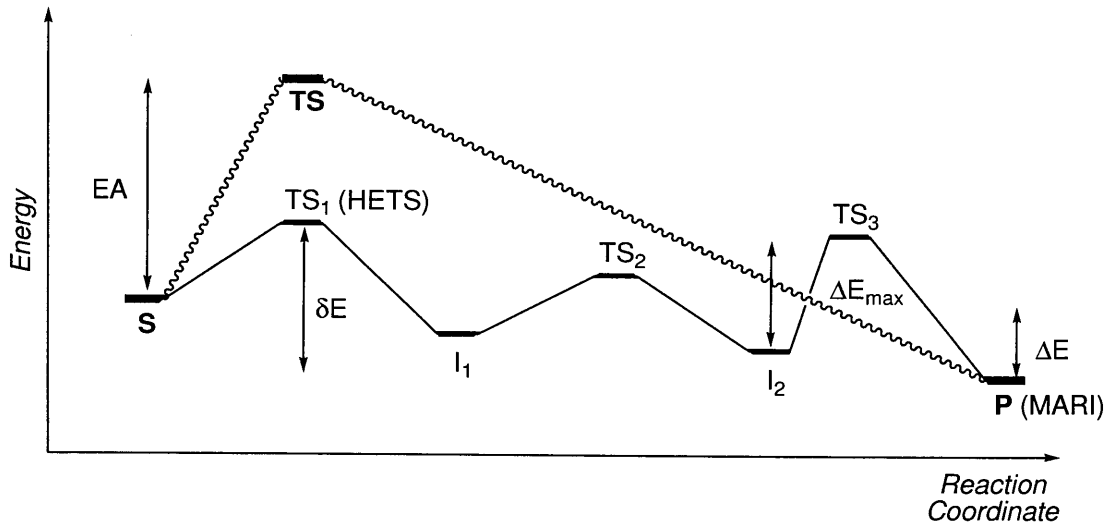

Figure 2: *energy diagram representing a thermal process and its catalysed version*

This sequence goes from sustrates (**S**) to products (**P**) via a transition state (**TS**). The whole process is thermodynamically favourable by ΔE.

The catalysed reaction does not change the global energy (ΔE) of the reaction,[3] but it proceeds *via* lower-energy transition states (TS_1-TS_3) and relatively unstable intermediates (I_1 and I_2). The energy difference between the lowest-energy (also called most abundant) intermediate (MARI) and the highest-energy transition state (HETS) is called the *energetic span* of the reaction (δE).[4] An efficient process should have the smallest possible value for δE, as the turnover frequency of the catalyst (TOF, number of cycles performed by each molecule of catalyst by unit of time) is limited by δE.[5] Therefore the most general way of improving a catalytic process (apart from preventing catalyst decomposition) consists of stabilising the HETS and/or destabilising the MARI.[1, 5, 6] On the other hand, ΔE_{max} (the highest activation energy in the catalysed reaction, I_2/TS_3 in ***Figure 2***) often determines the so-called "rate determining step" (*r.d.s.*) of the reaction. If a *r.d.s.* exists (*i.e.* if all the other activation energies can be neglected, which is not always possible[7]), improvement of the reaction kinetics can only be achieved by lowering the energy of this step. If the maximum activation energy cannot be easily overcome and causes the catalyst to be "stored" along the reaction pathway, steady state conditions may not be reached and catalysis (in the true sense) becomes impossible, with only a low turnover number (TON, the number of cycles performed by each molecule of catalyst) being achieved as a result. These considerations are important because they underline the differences between true catalytic conditions (*i.e.* steady state conditions, high TONs) and "pseudo-catalytic" or substoichiometric conditions (more complex kinetics, low TONs).

Homogeneous catalysis is perhaps the most important application of the organometallic chemistry of transition metals.[1, 6] This is partly due to the ability of transition metals to change oxidation states very easily. A typical example is Pd, which commonly exists in 0 and +II oxidation states (the +IV state, although a rarer occurrence, can sometimes play a role in catalysis[8]). The ease with which Pd goes from one oxidation state to another enables a variety of fundamental processes (*e.g.* oxidative

addition, reductive elimination) involving organic ligands to take place, sometimes under very mild conditions. Another reason for the success of transition metals in homogeneous catalysis is the often exacerbated reactivity of metal-bound organic molecules compared to their free counterparts. For example, Zr(IV)-bound ethylene is prone to intramolecular nucleophilic attack by an alkyl group in the polymerisation reaction shown in ***Scheme 1***.

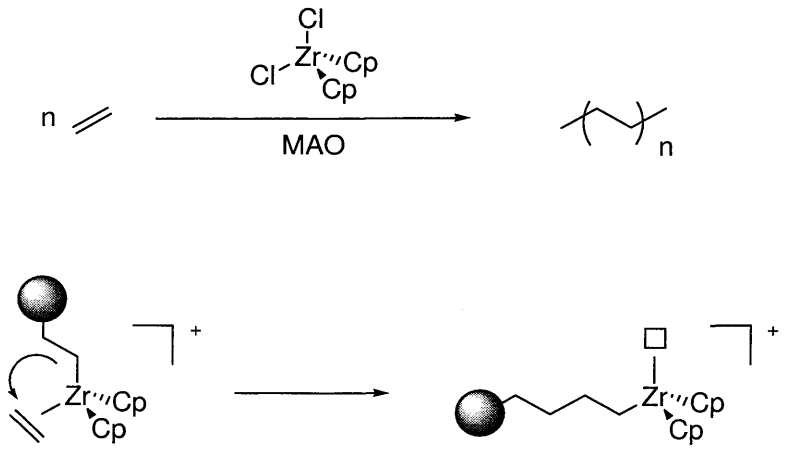

Scheme 1: *electrophilicity of Zr-bound ethylene in Zr polymerization of ethylene*

Finally, organometallic compounds are generally well-defined species that can be studied using a variety of solution-phase analytical techniques such as NMR spectroscopy or high pressure IR. This makes the *in situ* investigation of mechanisms in homogeneous catalysis an easier task than in heterogeneous catalysis.[9, 10]

1.1.2 Fundamental organometallic reactivity and catalyst design

In transition metal catalysis, a catalytic cycle is made of a combination of elementary steps. For example, the Pd-catalysed Suzuki-Miyaura coupling of aryl halides and boronic acids follows the simplified mechanism shown in ***Figure 3***:[1]

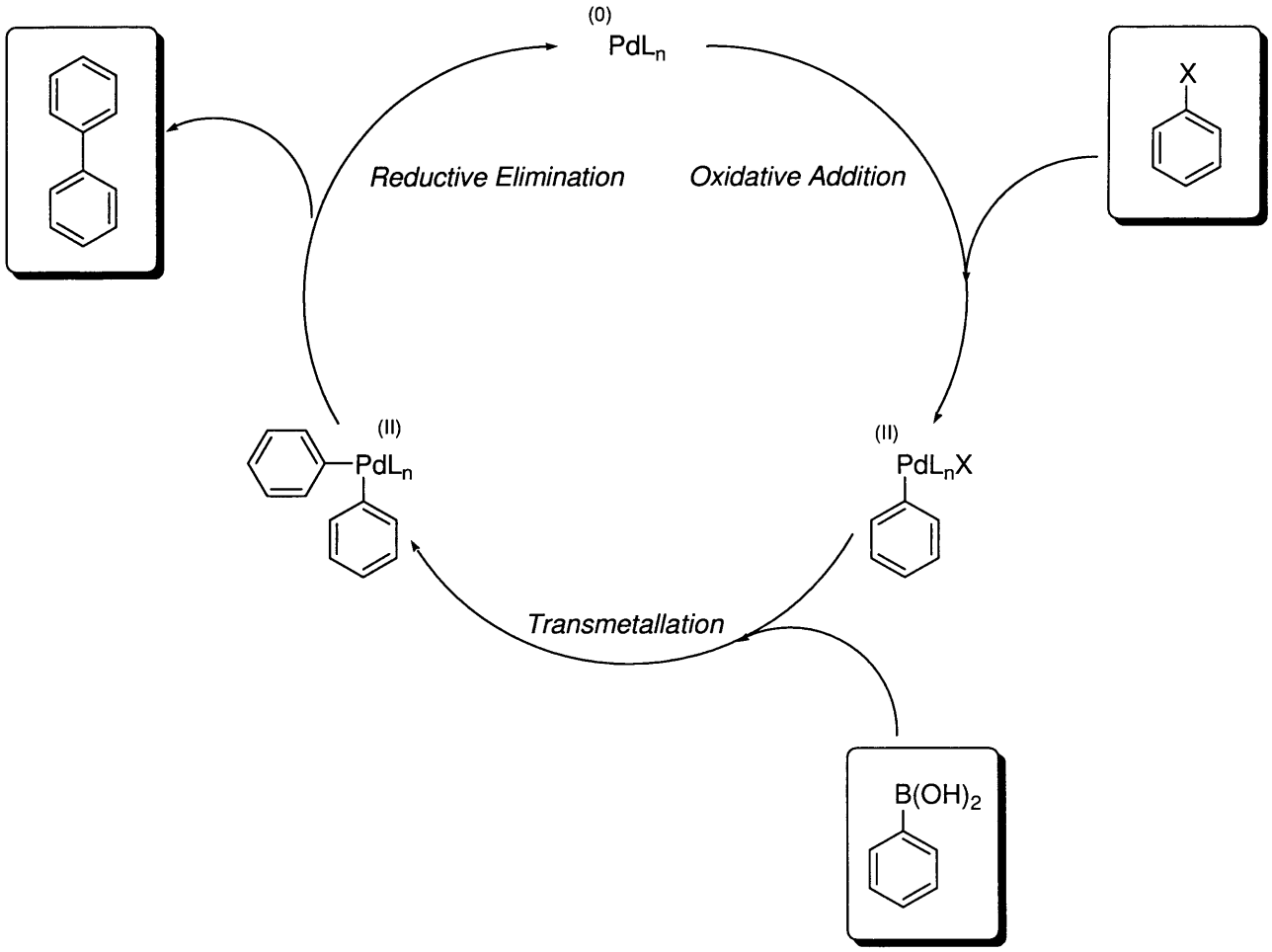

Figure 3: *simple organometallic reactions observed in the Suzuki-Miyaura cross-coupling reaction*

In the case of aryl chlorides or deactivated aryl bromides as coupling partner, oxidative addition is often the rate-determining step. Therefore, research efforts to develop more active catalysts have focused on this step in the last few years.[11] In the following, some simple organometallic reactions are described, together with general ways of accelerating these steps when they occur in catalytic

cycles. It must be remembered that accelerating one step might slow down another one to the extent that no beneficial effect is observed, and that (as mentioned above) the only effective way to increase reaction efficiency is to destabilise the MARI or stabilise the HETS. However it is always useful to have a good understanding of the general rules that govern elementary reactions in catalytic cycles. The following reactions are all relevant to the Ni and Pd-catalysed alkenylation of azolium salts discussed in Chapter 2.

1.1.2.1 Oxidative addition[12]

The first step in many transition metal catalysed processes, including Pd-catalysed cross-coupling reactions (Heck, Suzuki-Miyaura, Stille...),[1] oxidative addition is commonly encountered with electron-rich late transition metals. ***Scheme 2*** shows the general reaction scheme, illustrated by an example from the literature.[13]

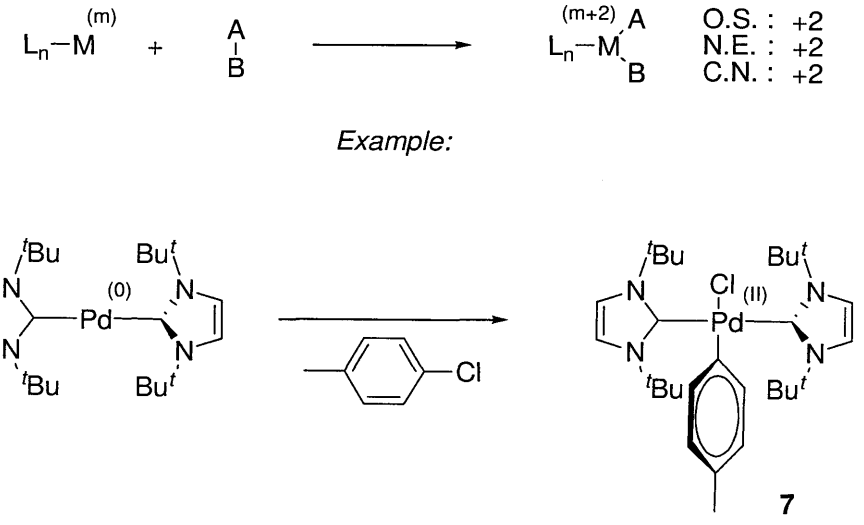

Scheme 2: *oxidative addition*

Oxidative addition to a metal in the m oxidation state leads to a new species with increased oxidation state (O.S.), number of electrons (N.E.) and coordination number (C.N.).

The geometry of the resulting complex is *cis* (i.e. the new ligands are *cis* to each other). The product in the example (**7**) is *trans* because the reaction proceeds first by dissociation of one of the two N-heterocyclic carbene (NHC) ligands, then oxidative addition and finally recoordination of the dissociated NHC.[13]

Because the coordination number increases by +2, a very effective way of promoting oxidative addition is to enforce coordinative unsaturation. Thus, so-called "monoligated" Pd(0) species (see Chapter 4) generated with bulky, electron-rich ligands, are very efficient in reactions where oxidative addition is the rate determining step.[11, 14, 15]

Another important strategy is the use of electron-rich ancillary ligands. In the example shown in ***Figure 4***, the strong electron-donating abilities of NHCs (see section **1.2.1**) enable the oxidative addition of *p*-chlorotoluene, a notoriously challenging substrate.

An important feature of oxidative addition not shown in ***Figure 4*** is the change of geometry resulting from the increased coordination number. Thus, square planar complexes become octahedral, linear complexes become square planar and so on. Therefore, one way of facilitating this step is to use chelating ligands with small bite angles, which will both stabilise the product of the reaction and destabilise the starting material. An example of such a strategy is Whiteside's compound **8**, a Pt(II) complex of bis(dicyclohexylphosphino)ethane which irreversibly loses neopentane upon thermal activation. The resulting unsaturated, strained Pt(0) complex is so reactive that it undergoes oxidative addition of cyclohexane (***Scheme 3***).[16]

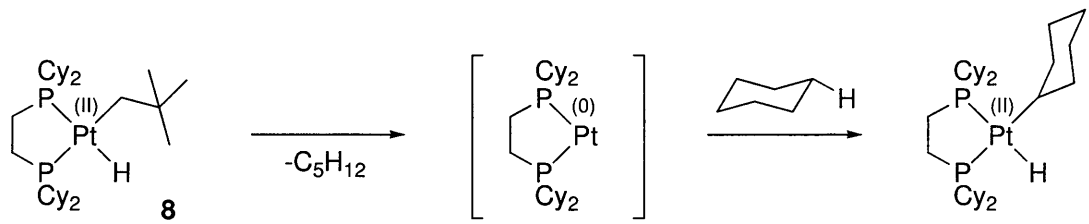

Scheme 3: *oxidative addition promoted by chelation*

1.1.2.2 Reductive elimination

Reductive elimination (***Scheme 4***) is the reverse reaction of oxidative addition. If oxidative addition is the first step of many transition metal catalysed reactions, reductive elimination is often a product forming step.

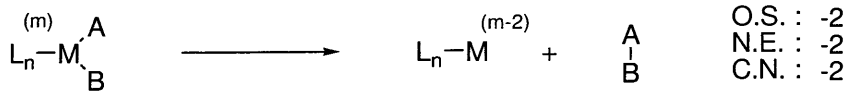

Example:

9 **10**

Scheme 4: *reductive elimination*

In the example shown above, reductive elimination of PhI happens from a cationic Pt(IV) intermediate (generated by the loss of I^- from **9**).[17] Coordinative unsaturation is sometimes a prerequisite for the reaction to take place, and this result is counterintuitive because unsaturation also helps oxidative addition (see section **1.1.2.1**).[18] However, unsaturated complexes are more prone to reductive elimination than saturated species. This is because coordinatively unsaturated species are less stable than saturated ones, thus lowering the barrier to reductive elimination (see chapter 4 for an example). In this example, lost I^- coordinates to the product of the reaction, thereby exerting a stabilising effect on the reductive elimination product.

Bulky and/or π-acid spectator ligands are generally effective at promoting reductive elimination. Indeed, bulky spectator ligands tend to force together the ligands to be eliminated, and they also

prevent reverse oxidative addition. On the other hand, π-acid ligands destabilise metals in a higher oxidation state and tend to favour a lower oxidation state that they can stabilise by back-donation.[1] These effects have been highlighted in Cavell's work on the reductive elimination from Pd(II) alkyl NHC species.[19]

In most cases oxidative addition and reductive elimination form a reversible process so that it is possible to tune reaction conditions in order to shift the equilibrium towards one or the other. ***Scheme 5*** illustrates this concept. In this example, addition of an olefin to Pt(II) NHC hydride **11** causes reductive elimination of an imidazolium salt. In the case of styrene, 50% conversion is observed. However, when the much stronger π-acid dimethylfumarate (dmfu) is used, the equilibrium shifts completely towards reductive elimination, because electron-rich Pt(0) product **12** is stabilised by the π-accepting ability of dmfu.[20]

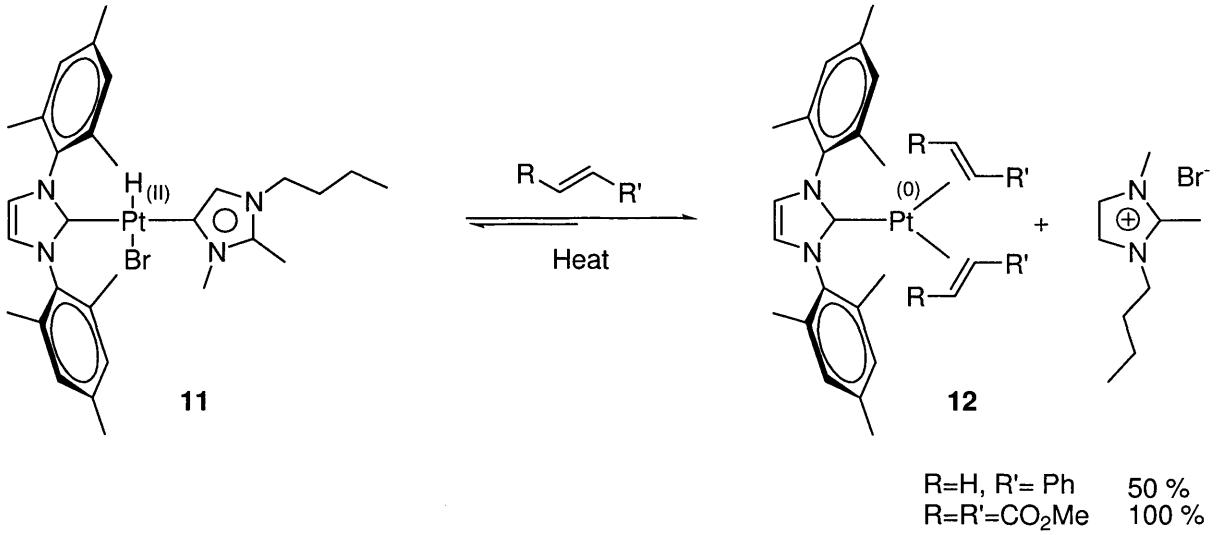

Scheme 5: *equilibrium between reductive elimination and oxidative addition in a Pt(II) complex*

Similarly to oxidative addition, reductive elimination can be promoted by enforcing the right geometry. For example, electron-rich d^{10} metals with two ligands prefer to adopt a linear geometry.[21] Starting from a square planar d^8 complex, reductive elimination can be promoted by a chelating

ligand with a large natural bite angle such as XANTPHOS, a bis(phosphine) developed by Van Leeuwen (***Figure 4***).[6, 22] This ligand was shown to accelerate reductive elimination by destabilising the square planar starting material and lowering the energy of the transition state.[23] Chelating ligands with smaller bite angles on the other hand can prevent reductive elimination.[24]

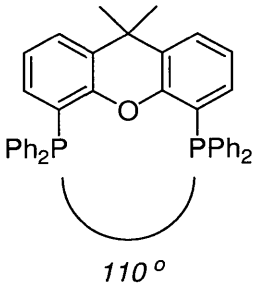

Figure 4: *XANTPHOS ligand*

These considerations are mostly valid for spectator ligands (*i.e.* not the reductively eliminated ones). They are important because the design of an efficient catalytic system should be based on the catalyst itself, not the substrate.

As mentioned previously, reductive elimination is accelerated by electron-poor spectator ligands. By contrast, Hartwig has shown in an elegant study on Pt(II) complexes that elimination of two identical aryl ligands with an electron withdrawing group (*i.e.* CF_3) was slower than that of aryl ligands with an electron donating group (*i.e.* NMe_2). This is due to ground-state stabilisation of the Pt(II) complex because of the stronger metal-ligand bonds (***Scheme 6***).[25]

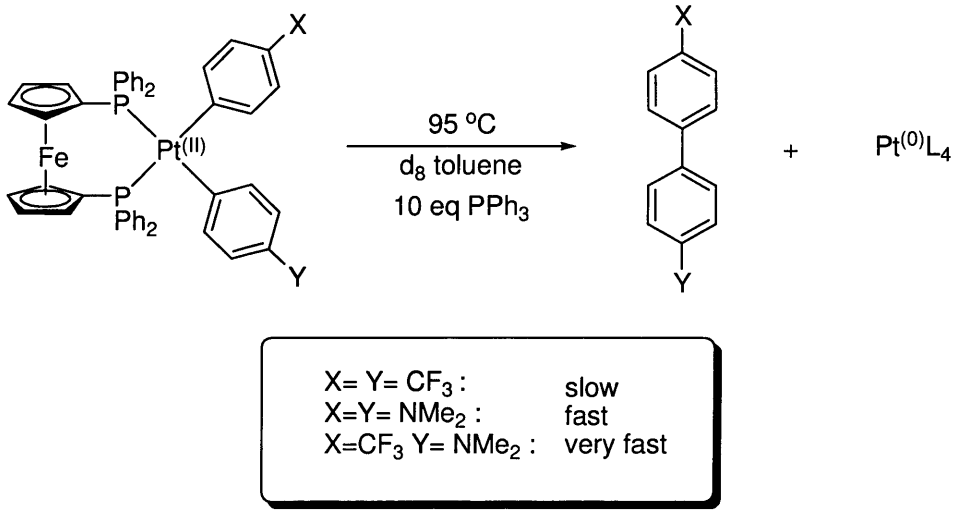

Scheme 6: *reductive elimination of electronically dissimilar ligands*

Strikingly, reductive elimination was even faster for electronically dissimilar ligands ($X=CF_3$ and $Y=NMe_2$). This is due to a synergistic effect of the two aryls, lowering the energy of the transition state by enabling a favourable charge transfer between the electron donating aryl (acting as a nucleophile) and the electron withdrawing aryl (acting as an electrophile). This work highlights the importance of ground-state and transition state effects on reaction rates, the latter being more difficult to predict without theoretical data.

1.1.2.3 β hydride elimination

β hydride elimination is a very common reaction for σ-bound alkyl complexes with hydrogens in the β position. It is usually not a desired reaction in catalysis, except for example in the coupling of aryl halides with olefins (the so-called Heck reaction),[1, 26-28] and in olefin isomerisation[29] or oligomerisation reactions.[30-33] In other reactions such as the Negishi coupling of alkyl organozincs and alkyl bromides, it severely limits the development of efficient catalysts.[34-37] As shown in ***Scheme 7***, a coplanar arrangement is required between the metal, the C-C and the C-H bonds of the alkene:

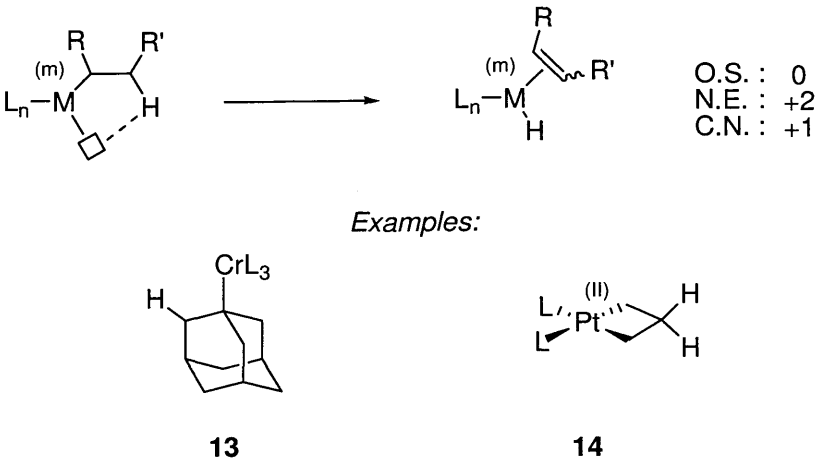

Scheme 7: *β hydride elimination*

The complexes in ***Scheme 7*** are example of compounds which do not undergo β hydride elimination. The adamantyl ligand in Cr(IV) complex **13** prevents elimination because the resulting bridgehead olefin is too unstable to form. In the case of Pt(II) complex **14**, a coplanar arrangement cannot be achieved because of the steric requirements of the metallacyclobutane ring. Another common way of preventing β hydride elimination is to saturate the alkyl complex so that no free coordination site is available for the incoming hydride.[1]

1.1.2.4 Olefin insertion

Olefin insertion into M-H or M-alkyl bonds is a very useful reaction since olefins are readily available and the reaction leads to C-C bond formation, either directly (M-alkyl insertion) or indirectly (M-H insertion followed by reductive elimination). It is the key step in many industrially relevant processes such as ethylene oligomerisation,[30-33] ethylene polymerisation,[38-41] or hydrocyanation of butadiene.[42] In the Ni and Pd-catalysed alkenylation of azolium salts described in Chapter 2, olefin insertion is also central to the overall catalytic cycle. The main features of this elementary reaction are shown in ***Scheme 8***.

Olefin insertion does not change the oxidation state of the metal; therefore it is observed across the periodic table from d^0 metals such as Zr(IV),[40] to electron-rich d^8 metals such as Ni(II).[38, 39, 41, 43] It is sometimes referred to as migratory insertion. This is because it is actually a nucleophilic addition of the hydride or the alkyl on the electrophilic coordinated olefin. Therefore the vacant site generated during this reaction is situated at the nucleophile coordination site.

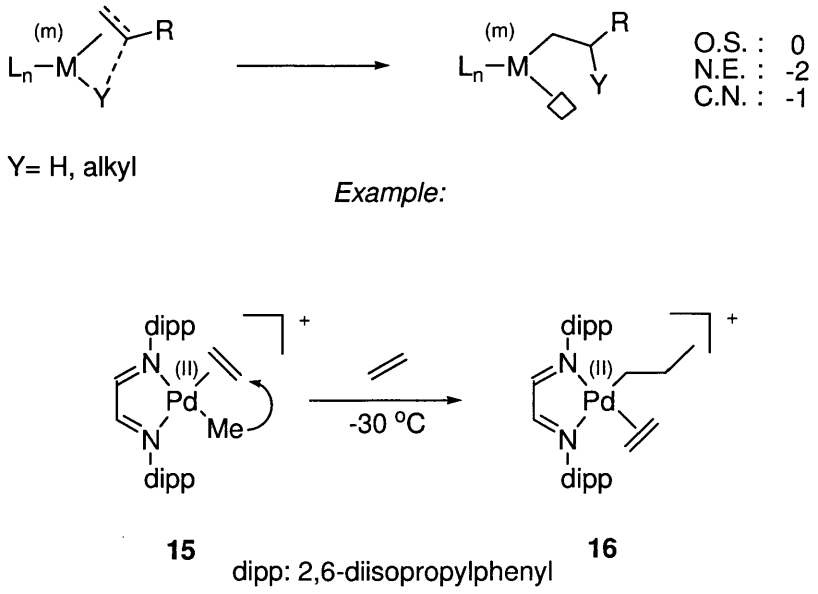

Scheme 8: *olefin insertion*

Because the coordination number of the metal decreases by one, excess olefin (as in the case of ethylene polymerisation) can fill the vacant site and drive the equilibrium forward by preventing reverse β hydride elimination.[40] ***Scheme 8*** shows an insertion reaction in the Pd(II)-catalysed ethylene polymerisation reported by Brookhart.[41] Ethylene insertion was observed at low temperature in cationic Pd(II)-Me complex **15**. The high affinity of cationic Pd(II)-alkyl complexes for olefins prevents β hydride elimination,[44] by ensuring constant occupation of the vacant sites by ethylene (complex **16**).

1.1.3 Homogeneous catalysis and fine organic synthesis

Homogeneous catalysis has enabled the development of several bulk chemical processes, such as alkene hydroformylation,[45, 46] alkene oxidation (the so-called "Wacker Process"),[47-50] butadiene hydrocyanation (for the production of Nylon 6,6),[42] and other alkene transformation reactions.[29, 31, 33, 40, 41, 43, 51] However, it is in the field of fine organic synthesis that its achievements are most spectacular. In the past decade, two Nobel Prizes have been awarded to researchers in the field, thus acknowledging the outstanding contributions of homogeneous catalysis to modern synthetic chemistry.[52-57] The reactions discussed in the following have now reached a level of technical maturity allowing their application to the large-scale preparation of fine chemicals. Other technologies, notably Pd-catalysed reactions such as Suzuki-Miyaura,[58] Heck[26] and Buchwald-Hartwig[59] coupling methodologies will doubtlessly reach similar status in the coming years.[59-63]

1.1.3.1 Asymmetric olefin hydrogenation

Noyori and Knowles were awarded the Nobel Prize in chemistry (2001) for the independent development of asymmetric hydrogenation (***Scheme 9***).[56, 57]

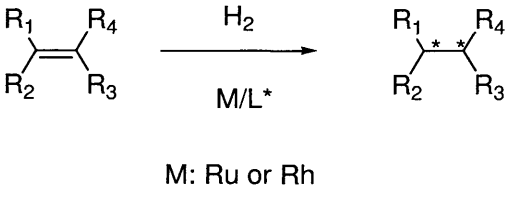

Scheme 9: *Ru and Rh-catalysed asymmetric hydrogenation of olefins*

Asymmetric hydrogenation of unsaturated substrates was rapidly acknowledged as an extremely useful methodology. Indeed, the product of the reaction is generated with perfect atom economy,[64] and up to two chiral centres are generated in a single step. The development of chelating chiral

bis(phosphine) ligands DIPAMP and BINAP (***Figure 5***), together with extraordinary substrate scope and scalability, were keys to the success of this methodology.

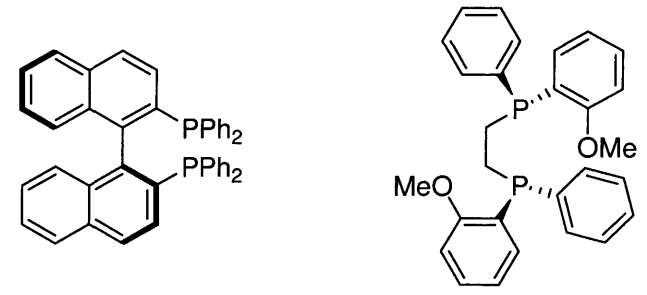

(S)-BINAP
Noyori

(R,R)-DIPAMP
Knowles

Figure 5: *chiral ligands used in asymmetric hydrogenation*

The combination of those three factors resulted in a number of industrial syntheses of fine chemicals such as L-DOPA (a drug for Parkinson's disease)[57] and naproxen (a pain reliever) (***Scheme 10***).[65]

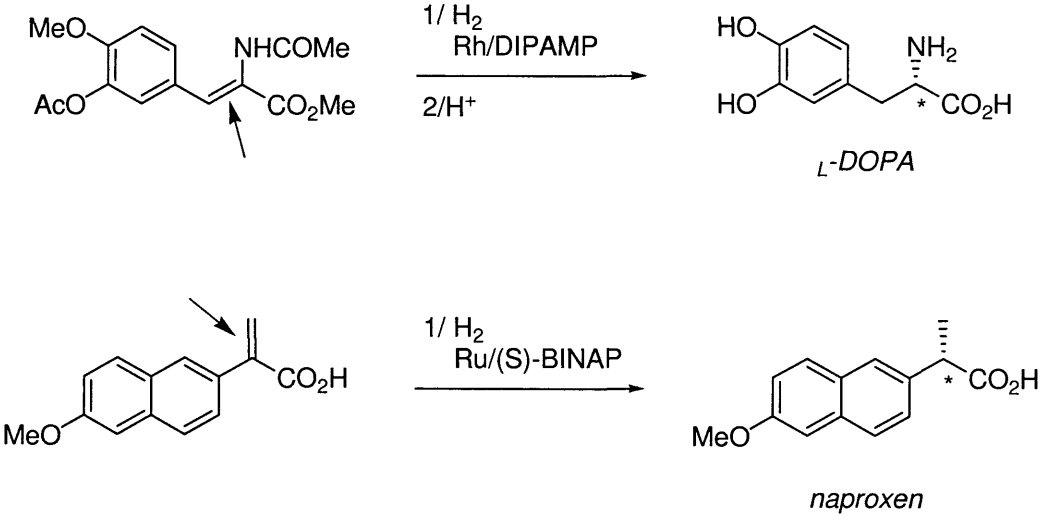

Scheme 10: *asymmetric hydrogenations on an industrial scale.*[66]

1.1.3.2 Olefin metathesis

The 2005 Nobel Prize in chemistry was awarded to Chauvin, Grubbs and Schrock for the development of homogeneous olefin metathesis.[52-54] Since the early studies in the 1970s, the reaction has been declined in many variants (***Scheme 11***), but the general concept remains the same: metal carbenes are able to undergo ligand exchange with olefins *via* metallacyclobutane intermediates (Chauvin mechanism, ***Scheme 12***).

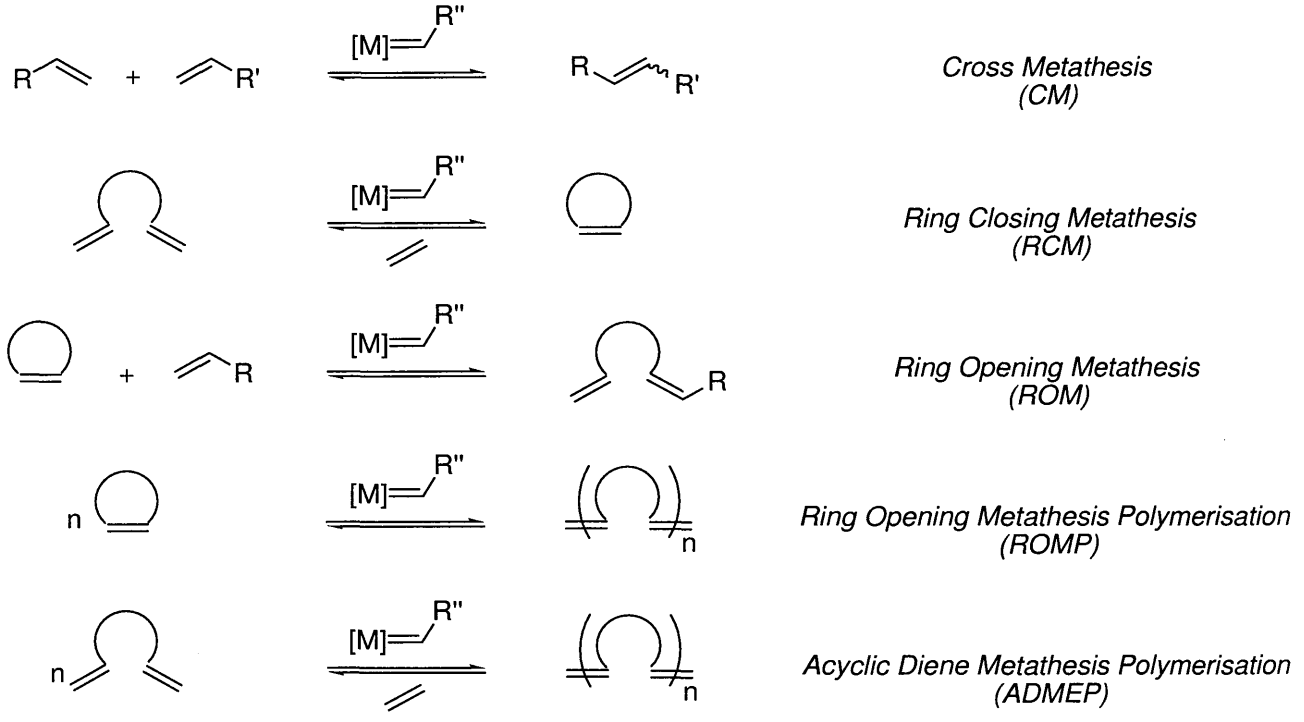

Scheme 11: *homogeneous olefin metathesis*

Olefin metathesis is perhaps the most typical example of how mechanistic information about a particular metal-catalysed reaction can be exploited to develop extremely efficient catalysts. The Chauvin mechanism involving metal carbenes and metallacyclobutane intermediates (***Scheme 12***) became the basis of the so-called Grubbs and Schrock catalysts (***Figure 6***). In this respect, the work

of Chauvin, Grubbs and Schrock is an inspiration to every chemist involved in the field of homogeneous catalysis.

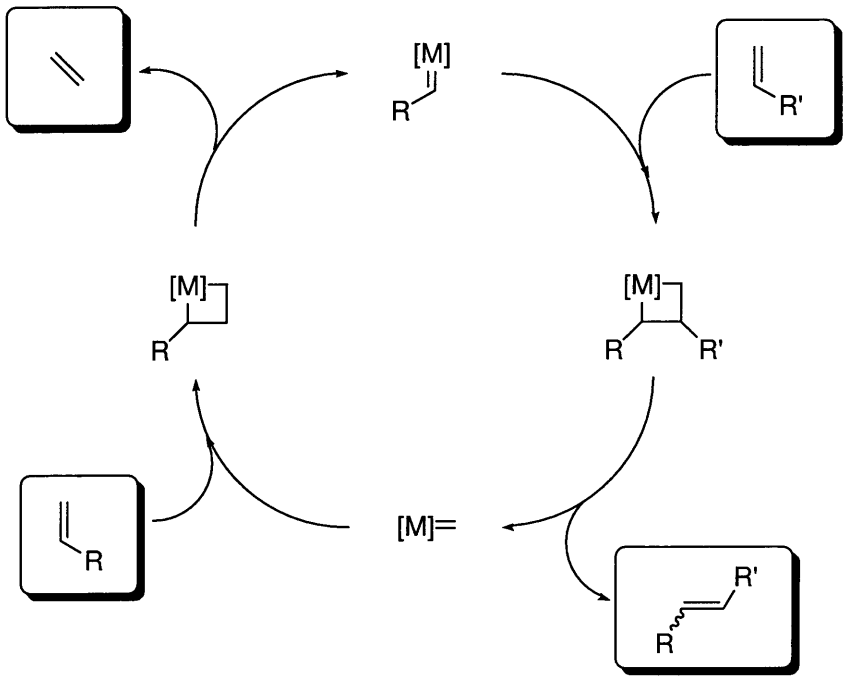

Scheme 12: *accepted "Chauvin" mechanism of olefin metathesis*

The reaction (particularly RCM, ***Scheme 11***) has gradually been adopted by chemists as a prime tool for challenging syntheses, especially of natural products.[67] Asymmetric variants have also been developed with chiral catalysts.[52, 53, 67, 68] The widespread adoption of olefin metathesis is certainly due to its synthetic potential (formation of C=C double bonds from simple olefins) and led in turn to the attention it has received from organic and inorganic chemists alike, both in academia and in industry.

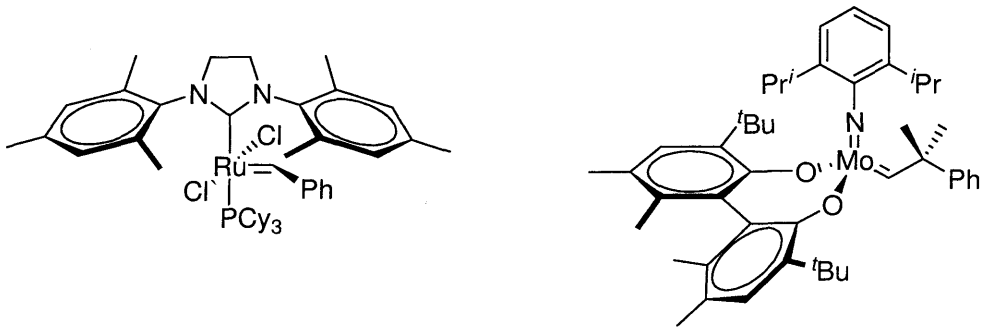

Figure 6: *olefin metathesis catalysts*

Several commercial applications of this reaction have now been developed. ***Scheme 13*** shows the synthesis of antiviral agent **17**. This compound was produced by RCM on a 400 kg scale for clinical trials in the treatment of hepatitis.[69]

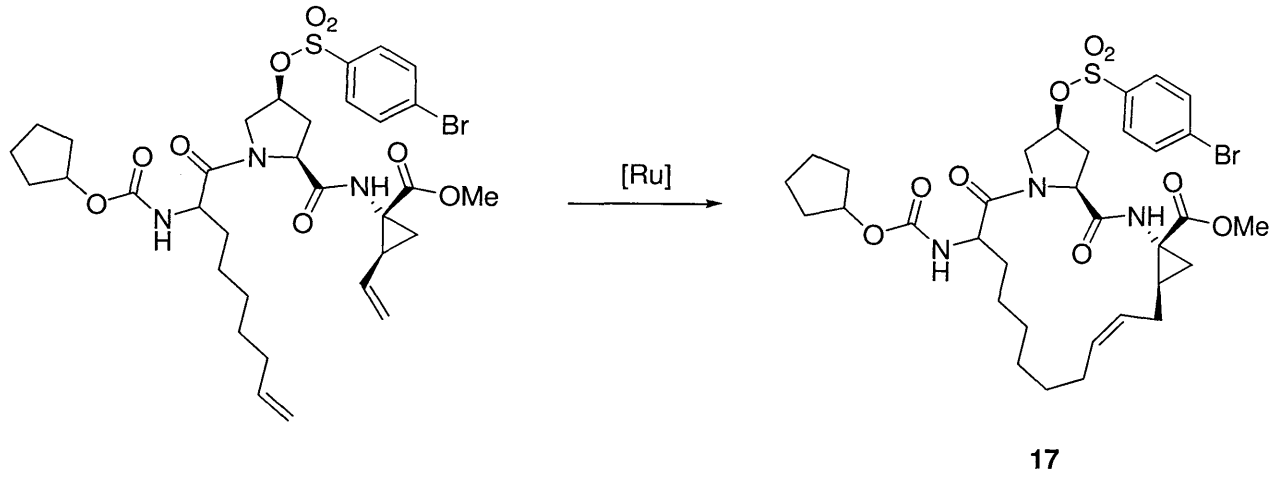

Scheme 13: *example of the application of RCM on industrial scale*

1.2 NHCs as ligands for transition metals

1.2.1 Background

Carbenes are species possessing a divalent carbon atom.[70] As a consequence they break the octet rule, as there are only 6 electrons around C. They were long considered to be transient species in the free state for this reason until Bertrand[71] and Arduengo[72] isolated the first examples of stable free carbenes (***Figure 7***). Carbene A is the first reported example of a so-called free N-heterocyclic carbene or NHC.

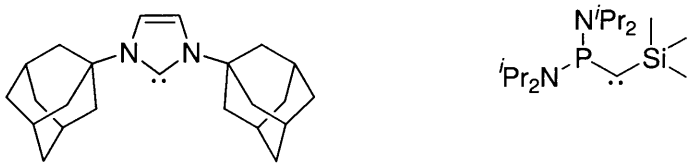

A *(1991)* **B** *(1988)*

Figure 7: *first stable carbenes*

Figure 8 shows the different electronic states adopted (at least in theory) by free carbenes:

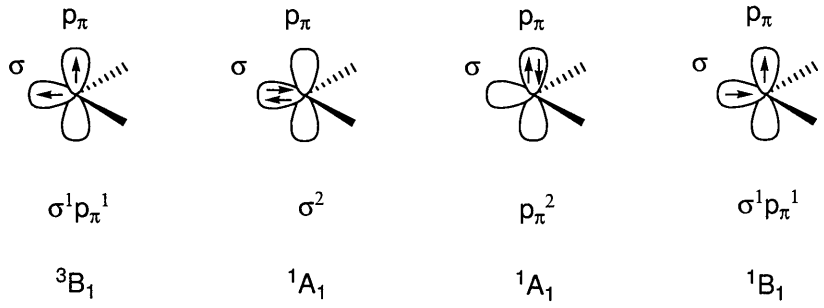

Figure 8: *electronic states of carbenes*[73]

In theory, carbenes can exist in four electronic states. The triplet state $^3B_1$ consists of two unpaired electrons in the σ and p_π orbitals. There are two different singlet states ($^1A_1$) with paired electrons in the σ or p_π orbital. Finally, an excited singlet state can also be envisaged ($^1B_1$), consisting of two unpaired electrons with antiparallel spins. Of the four different carbene electronic structures in ***Figure 8***, only the two ground state singlets (paired electrons in the same orbital) have been observed as stable species.[70, 74-76]

Carbenes are obviously highly energetic and the two substituents on the carbon determine their electronic state and stability.[70, 76]

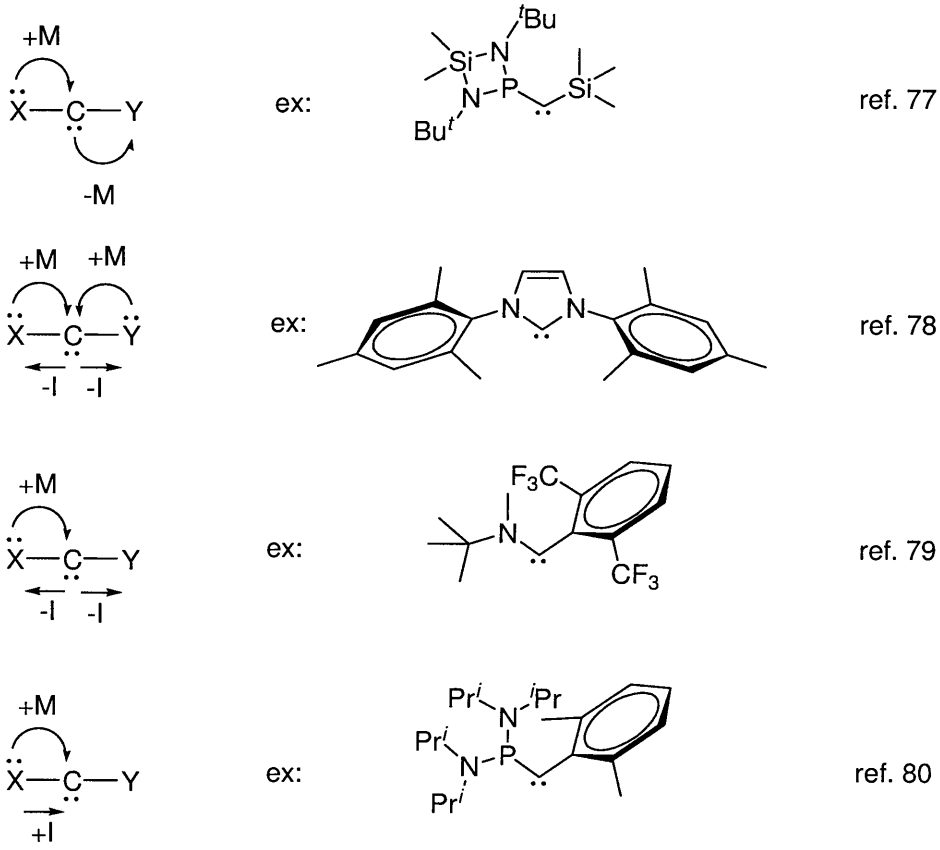

Figure 9: *electronic stabilisation of singlet carbenes*[77-80]

Because ground state singlet carbenes possess a fully occupied orbital and an empty one, the most general way of stabilising them consists in removing electron density from the occupied orbital whilst partially filling the empty orbital. This can be achieved by a variety of means, using both mesomeric and inductive effects as shown in ***Figure 9***.

In the case of NHCs, the combination of mesomeric donation (from the lone pair on the nitrogens) and negative inductive effect (due to the higher electronegativity of N)[81] effectively stabilises these compounds. This had been acknowledged for more than 20 years (by Ofele[82] and Wanzlick[83]) before Arduengo reported the first stable NHC.[72]

Obviously, steric bulk is also an important factor and it is believed that bulky substituents kinetically stabilise carbenes.[70] However, there are some exceptions such as tetramethylimidazol-2-ylidene (tmiy, ***Figure 11***). This highlights the sometimes unpredictable stability pattern of singlet carbenes.[76]

1.2.2 Types of NHCs

N-heterocyclic carbenes (NHCs) are carbenes originally based on N-containing heterocyles such as imidazoles (I_U), imidazolines (I_S),[84] and triazoles (T).[85] Other heterocyclic structures have appeared (and continue to do so) since the first studies,[78, 82, 83, 86] including oxazoles (O),[87] benzothiazoles (B_T)[88, 89], pyridines (Py),[90-94] benzimidazoles (B_N)[95] or 1,2-piperazine (Pip)[96] (***Figure 10***).

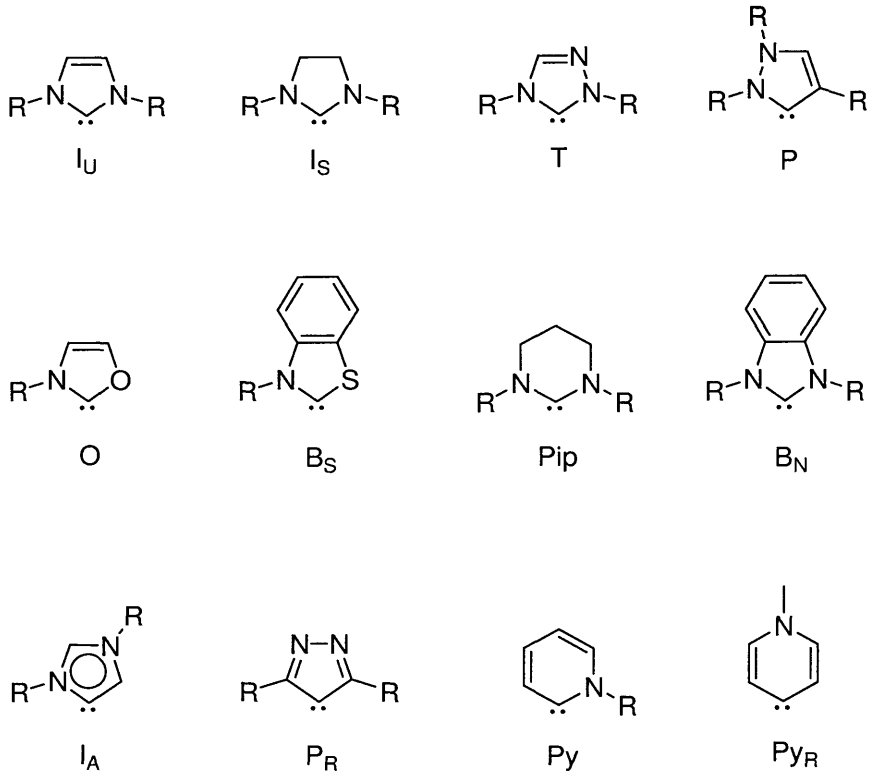

Figure 10: *common types of NHCs*[97]

The most common NHCs are imidazol-2-ylidenes of type I_U and I_S (***Figure 10***).[70, 78, 85, 98, 99] Examples of these compounds, most of which are commonly used in homogeneous catalysis, are shown in ***Figure 11***.

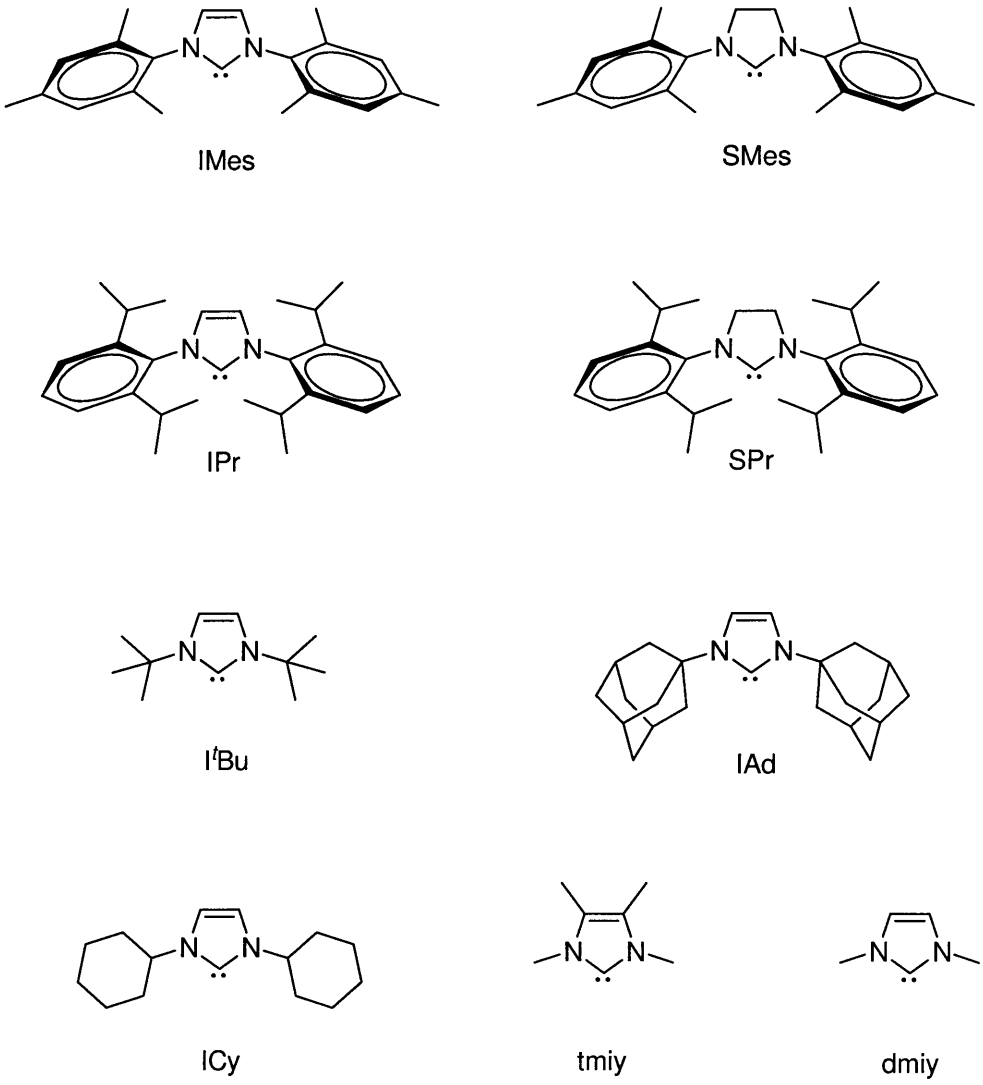

Figure 11: *common NHCs based on the imidazole ring*

These compounds are sometimes referred to as "normal NHCs" , as opposed to the recently appeared "abnormal NHCs" which bind to metals by the C4 or C5 position of the imidazole ring (***Figure 10***, I_A. See also ***Scheme 3***).[20, 100-103] Finally, so-called "remote-NHCs" have recently appeared in the literature.[91, 104] The nitrogen atom in these compounds (based on the pyrazole or pyridine ring: ***Figure 10***, P_R and Py_R) is not directly linked to the carbene centre.[105] Because the most common types of NHCs are I_U and I_S, the term NHC refers to these throughout this thesis.

1.2.3 Ligand properties

1.2.3.1 NHCs vs Fischer and Schrock carbenes

Although free carbenes have been known for less than 20 years,[71, 72] carbene complexes of transition metals have a long history. Fischer,[106] then Schrock,[107] introduced carbene-bound complexes in the 60s-70s, and Lappert studied the organometallic chemistry of NHCs long before Arduengo's work.[98] The generally held view is that carbene complexes can be classified into Fischer-type or Schrock-type species(***Figure 12***).[1]

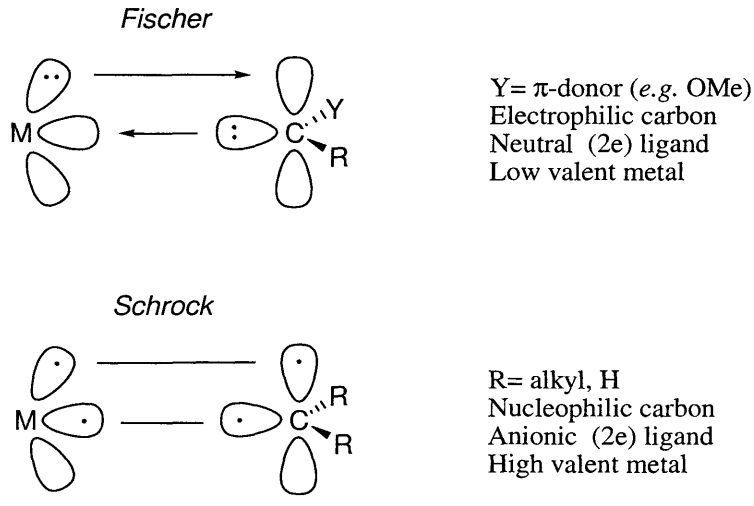

Figure 12: *Fischer and Schrock carbene metal complexes*

Fischer carbene complexes are related to NHC complexes in that the carbene in these species can be considered as a neutral ligand. Moreover it is in the singlet state like NHCs, and the central carbon atom bears substituents with inductive-acceptor and mesomeric-donor properties (*e.g.* OMe). However, Fischer carbenes are good π-acceptors with strong back-bonding from the metal to the carbene whereas the π-accepting abilities of NHCs are variable (see section **1.2.3.3**), to the extent that unlike Fischer carbenes,[70, 108] they can stabilise early transition metals in high oxidation states

without back-donating abilities (e.g. Ti(IV)[109]). Finally, NHCs can usually be considered as spectator ligands (although this is not always the case, see section **1.2.3.3**), whereas Fischer carbenes undergo a variety of reactions, including cyclopropanation and metathesis.[1, 110, 111]

1.2.3.2 Steric and electronic properties: NHCs *vs* phosphines

Since the isolation of the first NHC based on the imidazole ring by Arduengo,[72] this class of ligand has been thoroughly studied and chemists now have a better understanding of their properties as ligands. Because they are neutral 2e ligands, and due to their affinity for transition metals, NHCs have been used to replace phosphines in a number of transition metal catalysed reactions.[85] For example, the replacement of bulky trialkylphosphines by NHCs to generate catalysts for olefin metathesis[53] or Buchwald amination[13, 112, 113] has been described (***Figure 13***):

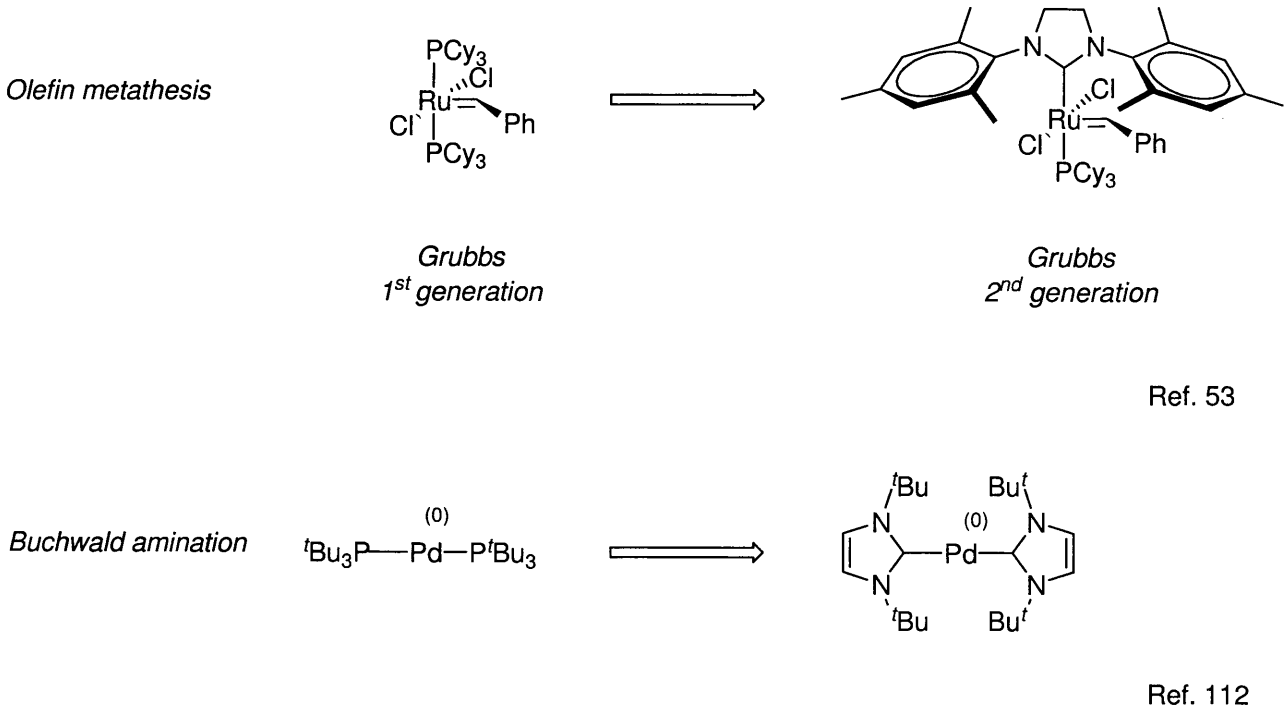

Figure 13: *NHCs vs phosphines in metal catalysts*

The fact that NHCs can be used to replace bulky electron-rich trialkylphosphines such as PCy_3 or P^tBu_3 is no coincidence. Stable carbenes such as IMes or IPr often possess bulky groups on the nitrogens, and they also are strongly basic. Although these features (high bond dissociation energies, comparable steric bulk to bulky tertiary phosphines, strong σ-donor properties) had been recognized early on,[70, 85, 108] no systematic investigation of the fundamental properties of NHCs as ligands had been reported until major studies by Nolan,[99, 114] Cavallo[115, 116] and Cavell.[117]

1.2.3.2.1 Basicity of NHCs

An *ab initio* DFT study by Cavell and Yates focused on the determination of the pK_bs of NHCs in various solvents.[117] Basicity directly correlates to the σ-donor properties of ligands such as NHCs or phosphines; therefore it is a useful indicator of ligand properties.[118] However, basicity does not measure the *net electron-donating ability*, since the latter is a balance between σ-donor, π-acceptor and π-donor abilities.[119] ***Figure 14*** shows some NHCs and their calculated pK_bs in water.

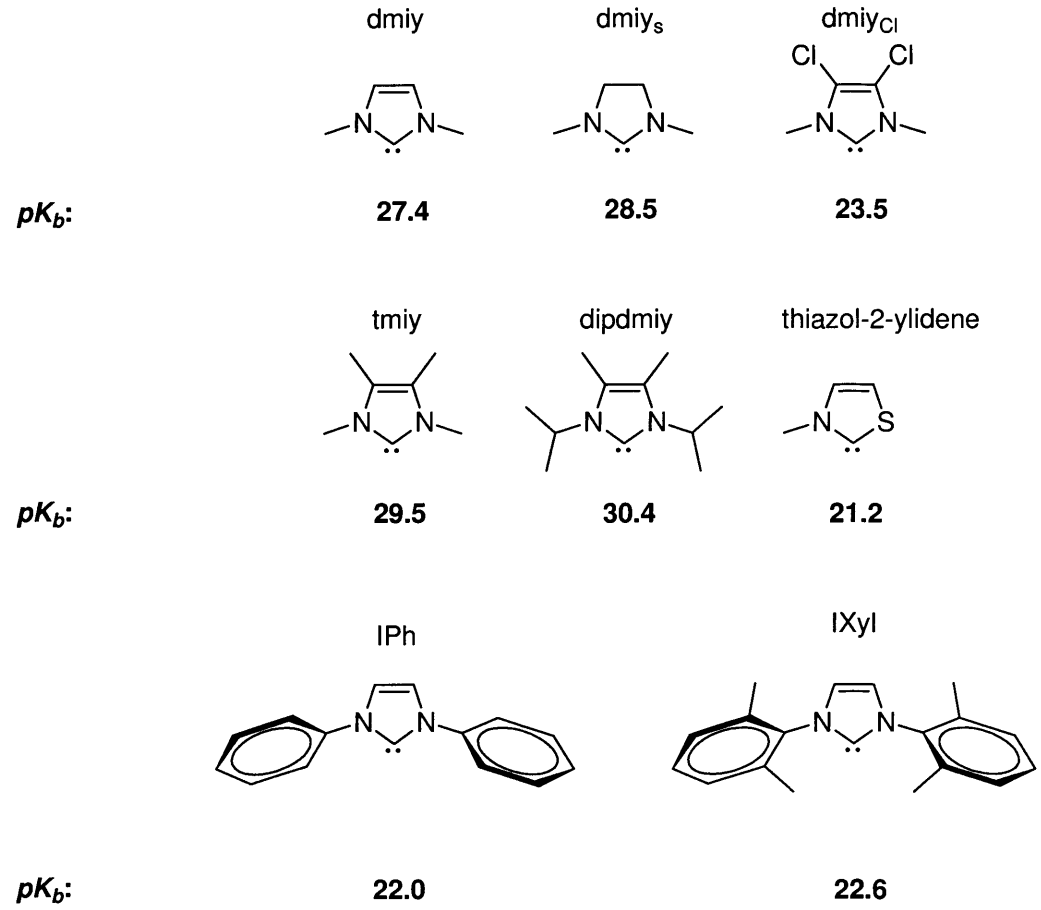

Figure 14: *calculated pK_bs of some NHCs in water*

As a comparison, the pK_b of P^tBu_3 (the most basic phosphine used in homogeneous catalysis) in water is 11.40.[117] Therefore, even the least basic NHC of the calculated set of carbenes (thiazol-2-ylidene, pK_b= 21.2) is considerably more basic than the most basic phosphine. Interestingly, for NHCs with the same type of substituents on the nitrogens (*i.e.* alkyl or aryl), the basicity does not vary much. For example, tmiy and dipdmiy have very close pK_bs (29.5 and 30.4 respectively). The difference between saturated and unsaturated NHCs is also quite small: dmiy and dmiy$_s$ only differ by one pK_b unit (27.4 *vs* 28.5). On the other hand, the introduction of electron-withdrawing substituents on the imidazole ring (dmiy$_{Cl}$, pK_b= 23.5) has a marked effect on the basicity.

Overall, these results confirm the common understanding that NHCs are very basic ligands, much more so than phosphines.

1.2.3.2.2 Steric and electronic properties of NHCs compared with phosphines

Studies of the steric and electronic properties of phosphines conducted by Tolman in the 70s have had a profound impact on organometallic chemistry and homogeneous catalysis.[111, 118-121] Tolman defined his phosphine parameters θ (a.k.a. cone angle, measuring steric bulk) and ν (a.k.a. electronic parameter, measuring net electron-donating ability) to quantify steric and electronic properties associated with phosphines, and in turn to help predict the behaviour of phosphine metal complexes. The cone angle θ of a phosphine is measured in ° and represents the angle of a cone in which the metal is the apex and the outermost phosphine substituents touch the surface (***Figure 15***).[122]

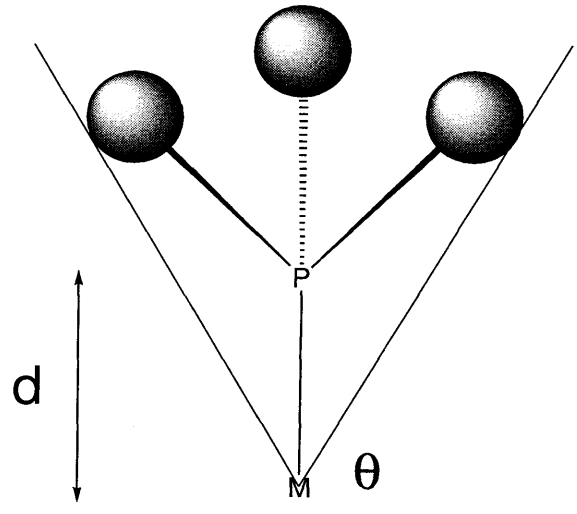

Figure 15: *determination of the cone angle of a phosphine*

The distance d between the phosphorus atom and the metal is fixed at 2.28 Å, which is a rough average of distances observed experimentally in phosphine complexes.[120]

The electronic parameter ν (measured in cm^{-1}) corresponds to the A_1 stretching vibration of CO in $Ni(CO)_3L$ complexes (where L= phosphine) formed by the addition of 1 eq of phosphine to $Ni(CO)_4$ (***Figure 16***).

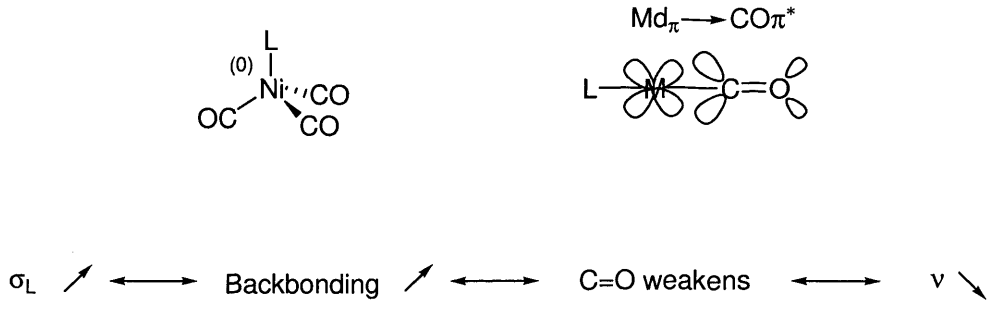

Figure 16: *determination of the electronic parameter of a phosphine*

As a consequence, ν measures the net electron donating ability of a phosphine. Indeed, as shown in ***Figure 16***, the π^* orbital of a CO ligand can accept electron back-donation from one of the metal's d orbitals. The more electron-rich the metal, the more back-donation occurs. Therefore, electron-rich ligands induce more back-donation, thus weakening the C=O bond and decreasing the stretching frequency.

Tolman parameters can be used to plot a so-called "Tolman map", a very useful graphic tool to visually compare phosphine properties (see Chapter 2). Unfortunately, NHCs cannot be plotted on a Tolman map because the cone angle is not a relevant parameter to measure their steric bulk. Indeed, substituents in NHCs point towards the metal whereas phosphine substituents point away from it (umbrella shape). However, Nolan and Cavallo have shown that ν can be obtained for NHCs, as $Ni(CO)_3NHC$ complexes are conveniently synthesised from $Ni(CO)_4$ and free NHCs.[99, 114, 123] Moreover, in order to compare steric properties of phosphines and NHCs, Nolan and Cavallo introduced the buried sphere volume ($\%V_{Bur}$) concept: $\%V_{Bur}$ represents the "amount of volume of a sphere centered on the metal, buried by overlap with atoms of the various NHC ligands. The volume

of this sphere would represent the space around the metal atom that must be shared by the different ligands upon coordination"[115]. ***Figure 17*** illustrates this concept:

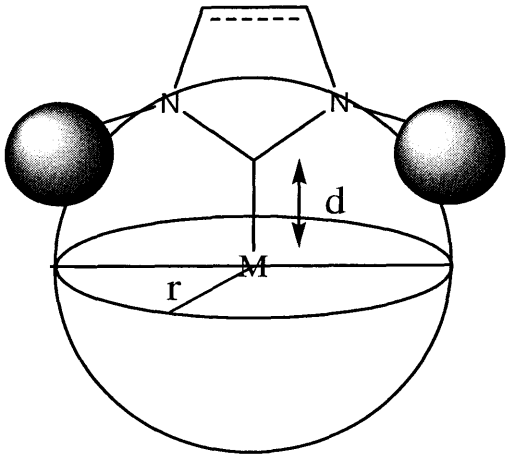

Figure 17: *determination of the buried sphere volume* $\%V_{Bur}$ *of an NHC*

The buried sphere volume tool can also be used for phosphines, and varying d (ligand to metal distance) and r (radius of the coordination sphere) allows one to calculate $\%V_{Bur}$ for different metals as well. The advantage of using $\%V_{Bur}$ is that ligands with widely different geometries can be compared.[99, 115] Thus, it is now possible to compare steric and electronic properties of NHCs and phosphines. By conducting dynamic IR experiments on $Ni(CO)_3L$ complexes (where L= NHC), Nolan also estimated bond dissociation energies (BDE) of NHCs in these complexes and compared the values obtained to those of phosphines (***Table 1***):[99]

Table 1: *steric and electronic comparison of phosphines with NHCs*[124]

[a]: $Ni(CO)_3L$ not stable. [b]: literature value not given.

Ligand	ν (cm^{-1})	$\%V_{Bur}$	BDE ($kcal.mol^{-1}$)
I^{t}Bu	*NA*[a]	37	24.0
IAd	*NA*[a]	37	20.4
IPr	2051.5	29	38.5
SIPr	2052.2	30	38.0
IMes	2050.7	26	41.1
SIMes	2051.5	27	40.2
ICy	2049.6	23	39.6
PPh_3	2068.9	22	26.7
PCy_3	2056.4	26	*NA*[b]
P^tBu_3	2056.1	30	28.0

These results clearly establish that:

- NHCs have much stronger net electron-donating abilities than even the most basic phosphine P^tBu_3.
- In terms of steric bulk, IMes and SIMes are best compared with PCy_3 whilst IPr and SIPr are closer to P^tBu_3. These ligands are all commonly used in cross-coupling reactions,[28, 36, 58, 125-127] therefore it is interesting to be able to compare them.
- Finally ***Table 1*** shows that, for comparable steric bulk, the BDEs of NHCs are considerably higher than those of phosphines (for example compare P^tBu_3, 28.0 kcal.mol^{-1} and SIPr, 38.0 kcal.mol^{-1} for a $\%V_{Bur}$ value of 30 %). This is especially important in catalysis, where ligand dissociation is a common catalyst deactivation pathway.

1.2.3.3 Nature of the NHC-metal bond: π interactions

The question of the nature of the bonding in NHC complexes arose very early after the isolation of the first free NHC. Due to the lone pair on the carbon atom, NHCs are primarily σ-donors.[70] In 1994, Arduengo reported homoleptic complexes of Ni(0) and Pt(0) (***Figure 18***) and concluded (on the basis of structural data) that π back-donation from the metal to the NHC was significant.[128]

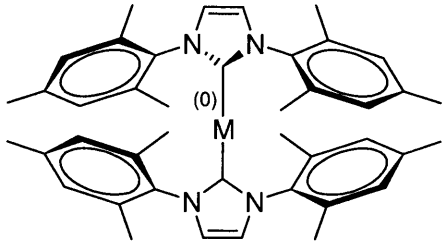

M= Ni, Pt

Figure 18: *homoleptic NHC complexes reported by Arduengo*

However, Green and coworkers later reported that π-bonding in similar Pt(0) and Pd(0) complexes was minimal, and that the metal-ligand interaction should be regarded as a pure σ bond.[129] This study, which was conducted by photoelectron spectroscopy and DFT calculations,[130] became a reference when discussing the σ-donating and π-accepting properties of NHCs.[131] Perhaps the fact that NHCs can bind in the absence of back-donation (for example in the cases of d^0, alkali or alkaline earth metals[70]) persuaded researchers in the field that NHCs were pure σ-donor ligands. Also, the kinetic stability of free NHCs is due to donation of the nitrogens' lone pairs into the empty p_π orbital; therefore it is tempting to assume that this happens in NHC complexes as well, in which case there is no need for π back-donation from the metal to stabilise the empty orbital.[108, 132, 133] In addition, Frenking investigated the bonding in group 11 NHC complexes by charge decomposition analysis (CDA) and concluded that π interactions in these complexes were minimal.[133]

However, some reports appeared after 2001, which challenged the widely accepted view that NHCs were pure σ-donors.[134-137] A convincing manifesto for π-accepting abilities was provided by the work of Meyer on homoleptic group 11 metal complexes of a tripodal carbene ligand (***Figure 19***):

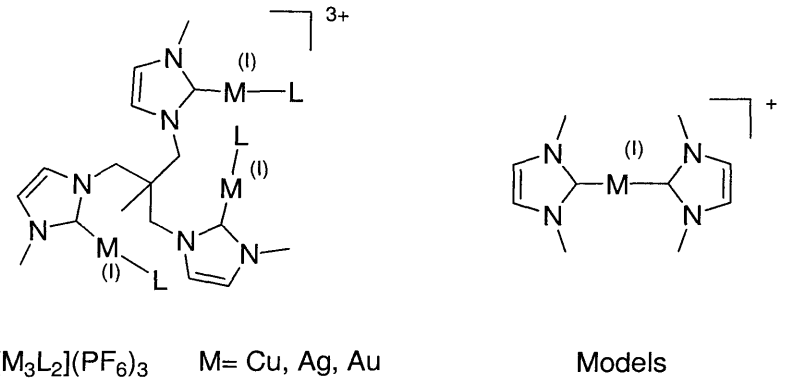

Figure 19: *homoleptic Cu(I), Ag(I) and Au(I) NHC complexes*

The carbene-metal bond in these compounds was studied computationally (by energy decomposition analysis a.k.a. EDA) using the simple $[M(dmiy)_2]^+$ cations as models (***Figure19***). Meyer found that π back-donation contributed 15-30 % of the total interaction.[134, 136] Frenking confirmed these results in a very similar study (also using EDA).[132] Recently, a computational assessment (by EDA) conducted by Jacobsen on a large number of model NHC complexes came to the same conclusions, *i.e.* NHCs do have some π-accepting character, especially in electron-rich complexes of late transition metals.[138] Not surprisingly however, NHC complexes of d^0 metals such as Sm(III),[139] Ti(IV),[140, 141] or Zr(IV)[141] have no π accepting character.

Whilst π-acidity is gradually being recognised as a feature of NHCs, π-basicity was unknown until Nolan reported two rare examples of 14-electron Ir(III) and Rh(III) complexes stabilized by a bulky NHC (***Figure 20***).[142]

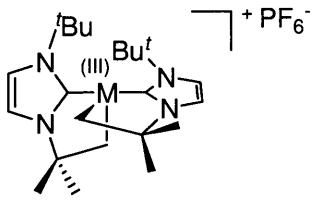

18 M=Ir
19 M= Rh

Figure 20: *14- electron complexes of group 9 metals isolated by Nolan*

Electron-deficient complexes are usually stabilised by agostic C-H interactions, *i.e.* a C-H bond of the ligand donates electron density to an empty d orbital on the metal.[1] Nolan performed DFT calculations on **18** and **19** and did not find any evidence of agostic interaction. These 14 electron complexes appear to be stabilised by π-donation from the NHC to the metal. Jacobsen later found evidence of π-donation in electron-poor complexes.[138]

The body of work on NHCs and their complexes shows a more complex picture of the nature of the NHC-metal bond than the original one. Whilst it remains true that NHCs can bind to metals devoid of π back-donating ability (which is easily explained by the fact that free NHCs are stable), they usually interact by a combination of σ donation, π back-donation (electron rich metals) and in some cases (electron-poor metals) π donation. This electronic flexibility is certainly a key factor in their success as ligands for transition metals.

1.2.4 Synthesis of NHC complexes

There are several ways of preparing NHC complexes. They can be divided into three main classes: use of free NHCs, reaction of NHC precursors, and template synthesis. A mini-review on this topic was published a decade ago.[143] Since then, new methods have appeared in the literature. In the following, the main strategies for the synthesis of these important species are presented.

1.2.4.1 Use of free NHCs to generate NHC complexes

The simplest method to prepare NHC complexes is the use of a free NHC that can be added to a suitable metal precursor to generate the desired product. The key step in this strategy is the generation of the free carbene. The spur of interest in NHCs since the isolation of the first free NHC is a testimony to the convenience and usefulness of this method. Historically, free NHCs have mostly been prepared by deprotonation of imidazolium salts using different bases (***Scheme 14***).

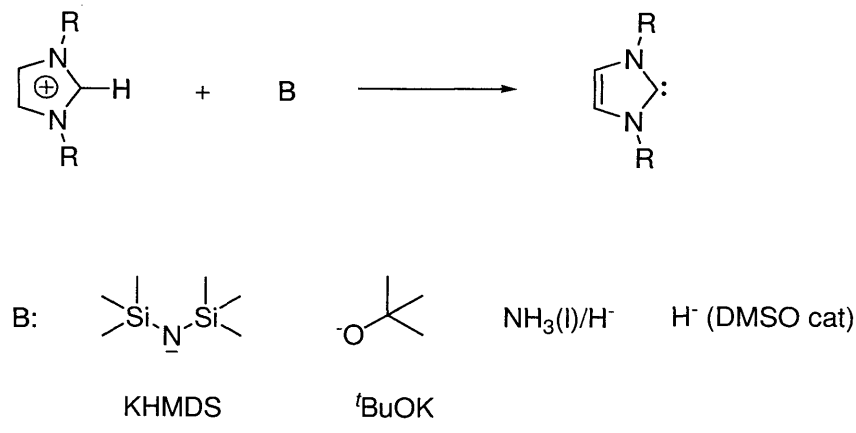

Scheme 14: *deprotonation of imidazolium salts to prepare free NHCs*

In the early days, the use of NaH with catalytic DMSO or ^{t}BuOK was common;[72, 78] then Herrmann devised a method using liquid ammonia.[144] Nowadays, the stoichiometric use of strong hindered bases such as KHMDS or ^{t}BuOK seems to be a method of choice, not least because the by-

products (^{t}BuOH and $(Me_3Si)_2NH$) are volatile, allowing for easy work-up.[145] However, Bertrand has reported the formation of imidazolium/base adducts, indicating that deprotonation is not always trivial.[146] It is worth noting that deprotonation can be done *in situ*, especially in the case of reactive carbenes or on a large scale. In this case, an imidazolium salt is deprotonated in solution and the resulting free carbene can be transferred to a suitable metal precursor. For example, Nolan developed a multigram procedure for the synthesis of **20**, very active cross-coupling catalyst (***Scheme 15***. See also chapters 3 and 4).[147]

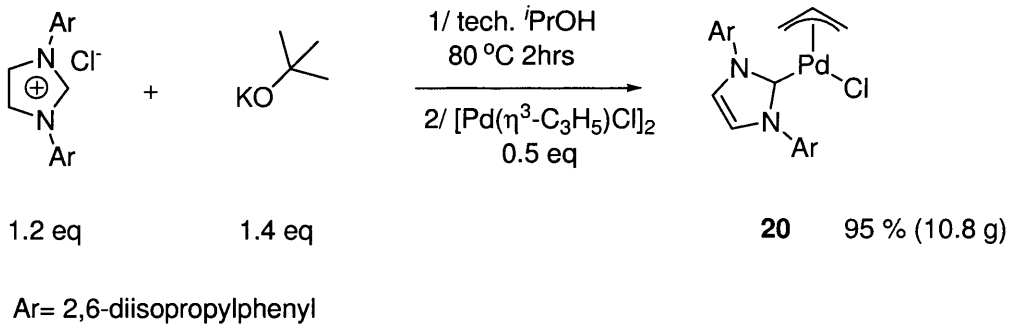

Scheme 15: *in situ deprotonation of an imidazolium salt in the synthesis of a Pd(II) complex*

NHCs with alkyl substituents on the nitrogens (such as tmiy or dipdmiy) are more basic than NHCs bearing aryl substituents (see section **1.1.6.2.1**).[117] Consequently, the corresponding imidazolium salts can be difficult to deprotonate. Moreover, their synthesis can sometimes be troublesome. Therefore, a convenient way of accessing free NHCs is the potassium reduction of imidazol-2-thiones developed by Kuhn (***Scheme 16***).[148]

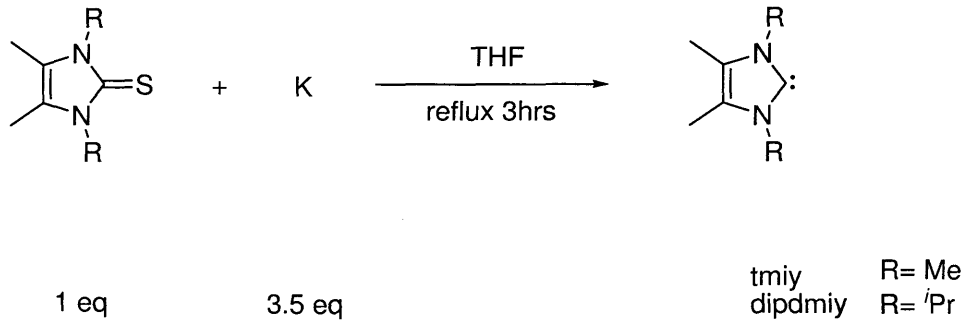

Scheme 16: *synthesis of free NHCs by reduction of thiones*

Finally, an elegant method to deprotonate imidazolium salts has recently been reported by Astruc (***Scheme 17***).[149]

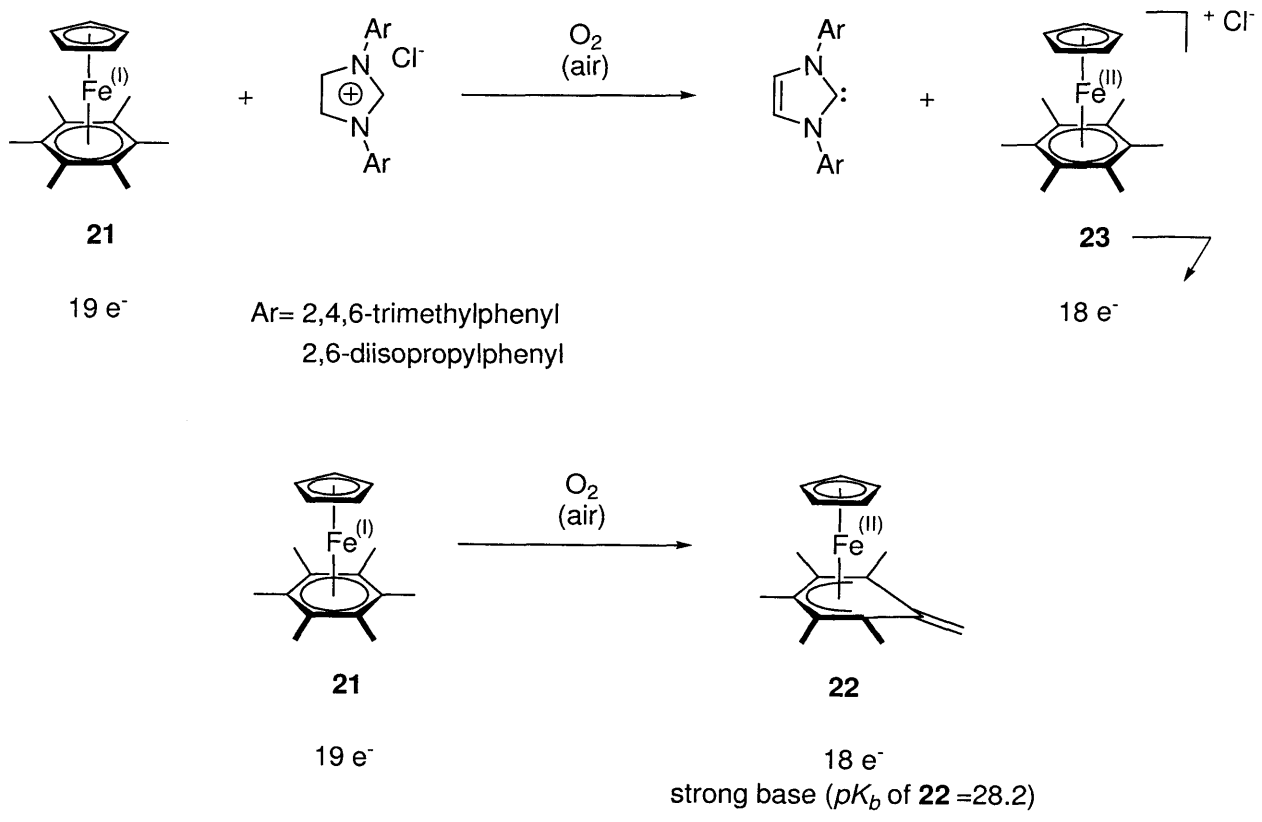

Scheme 17: *use of an electron reservoir complex to generate free NHCs*

It is thought that the 19 electron Fe(I) complex **21** reacts with air to generate **22**, a strong base which can then deprotonate imidazolium salts. The by-product of the reaction **23**, precipitates from the reaction mixture and can be reduced with Na/Hg to regenerate **21**.

1.2.4.2 Synthesis of NHC complexes from NHC precursors

1.2.4.2.1 Base-mediated metalation of imidazolium salts

NHCs are strong bases (see section **1.1.6.2.1**);[117] therefore they are moisture sensitive. In addition, they cannot always be isolated as free carbenes, although they readily form metal complexes. Actually, before Arduengo's seminal work,[72] preparation of NHC complexes required the use of NHC precursors or template synthesis (see section **1.1.7.3**).[83, 98, 150] Nowadays, it is still possible to avoid using free NHCs to generate metal complexes. A very common strategy is the deprotonation of imidazolium salts with a weak base. In contrast to the *in situ* deprotonation of imidazolium salts, which generates stoichiometric amounts of free NHCs (see previous section), this method relies on the presence of a metal precursor to drive the reaction to completion. Therefore it is better described as base-mediated metalation of imidazolium salts. For example, Ofele reported Cr(0) NHC complex **24** some 39 years ago (***Scheme 18***).[82]

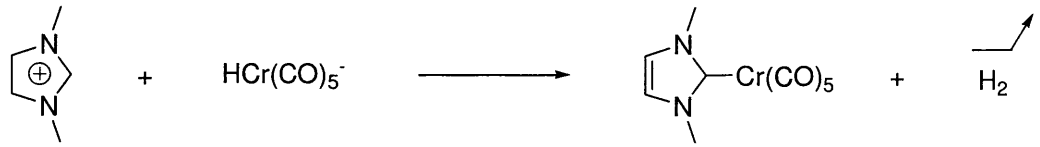

24

Scheme 18: *metalation of an imidazolium salt to generate a Cr(0) NHC complex*

In Ofele's example, the metal precursor is also the base. This is also the case in the synthesis of Ag(I) NHC complexes from imidazolium salts first described by Lin.[151] For example, complex **25** can be prepared under mild conditions (***Scheme 19***).[152]

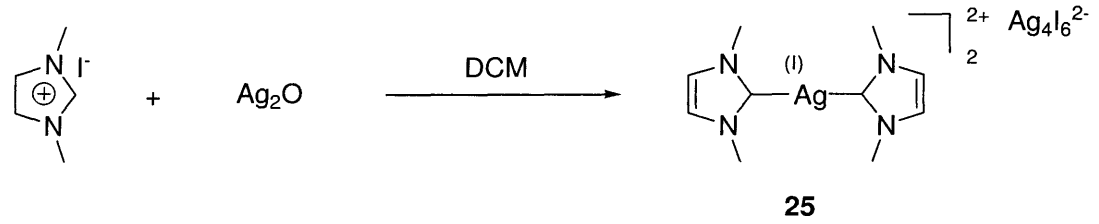

25

Scheme 19: *synthesis of an NHC transfer agent*

Complex **25** is a so-called carbene transfer agent, because it undergoes transmetalation reactions with other complexes (see Chapter 3 for example). The transferred NHC (dmiy) can also be prepared by deprotonation of 1,3-dimethylimidazolium, but it is somewhat unstable and requires strictly anhydrous conditions.[78] By contrast, the reaction depicted in ***Scheme 19*** is rapid (1 hour) and does not require any special precautions to exclude air or moisture.[153] This is a general feature of Ag(I) NHC complexes;[151, 154] therefore this class of compounds is commonly used to transfer NHCs to other metals. For example, Pd(II) complex **26**, an extremely efficient catalyst for Heck and Suzuki reactions, was obtained in this way.[155]

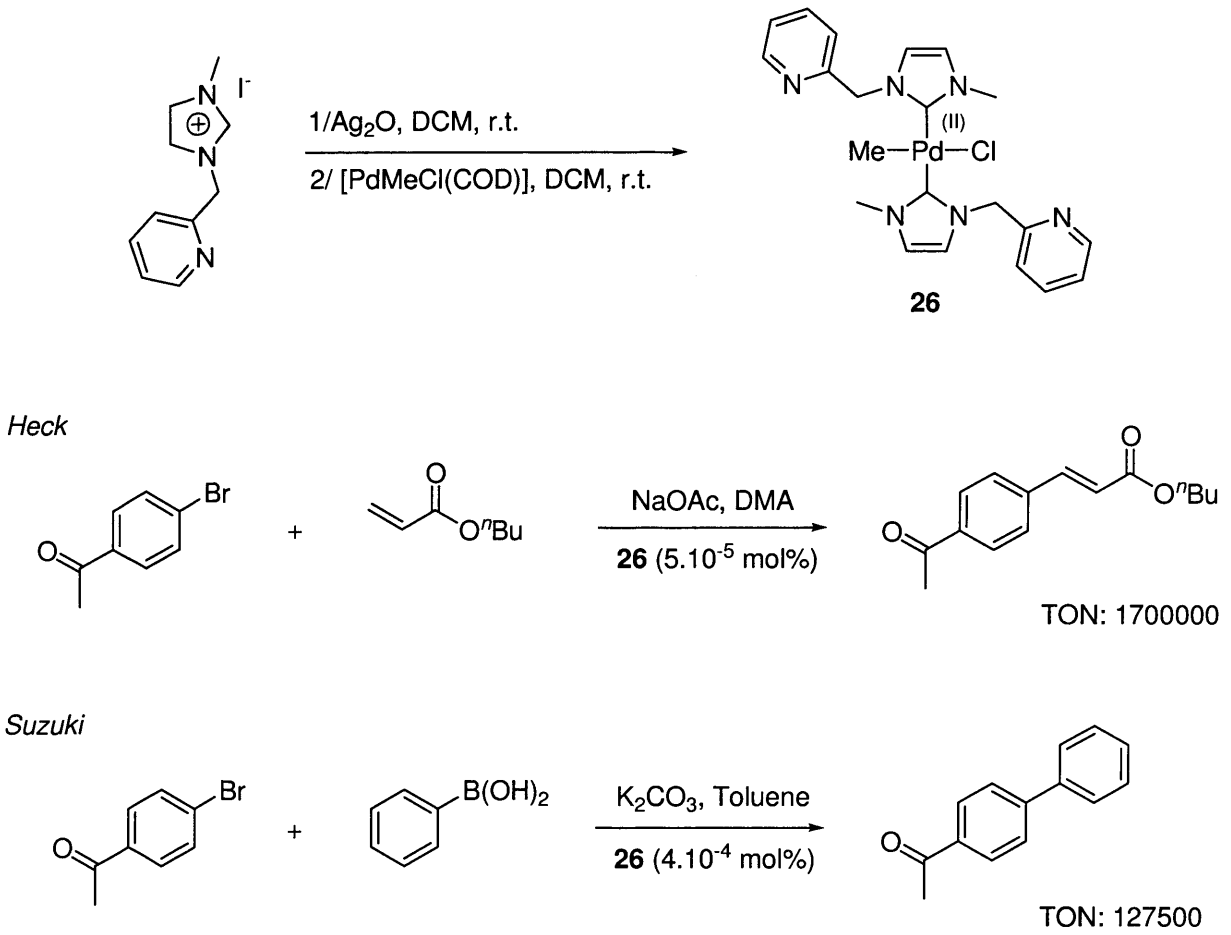

Scheme 20: *synthesis and application of a Pd(II) catalyst via Ag(I) transmetalation*

Other examples of base-mediated metalations of imidazolium salts include the synthesis of Pd(II) complexes from $Pd(OAc)_2$.[156] This reaction is akin to the well-known metalation of aromatic C-H bonds by $Pd(OAc)_2$.[157, 158]

1.2.4.2.2 Other metalation reactions

Imidazolium salts can also be used to generate NHC complexes without the need of a base. This area was pioneered by Cavell, who showed that imidazolium salts oxidatively add to group 10 metals to give metal hydrides (see Chapter 2 for detailed discussion).[20, 159-163] Later, Crabtree reported a similar reaction with Ir (***Scheme 21***).[164]

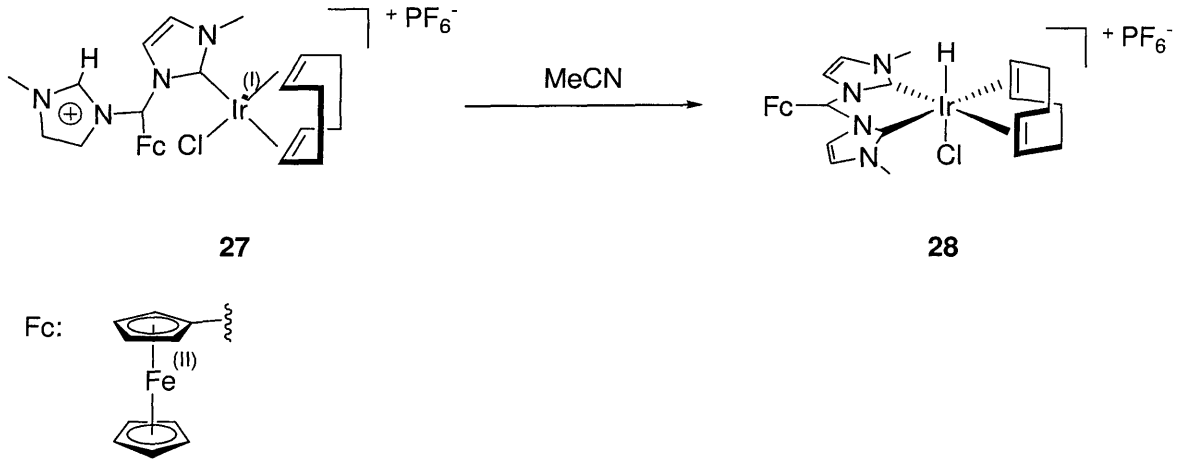

Scheme 21: *oxidative addition of an imidazolium salt to Ir(I)*

Complex **27**[165] evolves to **28** upon standing at room temperature in NMR solvents. Key to the formation of **28** are the proximity of the imidazolium C-H bond to the metal, and the electron-rich character of Ir(I) (enhanced by coordination of an NHC). Thus, for electron-rich transition metals prone to oxidative addition, this strategy can be quite successful.

A new type of imidazolium salt has recently been developed by Crabtree with the aim of providing convenient NHC precursors for NHC complexes. These zwitterionic species, which can be seen as NHC-CO_2 adducts, undergo metalation with a variety of late transition metals.[166] ***Scheme 22*** shows the synthesis of Rh(I) complex **29** using this strategy.

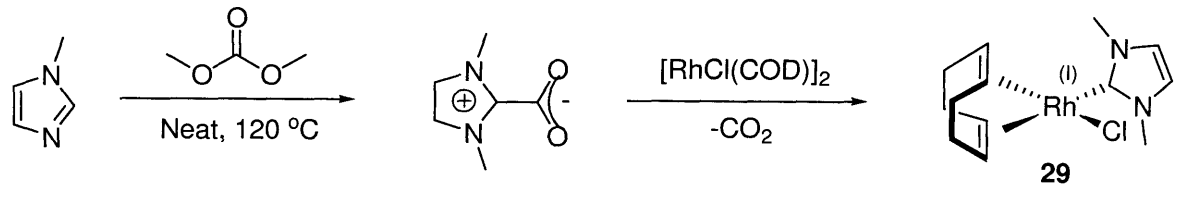

Scheme 22: *synthesis of a Rh(I) NHC complex from a zwitterionic imidazolium precursor*

Beside the use of imidazolium salts, other strategies based on the metalation of a suitable precursor exist. An early example is the use of electron-rich olefins (EROs) by Lappert.[98] ***Scheme 23*** shows the formation of Rh(I) complex **30** in which the cationic part bears a chelating saturated NHC.[167]

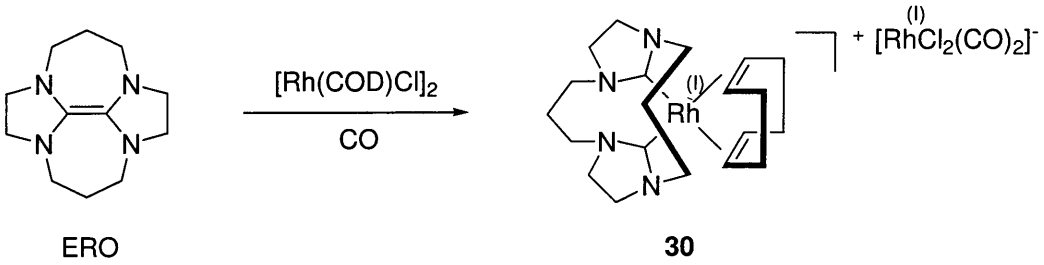

Scheme 23: *metalation of an electron-rich olefin (ERO)*

1.2.4.3 Template synthesis of NHC complexes

Template synthesis of Fischer carbene complexes (see section **1.1.7.2**) was an established method when the first free NHC was reported. This strategy relies on nucleophilic attack of a protic nucleophile on the coordinated carbon of an isocyanide (***Scheme 24***). A review of this topic was published by Hahn.[168]

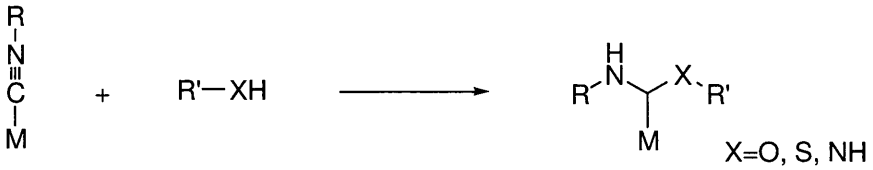

Scheme 24: *nucleophilic attack of coordinated isocyanide yielding a carbene*

With the renewed interest in NHC chemistry, template synthesis of these species is increasingly recognised as an interesting route to otherwise elusive species. For example, Hahn reported the template synthesis of **31**, a W(0) complex bearing one of the simplest NHCs of all, namely imidazolin-2-ylidene. Complex **31** can be further functionalised by alkylation of the two nitrogens to give **32** (***Scheme 25***).

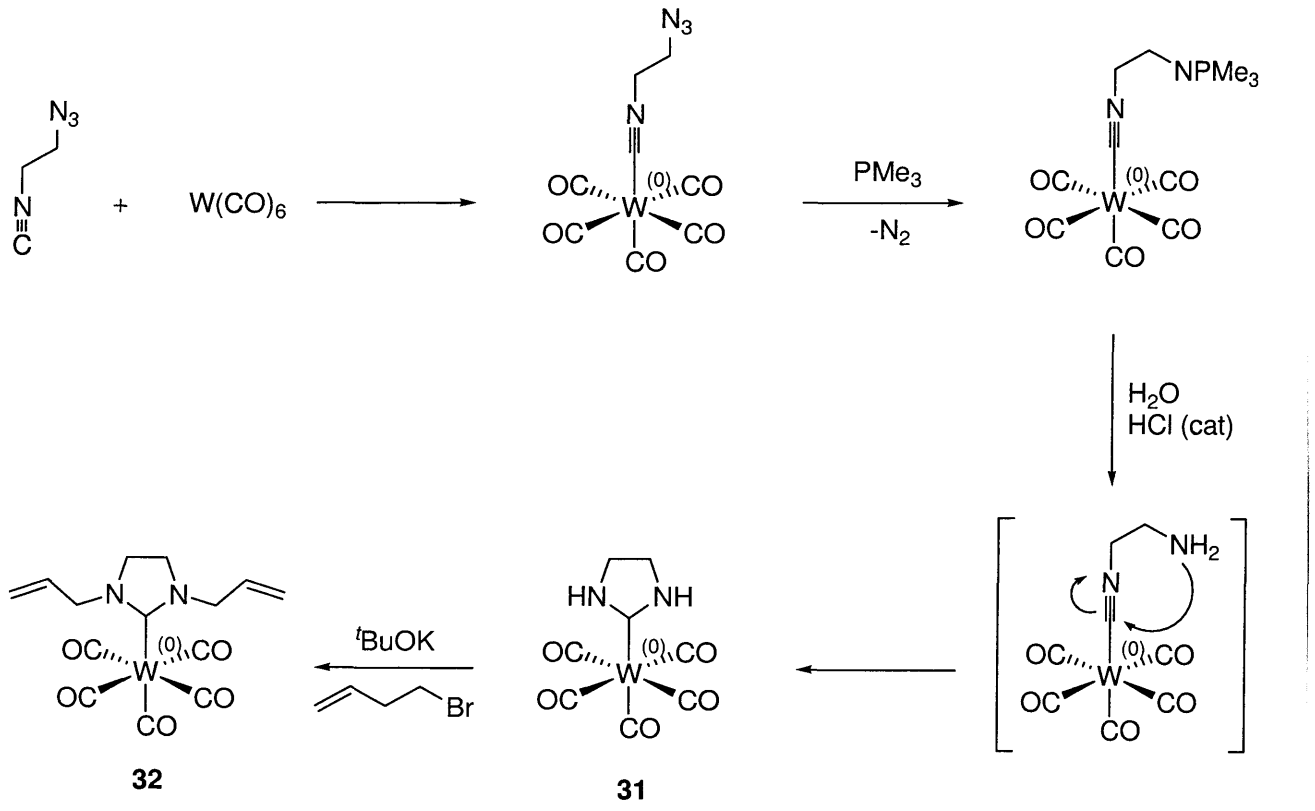

Scheme 25: *template synthesis of a W(0) NHC complex*

1.2.5 Stability of NHC complexes

Because of their ability to stabilise a great variety of metal complexes,[70, 108] and their relative inertness compared to Fischer carbenes, NHCs were rapidly applied as substitutes for phosphines in homogeneous catalysis (see section **1.1.6**).[85] NHCs generally have very high bond dissociation energies (BDE) in transition metal complexes;[99] therefore, a commonly held view is that they are spectator ligands.[1, 110, 111] However, NHC complexes sometimes display unexpected behaviour such as reductive elimination, enhanced intra- and intermolecular reactivity and even dissociation. A very comprehensive review of the stability and reactivity of NHC complexes was published by Crudden and Allen in 2004;[110] therefore the following sections only discuss the most representative examples of unexpected reactivities.

1.2.5.1 Reductive elimination of NHC complexes

Reductive elimination (see section **1.1.2.2**) to form a C-C bond is the last step of many transition metal catalysed processes (e.g. cross-coupling reactions).[1] The relative ease of this reaction is caused by the strength of the C-C bond, acting as a thermodynamic sink and allowing the reduced metal fragment to oxidatively add to another substrate and continue the catalytic cycle.[1] NHCs are C-bound ligands; therefore it is not entirely unexpected that they should reductively eliminate from complexes containing other C-bound ligands. Cavell first demonstrated that group 10 metal complexes containing NHCs and hydrocarbyl ligands (such as methyl, aryl or acyl) decomposed to yield azolium salts (***Scheme 26***).[19, 163, 169, 170]

As shown in ***Scheme 26***, Pd(II) and Ni(II) complexes **33-37** all decompose yielding C2-subsituted imidazolium salts, a process which can be exploited for the synthesis of functionalised azolium salts (see Chapters 2 and 4). Interestingly, complex **36** can either decompose directly or undergo CO insertion before decomposing. It appears that reductive elimination in NHC complexes

of group 10 metals is a very general phenomenon, and it represents a severe limitation to the use of NHCs in Ni, Pd and Pt-catalysed reactions.[169]

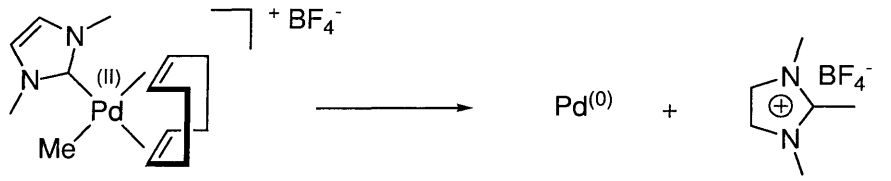

33

Ref. 170

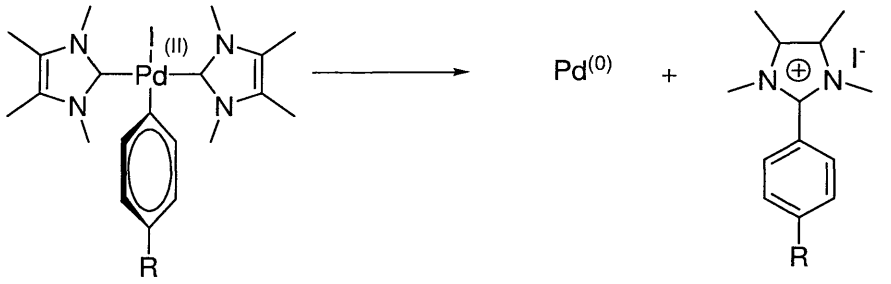

34 R= H
35 R= NO_2

Ref. 163

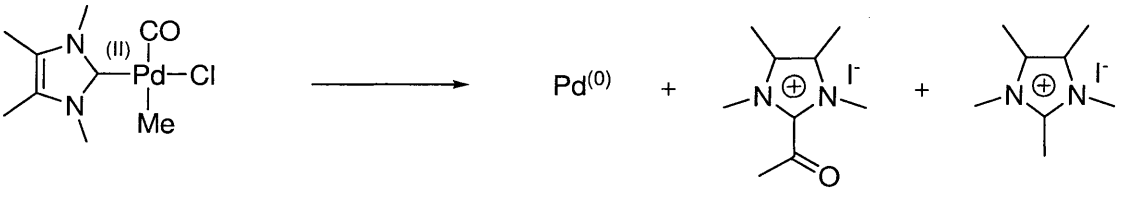

36

Ref. 155

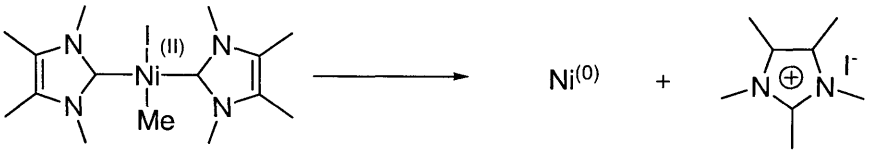

37

Ref. 163

Scheme 26: *reductive elimination of group 10 metal complexes of NHCs*[155, 163, 170]

Because of these implications for catalysis, a series of experimental and DFT studies were conducted on Pd complexes (***Scheme 27***),[19, 24, 171] with the following results:

- The mechanism of this reaction is a concerted 3-centre reductive elimination as shown in ***Scheme 27***.[19]
- The reaction is accelerated by electron-poor and/or bulky spectator ligands such as phosphites, PCy_3 or NHCs with bulky alkyl groups.[19, 171]
- Chelating ligands with small bite angles retard the reaction by destabilising the transition state and the resulting Pd(0) complex.[24]
- The barrier to elimination is lower for electronically dissimilar groups, consistent with Hartwig's work on biaryl elimination from group 10 metals (see section **1.1.2.2**).[25] Thus, CH_3^- being a strongly basic ligand, NHCs with electron releasing substituents (such as alkyl groups) are expected to be more resilient towards reductive elimination.[171]

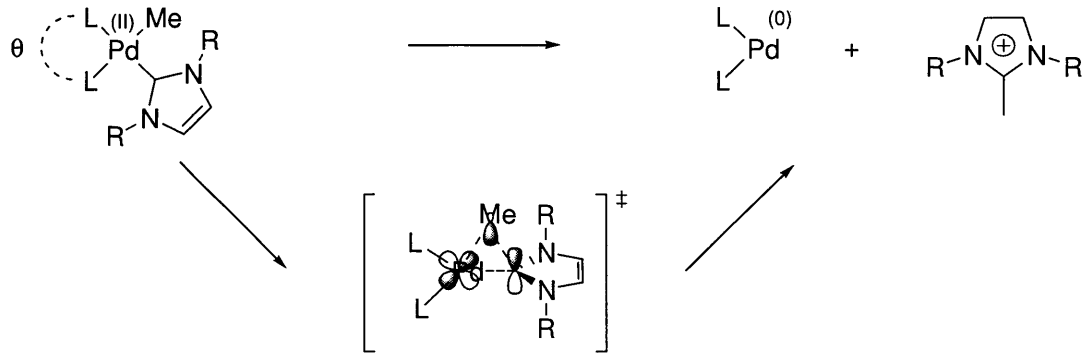

Scheme 27: *reductive elimination of Pd(II) methyl NHC complexes*

In line with this work, Cloke has recently reported several stable examples of Pd(II) complexes containing bulky NHCs and neopentyl (***Figure 21***). It would seem that the steric bulk of neopentyl prevents reductive elimination. Indeed, the energy of the transition state, with the neopentyl sitting above the carbene ring, is probably very high, hence the kinetic stability of these species.[172]

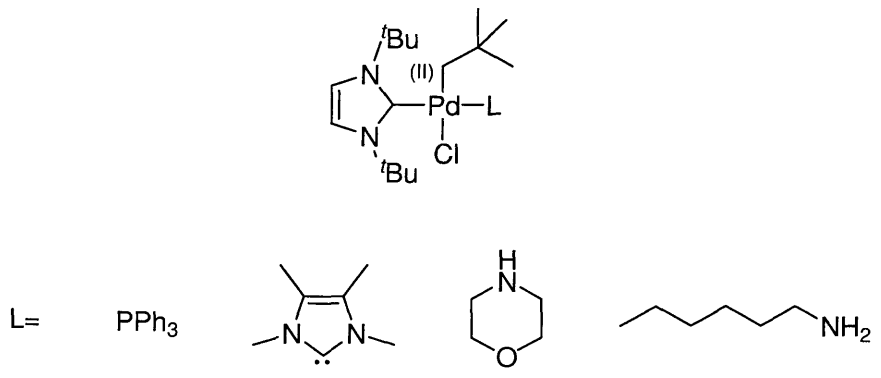

Figure 21: *examples of stable Pd(II) alkyl NHC complexes*

Other examples of reductive elimination from Pd(II) NHC complexes include a report by Grushin of reductive elimination of a Pd(II) complex containing an aryl ligand and IPr (see Chapter 4). [173] In addition, Danopoulos has reported pincer complex **38**, apparently formed by migration of Me from Pd to the NHC (***Scheme 28***), which suggests a mechanism different from the concerted reductive elimination proposed by Cavell. However this is an isolated example, in contrast with the generality observed with Cavell's examples.

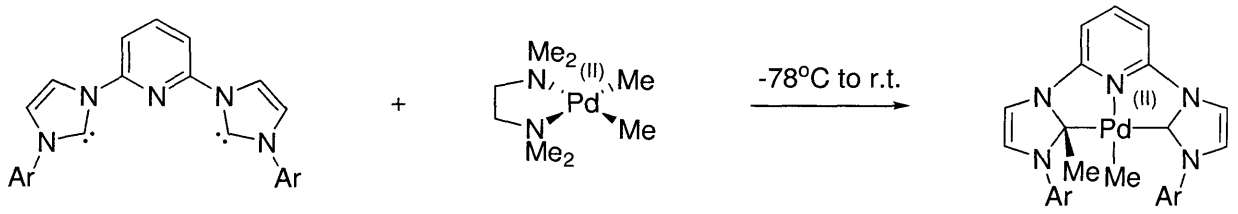

Ar= 2,6-diisopropylphenyl

38

Scheme 28: *methyl migration from Pd to an NHC*

1.2.5.2 Intra- and intermolecular bond activation by NHC complexes

The strong σ-donor properties of NHCs can significantly increase the reactivity of late transition metal complexes. For example, low-valent metals in the d^{10} (*e.g.* Pd(0)) or d^8 (*e.g.* Rh(I)) configuration can undergo oxidative addition to adopt a d^8 (*e.g.* Pd(II)) or d^6 (*e.g.* Rh(III)) configuration.[1] As discussed in section **1.2.1.1**, electron-rich ligands as well as coordinative unsaturation greatly enhance the reactivity of such metals towards oxidative addition. Therefore it is not so surprising that NHCs should promote the activation of otherwise unreactive bonds. Crudden reviewed the different examples of C-H and C-C activation promoted by NHCs in 2004.[110]

An early example of intramolecular C-H bond activation was reported by Nolan in 2000 (***Scheme 29***).[174]

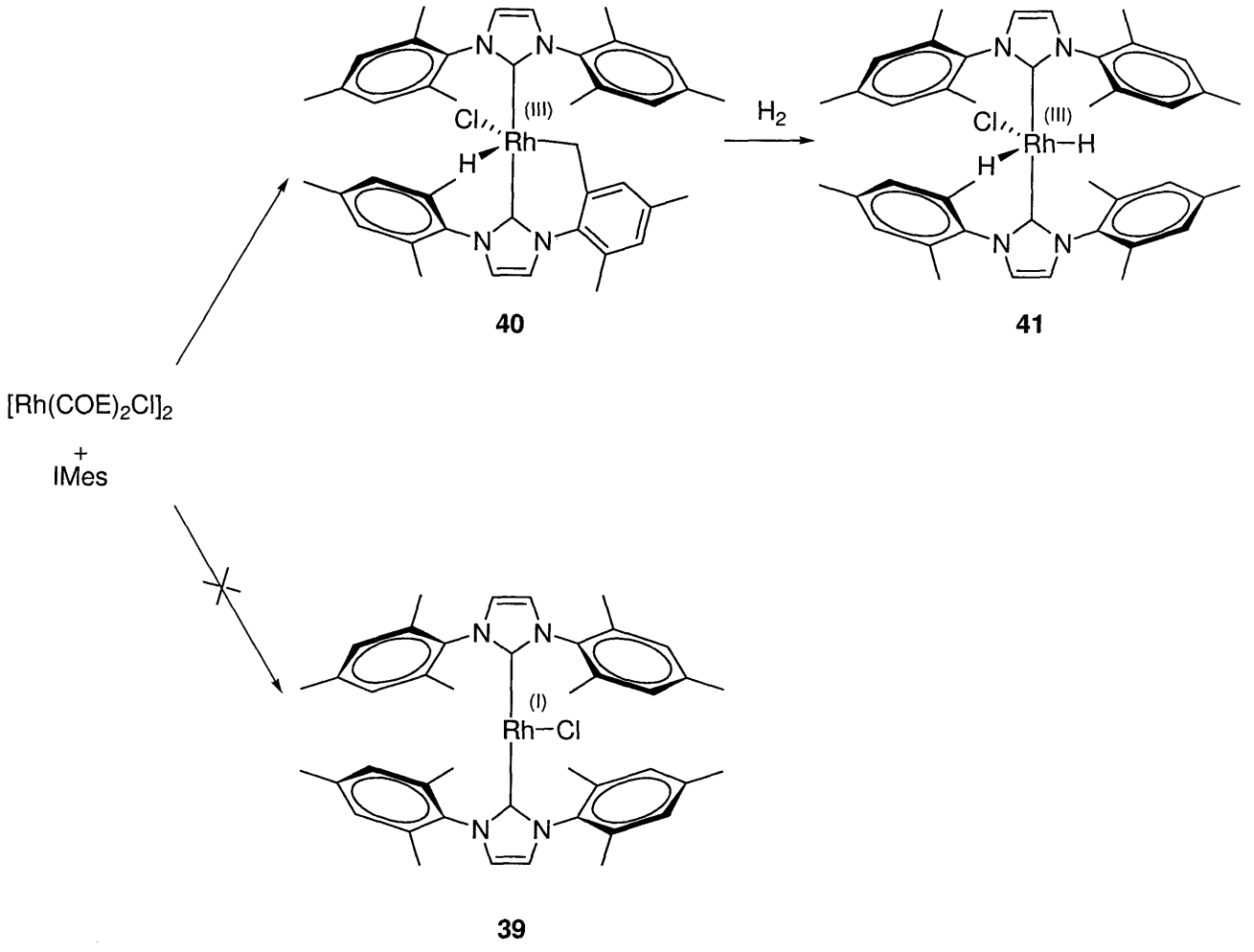

Scheme 29: *intramolecular C-H activation promoted by IMes*

In an attempt to generate coordinatively unsaturated Rh(I) complex **39**, the authors obtained Rh(III) hydride **40**, probably resulting from the oxidative addition of a benzylic C-H bond of IMes to Rh. This reaction occurred under very mild conditions at room temperature. Interestingly, hydrogenation of **39** regenerated this bond and gave Rh(III) dihydride **41**.

More recently, Cloke reported unexpected intramolecular activation of a C-N bond in a Ni(0) complex of I^{t}Bu (***Scheme 30***):[175]

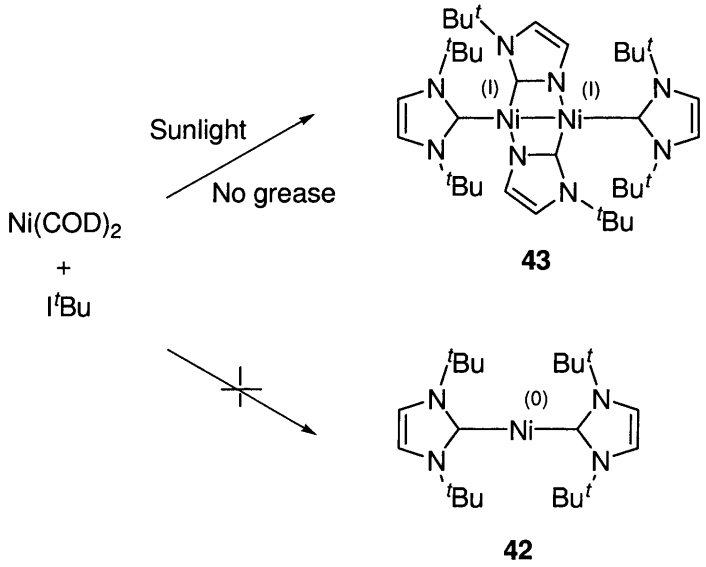

Scheme 30: *C-N activation promoted by I^tBu*

Whereas homoleptic Ni(0) complexes of IMes or IPr can be synthesised in solution from $Ni(COD)_2$ and the free NHC, compound **42** is prepared by metal vapour synthesis (MVS). In an attempt to develop a solution phase route to this compound the authors obtained **43**. The reaction, which requires sunlight, probably goes *via* an intramolecular C-H activation sequence, although no Ni-hydride was detected. In the presence of silicone grease, compound **43** is not obtained, instead an intermolecular Si-O bond activation occurs, yielding compound **44** (***Figure 22***):

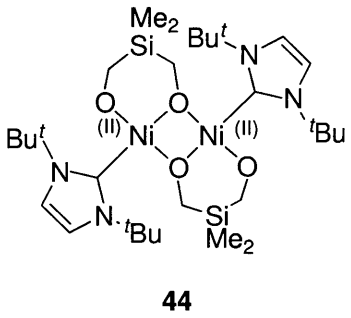

Figure 22: *product of Si-O activation promoted by I^tBu*

Finally Whittlesey has reported several cases of unexpected bond activation promoted by NHCs in Ru and Rh complexes.[100, 176-180] ***Scheme 31*** shows an intriguing example of transformation from normal to abnormal NHC followed by C-H activation in a Ru carbonyl cluster:[100]

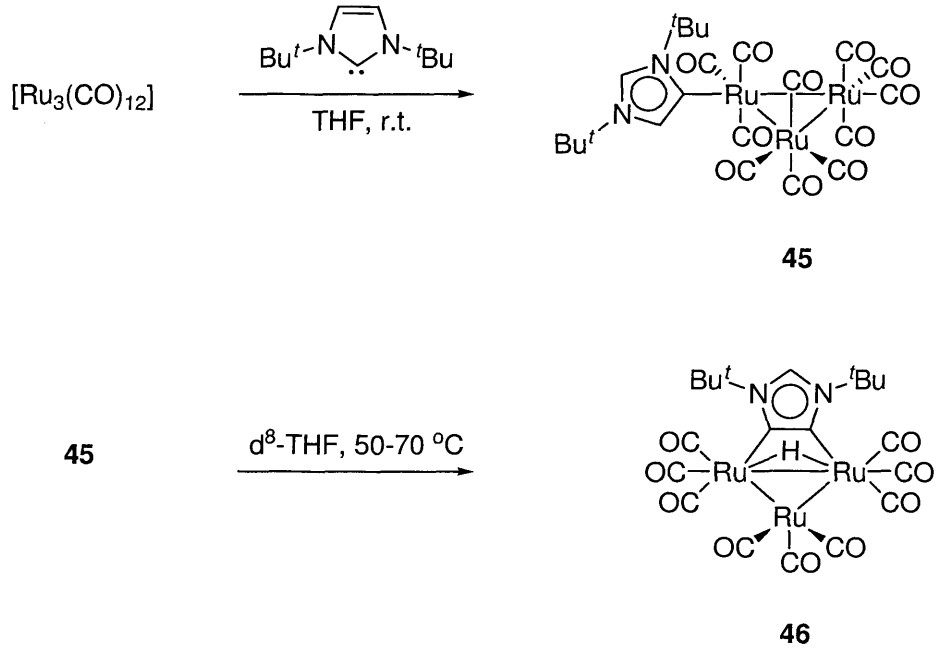

Scheme 31: *unexpected reaction sequence in an NHC Ru carbonyl cluster*

This unusual sequence is thought to arise from the high steric bulk of I'Bu, causing preferential binding at the C4 position (rather than C2) in complex **45**. This compound then undergoes C-H activation upon heating to yield hydride **46**. The high basicity of abnormal I'Bu (together with the spatial proximity of the C-H bond) is probably responsible for this reactivity.

1.2.5.3 Unexpected ligand dissociation

As discussed in section **1.1.6.2**, NHCs generally have higher bond dissociation energies than phosphines. As a consequence, a commonly held view about NHCs is that they are stable towards dissociation.[110] Whilst small NHCs such as dmiy might not dissociate easily (see Chapter 2 for example), more bulky ligands (such as I^{t}Bu) can sometimes be displaced (***Scheme 32***):

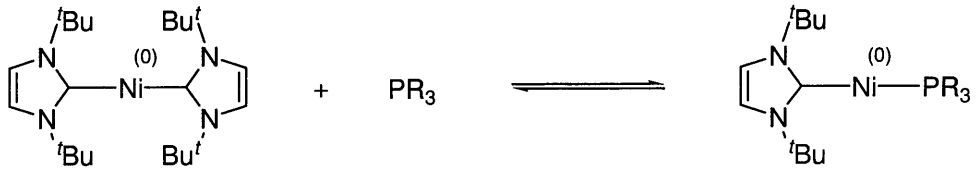

47

48 R=*o*-tolyl 33 % (16 hr, 60 °C)
49 R=Cy 100 % (15 min, r.t.)

Scheme 32: *dissociation equilibrium between I^{t}Bu* and PR_3

Compound **47** is susceptible to ligand exchange reactions with phosphines. Replacement of I^{t}Bu by bulky P(*o*-tolyl)$_3$ (complex **48**) requires elevated temperatures, but changing the phosphine to PCy_3 (a significantly less bulky ligand than I^{t}Bu or P(*o*-tolyl)$_3$, see section **1.1.6.2**, ***Table 1***) causes the equilibrium to switch towards mixed complex **49**.[181] This work indicates that NHCs can sometimes have smaller BDEs than phosphines, and more generally that the metal-NHC bond is not always completely inert. This is especially true for electron-rich, low valent metals (such as Ni(0)) in which the strong σ-donor properties of NHC may cause a preference of the metal for less electron-rich ligands such as phosphines.

1.3 Bibliography and notes

1. Crabtree, R. H., *The organometallic chemistry of the transition metals*. 3rd ed.; Wiley: New York, 2000.
2. adapted from ref. 1, page 222.
3. therefore a catalyst cannot be used to enable a thermodynamically unfavourable reaction.
4. Kozuch, S.; Shaik, S., *J. Am. Chem. Soc.* **2006,** 128, 3355-3365.
5. Kozuch, S.; Amatore, C.; Jutand, A.; Shaik, S., *Organometallics* **2005,** 24, 2319-2330.
6. Van Leeuwen, P. W. N. M., *Homogeneous catalysis*. Kluwer Academic Publishers: Dortrecht, 2004.
7. Campbell, C. T., *J. Catal.* **2004,** 204, 520-524.
8. Deprez, N. R.; Kalyani, D.; Krause, A.; Sanford, M. S., *J. Am. Chem. Soc.* **2006,** 128, 4972-4973.
9. Brown, J. M., *J. Organomet. Chem.* **2004,** 689, 4006-4015.
10. Heaton, B., *Mechanisms in homogeneous catalysis*. 1st ed.; Wiley-VCH: Weinheim, 2005.
11. Christmann, U.; Vilar, R., *Angew. Chem. Int. Ed.* **2005,** 44, 366-374.
12. oxidative addition may happen via three types of mechanisms: concerted, S_N2 and radical (see ref. 1). Only the most common concerted mechanism is discussed here.
13. Lewis, A. K. de K.; Caddick, S.; Cloke, F. G. N.; Billingham, N. C.; Hitchcock, P. B.; Leonard, J., *J. Am. Chem. Soc.* **2003,** 125, 10066-10073.
14. Galardon, E.; Ramdeehul, S.; Brown, J. M.; Cowley, A.; Hii, K. K.; Jutand, A., *Angew. Chem. Int. Ed.* **2002,** 41, 1760-1763.
15. Ahlquist, M.; Norrby, P.-O., *Organometallics* **2007,** 26, 550-553.
16. Hackett, M.; Whitesides, G. M., *J. Am. Chem. Soc.* **1988,** 110, 1449-1462.
17. Maitlis, P. M.; Haynes, A.; James, B. R.; Catellani, M.; Chiusoli, G. P., *Dalton. Trans.* **2004,** 3409-3419.
18. in the example, I^- is replaced by a molecule of solvent; therefore the complex is coordinatively saturated.
19. McGuinness, D. S.; Saendig, N.; Yates, B. F.; Cavell, K. J., *J. Am. Chem. Soc.* **2001,** 123, 4029-4040.
20. Bacciu, D.; Cavell, K. J.; Fallis, I. A.; Ooi, L.-l., *Angew. Chem. Int. Ed.* **2005,** 44, 5282-5284.
21. Jean, Y., *Molecular orbitals of transition metal complexes*. English ed.; Oxford university press: Oxford, 2005.
22. Grushin, V. V.; Marshall, W. J., *J. Am. Chem. Soc.* **2006,** 128, 12644-12645.
23. Zuidema, E.; Van Leeuwen, P. W. N. M.; Bo, C., *Organometallics* **2005,** 24, 3703-3710.
24. Graham, D. C.; Cavell, K. J.; Yates, B. F., *Dalton. Trans.* **2005**, 1093-1100.
25. Shekhar, S.; Hartwig, J. F., *J. Am. Chem. Soc.* **2004,** 126, 13016-13027.
26. Knowles, J. P.; Whiting, A., *Organic & Biomolecular Chemistry* **2007,** 5, 31-44.
27. Amatore, C.; Godin, B.; Jutand, A.; Lemaître, F., *Chem.Eur.J.* **2007,** 13, 2002-2011.
28. Littke, A. F.; Fu, G. C., *J. Am. Chem. Soc.* **2001,** 123, 6989-7000.
29. Cramer, R.; Lindsey, R. V., *J. Am. Chem. Soc.* **1966,** 88, 3534-3544.
30. Wass, D. F., *Dalton Transactions* **2007**, 816-819.
31. Speiser, F.; Braunstein, P.; Saussine, L., *Acc. Chem. Res.* **2005,** 38, 784-793.
32. Carter, A.; Cohen, S. A.; Cooley, N. A.; Murphy, A.; Scutt, J.; Wass, D. F., *Chem. Commun.* **2002**, 858-859.
33. Peuckert, M.; Keim, W., *Organometallics* **1983,** 2, 594-597.

34. Hadei, N.; Kantchev, E. H. B.; O'Brien, C. J.; Organ, M. G., *J. Org. Chem.* **2005,** 70, 8503-8507.
35. Hadei, N.; Kantchev, E. A. B.; O'Brien, C. J.; Organ, M. G., *Org. Lett.* **2005,** 7, 3805-3807.
36. Netherton, M. R.; Dai, C.; Neuschutz, K.; Fu, G. C., *J. Am. Chem. Soc.* **2001,** 123, 10099-10100.
37. Andrus, M. B.; Song, C., *Org. Lett.* **2001,** 3, 3761-3764.
38. Ketz, B. E.; Ottenwaelder, X. G.; Waymouth, R. M., *Chem. Commun.* **2005**, 5693-5695.
39. Li, W.; Sun, H.; Chen, M.; Wang, Z.; Hu, D.; Shen, Q.; Zhang, Y., *Organometallics* **2005,** 24, 5925-5928.
40. Alt, H. G.; Koppl, A., *Chem. Rev.* **2000,** 100, 1205-1222.
41. Johnson, L. K.; Killian, C. M.; Brookhart, M., *J. Am. Chem. Soc.* **1995,** 117, 6414-6415.
42. McKinney, R. J.; Roe, D. C., *J. Am. Chem. Soc.* **1986,** 108, 5167-5173.
43. Shultz, C. S.; DeSimone, J.; Brookhart, M., *Organometallics* **2001,** 20, 16-18.
44. β-alkyl elimination is thermodynamically and kinetically less favourable than β-hydride elimination; therefore only the latter is an issue, see ref. 1.
45. Clarke, M. L.; Ellis, D.; Mason, K. L.; Orpen, A. G.; Pringle, P. G.; Wingad, R. L.; Zaher, D. A.; Baker, R. T., *Dalton Trans.* **2005**, 1294-1300.
46. Tucci, E. R., *Ind. Eng. Chem. Prod. Res. Develop.* **1970,** 9, 516-521.
47. Keith, J. A.; Oxgaard, J.; Goddard, W. A. III., *J. Am. Chem. Soc.* **2006,** 128, 3132-3133.
48. Baeckvall, J. E.; Akermark, B.; Ljunggren, S. O., *J. Am. Chem. Soc.* **1979,** 101, 2411-2416.
49. Stille, J. K.; Divakaruni, R., *J. Am. Chem. Soc.* **1978,** 100, 1303-1304.
50. Siegbahn, P. E. M., *J. Am. Chem. Soc.* **1995,** 117, 5409-5410.
51. Musco, A., *J. Chem. Soc. Perkin. Trans. 1* **1980**, 693-698.
52. Schrock, R. R., *Angew. Chem. Int. Ed.* **2006,** 45, 3748-3759.
53. Grubbs, R. H., *Angew. Chem. Int. Ed.* **2006,** 45, 3760-3765.
54. Chauvin, Y., *Angew. Chem. Int. Ed.* **2006,** 45, 3740-3747.
55. Sharpless, K. B., *Angew. Chem. Int. Ed.* **2002,** 41, 2024-2032.
56. Noyori, R., *Angew. Chem. Int. Ed.* **2002,** 41, 2008-2022.
57. Knowles, W. S., *Angew. Chem. Int. Ed.* **2002,** 41, 1998-2007.
58. Marion, N.; Navarro, O.; Mei, J.; Stevens, E. D.; Scott, N. M.; Nolan, S. P., *J. Am. Chem. Soc.* **2006,** 128, 4101-4111.
59. Buchwald, S. L.; Mauger, C.; Mignani, G.; Scholz, U., *Adv. Synth. Cat.* **2006,** 348, 23-39.
60. Blaser, H.-U.; Indolese, A.; Naud, F.; Nettekoven, U.; Schnyder, A., *Adv. Synth. Cat.* **2004,** 346, 1583-1598.
61. Farina, V., *Adv. Synth. Cat.* **2004,** 346, 1519-1521.
62. Farina, V., *Adv. Synth. Cat.* **2004,** 346, 1553-1582.
63. Catellani, M.; Motti, E.; Ca', N. D.; Ferraccioli, R., *Eur. J. Org. Chem.* **2007**, 4153-4165.
64. Barry, M. T., *Angew. Chem. Int. Ed.* **1995,** 34, 259-281.
65. Ohta, T.; Takaya, H.; Kitamura, M.; Nagai, K.; Noyori, R., *J. Org. Chem.* **1987,** 52, 3174-3176.
66. arrows indicate the hydrogenated bonds and stars indicate the resulting asymmetric carbon atoms.
67. Nicolaou, K. C.; Bulger, P. G.; Sarlah, D., *Angew. Chem. Int. Ed.* **2005,** 44, 4490-4527.
68. Funk, T. W.; Berlin, J. M.; Grubbs, R. H., *J. Am. Chem. Soc.* **2006,** 128, 1840-1846.
69. Nicola, T.; Brenner, M.; Donsbach, K.; Kreye, P., *Org. Proc. Res. Dev.* **2005,** 9, 513-515.
70. Bourissou, D.; Guerret, O.; Gabbai, F. P.; Bertrand, G., *Chem. Rev.* **2000,** 100, 39-91.
71. Igau, A.; Grutzmacher, H.; Baceiredo, A.; Bertrand, G., *J. Am. Chem. Soc.* **1988,** 110, 6463-6466.
72. Arduengo, A. J.; Harlow, R. L.; Kline, M., *J. Am. Chem. Soc.* **1991,** 113, 361-363.
73. adapted from ref 76.

74. Hahn, F. E., *Angew. Chem. Int. Ed.* **2006,** 45, 1348-1352.
75. Wolfgang, K., *Angew. Chem. Int. Ed.* **2004,** 43, 1767-1769.
76. Canac, Y.; Soleilhavoup, M.; Conejero, S.; Bertrand, G., *J. Organomet. Chem.* **2004,** 689, 3857-3865.
77. Kato, T.; Gornitzka, H.; Baceiredo, A.; Savin, A.; Bertrand, G., *J. Am. Chem. Soc.* **2000,** 122, 998-999.
78. Arduengo, A. J. III.; Dias, H. V. R.; Harlow, R. L.; Kline, M., *J. Am. Chem. Soc.* **1992,** 114, 5530-5534.
79. Sole, S.; Gornitzka, H.; Schoeller, W. W.; Bourissou, D.; Bertrand, G., *Science* **2001,** 292, 901-902.
80. Despagnet, E.; Gornitzka, H.; Rozhenko, A. B.; Schoeller, W. W.; Bourissou, D.; Bertrand, G., *Angew. Chem. Int. Ed.* **2002,** 41, 2835-2838.
81. also referred to as "push-pull" effect.
82. Ofele, K., *J. Organomet. Chem.* **1968,** 12, P42-P43.
83. H.-W. Wanzlick, H. J. S., *Angew. Chem. Int. Ed.* **1968,** 7, 141-142.
84. commonly referred to as "unsaturated" NHCs.
85. Herrmann, W. A., *Angew. Chem. Int. Ed.* **2002,** 41, 1290-1309.
86. Arduengo III, A. J.; Harlow, R. L.; Kline, M., *J. Am. Chem. Soc.* **1991,** 113, 361.
87. Tubaro, C.; Biffis, A.; Basato, M.; Benetollo, F.; Cavell, K. J.; Ooi, L., *Organometallics* **2005,** 24, 4153-4158.
88. Calò, V.; Nacci, A.; Monopoli, A., *J. Organomet. Chem.* **2005,** 690, 5458-5466.
89. Huynh, H. V.; Meier, N.; Pape, T.; Hahn, F. E., *Organometallics* **2006,** 25, 3012-3018.
90. Doris, K., *Angew. Chem. Int. Ed.* **2007,** 46, 3405-3408.
91. Schneider, S. K.; Julius, G. R.; Loschen, C.; Raubenheimer, H. G.; Frenking, G.; Herrmann, W. A., *Dalton. Trans.* **2006**, 1226-1233.
92. Alcazaro, M.; Roseblade, S. J.; Cowley, A. R.; Fernández, R.; Brown, J. M.; Lassaletta, J. M., *J. Am. Chem. Soc.* **2005,** 127, 3290-3291.
93. Albrecht, M.; Stoeckli-Evans, H., *Chem. Commun.* **2005**, 4705-4707.
94. Owen, J. S.; Labinger, J. A.; Bercaw, J. E., *J. Am. Chem. Soc.* **2004,** 126, 8247-8255.
95. Huynh, H. V.; Holtgrewe, C.; Pape, T.; Koh, L. L.; Hahn, E., *Organometallics* **2006,** 25, 245-249.
96. Jazzar, R.; Liang, H.; Donnadieu, B.; Bertrand, G., *J. Organomet. Chem.* **2006,** 691, 3201-3205.
97. some of these compounds have not been isolated as free species, but metal complexes bearing them were reported.
98. Lappert, M. F., *J. Organomet. Chem.* **2005,** 690, 5467-5473.
99. Dorta, R.; Stevens, E. D.; Scott, N. M.; Costabile, C.; Cavallo, L.; Hoff, C. D.; Nolan, S. P., *J. Am. Chem. Soc.* **2005,** 127, 2485-2495.
100. Ellul, C. E.; Mahon, M. F.; Saker, O.; Whittlesey, M. K., *Angew. Chem. Int. Ed.* **2007,** 46, 6343-6345.
101. Lebel, H.; Janes, M. K.; Charette, A. B.; Nolan, S. P., *J. Am. Chem. Soc.* **2004,** 126, 5046-5047.
102. Chianese, A. R.; Kovacevic, A.; Zeglis, B. M.; Faller, J. W.; Crabtree, R. H., *Organometallics* **2004,** 23, 2461-2468.
103. Appelhans, L. N.; Zuccaccia, D.; Kovacevic, A.; Chianese, A. R.; Miecznikowski, J. R.; Macchioni, A.; Clot, E.; Eisenstein, O.; Crabtree, R. H., *J. Am. Chem. Soc.* **2005,** 127, 16299-16311.
104. Han, Y.; Huynh, H. V., *Chem. Commun.* **2007**, 1089-1091.
105. free abnormal NHCs and remote NHCs have not yet been isolated; therefore they have only been observed as ligands bound to transition metals.
106. Fischer, E. O.; Maasböl, A., *Angew. Chem. Int. Ed.* **1964,** 3, 580-581.

107. Schrock, R. R., *J. Am. Chem. Soc.* **1974,** 96, 6796-6797.
108. Herrmann, W. A.; Köcher, C., *Angew. Chem. Int. Ed.* **1997,** 36, 2162-2187.
109. Herrmann, W. A.; Ofele, K.; Elison, M.; Kuhn, F. E.; Roesky, P. W., *J. Organomet. Chem.* **1994,** 480, C7-C9.
110. Crudden, C. M.; Allen, D. P., *Coord. Chem. Rev.* **2005,** 248, 2247-2273.
111. Crabtree, R. H., *J. Organomet. Chem.* **2005,** 690, 5451-5457.
112. Caddick, S.; Cloke, F. G. N.; Hitchcock, P. B.; Leonard, J.; Lewis, A. K. d. K.; McKerrecher, D.; Titcomb, L. R., *Organometallics* **2002,** 21, 4318-4319.
113. Caddick, S.; Cloke*, F. G. N.; Clentsmith, G. K. B.; Hitchcock, P. B.; McKerrecher, D.; Titcomb, L. R.; Williams, M. R. V., *J. Organomet. Chem.* **2001,** 617-618, 635-639.
114. Diez-Gonzalez, S.; Nolan, S. P., *Coord. Chem. Rev.* **2007,** 251, 874-883.
115. Cavallo, L.; Correa, A.; Costabile, C.; Jacobsen, H., *J. Organomet. Chem.* **2005,** 690, 5407-5413.
116. Hillier, A. C.; Sommer, W. J.; Yong, B. S.; Petersen, J. L.; Cavallo, L.; Nolan, S. P., *Organometallics* **2003,** 22, 4322-4326.
117. Magill, A. M.; Cavell, K. J.; Yates, B. F., *J. Am. Chem. Soc.* **2004,** 126, 8717-8724.
118. Tolman, C. A., *J. Am. Chem. Soc.* **1970,** 92, 2953-2956.
119. Perrin, L.; Clot, E.; Eisenstein, O.; Loch, J.; Crabtree, R. H., *Inorg. Chem.* **2001,** 40, 5806-5811.
120. Tolman, C. A., *Chem. Rev.* **1977,** 77, 313-348.
121. Tolman, C. A., *J. Am. Chem. Soc.* **1970,** 92, 2956-2965.
122. for non-symmetrical phosphines and those with a cone angle superior to 180 °, slightly more sophisticated methods are used to calculate θ, see ref. 121.
123. Dorta, R.; Stevens, E. D.; Hoff, C. D.; Nolan, S. P., *J. Am. Chem. Soc.* **2003,** 125, 10490-10491.
124. adapted from ref. 99.
125. Hills, I. D.; Fu, G. C., *J. Am. Chem. Soc.* **2004,** 126, 13178-13179.
126. Hills, I. D.; Netherton, M. R.; Fu, G. C., *Angew. Chem. Int. Ed.* **2003,** 42, 5749-5752.
127. Netherton, M. R.; Fu, G. C., *Org. Lett.* **2001,** 3, 4295-4298.
128. Arduengo III, A. J.; Gamper, S. F.; Calabrese, J. C.; Davidson, F., *J. Am. Chem. Soc.* **1994,** 116, 4391-4394.
129. Green, J. C.; Scurr, R. G.; Arnold, P. L.; Cloke, G. N., *Chem. Commun.* **1997**, 1963-1964.
130. the NHCs in this work were 1,3-di(*tert*butyl)imidazol-2-ylidene and 1,3-dihydroimidazol-2-ylidene.
131. this work has been cited 49 times since its publication, and in all major reviews on NHCs since 1997. source: ISI Web of Knowledge™.
132. Nemcsok, D.; Wichmann, K.; Frenking, G., *Organometallics* **2004,** 23, 3640-3646.
133. Boehme, C.; Frenking, G., *Organometallics* **1998,** 17, 5801-5809.
134. Hu, X.; Castro-Rodriguez, I.; Olsen, K.; Meyer, K., *Organometallics* **2004,** 23, 755-764.
135. Termaten, A. T.; Schakel, M.; Ehlers, A. W.; Lutz, M.; Spek, A. L.; Lammertsma, K., *Chem. Eur. J.* **2003,** 9, 3577-3582.
136. Hu, X.; Tang, Y.; Gantzel, P.; Meyer, K., *Organometallics* **2003,** 22, 612-614.
137. Deubel, D. V., *Organometallics* **2002,** 21, 4303-4305.
138. Jacobsen, H.; Correa, A.; Costabile, C.; Cavallo, L., *J. Organomet. Chem.* **2006,** 691, 4350-4358.
139. Maron, L.; Bourissou, D., *Organometallics* **2007,** 26, 1100-1103.
140. Mungur, S. A.; Blake, A. J.; Wilson, C.; McMaster, J.; Arnold, P. L., *Organometallics* **2006,** 25, 1861-1867.
141. Niehues, M.; Erker, G.; Kehr, G.; Schwab, P.; Fröhlich, R., *Organometallics* **2002,** 21, 2905-2911.

142. Scott, N. M.; Dorta, R.; Stevens, E. D.; Correa, A.; Cavallo, L.; Nolan, S. P., *J. Am. Chem. Soc.* **2005,** 127, 3516-3526.
143. Manfred, R., *Angew. Chem. Int. Ed.* **1996,** 35, 725-728.
144. Herrmann, W. A.; Köcher, C.; Gooßen, L. J.; Artus, G. R. J., *Chem.Eur.J.* **1996,** 2, 1627-1636.
145. KHMDS usually give better results with less acidic imidazolium salts. D.J. Beetstra, personal communication.
146. Cattoën, X.; Bourissou, D.; Bertrand, G., *Tetrahedron Lett.* **2006,** 47, 531-534.
147. Navarro, O.; Nolan, S., *Synthesis* **2006**, 366-367.
148. Kuhn, N.; Kratz, T., *Synthesis* **1993**, 561-562.
149. Mery, D.; Aranzaes, J. R.; Astruc, D., *J. Am. Chem. Soc.* **2006,** 128, 5602-5603.
150. Denk, M. K.; Hezarkhani, A.; Zheng, F.-L., *Eur. J. Inorg. Chem.* **2007,** 2007, 3527-3534.
151. Wang, H. M. J.; Lin, I. J. B., *Organometallics* **1998,** 17, 972-975.
152. Chen, W.; Liu, F., *J. Organomet. Chem.* **2003,** 673, 5-12.
153. **10** is light sensitive though.
154. Garrison, J. C.; Youngs, W. J., *Chem. Rev.* **2005,** 105, 3978-4008.
155. McGuinness, D. S.; Cavell, K. J., *Organometallics* **2000,** 19, 741-748.
156. Herrmann, W. A.; Elison, M.; Fischer, J.; Kocher, C.; Artus, G. R. J., *Angew. Chem. Int. Ed.* **1995,** 34, 2371-2375.
157. Zaitsev, V. G.; Shabashov, D.; Daugulis, O., *J. Am. Chem. Soc.* **2005,** 127, 13154-13155.
158. Davies, D. L.; Donald, S. M. A.; Macgregor, S. A., *J. Am. Chem. Soc.* **2005,** 127, 13754-13755.
159. Hawkes, K. J.; McGuinness, D. S.; Cavell, K. J.; Yates, B. F., *Dalton. Trans.* **2004**, 2505-2513.
160. Clement, N. D.; Cavell, K. J.; Jones, C.; Elsevier, C. J., *Angew. Chem. Int. Ed.* **2004,** 43, 1277-1279.
161. McGuinness, D. S.; Cavell, K. J.; Yates, B. F.; Skelton, B. W.; White, A. H., *J. Am. Chem. Soc.* **2001,** 123, 8317-8328.
162. McGuinness, D. S.; Cavell, K. J.; Yates, B. F., *Chem. Commun.* **2001**, 355-356.
163. McGuinness, D. S.; Cavell, K. J.; Skelton, B. W.; White, A. H., *Organometallics* **1999,** 18, 1596-1605.
164. Viciano, M.; Mas-Marzá, E.; Poyatos, M.; Sanaú, M.; Crabtree, R. H.; Peris, E., *Angew. Chem. Int. Ed.* **2005,** 44, 444-447.
165. obtained by base-mediated metalation of a chelating imidazolium salt, see previous section.
166. Voutchkova, A. M.; Appelhans, L. N.; Chianese, A. R.; Crabtree, R. H., *J. Am. Chem. Soc.* **2005,** 127, 17624-17625.
167. Hitchcock, P. B.; Lappert, M. F.; Terreros, P.; Wainwright, K. P., *J. Chem. Soc. Chem. Commun.* **1980**, 1180-1182.
168. Tamm, M.; Ekkehardt Hahn, F., *Coord. Chem. Rev.* **1999,** 182, 175-209.
169. Cavell, K. J.; McGuinness, D. S., *Coord. Chem. Rev.* **2004,** 248, 671-679.
170. McGuinness, D. S.; Green, M. J.; Cavell, K. J.; Skelton, B. W.; White, A. H., *J. Organomet. Chem.* **1998,** 565, 165-178.
171. Graham, D. C.; Cavell, K. J.; Yates, B. F., *Dalton. Trans.* **2006**, 1768-1775.
172. Esposito, O.; Lewis, A. K. de K.; Hitchcock, P. B.; Caddick, S.; Cloke, F. G. N., *Chem. Commun.* **2007**, 1157-1159.
173. Marshall, W. J.; Grushin, V. V., *Organometallics* **2003,** 22, 1591-1593.
174. Huang, J.; Stevens, E. D.; Nolan, S. P., *Organometallics* **2000,** 19, 1194-1197.
175. Caddick, S.; Cloke, F. G. N.; Hitchcock, P. B.; Lewis, A. K. d. K., *Angew. Chem. Int. Ed.* **2004,** 43, 5824-5827.

176. Burling, S.; Mahon, M. F.; Powell, R. E.; Whittlesey, M. K.; Williams, J. M. J., *J. Am. Chem. Soc.* **2006,** 128, 13702-13703.
177. Diggle, R. A.; Macgregor, S. A.; Whittlesey, M. K., *Organometallics* **2004,** 23, 1857-1865.
178. Burling, S.; Mahon, M. F.; Paine, B. M.; Whittlesey, M. K.; Williams, J. M. J., *Organometallics* **2004,** 23, 4537-4539.
179. Chilvers, M. J.; Jazzar, R. F. R.; Mahon, M. F.; Whittlesey, M. K., *Adv. Synth. Cat.* **2003,** 345, 1111-1114.
180. Jazzar, R. F. R.; Macgregor, S. A.; Mahon, M. F.; Richards, S. P.; Whittlesey, M. K., *J. Am. Chem. Soc.* **2002,** 124, 4944-4945.
181. Titcomb, L. R.; Caddick, S.; Cloke, F. G. N.; Wilson, D. J.; McKerrecher, D., *Chem. Commun.* **2001**, 1388-1389.

2 Chapter two: C2-Alkenylation of Azolium Salts and Activated Azoles Catalysed by Ni and Pd

2.1 Background (previous work, related reactions)

This chapter describes the application of redox reactions of NHC complexes of Ni and Pd to the C2-functionalisation of imidazolium salts and related compounds (***Figure 1***).

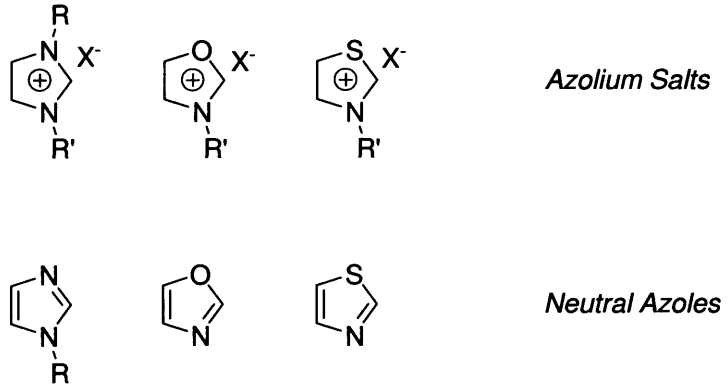

Figure 1: *some azolium salts and neutral azole heterocycles*

2.1.1 Oxidative addition of imidazolium salts to late transition metals yielding NHC metal hydrides

Whilst in general, NHC complexes are considered to be very stable species, due to the high bond dissociation energies (BDE) of NHCs,[1] previous work in the Cavell group has shown that Pd- and Ni-hydrocarbyl complexes of NHCs readily decompose by reductive elimination to yield 2-substituted imidazolium salts.[2-5] Subsequent studies demonstrated that the "reverse" reaction (*i.e.*

oxidative addition of imidazolium salts to zerovalent group 10 metals) is also possible.[4, 6-10] ***Scheme 1*** illustrates this relationship between NHC complexes and imidazolium salts.

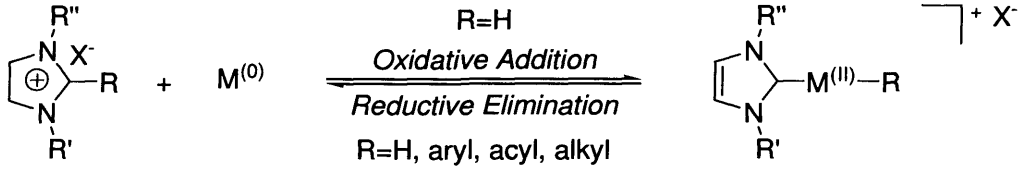

Scheme 1: *redox reactions of group 10 metals involving imidazolium salts and NHCs*

A feature of this oxidative addition chemistry is the use of what is effectively an imidazolium based ionic liquid (IL), to directly form metal carbene hydride complexes. It is a well-known fact that ILs can generate NHCs under basic reaction conditions,[11-14] but until this seminal work, there was no evidence that NHC complexes formed without the need of a base. Carbene-metal-hydride complexes were first isolated for Pt[9, 15] and then subsequently for Ni and Pd (***Figure 2***).[4, 8]

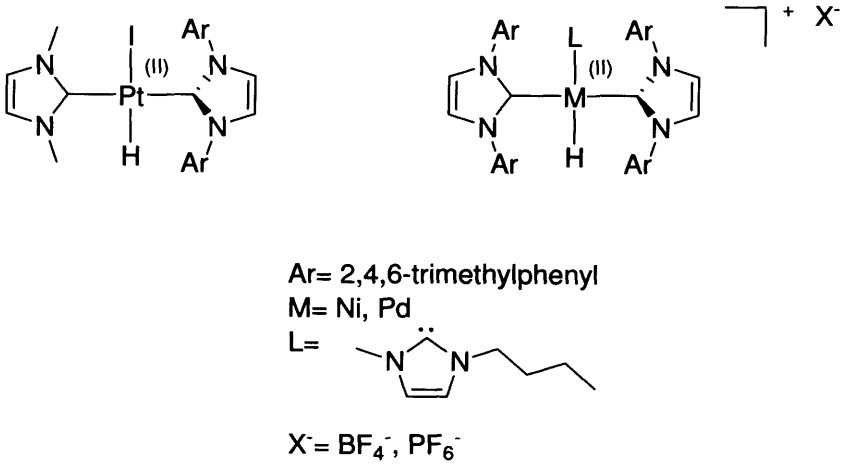

Figure 2: *group 10 metal hydride/NHC complexes isolated by direct oxidative addition of imidazolium salts.*[8, 15]

More recently, Crabtree reported the isolation of an Ir hydride starting from $[Ir(COD)Cl]_2$ and an imidazolium salt with the help of a base. Interestingly, the Rh analogue of this complex could not be obtained.[16] In addition, Finke published a study in which an imidazolium salt underwent reversible oxidative addition to colloidal $Ir^{(0)}$.[17] Finally, Cavell and Yates conducted a theoretical study of the oxidative addition of imidazolium salts to Rh(I), and found that the resulting hydrides would probably decompose by reductive elimination.[7] These results indicate that group 9 metal hydrides formed by oxidative addition of imidazolium salts are generally less stable than their group 10 metal counterparts.

These features of imidazolium salts and NHCs (*i.e.* the ability to undergo oxidative addition/reductive elimination) make the former potential substrates for metal-catalysed functionalisation at the C2 position. It is also worth noting that in recent years, so-called "abnormal" NHCs have emerged as ligands for transition metals.[4, 18, 19] These species are based on the imidazole ring, like their "normal" counterparts, but due to geometrical constraints or blocking of the C2 position, they bind at the C4 or C5 position. Work in the Cavell group has shown that they are also susceptible to the same type of redox processes as normal NHCs.[4] This is likely to open new opportunities for the functionalisation of the imidazole core at the C4 or C5 position.

2.1.2 Heterocycle functionalisation proceeding *via* NHC complexes

Nitrogen-containing heterocycles usually bind to transition metals by the nitrogen atom. However, Taube showed some *32 years ago* (long before the term "N-heterocyclic carbene" was first coined) that the caffeine ligand in xanthine ruthenium ammine complexes binds by a carbon atom. Thus, a Ru(III) NHC complex (***Figure 3***) was isolated and characterized by X-ray crystallography.[20] The chloride ligand *trans* to caffeine was found to be much more labile than the *cis* one, as one would expect from the σ-donor properties of NHCs.

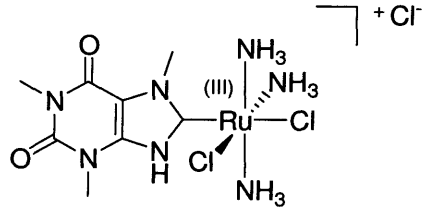

Figure 3: *C-bound caffeine in a Ru(III) complex*[20]

Later, Crabtree and Eisenstein studied the binding of transition metal complexes of imidazole by DFT.[21] Their work stemmed from Taube's observation that imidazole is a *free imidazol-2-ylidene tautomer*. Thus, NHC complexes are imidazole complex tautomers (***Scheme 2***).

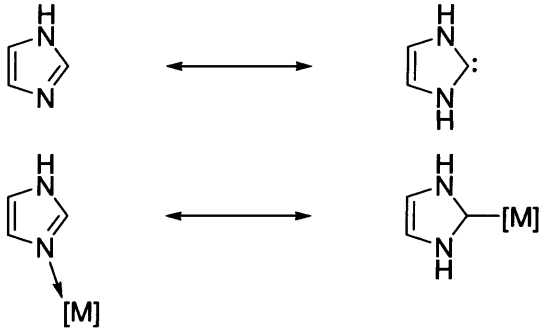

Scheme 2: *tautomerism between imidazole and imidazol-2-ylidene, and imidazole complexes and NHC complexes*

In their work, Crabtree and Eisenstein noted that, although C-binding might be favourable in some cases, interconversion between imidazole and NHC binding would probably require some sort of acid catalysis (as in Taube's example). Shortly after this, Bergman and Ellman reported the first example of heterocycle C-H functionalisation proceeding via an NHC intermediate (*i.e.* a Rh(III) benzimidazol-2-ylidene complex, see ***Scheme 3***), thus definitely establishing the usefulness of N- to C-binding interconversion in catalysis.[22] Importantly, the authors used PCy_3.HCl as a source of PCy_3, giving credit to the hypothesis of an acid-catalysed switch from N-binding to C-binding. Other studies exploiting imidazole-NHC tautomerism have appeared in the literature, notably for the synthesis of transition metal complexes.[23-25]

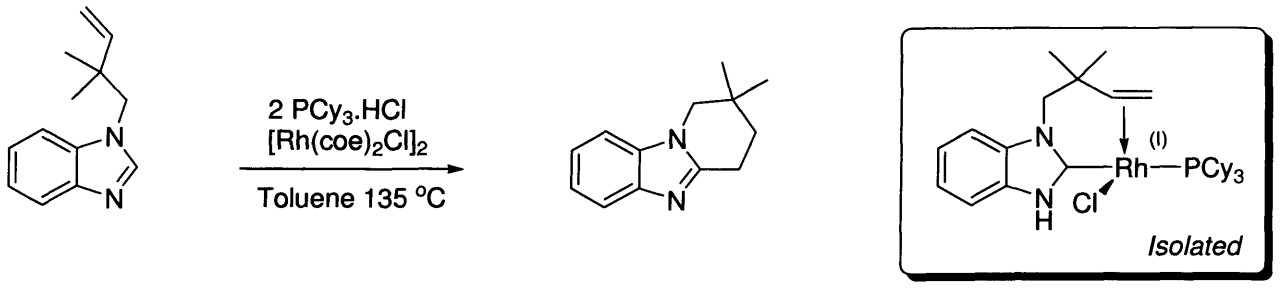

Scheme 3: *alkenylation of benzimidazole proceeding via an NHC intermediate*

Since this seminal study, Bergman and Ellman have published a number of papers detailing both mechanistic and synthetic aspects of their work.[26-36] The reaction proceeds from a Rh(I) NHC complex (such as the one in ***Scheme 3***) to a Rh(III) hydride which undergoes intra- or intermolecular olefin insertion followed by reductive elimination of the cyclic product.[37] ***Scheme 4*** shows the synthesis of a biologically active compound using this methodology.[26]

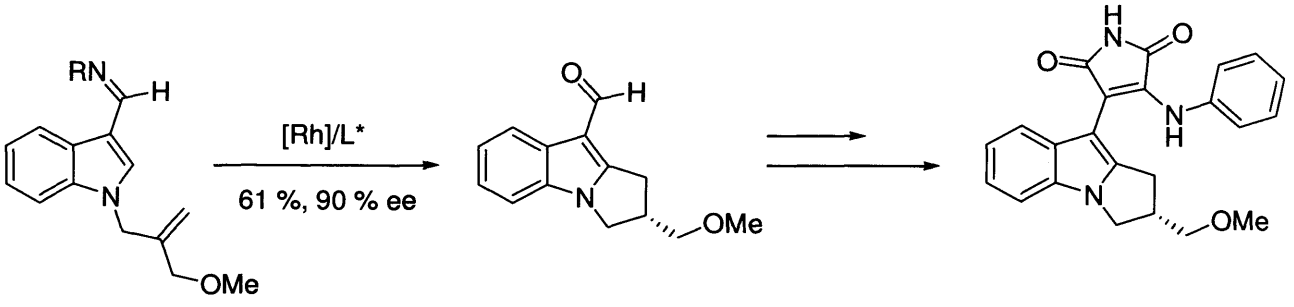

Scheme 4: *application of the Rh-catalysed alkenylation of N-heterocycles to the synthesis of a protein kinase C inhibitor*[26]

The scope of this reaction was recently extended to pyridines,[38] which is not totally unexpected considering the emergence of pyridine-2-ylidenes as ligands for transition metals. [24, 25]

Recent studies in the Cavell group have combined the redox reactions discussed in section **2.1.1** to generate an atom-efficient coupling reaction between azolium salts and alkenes,[10] and in turn, to

demonstrate the *in situ* formation of reactive carbene metal hydride complexes. A range of olefins were successfully coupled to give the 2-substituted product (***Scheme 5***).[12]

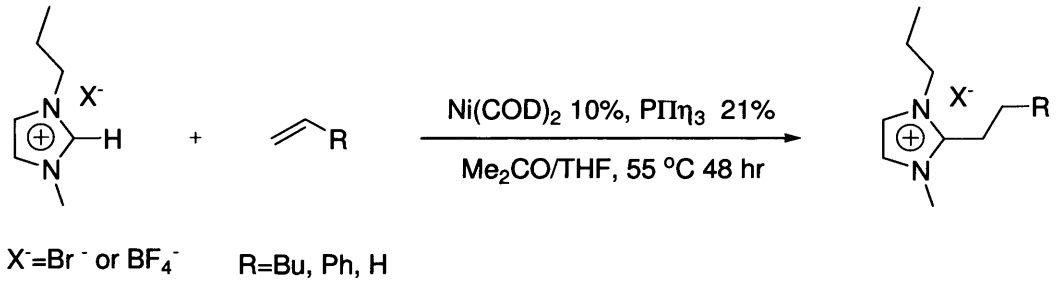

Scheme 5: *Reaction of olefins with N-alkyl azolium salts*[10]

With the current interest in ionic liquids (ILs) based on imidazolium salts as "green" media for chemical reactions,[39-43] this reaction provides a useful, modular approach to the synthesis of finely tuned ILs, using simple imidazolium salts as building blocks. With increasing pressure on chemists to develop cleaner, atom-efficient reactions, direct functionalisation of C-H bonds is becoming a strategically important area of chemistry (see chapter 1). In this context, this olefin/azolium salt coupling reaction bears considerable potential, and one of the aims of the work discussed in this thesis was to better understand and broaden the scope of this unique process.

2.2 Results and discussion

2.2.1 Intermolecular coupling of azolium salts

2.2.1.1 Catalysis with Ni

2.2.1.1.1 Combined experimental and theoretical study of ligand effects

Despite striking similarities with Bergman's heterocycle alkenylation, the reaction depicted in ***Scheme 5*** does not require Brønsted acid catalysis to generate the NHC intermediate, probably because of the ease with which oxidative addition occurs. Based on the stoichiometric studies discussed above, it was initially proposed that the catalytic cycle, using the catalyst system $Ni(COD)_2/PPh_3$, proceeds *via* a mechanism involving oxidative addition of the azolium salt, replacement of a weakly bound ligand by alkene, followed by insertion of the alkene into the metal hydride bond and finally, reductive elimination of the product ("redox mechanism", ***Figure 4***).[10]

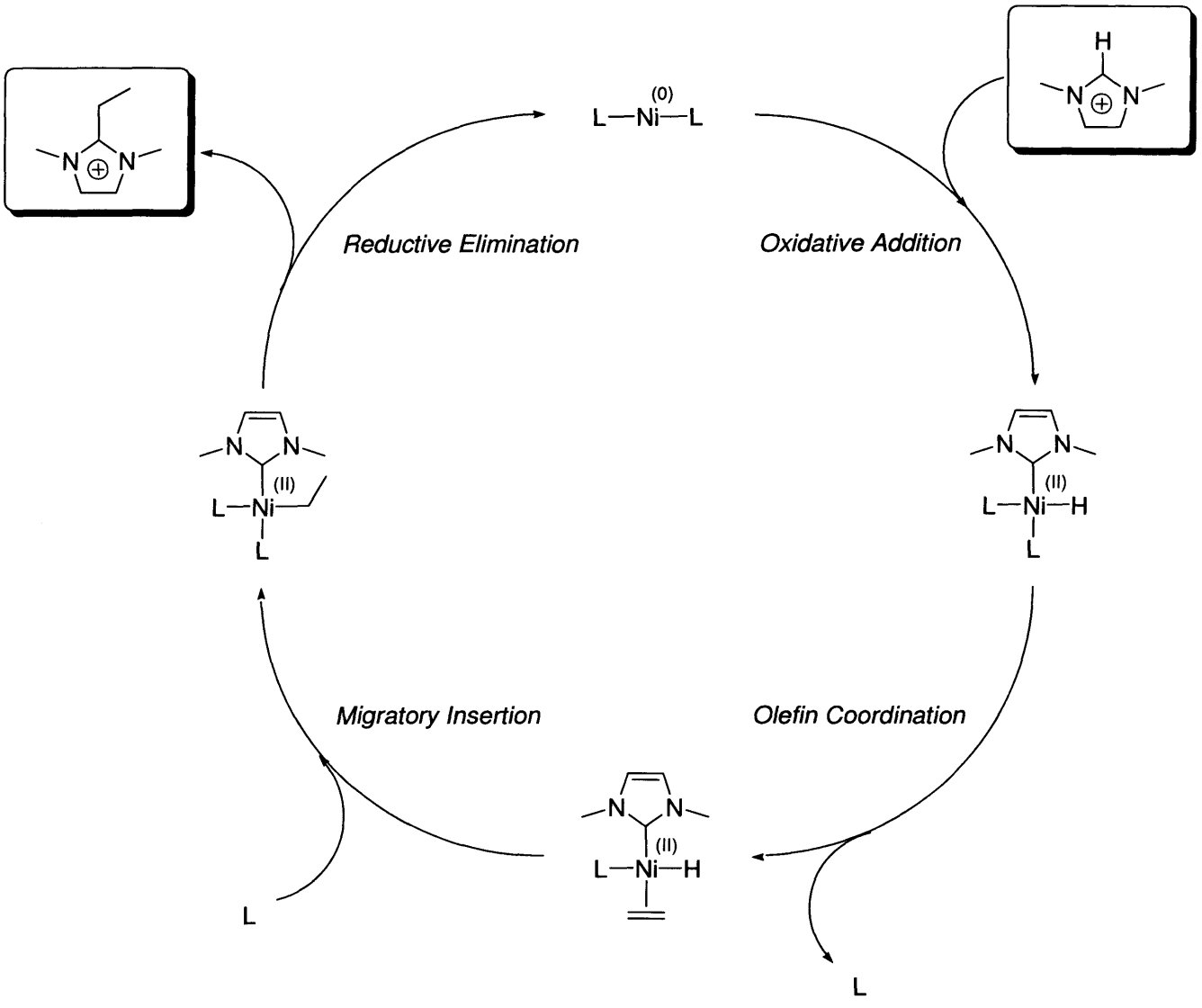

Figure 4: *proposed "redox" mechanism for the reaction of olefins with imidazolium salts*

This catalytic cycle should be regarded as a "textbook" mechanism. Indeed, it leaves a number of issues unsolved, in particular the exact geometry (*i.e. cis* or *trans*) of the Ni hydride and the coordination number (*i.e.* 4 or 3) of the different intermediates. In order to optimise and broaden the scope of this process, a combined experimental and computational study was undertaken.[44] DFT calculations on different catalytic systems were conducted by Kirsty J. Hawkes and Brian F. Yates at the University of Tasmania.[45]

Investigations reveal how changes in electronic and steric properties of the ligand dramatically influence the outcome of the reaction. This section describes the benchmark reaction of 1-propyl-3-methylimidazolium bromide ([pmim]Br) with ethylene catalysed by *in situ* Ni(0) catalysts (formed by mixing $Ni(COD)_2$ and a phosphine or NHC ligand). A summary of the computational investigation of the reaction mechanism (using the model system ethylene and 1,3-dimethylimidazolium, with a range of NiL_1L_2 catalyst systems) will also be presented.

The ligands employed in the reaction may be interpreted in terms of the "Tolman map" [46-48] plotted in ***Figure 5***. The Tolman map classifies phosphines according to their cone angle θ, which represents the angle of a fictive cone in which the umbrella-shaped phosphines could fit (therefore the bulkier the phosphine, the larger θ), and their electronic parameter ν, which is the frequency of the A_1 vibration of CO in $Ni(CO)_3L$ (where L is a phosphine). For strongly electron donating phosphines, π back donation from Ni to the π^* orbital of CO is greater, thus weakening the C=O bond and decreasing the vibration frequency.[49] Nolan and coworkers prepared a series of $Ni(CO)_3L$ complexes (where L= NHC) and concluded that even the less electron-donating NHCs are much stronger σ-donors than the most basic phosphines such as P^tBu_3.[50, 51] Whilst NHCs cannot be represented on a Tolman map because the cone angle model is unsuitable for characterisation of their steric properties, the same authors introduced the buried sphere volume (V_{bur}%) concept and they were able to conclude that, in terms of steric bulk, IMes is comparable with PCy_3, while IPr is closer to P^tBu_3.[51, 52] However, as noted in Chapter 1, phosphines and NHC have widely different geometries and comparisons between them should be made with care.

The phosphines employed in the present study encompass a wide range of electronic and steric properties, with PPh_3 and P^tBu_3 lying at each extreme of the basicity scale, and P(*o*-tolyl)$_3$ and PMe_2Ph occuping the positions of most and least bulky ligands respectively. Comparisons between PPh_3 and P(*p*-$C_6H_4OMe)_3$ on one hand, and between P(*p*-$C_6H_4OMe)_3$ and $P(CH_2Ph)_3$ (a.k.a. PBz_3)

on the other, provide an insight into the effect of independently varying ligand basicity, and steric bulk.

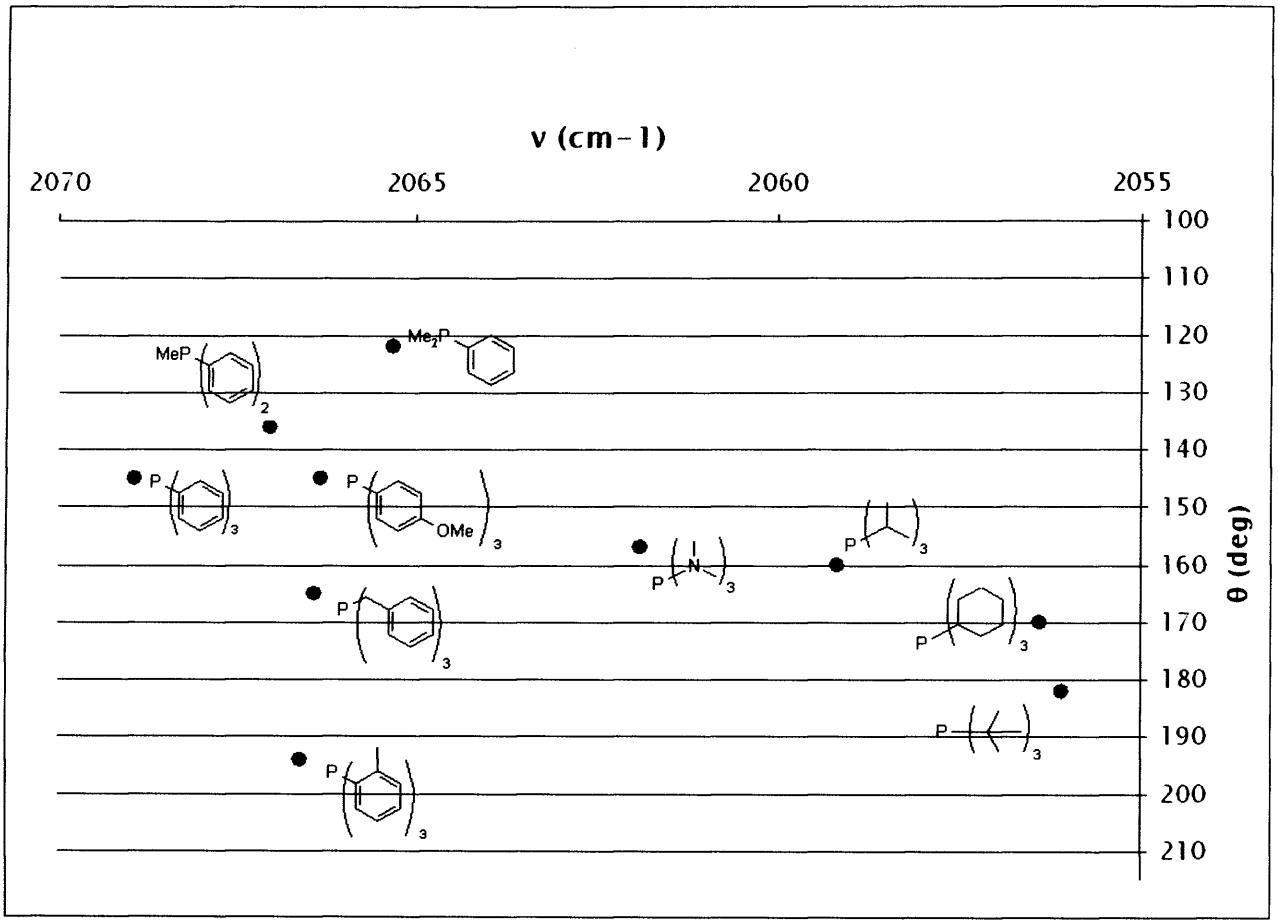

Figure 5: *Tolman map of tested monoligating phosphines*

Table 1 shows the results obtained for the catalytic 2-substitution of [pmim]Br employing a range of different ligands sorted from least to most bulky (except for *bis*(diphenylphosphino)butane, dppb, which cannot be compared to monodentate ligands). The catalytic reaction generally proceeds best with 2.1 eq. of ligand with respect to Ni (compare entries 3 & 4; 6 & 7; 12 & 13), with the notable exception of the very bulky IPr where excess ligand inhibits the reaction (entries 18 & 19). In some cases, addition of further phosphine led to some reduction in performance, whilst it also helped suppress catalyst decomposition.

Table 1: *selected results with Ni(COD)$_2$*[a]

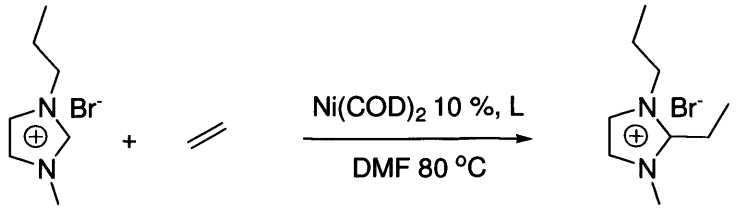

Entry	Ligand	Conv (%)
1	dppb* (11 %)	11
2	PMe_2Ph (21 %)	95
3	$PMePh_2$ (11 %)	43†
4	$PMePh_2$ (21 %)	94
5	$PMePh_2$ (31 %)	81
6	PPh_3 (11 %)	<5†
7	PPh_3 (21 %)	24
8	P(*p*-$C_6H_4OMe)_3$ (21 %)	39
9	$P(NMe_2)_3$ (21 %)	<5†
10	P(^{i}Pr$_3$) (21 %)	88
11	$P(Bz)_3$ (21 %)	45
12	PCy_3 (11 %)	87
13	PCy_3 (21 %)	94
14	P(^{t}Bu)$_3$ (21 %)	>95
15	P(*o*-tolyl)$_3$ (21 %)	<5†
16	IMes (11 %)	94
17	IMes (21 %)	>95
18	IPr (21 %)	8
19	IPr (11 %)	93

[a]Reagents and conditions : 1-propyl-3-methylimidazolium bromide 0.73 mmol, $Ni(COD)_2$ 10 mol%, Ligand (x mol%), DMF 3 mL, C_2H_4 1 bar 80 °C, 5 hr. Generally based on the average of two runs. † Rapid catalyst decomposition was observed.* *Bis*(diphenylphosphino)butane.

Table 2: *selected results at low catalyst loading*[a]

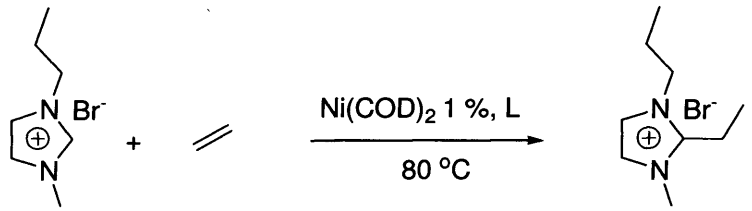

Entry	Solvent	Ligand	Conv (%)
1	DMF	PCy_3 (2.1 %)	<5
2	DMF	PCy_3 (1.1 %)	<5
3	DMF	$P(^tBu)_3$ (2.1 %)	<5
4	DMF	IMes (1.1 %)	<5
5	DMF	IPr (1.1 %)	<5
6	DMF	PMe_2Ph (2.1 %)	26
7	DMA	PMe_2Ph (2.1 %)	<5
8	DMSO	PMe_2Ph (2.1 %)	<5
9	NMP	PMe_2Ph (2.1 %)	83
10	THF/NMP (1/3)	PMe_2Ph (2.1 %)	62
11	THF/NMP (2/1)	PMe_2Ph (2.1 %)	52

[a]Reagents and conditions : 1-propyl-3-methylimidazolium bromide 0.73 mmol, $Ni(COD)_2$ 1 mol%, Ligand (x mol%), Solvent 3 mL, C_2H_4 1 bar 80 °C, 5 hr. Generally based on the average of two runs.

Several of the more efficient catalyst systems were further tested using a low catalyst loading (1 mol%) and only PMe_2Ph was found to give good conversions (***Table 2***). It became apparent that catalytic systems which displayed comparable activities at 10 % [Ni] loading gave different activities under the new conditions (*e.g.* PCy_3 and PMe_2Ph, ***Table 1*** entries 2 & 13 and ***Table 2*** entries 1 & 6 or 9). A large improvement in catalytic activity was observed when changing the solvent from DMF to NMP (entries 6 and 9). Moreover, using mixtures of NMP/THF eroded the observed conversion (entries 9-11), pointing to the importance of solvent polarity.

At this point it is useful to present the results of the theoretical study using DFT calculations. Indeed, ***Table 1*** shows that very different ligands (*e.g.* PMe_2Ph or $PMePh_2$ and PCy_3 or P^tBu_3) could give similar activities using the same conditions, an observation which is not easily rationalised without the insight provided by theoretical calculations.

As mentioned above, a mechanism involving four main steps was envisaged (***Figure 4***). A more detailed reaction sequence came out of the calculations (***Figure 6***): oxidative addition of the imidazolium salt (**1** → **4**), coordination of ethylene (**4** → **6b**), insertion of ethylene into the metal hydride bond (**6b** → **9**), and reductive elimination of the coupled product (**9** → products). Transition states are indicated by the symbol (**TS**).

This mechanism was explored using a range of ligand sets with varying degrees of bulk and basicity to reflect the catalysts employed in the catalytic experiments. The ligand set used includes $L_1 = L_2$ = 1,3-dimethylimidazol-2-ylidene (dmiy); L_1 = dmiy, L_2 = trimethylphosphine (PMe_3); $L_1 = L_2 = PMe_3$; $L_1 = L_2$ = triphenylphosphine (PPh_3); $L_1 = L_2$ = tri-(*tert*-butyl)phosphine (P^tBu_3) (***Figure 7***).

Figure 7: *ligands used in the computational study*

Full energy diagrams for each system are presented in ***Figures 8*** to ***12***.

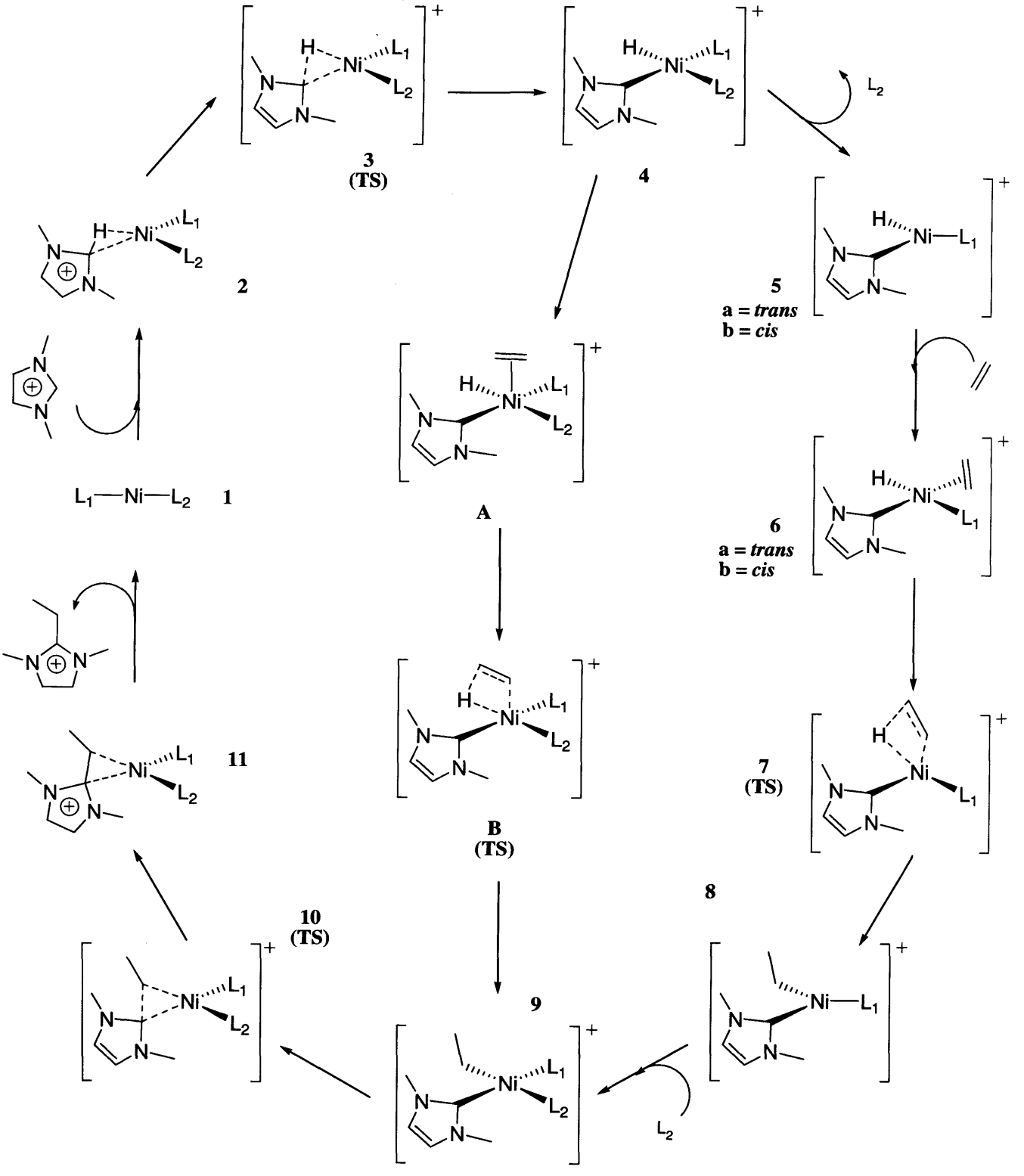

Figure 6: *full catalytic cycle for the coupling of ethylene and imidazolium salts*

The mechanism depicted in ***Figure 6*** is significantly more complex than the "textbook" mechanism. Indeed, once oxidative addition has occurred, dissociation of one of the two ancillary ligands is the preferred route (as opposed to a 5-coordinate route involving structures **A** and **B**). This gave rise to two cases: dissociation *trans* to the hydride (intermediate **5a**, energetically favoured but in this case a rearrangement has to take place before olefin insertion can occur), or *cis* dissociation (this represents a larger activation energy, but no rearrangement is required for olefin insertion). Because no energy minima were found when investigating a rearrangement, it was concluded that the worst-case scenario would be *cis* dissociation. For the more compact ligand systems such as PMe_3 or dmiy, ligand dissociation represents the most energy-demanding step (regardless of the preferred site of dissociation), whilst reductive elimination is the rate determining step for the two bulkier phosphines PPh_3 and P^tBu_3.

Another subtlety of the computational mechanism is the fate of the dissociated ancillary ligand: for dmiy and PMe_3, dissociation occurs after oxidative addition, and recoordination takes place straight after olefin insertion. For PPh_3, which can be considered a borderline ligand in terms of bulk, two cases were observed: one exactly similar to PMe_3 ("associative" route), and the other in which recoordination takes place after reductive elimination ("monophosphine" or "dissociative" route). Finally, the bulk of P^tBu_3 causes immediate dissociation; therefore the active catalytic species is a monoligated Pd-P^tBu_3 complex (*i.e.* L_2 is not present except for intermediate **1**).

From these results, the NiL_1L_2 catalytic systems appear to fall into 3 separate categories:

- Case 1: for the smallest, less easily dissociated ligands such as dmiy and PMe_3, 4-coordinate complexes would be favoured and as a result the most energy demanding step becomes ligand dissociation prior to ethylene coordination (***Figures 8 to 10***).
- Case 2: for larger, labile phosphines, ethylene is more easily coordinated and reductive elimination becomes the rate determining step. Calculations indicate two possible routes, with one or two phosphine ligands on Ni (***Figure 11***).
- Case 3: for very bulky, more readily dissociated ligands (*e.g.* P^tBu_3), catalysis proceeds via more compact mono-phosphine intermediates in which ethylene coordination is challenging, but reductive elimination remains the rate determining step (***Figure 12***).

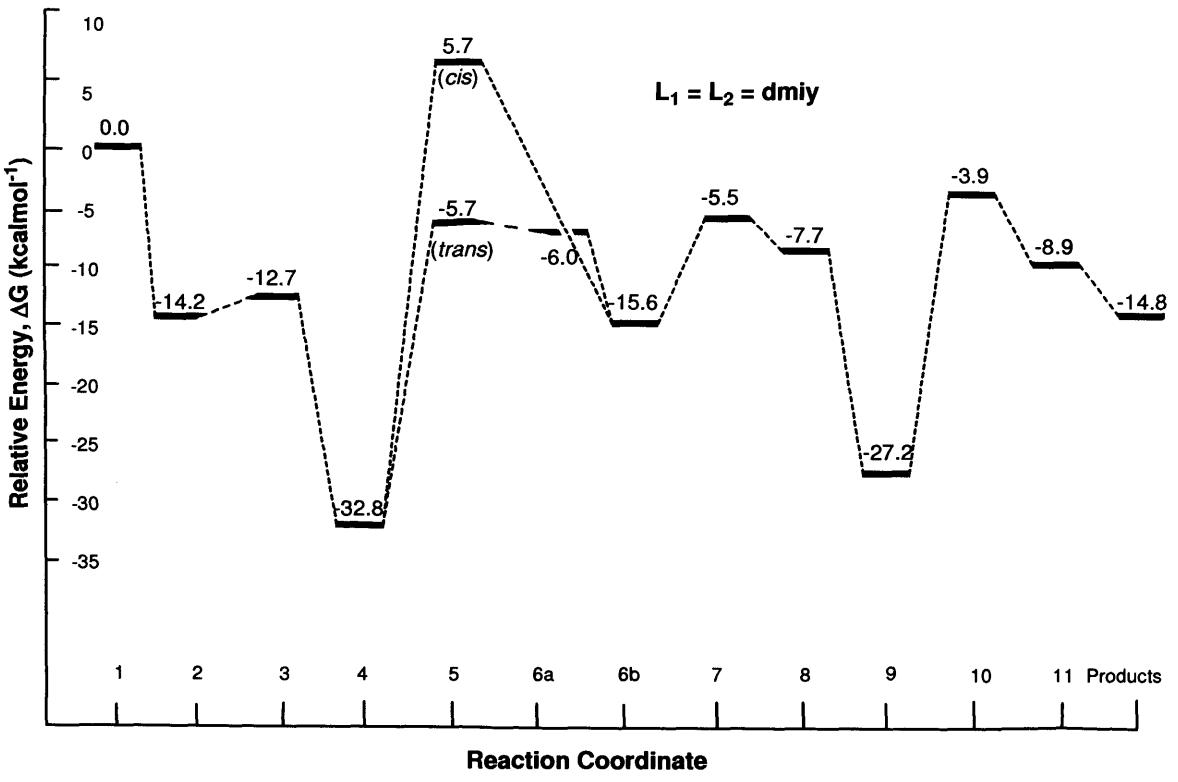

Figure 8: *full energy diagram for the $Ni(dmiy)_2$ system*

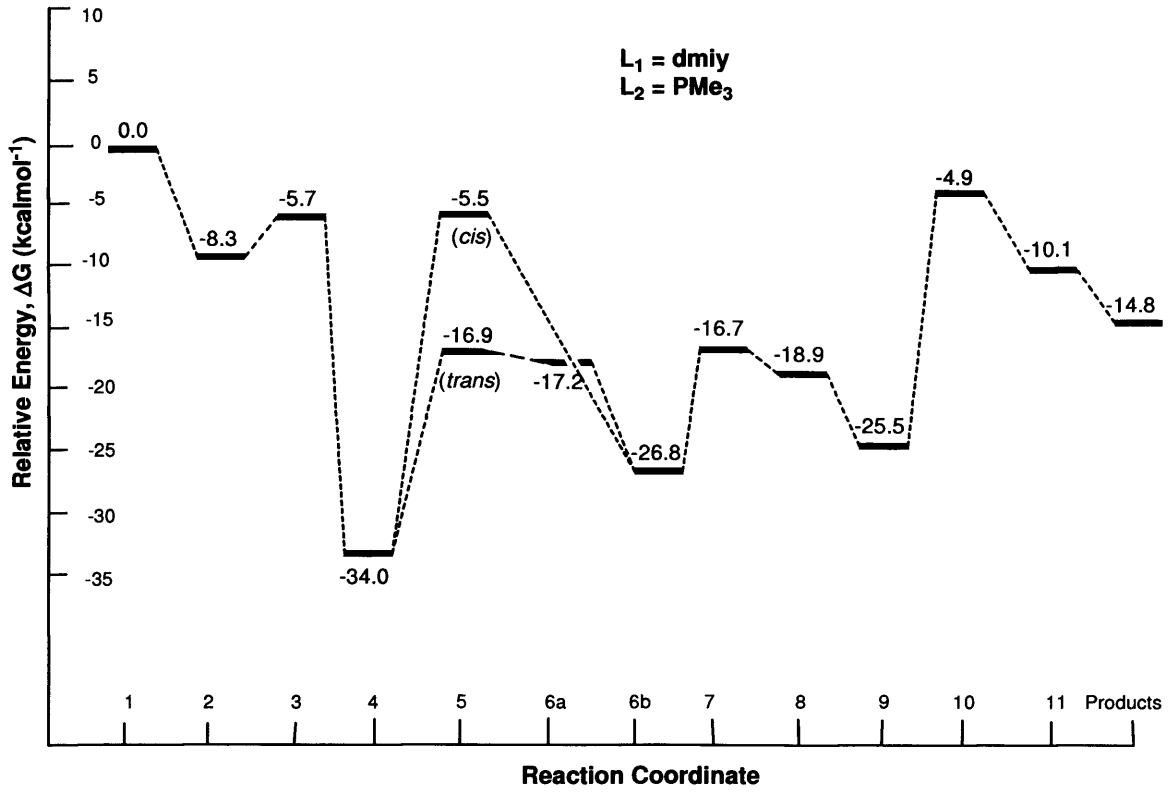

Figure 9: *full energy diagram for the Ni(dmiy)(PMe_3) system*

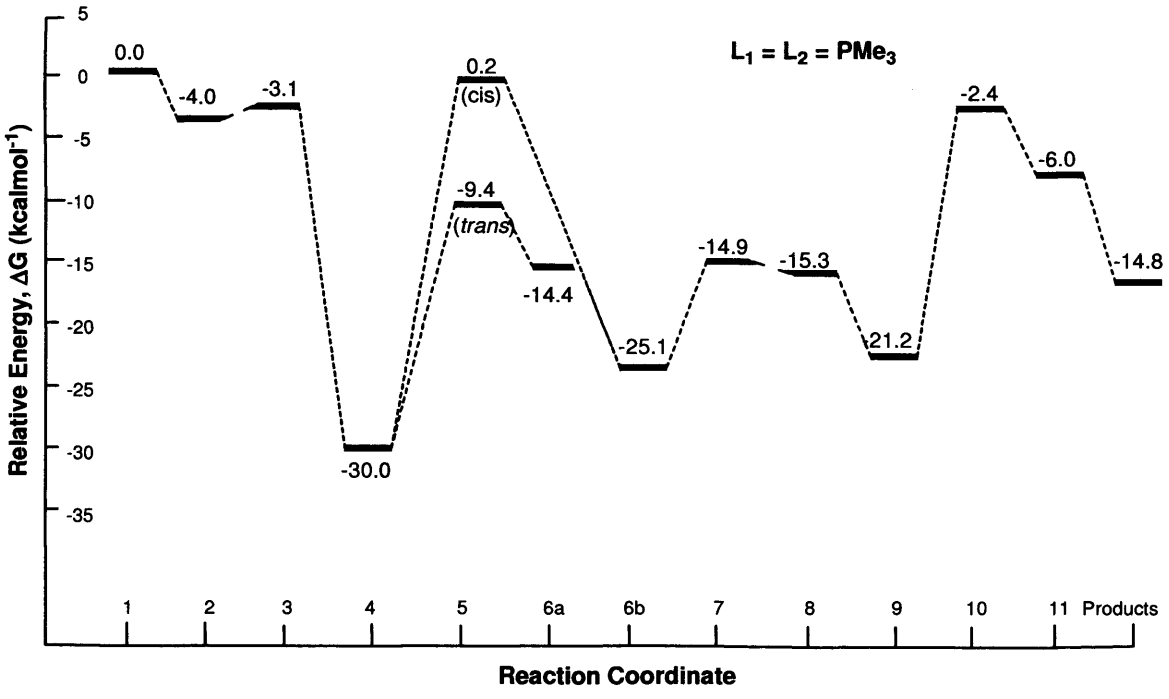

Figure 10: *full energy diagram for the Ni(PMe_3)$_2$ system*

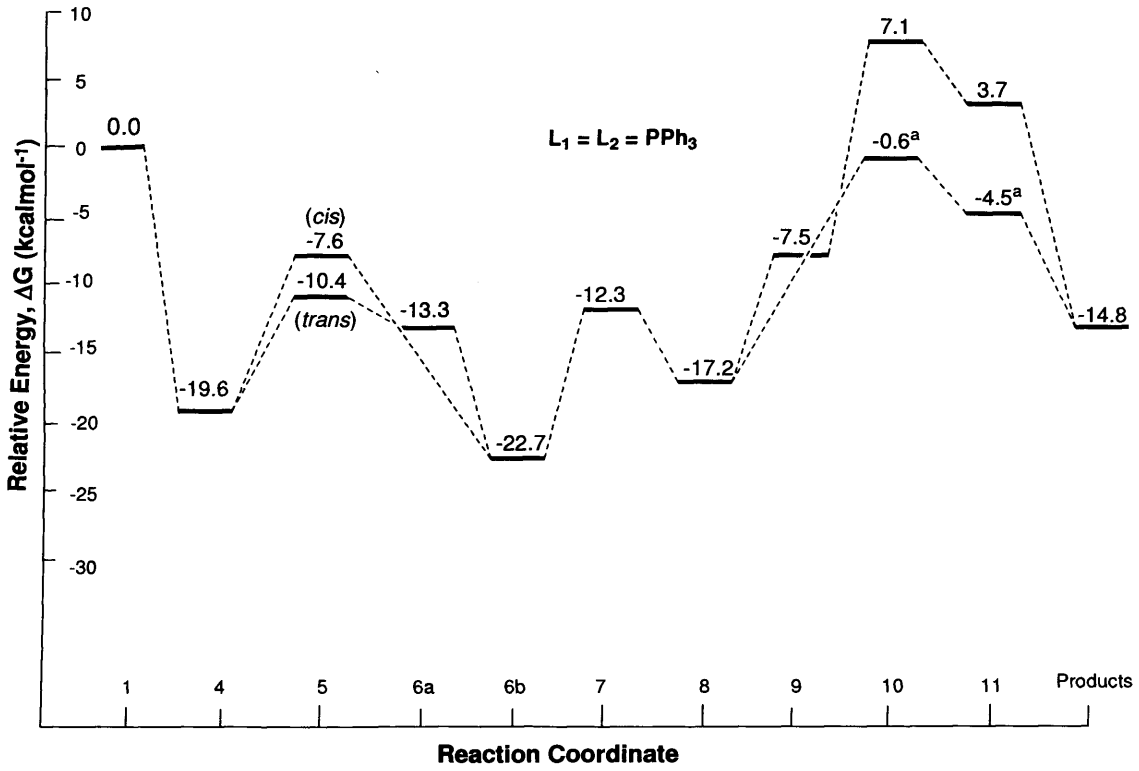

Figure 11: full energy diagram for the $Ni(PPh_3)_2$ system. [a] mono-phosphine reductive elimination

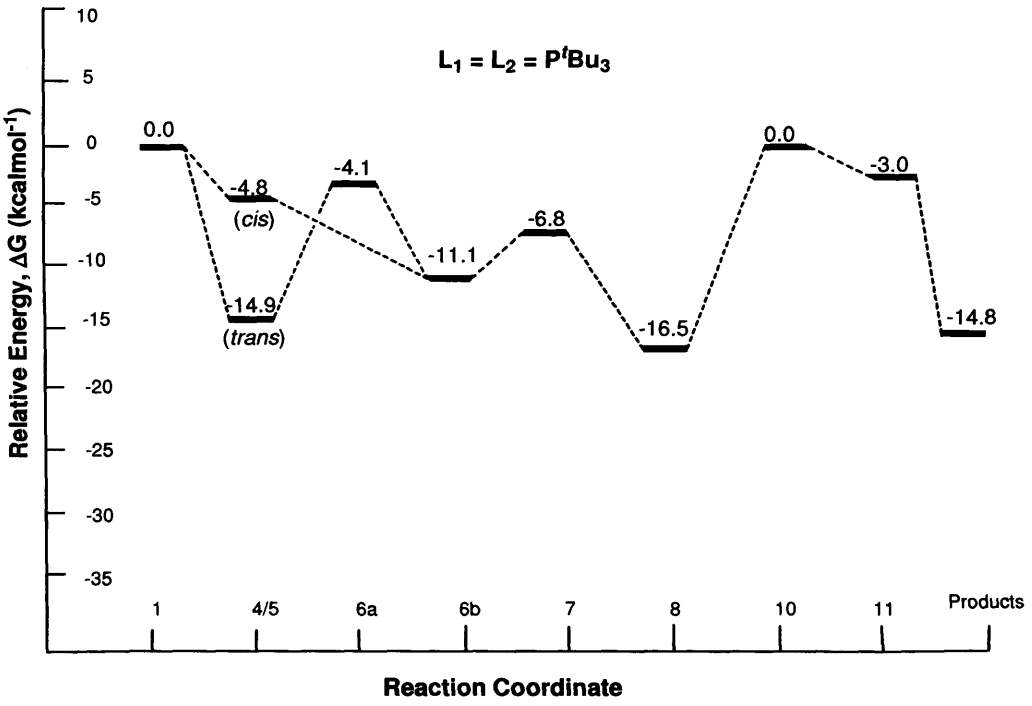

Figure 12: full energy diagram for the $Ni(P^tBu_3)_2$ system

It was initially difficult to interpret the experimental results, but when taken in conjunction with the computational studies, it becomes apparent that the reaction is a complex, and "flexible" process, in which different rate determining steps operate depending on the ancillary ligand employed. There is, in general, good agreement between the experimental observations and the theoretical results

Steric bulk appears to be the predominant factor affecting the rate determining step (*r.d.s.*). Just where the reaction changes from a mono- to di-phosphine system is unclear, but experiments seem to indicate that it could be where cone angles are around 160 °. Indeed, if one compares the activities of electronically similar P(*p*-$C_6H_4OMe)_3$ and PBz_3 (***Table 1***, entries 8 & 11), it appears that despite the much bulkier nature of the latter (θ= 165° *vs* 145 °), their efficiencies are extremely close (45 % vs 39 % conversion). If the same mechanism was operating for both systems, PBz_3 should greatly accelerate the reaction by facilitating reductive elimination. The fact that this does not happen indicates that somewhat different mechanisms might operate. With this in mind, the experimental results can also be divided into 3 broad classes. As observed from the computational studies, Case 1 represents phosphine cone angles of less than 140°, Case 2 operates for cone angles between 140° and around 160° and Case 3 is in operation when cone angles exceed 160° (***Table 3***).

Table 3: *experimental results grouped in three cases*[a]

Case	Ligand	Conv (%)
1	PMe_2Ph (21 %)	95
1	$PMePh_2$ (11 %)	43[†]
1	$PMePh_2$ (21 %)	94
1	$PMePh_2$ (31 %)	81
2	PPh_3 (21 %)	24
2	$P(p\text{-}eC_6H_4OM)_3$ (21 %)	39
3	P^iPr_3 (21 %)	88
3	PBz_3 (21 %)	45
3	PCy_3 (21 %)	94
3	$P(^tBu)_3$ (21 %)	>95
3	IMes (11 %) (~PCy_3)	94
3	IMes (21 %)	>95
3	IPr (21 %) (~P^tBu_3)	8
3	IPr (11 %)	93

[a] See ***Table 1*** for reaction conditions.

Consistent with the theoretical studies, it was noted that for smaller and more basic phosphines, such as PMe_2Ph and $PMePh_2$, the metal can accommodate 2 equivalents of ligand and any excess phosphine (more than 2 eq) retards the reaction by competing with incoming substrate, for example the case of $PMePh_2$ (***Table 3*** case 1): 1.1 eq of ligand catalysed the reaction, albeit with significant catalyst decomposition, while 2.1 eq gave the best results. A significant decrease in activity was observed when 3.1 eq of ligand was used, which is consistent with ligand dissociation being the *r.d.s.*

In terms of steric influence, calculations found PPh_3 to be a borderline case, with both associative and dissociative mechanisms possibly operating and reductive elimination the *r.d.s.* (Case 2).

Replacing PPh_3 by $P(p\text{-}C_6H_4OMe)_3$ (*i.e.* increasing basicity but leaving bulk unchanged, ***Table 3***, case 2) generates an increase in yield. This result is attributed to reduced catalyst decomposition, with the more basic ligand stabilising the Ni intermediates.

For larger phosphine ligands, a dissociative mechanism is expected to operate uniformly. Here, due to steric constraints, ethylene coordination is challenging, but reductive elimination remains the rate determining step (Case 3). In the cases of PCy_3 (θ = 170 °) and P^tBu_3 (θ = 182 °), a small excess of ligand was beneficial; no nickel black was observed with 2.1 eq (***Table 1***, entries 12, 13 and 14). For these systems, a small amount of additional ligand may simply improve catalyst stability without significantly affecting the ligand dissociation equilibrium.

As mentioned previously, IMes may be considered similar in bulk to PCy_3, and IPr similar to P^tBu_3, which most closely links them to Case 3. Interestingly, only the IMes system demonstrated good activity when 2.1 eq. of ligand was used (***Table 1***, entry 17). Using proportions of 1.1 eq. both ligand systems demonstrated very high activities (***Table 1***, entries 16 and 19). The extremely bulky nature of IPr and the intrinsically strong coordinating ability of carbenes probably explain this observation. Although IPr is comparable to P^tBu_3 in terms of steric bulk, it forms stronger ligand to metal bonds. Thus $Ni(IPr)_2$ can be synthesised from $Ni(COD)_2$ and free IPr,[53] whereas $Ni(P^tBu_3)_2$ has never been isolated (in this case the complex formation equilibrium strongly favours phosphine dissociation).[54] Therefore, it is likely that under our conditions, the sterically crowded but stable $Ni(IPr)_2$ forms and is unable to enter the catalytic cycle. In contrast, activity is retained in the case of the less sterically demanding IMes (entries 16-17).[55]

Finally, a hemilabile chelating phosphine, namely dppb *bis*-(diphenylphosphino)butane gave poor results, most probably because of considerably slower and/or thermodynamically disfavoured reductive elimination from a chelate complex.[5] This would confirm that chelation is an effective way of stabilising hydrocarbyl complexes of NHCs under catalytic conditions.[2]

2.2.1.1.2 Conclusions from the combined experimental and computational study

The combined experimental and DFT study of the reaction of ethylene with imidazolium salts has provided valuable insight into this process. It was found that the catalytic reaction is relatively complex, with a number of possible rate determining steps apparent, each of which can become dominant when ligands are changed. The trends in catalytic behavior can now be understood with some confidence: systems incorporating smaller ligands such as PMe_3 or dmiy are better described by an associative route, in which ligand dissociation is the rate determining step. This was confirmed experimentally in the case of $PMePh_2$. Larger ligands such as PPh_3 and P^tBu_3 are expected to proceed via a "monophosphine" route, in which the rate determining step would be reductive elimination. The two NHC ligands tested (IMes and IPr) also seem to belong to this category, indicating that care must be taken using simple carbenes such as dmiy to model their behavior.

In terms of reaction optimisation, it is somewhat puzzling that ligands such as IMes or PCy_3 fail to give any activity when [Ni] catalyst loading is lowered to 1 % (***Table 2***, entries 1, 2, 4 and 5). A possible explanation for this would be poisoning of the catalyst by the large excess of ethylene at low loading. Indeed, reductive elimination (the rate determining step for those systems) is expected to proceed from unstable 14-electron 3-coordinate NHC/ethyl Ni complexes, as 4-coordinate intermediates with two NHCs cannot form. Coordination of the smaller ethylene at this stage to give stable 16-electron 4-coordinate complexes would thus inhibit the reaction. On the other hand, the smaller PMe_2Ph gave good activity at 1% catalyst loading, which is consistent with phosphine dissociation being the rate-determining step. In this case, an excess of ethylene is not expected to be detrimental to the reaction rate, and in fact it could help shift the ligand exchange equilibrium towards the olefin complex.

2.2.1.2 Catalysis with *in situ* Pd catalysts

As discussed above, Pd complexes of NHCs can follow the same reactivity pattern as their Ni counterparts (*i.e.* oxidative addition of imidazolium salts and reductive elimination of alkyl NHC complexes).[2, 3, 5, 6, 8, 56] However, previous attempts at developing a Pd-catalysed version of the coupling of azolium salts and olefins had thus far all but failed. ***Table 4*** shows that Pd can actually perform the same reaction, but unlike the Ni-catalysed process, the range of *in situ* catalysts that enable the reaction is much more limited.

Table 4: *selected results with* $Pd(dba)_2$

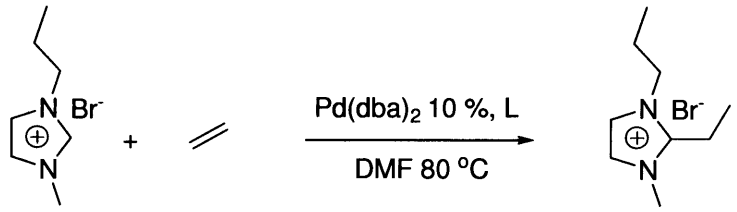

Entry	Ligand	Conv (%)
1	PPh_3 11%	<5
2	PPh_3 21%	<5
3	P^tBu_3 11%	<5
4	P^tBu_3 21%	<5
5	**PCy_3 21%**	**22**
6	**PCy_3 11%**	**88**
7	IMes 11%	17
8	IMes 21%	18
9	$PMePh_2$ 11%	<5
10	$PMePh_2$ 21%	<5

[a] Reagents and conditions : 1-propyl-3-methylimidazolium bromide [pmim]Br 0.73 mmol, $Pd(dba)_2$ 10 mol%, Ligand (x mol%), DMF 3 mL, C_2H_4 1 bar 80 °C, 24 hr. Generally based on the average of two runs.

Of the ligands (PPh_3, P^tBu_3, PCy_3, $PMePh_2$ and IMes) tested in this reaction, only PCy_3 (entries 5 & 6) gave good activity. A striking observation is the fact that more than 1 eq of phosphine with respect to Pd significantly inhibited the reaction. This suggested that monoligated Pd (see chapter 4) might be the active catalyst and led to the development of mixed phosphine carbene π-allyl Pd(II) complexes described in chapters 3 and 4.

2.2.2 Intramolecular coupling of azolium salts

2.2.2.1 Coupling using *in situ* Ni catalysts

The success of the intermolecular coupling of azolium salts with ethylene indicated that an intramolecular version of this process could be envisaged. Suitable substrates for this reaction would be simple alkenylazolium salts such as those depicted in ***Figure 13***. The synthesis of mono or di-subsituted azolium salts was initially realised by Swee Kuan Yen during her time as an exchange student in the Cavell group (***Scheme 6***). A simple alkylation of the corresponding imidazoles and thiazoles afforded compounds **1a-2H**. This work will be described in a paper elsewhere.

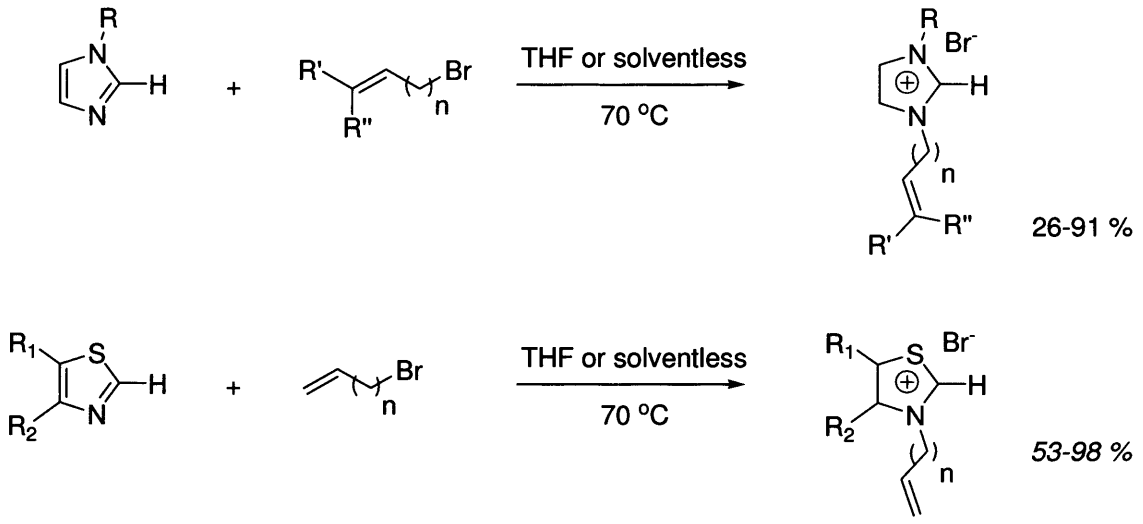

Scheme 6: *synthesis of azolium salts*

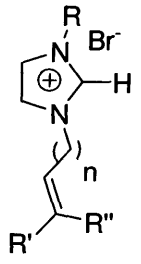

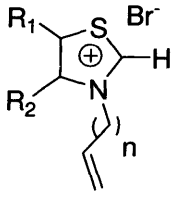

n= 1, R'= R"= H

1a: R= Me
1b: R= Bu
1c: R= 2,4,6-trimethylphenyl (Mes)
1d: R= 2,6-diisopropylphenyl (Dipp)

1e: R_1= R_2= H

n= 2, R'= R"= H

2a: R= Me
2b: R= Bu
2c: R= 2,4,6-trimethylphenyl (Mes)
2d: R= 2,6-diisopropylphenyl (Dipp)

2e: R_1= R_2= H
2f: R_1= H R_2= Me
2g: R_1= R_2= Me

n= 2, R'= R"= Me

2h: R= Me

Figure 13: *salts investigated in the intramolecular alkenylation of azolium salts*

Experimental conditions (the use of DMF as solvent, ligand-to-metal ratio...) were adapted from the intermolecular alkenylation described in section **2.2.1**.

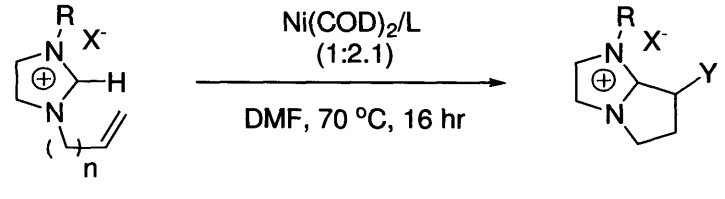

(n=1): no reaction (Y= H)
(n=2): conversion to products (Y= Me, ^{i}Pr)

Scheme 7: *2-substituted imidazolium coupling reaction*

An initial substrate screening using IMes as ancillary ligand was performed by Swee Kuan Yen. Allyl-substituted salts failed to give any products, whilst some butenyl analogues converted to the cyclised products (***Scheme 7*** and ***Table 5***).[57]

Table 5: intramolecular coupling results with different substrates

Entry	Substrate	Conv (%)[b]
1	**1a-1e**	0
2	**2a**	100[c]
3	**2b**	100[c]
4	**2c**	44
5	**2d**	0
6	**2e**	< 5
7	**2f**	< 5
8	**2g**	50
9	**2H**	100[c]

[a] Reagents and conditions: Catalyst [Ni(COD)$_2$] (10 mol%), substrate 0.7 mmol, IMes 0.15 mmol, DMF (4 mL), 70 °C, 16 hr. [b] Determined by ^{1}H NMR spectroscopy, average of two runs. [c] Products **3a**, **3b** and **3h** were isolated and fully characterised.

The inclusion of a further methylene group between the nitrogen and the alkene group, giving N-but-3-enyl substituted substrates **2a-h**, allows the formation of five-membered fused rings. When heated at 70 °C for 16 hours, the substrates converted to the C2-fused ring products **3a**, **3b** and **3h** (***Figure 14*** and ***Table 5***, entries 2, 3 and 9). These products were isolated and characterised by ^{1}H and ^{13}C NMR spectroscopy, high resolution electrospray mass spectrometry and microanalysis (except **3b** which was found to be too hygroscopic for the latter). The C2-H signal was absent from the ^{1}H NMR spectra of the products in D_2O and d_6-DMSO.

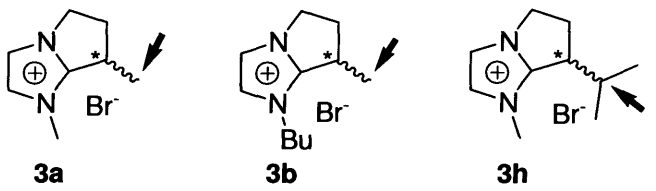

Figure 14: *isolated fused-ring imidazolium salts. Arrows indicate carbon atoms onto which hydride migration occurred.*

The lack of reactivity of allylimidazolium compared to butenylimidazolium salts can be explained in light of the mechanism shown in ***Figure 15***:

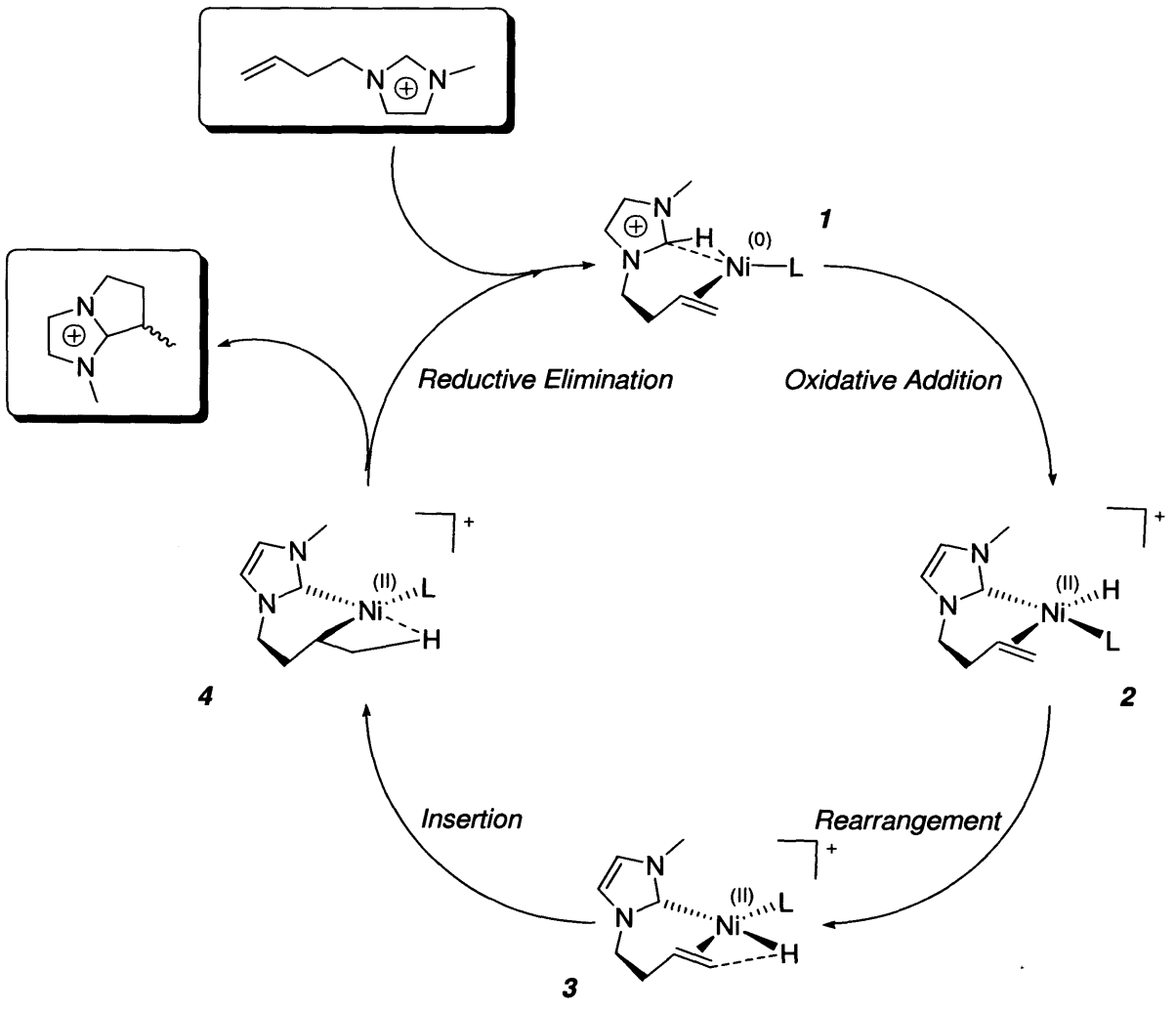

Figure 15: *proposed mechanism for the cyclisation reaction of alkenylimidazolium salts*

According to this mechanism, initial interaction of Ni with the C2-H bond of the imidazolium cation is facilitated by coordination of the olefinic moiety to the metal centre (intermediate ***1***). Oxidative addition then follows, and a rearrangement gives intermediate ***3***, in which the two carbon atoms of the olefin form a plane with Ni and H. This coplanar arrangement is well known to be an essential requirement for olefin insertion and its reverse reaction (*i.e.* β hydride elimination),[49] and this explains why allylimidazolium salts are unreactive: olefin insertion is not possible because hydride attack must happen at the fourth carbon atom on the alkenyl chain. It is worth noting that in the case of an alternative mechanism *via* a 5-coordinate Ni(II) intermediate ***2'*** (if Br^- remains in the first coordination sphere of the metal, or with bidentate ancillary ligands, *vide infra*),[58] this explanation remains valid, as shown in ***Figure 16***:

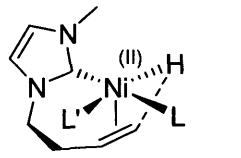

2'

L'= L or Br^-

Figure 16: *alternative 5-coordinate intermediate.*

It is interesting to note how the olefin insertion step does not display the same level of preference when it comes to the substitution pattern of the olefin. Indeed, formation of **3a** and **3b** occurs in an anti-Markovnikov fashion (*i.e.* hydride attacking the least substituted carbon), whereas **3h** results from a Markovnikov insertion (hydride attacking the most substituted carbon). This would seem to indicate that olefin insertion, provided it is geometrically possible, is not the rate determining step of the reaction.

The influence of the substitution on the second nitrogen atom is apparent in the results summarised in ***Table 5***: when the R group at the 3-position of **2a** was changed to mesityl (Mes), conversion to the fused ring product decreased to 44% (entry 8). Furthermore, when the diisopropylphenyl (Dipp) substituted imidazolium salt, **2d** was employed, no conversion was observed at all. This follows the expected reactivity pattern (methyl ~ butyl > Mes > Dipp) where the steric bulk of the N-substituent plays a part in the reaction efficiency. Again, the proposed mechanism accounts for these observations, as the rearrangement step required prior to olefin insertion would be disfavoured for bulky substituents at the 3-position of the imidazolium ring (this step brings ancillary ligand L and the carbene *cis* to each other).

The N-but-3-enyl substituted thiazolium salts **2e-g** were also investigated as substrates for the ring-fused catalytic reaction. Less than 5% conversion was noted for substrates **2e-f** (entries 11 & 12), and the solution turned dark brown immediately upon mixing of the catalyst and the substrates. However, 3-(3-butenyl)-4,5-dimethylthiazolium bromide **2f** showed 50% conversion to the ring-fused product (entry 13).[59] These results suggest catalyst poisoning by coordination of the thiazolium cation to nickel by the sulfur atom. However, **2f** has a methyl group adjacent to S, which might promote dissociation and thus allow the catalytic cycle to proceed in a similar fashion to imidazolium-based substrates.

With these encouraging results in hand, reaction conditions were optimised using the cyclisation of **2a** as a benchmark. Different ligands were tested, from the moderately basic and bulky PPh_3 to the highly basic and bulky Me_2IPr (***Figure 17***).

Carbene ligands

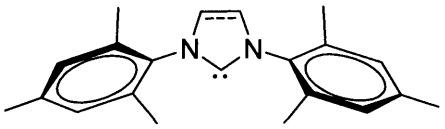

IMes, SMes

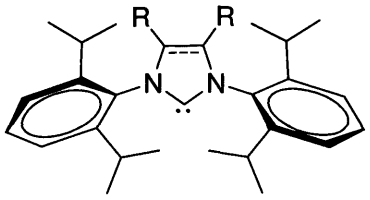

R=H: IPr, SPr
R=Me: Me_2IPr

Phosphine ligands

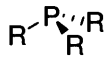

R=C_6H_6: PPh_3
R=C_6H_{11}: PCy_3
R= C_4H_9: P^tBu_3

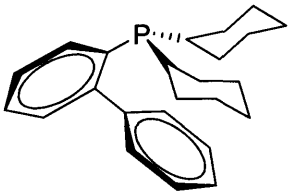

$PCy_2(Bip)$

Figure 17: *ligands tested in the optimisation studies*

Using a reduced catalyst loading of 5 %, the reaction proceeds to complete conversion in as little as 1 hour at 50 °C for the best ligands (***Table 6***, entries 3, 4, 5 & 8).

NHC ligands bearing a 2,6-diisopropylphenyl ring on both nitrogens (*i.e.* IPr, SPr, Me_2IPr) were found to give better results than those with 2,4,6-trimethylphenyl (IMes and SMes). It would thus seem that in the case of NHCs, the higher bulk of the former is beneficial for the reaction, which in turn suggests that reductive elimination or olefin insertion is the rate determining step. However, as mentioned previously, olefin insertion is unlikely to be the rate determining step.

Table 6: *Catalytic coupling results with different supporting ligand.*[a]

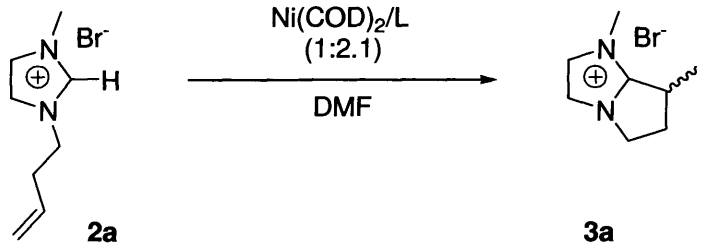

2a **3a**

Entry	Cat. loading	Ligand	Conv. (%)[b]
1	5 %	IMes	78
2	5 %	SMes	89
3	5 %	IPr	100
4[c,d]	2 %	IPr	100
5[e]	1 %	IPr	traces
6	5 %	SPr	100
7	5 %	Me_2IPr	100
8	5 %	PPh_3	30
9	5 %	PCy_3	94
10	5 %	$PCy_2(Bip)$	100
11[c,e]	2 %	$PCy_2(Bip)$	traces
9	5 %	P^tBu_3	35

[a] Reagents and conditions: $Ni(COD)_2$ (x mol%), substrate (**2a**) 0.7 mmol, supporting ligand (2.1x mol%), DMF (4 mL), 50 °C, 60 min. [b] Determined by ^1H NMR spectroscopy, average of two runs. [c] 3.5 mmol of substrate. [d] Reaction time was 20 hr. [e] 7.0 mmol of substrate

In the case of phosphines, a balance between bulk and electron donating ability seems necessary as neither PPh_3 (least basic and least bulky phosphine) nor P^tBu_3 (most basic and most bulky phosphine) is very effective in promoting the reaction. This balance would seem to be achieved with the Buchwald ligand $PCy_2(Bip)$. Overall, these results point to a possibly different mechanism (*e.g.* involving phosphine dissociation equilibria) for phosphines compared to NHCs.

Given the very fast conversion obtained for IPr at 5 % Ni loading (***Table 6***, entries 3 and 10) it was initially surprising that catalyst loading could not be lowered further than 2 % (entry 4). In this case, and although the reaction was performed over 20 hours, precipitation of the product was observed after 2 hours. When Ni loading was lowered to 1 %, almost complete inhibition was observed (entry 5). This observation (the same happens in the case of PCy_2(Bip), entries 10 & 11) suggests that catalyst deactivation probably occurs when substrate concentration far outweighs that of the catalyst. This could be due to catalyst poisoning by coordination of a second alkenylimidazolium to the metal centre via the alkene group. A similar observation was made in the intermolecular coupling of azolium salts with ethylene in the case of basic and bulky ligands (see this chapter, section **2.2.1.1**).

2.2.2.2 Attempts at coupling challenging substrates

As mentioned above, abnormal carbenes have emerged in the past few years and have shown similar redox chemistry to their C2-bound counterparts.[4] On this basis, one could expect that a C2-functionalised alkenylimidazolium salt such as **2i** would be suitable a substrate for the intramolecular alkenylation coupling. However, even under forcing conditions, no reaction was observed. This is likely be due to the difficulty of the oxidative addition step. Similarly, N-butenylimidazole did not undergo cyclisation (***Scheme 8***), indicating that some sort of activation (*e.g.* by Lewis or Brønsted acids) is required.

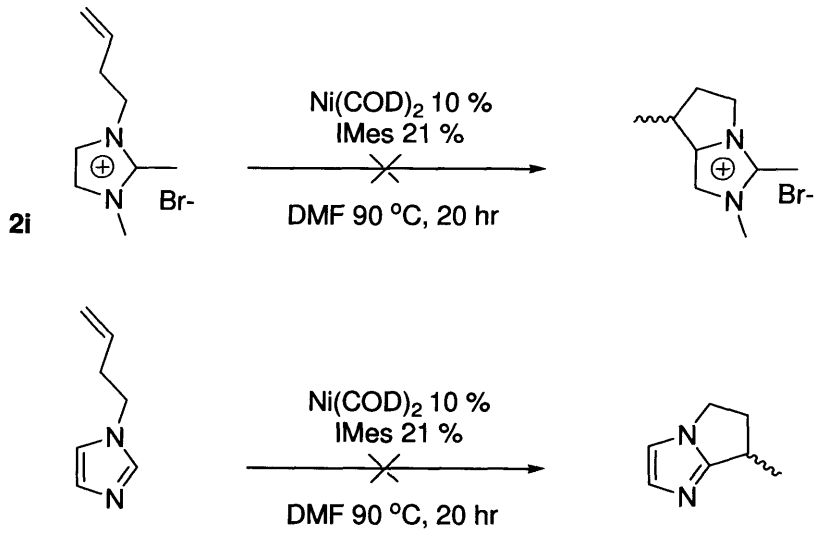

Scheme 8: *attempted coupling of challenging substrates*

2.2.2.3 Coupling using Pd catalysts

Pd catalysts were also found to promote the cyclisation of **2a**, albeit with significantly lower activity than the Ni system. The combination of 5 mol% $Pd(dba)_2$ and 2.1 eq. of IPr only gave 6 % coupled product at 70 °C (***Table 7***, entry 1). The use of the Buchwald phosphine was unsuccessful (entry 2), and raising the temperature to 90 °C only provided a slight increase in activity (entry 3).

Table 7: *catalytic Coupling Results with Pd(0) catalysts.*[a]

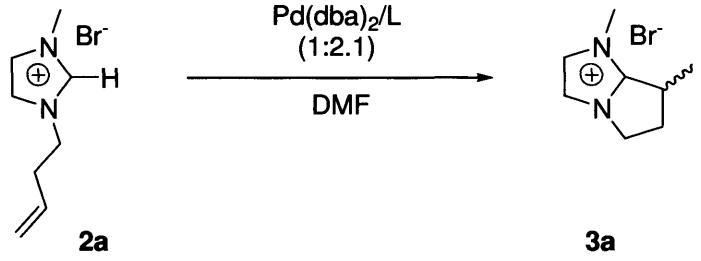

2a **3a**

Entry	Ligand	Temperature	Conv (%)[b]
1	IPr	70 °C	6
2	$PCy_2(Bip)$	70 °C	0
3	IPr	90 °C	20

[a] Reagents and conditions: $Pd(dba)_2$ (5 mol%), substrate (**2a**) 0.7 mmol, ligand 11 mol% , DMF (4 mL), 17 hr. [b] Determined by ^1H NMR spectroscopy, average of two runs.

Clearly, the Pd-catalysed version of this coupling reaction is much slower than the Ni one. This is unlikely to be due to slower reductive elimination as Pd has been found to eliminate 2-azolium salts more easily than Ni.[2, 3]

2.2.2.4 Towards chiral imidazolium salts

Despite the fact that the isolated fused-ring imidazolium salts **3a**, **3b** and **3h** are solids, they could potentially be modified by anion exchange to generate ionic liquids.[60, 61] ***Scheme 9*** shows an anion exchange reaction performed on **3a**.

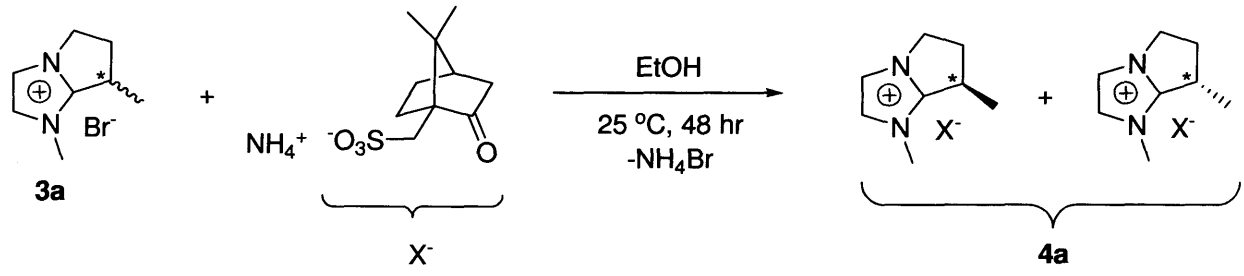

Scheme 9: *replacement of Br^- by (S)-10-camphorsulfonate in **3a**.*

Because **3a** and related compounds possess a chiral carbon situated at the β position from N, the resulting camphorsulfonate salt **4a** consists of a pair of diastereoisomers that one could selectively recrystallise to give an enantiomerically pure fused ring imidazolium salt. A second ion exchange on **4a**, for example by replacing camphorsulfonate with tetrafluoroborate BF_4^- or imidebis(triflate) NTf_2^-, would give a chiral ionic liquid.

It has not been possible so far to selectively recrystallise **4a**, thus preventing the application of this methodology for the preparation of chiral ILs. However, the formation of fused-ring imidazolium salts by intramolecular alkenylation would be an interesting methodology in itself if an asymmetric version could be developed. Therefore two chiral bidentate ligands ((S)-QUINAP and (R)-BINAP, ***Figure 18***) were tested in this reaction. [62]

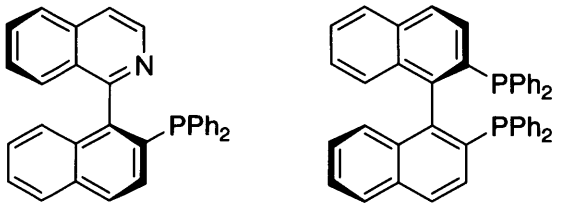

(S)-QUINAP *(R)-BINAP*

Figure 18: *chiral bidentate ligands tested in the cyclisation of* ***2a***

Unfortunately, although a reaction occurred, no conversion to **3a** was observed even at elevated temperatures, most probably because reductive elimination was prevented by the chelating effect of the ligands. The use of chiral monodentate NHCs and phosphines will thus have to be investigated in order to develop an asymmetric version of this reaction.

However, the formation of significant amounts (24% at 90 °C for (S)-QUINAP, 18 % for (R)-BINAP) of olefin isomerisation products **2a'** and **2a''** (***Scheme 10***) was observed. Z and E isomers were generated as a 50/50 mixture (see ^{1}H NMR spectra in appendix 2).

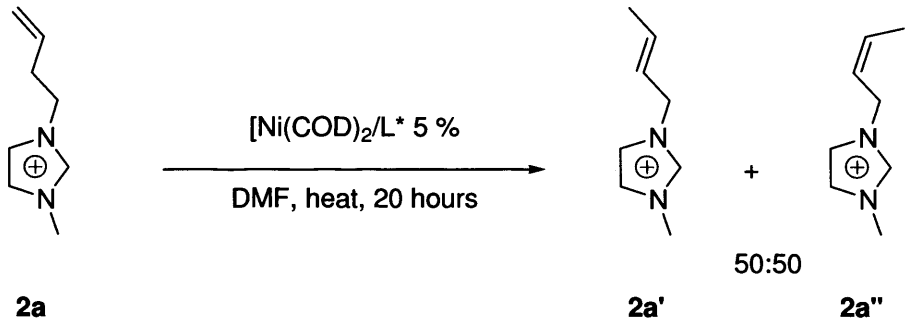

Scheme 10: *attempted asymmetric intramolecular coupling of* ***2a***

This result is extremely interesting, as it suggests the intermediacy of 5-coordinate Ni complexes, as shown in ***Figure 16***. A likely mechanism for the whole isomerisation sequence is depicted in ***Figure 19***.

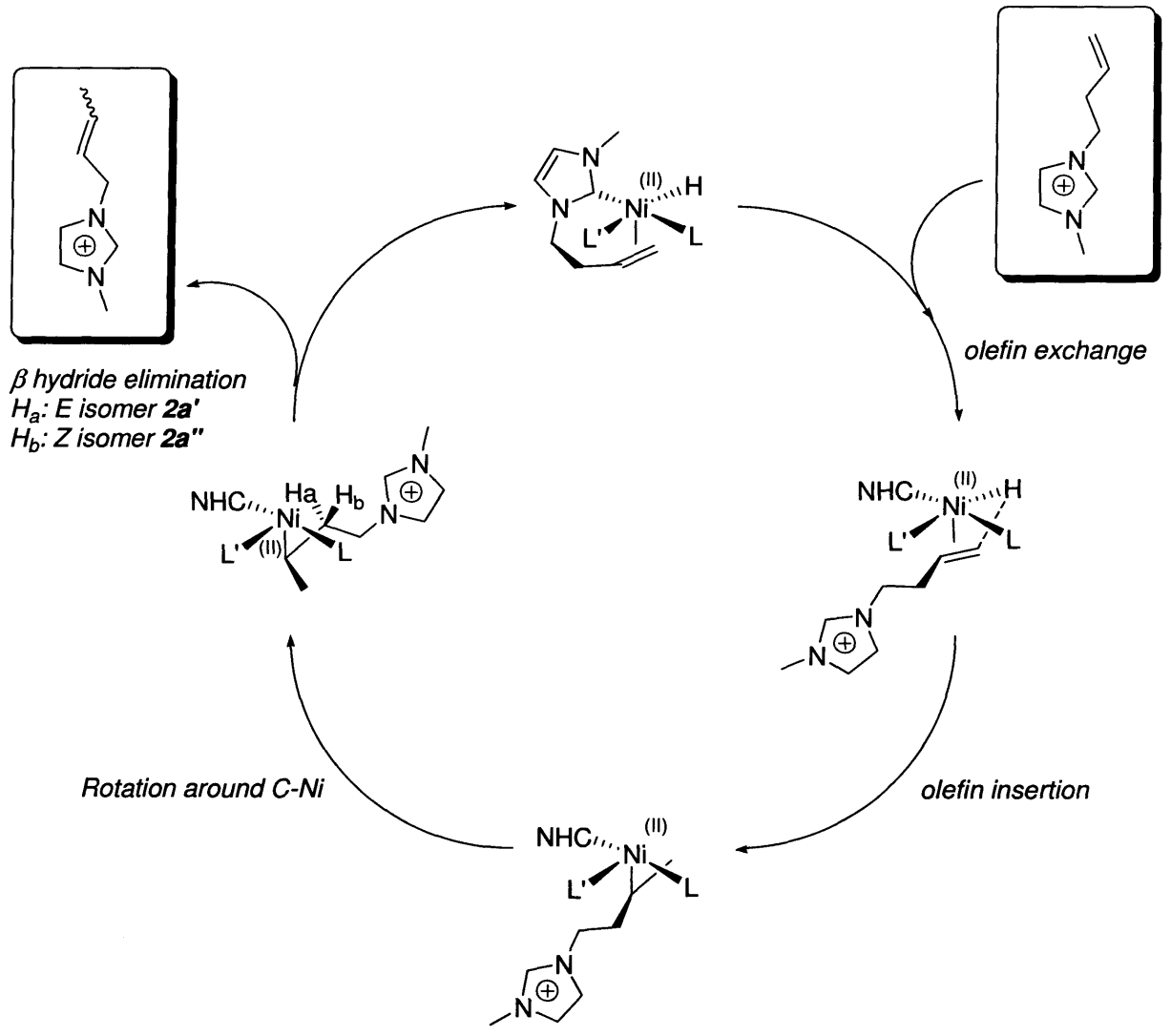

Figure 19: *proposed mechanism for the isomerisation of the olefinic part of* ***2a***

In this sequence, excess substrate coordinates to the Ni hydride intermediate. Anti-Markovnikov olefin insertion occurs, giving a σ-bound Ni alkylimidazolium. Rotation around the Ni-C bond followed by β hydride elimination of an hydrogen on the second methylene group of the imidazolium salt gives isomerisation products **2a'** and **2a"**. Whilst this mechanism explains the

isomerisation reaction and the absence of product **3a**, more work is needed in order to determine whether 5-coordinate Ni(II) intermediates do occur. The bromide anion could also play a role in the reaction.

It is worth noting the easy formation (starting from imidazolium salts) of hemilabile 5-coordinate Ni(II) hydrides (such as the one depicted in ***Figure 19***) as chiral catalysts for olefin isomerisation. This is an interesting prospect as olefin isomerisation can play an important role in homogeneously catalysed alkene transformation processes.[49] For example, the key step in the synthesis of (-)-menthol developed by Noyori is an asymmetric olefin isomerisation reaction (***Scheme 11***):[63, 64]

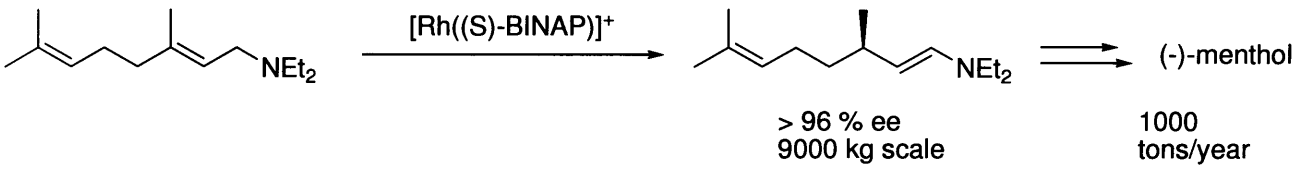

Scheme 11: *asymmetric olefin hydrogenation in the industrial synthesis of (-)-menthol*

2.2.2.5 Conclusions on the intramolecular alkenylation of imidazolium salts

A catalytic Ni(0)/Ni(II) redox sequence starting from alkenyl-substituted imidazolium salts has been applied to the construction of 5-membered fused ring imidazolium salts. This reaction occurs under mild conditions and represents a novel atom efficient catalytic reaction for the formation of substituted azolium salts. The fused ring products contain a chiral centre, and this feature can potentially be used to catalytically generate chiral ionic liquids in a minimum number of steps. Attempts at developing an asymmetric version for this reaction resulted in the isomerisation of the alkenyl side-chain by an intermolecular chain-walk mechanism.

Apart from its potential synthetic value, this reaction represents another example where imidazolium oxidative addition and carbene reductive elimination processes have been combined into the same catalytic cycle and illustrates the ease with which interconversion between azolium salts and N-heterocyclic carbene transition-metal complexes occurs even under mild conditions.

2.2.3 Coupling of neutral azoles

As mentioned above, direct functionalisation of azole heterocycles is related to the alkenylation of azolium salts developed in the Cavell group. ***Scheme 12*** shows how NH N-heterocyclic carbenes are related to N-alkyl NHCs such as those encountered in the reaction desribed in this chapter. It is worth noting that activation of the azole core by a Lewis acid (either stoichiometrically or catalytically) could achieve the same result.[65]

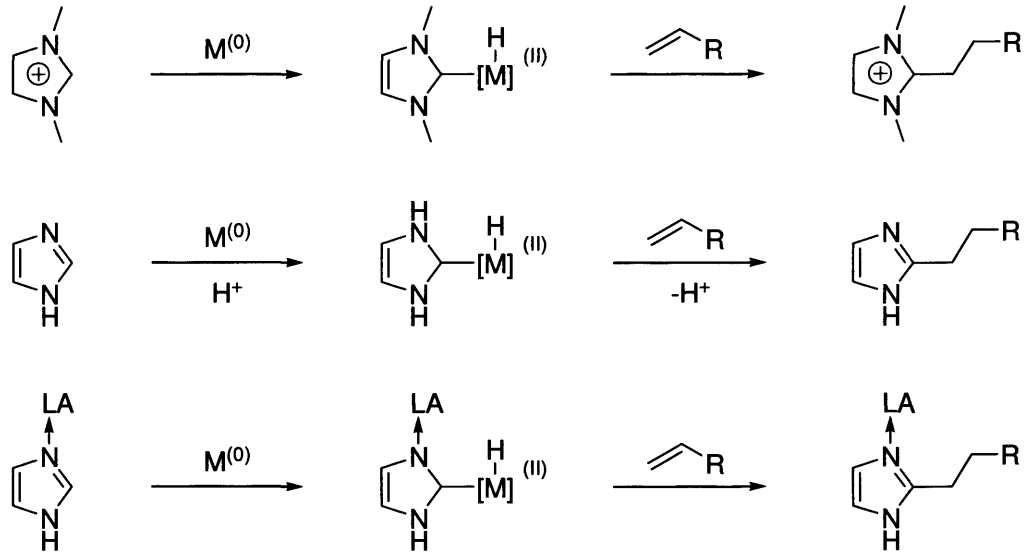

Scheme 12: *different mechanisms for the 2-alkenylation of azolium salts and neutral azoles*

As attempts at directly functionalising neutral azoles (such as N-methylimidazole) had failed,[66] and preliminary calculations indicated that oxidative addition of imidazole to Ni(0) would present a very large energy barrier,[67] one of the aims of this project was to explore the use of Lewis acids to activate azole heterocycles.

2.2.3.1 Activation with Lewis acids

A convenient way of qualitatively estimating the effect of Lewis acids on the acidity of the hydrogen atom at the C2 position of azoles is to measure the variations of the chemical shift of this proton by ^1H NMR spectroscopy. A larger difference from the chemical shift observed for free azoles should indicate greater acidification. Benzothiazole was found to be an especially suitable substrate for this purpose, since it readily formed soluble adducts in most deuterated solvents. Thus, ^1H NMR spectra of several benzothiazole-Lewis acid adducts (formed *in situ*) were recorded in $CDCl_3$ (***Table 8***). As a reference, entry 9 gives the value obtained with a Brønsted acid (*i.e.* HBF_4), and entry 10 gives that obtained for N-methylbenzothiazolium tetrafluoroborate.

Table 8: *C2-H chemical shift variation in $CDCl_3$ upon Lewis acid coordination to benzothiazole*

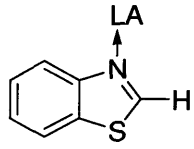

Entry	Lewis acid	C2-H Δδ (ppm)
1	LiOTf	0.09
2	$Mg(OTf)_2$	0.06
3	$Al(OTf)_3$	0.27
4	$Zn(OTf)_2$	0.32
5	**$AlCl_3$**	**0.57**
6	**$BF_3.Et_2O$**	**0.67**
7	**$B(C_6F_5)_3$**	**0.52**
8	**$B(OC_6F_5)_3$**	**1.07**
9	*HBF_4*	*0.69*
10	*"$Me^+BF_4^-$"*	*1.63*

Boron and aluminium based Lewis acids (entries 5-8 in bold) such as BF_3 or $Al(OTf)_3$ were found to induce the largest differences in chemical shifts relative to free benzothiazole. The influence of the solvent on the benzothiazole-$AlCl_3$ adduct was studied next (***Table 9***):

Table 9: *C2-H chemical shift variations in different solvents for benzothiazole-$AlCl_3$*

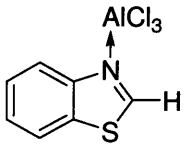

Entry	Solvent	C2-H Δδ
1	CD_2Cl_2	0.79
2	d_6-Acetone	0.98
3	d_6-DMSO	0.04
4	d_8-THF	0.08
5	d_3-MeCN	0.52

As expected, the variation in d_6-DMSO and d_8-THF was very small, probably because these solvents have a very strong affinity for Al(III) (due to the oxophilicity of this metal). Similar results would be expected with boron based Lewis acids. Therefore, B(III) and Al(III) Lewis acids were screened in the reaction of benzothiazole with ethylene in weakly coordinating solvents.

2.2.3.2 C2-ethylenation of benzothiazole

Table 10 summarises results obtained in the Ni-catalysed reaction of benzothiazole-Lewis acid adducts (formed *in situ* or introduced as an isolated solid in the case of the BF_3 adduct[68]) with ethylene. Only BF_3 (entries 1-6) gave satisfactory results, despite the fact that $B(C_6F_5)_3$ (entry 7) and $B(OC_6F_5)_3$ (entry 8) were also found to have a marked effect on the C2-H chemical shift of benzothiazole (***Table 8***). Perhaps the steric bulk of these species inhibits the reaction. The sensitivity

of the adducts towards oxygen containing coordinating solvent was reflected in the absence of conversion when DMF was used as a co-solvent with α,α,α-trifluorotoluene (BTF, entry 3).

Table 10: *Ni-catalysed C2 functionalisation of BF_3-activated benzothiazole*[a]

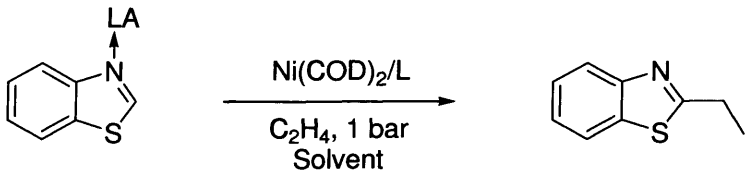

Entry	Lewis Acid	Ligand (eq/Ni)	Solvent	Conv. (%)[b]
1	BF_3	PCy_3 2.1 eq	BTF[c]	25
2	BF_3	PCy_3 1.1 eq	BTF	0
3	BF_3	PCy_3 2.1 eq	BTF/DMF (9:1)	0[d]
4	BF_3	IMes 2.1 eq	BTF	0
5	BF_3	PMe_2Ph 2.1 eq	BTF	28
6	BF_3	PMe_2Ph 2.1 eq	Toluene	50
7	$B(C_6F_5)_3$[e]	PCy_3 2.1 eq	BTF	0
8	$B(OC_6F_5)_3$[e]	PCy_3 2.1 eq	BTF	0

[a] *Reagents and conditions*: adduct 0.73 mmol, $Ni(COD)_2$ 10 mol%, Ligand x eq, solvent 3 mL, ethylene 1 bar 80 °C, 24 hr. Generally based on the average of two runs. [b] determined by GCMS. [c] α,α,α-trifluorotoluene. [d] 17 hr reaction. [e] 0.36 mmol of adduct was used.

The use of $Pd(dba)_2$ was also explored, as shown in ***Table 11***. Similarly to the Ni-catalysed reaction, bulky B(III) Lewis acids failed to give any conversion (entries 4 and 5). The use of $Al(OTf)_3$ (1 eq. added in situ) gave some activity (entry 3), as did that of BF_3 (entries 1 and 2).

Table 11:Pd-catalysed C2 functionalisation of BF_3-activated benzothiazole[a]

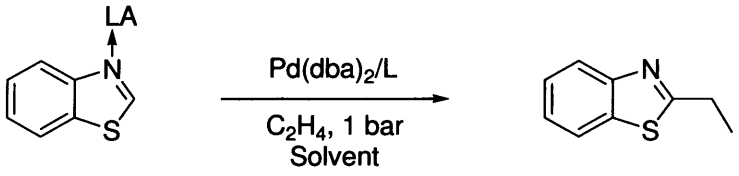

entry	Lewis Acid	Ligand (eq/Pd)	Solvent	Conv. (%)[b]
1	BF_3	PCy_3 21%	BTF[c]	45
2	BF_3	PCy_3 21%	Toluene	72
3	$Al(OTf)_3$	PCy_3 21%	BTF	46
4	$B(C_6F_5)_3$	PCy_3 21%	BTF	0
5	$B(C_6F_5)_3$	PCy_3 21%	BTF	0

[a] *Reagents and conditions*: adduct 0.73 mmol, $Ni(COD)_2$ 10 mol%, Ligand x eq, solvent 3 mL, ethylene 1 bar 80 °C, 24 hr. [b] Determined by GCMS, one run. [c] α,α,α-trifluorotoluene.

2.2.3.3 Conclusions on the coupling of neutral azoles

Attempts at applying the azolium alkenylation methodology to neutral azoles was met with limited success. B(III) and Al(III) Lewis acids used as stoichiometric additives enabled the Pd and Ni catalysed reaction to proceed, albeit with low TONs. However, the potential of direct methodologies for the functionalisation of heterocycles warrants a continued research effort in this direction.

2.3 Experimental Section

2.3.1 General conditions

All manipulations were carried out using standard Schlenk techniques under Ar or N_2 atmosphere, or using an MBRAUN M72 glovebox (N_2 atmosphere with <1 ppm O_2 and H_2O). THF and toluene were dried and freshly distilled before use (sodium benzophenone ketyl and sodium metal respectively). Acetone was dried and distilled over B_2O_3 and stored under inert atmosphere. Anhydrous DMF and NMP were purchased from Aldrich and transferred under Ar to a Young's Schlenk containing activated 4Å molecular sieve. Phosphine ligands were purchased from STREM. ^1H and ^{13}C NMR chemical shifts values are reported relative to tetramethylsilane using residual solvent peaks as a reference.[69]

NHC ligands were synthesised using reported procedures.[70] $Ni(COD)_2$ was synthesised from $Ni(acac)_2$ according to a known procedure,[71] except a larger excess of COD (3.5 eq) was used instead of the much more hazardous 1,3-butadiene.

Benzothiazole was purchased from Aldrich and purified by distillation under reduced pressure. Benzothiazole-BF_3 adduct was prepared according to a reported literature procedure.[68] Alkenylimidazolium salts **1a-2e** and **2a-2H** were synthesized using the procedure devised by Swee Kuan Yen during her time in our group.[72]

2.3.2 Procedures for the catalytic and reactivity studies

2.3.2.1 Procedure for ^{1}H NMR spectroscopy of benzothiazole-Lewis acid adducts

Benzothiazole (10 mg, 0.074 mmol, 1eq) and a Lewis acid (0.22 mmol, 3 eq, except for BF_3 where an equimolar amount of $BF_3.Et_2O$ was added) were mixed in the relevant deuterated solvent and submitted for ^{1}H NMR spectroscopy on a Bruker Avance 400 spectrometer (400.13 MHz, 298 K).

2.3.2.2 Procedure for the intermolecular functionalisation of azolium salts and Lewis acid activated azoles

A 60 ml Young's Schlenk was charged with bis-(cycloocta-1,5-diene) nickel(0) (20 mg, 0.073 mmol, 10 mol% in most cases), or $Pd(dba)_2$ (44 mg, 0.073 mmol, 10 mol%), a phosphine or NHC ligand (0.15 mmol, 21 mol%), and the substrate (0.73 mmol, 1 eq) in a glove box. The solvent (DMF in most cases) was then syringed under a flow of ethylene (or argon when a liquid olefin was used as coupling partner) into the reaction vessel and the orange/yellow solution heated to reaction temperature (80 °C in most cases). In the case of ethylene, the vessel was then pressurised to 1 bar with ethylene and closed. The solution was stirred for the required time (5 hr in most cases). The solvent was then removed *in vacuo* and the residue dissolved in d_6-DMSO and submitted for ^{1}H NMR spectroscopy.

2.3.2.3 Procedure for the intramolecular functionalisation of azolium salts.

A 60 ml Young's Schlenk was charged with *bis*(cycloocta-1,5-diene)nickel(0) (10 mg, 0.037 mmol, 5 mol% in most cases), or $Pd(dba)_2$ (44 mg, 0.073 mmol, 10 mol%), a phosphine or NHC ligand (0.077 mmol, 11 mol%), and the substrate (0.73 mmol, 1 eq) in a glove box. DMF was then syringed into the reaction vessel under a flow argon and the yellow solution was heated to reaction temperature (50 °C in most cases). The solution was stirred for the required time (1 hour in most

cases). The solvent was then removed *in vacuo* and the residue dissolved in d_6-DMSO and submitted for ^{1}H NMR spectroscopy.

2.3.3 Synthesis of new imidazolium salts

2.3.3.1 Synthesis of 1-(3-butenyl)-2,3-dimethylimidazolium bromide 2i

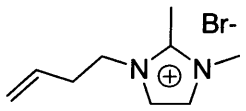

2i

1,2-Dimethylimidazole (1.941 g, 20.20 mmol, 1 eq) and 4-bromobut-1-ene (3.00 g, 22.22 mmol, 1.1 eq) were heated at 70 °C in a sealed pressure tube for 16 hours. The reaction mixture was cooled to room temperature, and excess 4-bromobut-1-ene was removed. The resulting yellow oil was washed 5 times with 10 mL of pre-dried Et_2O (HPLC grade, stored on Na wire) and dried under vacuum to afford a hygroscopic beige powder. The collected mass was 4.34 g (93 %) and the batch number was AN/570/C.

^{1}H NMR (d_6-DMSO, 500.13 MHz): δ (ppm) 7.69 (d, 1H, NCH, $^3J_{HH}$= 2.1 Hz), 7.66 (d, 1H, NCH, $^3J_{HH}$= 2.1 Hz), 5.74-5.84 (m, 1H, internal olefinic CH), 5.03-5.09 (m, 2H, terminal olefinic CH), 4.22 (t, 2H, NCH_2, $^3J_{HH}$= 7.0 Hz), 3.76 (s, 2H, NCH_3), 2.60 (s, 2H, CH_3), 2.45-2.52 (m, 2H, overlapping with solvent signal, CH_2).

^{13}C NMR ($CDCl_3$, 125.03 MHz): δ (ppm) 142.84 (s, NCN), 131.61 (s, internal olefinic CH), 122.00 (s, NCH), 120.61 (s, NCH), 118.58 (s, terminal olefinic CH), 47.22 (s, NCH_3), 35.24 (s, NCH_2), 33.21 (s, CH_3), 10.27 (s, CH_2).

High Resolution ESI_{pos}-MS (MeCN): found 151.1241 (calc 151.1235 dev: 4.0 ppm).

Anal. Calc. for $C_9H_{15}N_2Br$ (Mw = 231.13): C, 46.77; H, 6.54; N, 12.12; Br, 34.57. Found: C, 45.70; H, 6.44; N, 11.18; Br, 34.30. Off limits, probably due to an N-methylimidazolium impurity (seen by ^{1}H NMR spectroscopy).

2.3.3.2 Synthesis of *Rac*-1,7-dimethyl-6,7-dihydro-5H-pyrrole[1,2-α]imidazolium bromide 3a

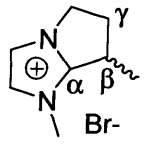

3a

This compound was isolated from the crude reaction mixture (*vide supra*) by precipitation from acetone. It was then dissolved in DCM and the solution was filtered through Celite®. Concentration of the filtrate followed by trituration in acetone/Et_2O afforded the pure compound in 80% yield (when the conversion was 100 %).

^{1}H NMR (D_2O, 500.13 MHz): δ (ppm) 7.24 (s, 2H, NCH), 4.23-4.28 (m, 1H, NCH_2), 4.10-4.15 (m, 1H, NCH_2), 3.77 (s, 2H, CH_3), 3.59-3.65 (m, 1H, CH *β* to N), 2.92-2.98 (m, 1H, CH_2 *γ* to N, H *anti* to CH_3), 2.34-2.40 (m, 1H, CH_2 *γ* to N, H *syn* to CH_3), 1.39 (d, 2H, CH_3, $^3J_{HH}$= 10.0 Hz). Chemical shifts of hydrogens on the carbon atom *γ* to N assigned by analogy with those of **3h** (obtained by gs-NOESY experiments).

^{13}C NMR (D_2O, 125.03 MHz): δ (ppm) 154.63 (s, NCN), 126.84 (s, NCH), 117.07 (s, NCH), 46.78 (s, NCH_2), 34.74 (s, NCH_3), 34.33 (s, CH *β* to N), 31.12 (s, CH_2 *γ* to N), 15.73 (s, CH_3).

High Resolution ESI_{pos}-MS (MeCN): found 137.1075 (calc 137.1079 dev: -2.9 ppm).

Anal. Calc. for $C_8H_{13}N_2Br$ (Mw = 217.11): C, 44.26; H, 6.04; N, 12.90. Found: C, 43.92; H, 6.04; N, 12.88.

2.3.3.3 Synthesis of 1,7-dimethyl-6,7-dihydro-5H-pyrrole[1,2-α]imidazolium (S)-10-camphorsulfonate 4a

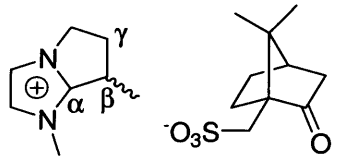

4a

Ammonium (S)-10-camphorsulfonate (1306 mg, 5.24 mmol, 1 eq) and **3a** (562 mg, 2.62 mmol, 1eq) were suspended in 10 mL of absolute EtOH. This mixture was stirred for 2 days at room temperature. It was then filtered through Celite®, evaporated, and the residue was suspended in 10 mL of a 5:1 mixture of DCM/EtOH. The insoluble ammonium (S)-10-camphorsulfonate was removed by filtration over Celite® and the solution was concentrated by evaporation. The resulting solid was triturated in acetone/Et_2O to afford a white solid. The collected mass was 872 mg (90 %) and the batch number was AN/576/A.

^{1}H NMR (D_2O, 500.13 MHz): δ (ppm) 7.16 (d, 2H, NCH overlapping with other NCH, $^3J_{HH}$= 1.9 Hz), 7.15(d, 2H, NCH overlapping with other NCH, $^3J_{HH}$= 1.9 Hz), 4.13-4.20 (m, 1H, NCH_2), 4.01-4.07 (m, 1H, NCH_2), 3.69 (s, 2H, CH_3), 3.46-3.55 (m, 1H, CH *β* to N), 3.16 (d, 1H, $CH_2SO_3^-$, $^2J_{HH}$= 14.9 Hz), 2.83-2.91 (m, 1H, CH_2 *γ* to N, H *anti* to CH_3), 2.75 (d, 1H, $CH_2SO_3^-$, $^2J_{HH}$= 14.9 Hz), 2.30-2.34 (m, 1H, CH_2 *γ* to N, H *syn* to CH_3), 2.24-2.35 (m, 3H), 2.04 (t, 1H, $COCH_2$, $^3J_{HH}$= 4.5 Hz), 1.94 (m, 1H, bridgehead CH), 1.89 (s, 1H, camphorsulfonate CCH_2), 1.85 (s, 1H, camphorsulfonate CH_2), 1.53 (m, 1H, camphorsulfonate CH_2), 1.34 (m 1H, camphorsulfonate CH_2), 1.30 (d, 2H, imidazolium CH_3, $^3J_{HH}$= 7.1 Hz), 0.92 (s, 2H, camphorsulfonate CH_3), 0.72 (s, 2H, camphorsulfonate CH_3). Chemical shifts of hydrogens on the carbon atom *γ* to N assigned by analogy with those of **2c** (obtained by gs-NOESY experiments)

^{13}C NMR (D_2O, 125.03 MHz): δ (ppm) 154.70 (s, NCN), 126.99 (s, NCH), 117.27 (s, NCH), 58.61 (s, CO), 48.25 (s, bridging C), 47.25 (s, $CH_2SO_3^-$), 46.95 (s, NCH_2), 42.71 (s,

camphorsulfonate CH_2), 42.38 (s, bridgehead CH), 34.76 (s, NCH_3), 34.44 (s, CH β to N), 31.15 (s, CH_2 γ to N), 26.31 (s, camphorsulfonate CH_2), 24.67 (s, camphorsulfonate CH_2), 19.03 (s, camphorsulfonate CH_3), 18.89 (s, camphorsulfonate CH_3), 15.82 (s, CH_3).

High Resolution ESI_{pos}-MS (MeCN): found 137.1075 (calc. 137.1079 dev: -2.9 ppm).

2.3.3.4 Synthesis of *Rac*-1-methyl-7-isopropyl-6,7-dihydro-5H-pyrrole[1,2-α]imidazolium bromide 3h

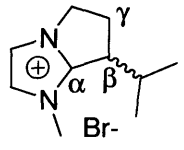

3h

This compound was isolated following the same procedure as that employed for the isolation of 1-7-dimethyl-6,7-dihydro-5H-pyrrole[1,2-α]imidazolium bromide **3a**. The isolated yield was 85 % (when the conversion was 100 %).

^{1}H NMR (CD_2Cl_2, 500.13 MHz): δ (ppm) 7.56 (d, 1H, NCH, $^3J_{HH}$= 1.9 Hz), 7.44 (d, 1H, NCH, $^3J_{HH}$= 1.9 Hz), 4.27-4.33 (m, 1H, NCH_2), 4.13-4.19 (m, 1H, NCH_2), 3.88 (s, 2H, CH_3), 3.73 (m, 1H, CH β to N), 2.78-2.87 (m, 1H, CH_2 γ to N, H *anti* to ^{i}Pr), 2.43-2.51 (m, 1H, CH_2 γ to N, H *syn* to ^{i}Pr), 2.26-2.36 (m, 1H, ^{i}Pr CH), 0.99 (d, 2H, ^{i}Pr CH_3, $^3J_{HH}$= 6.9 Hz), 0.73 (d, 2H, ^{i}Pr CH_3, $^3J_{HH}$= 6.8 Hz). Chemical shifts were assigned on the basis of gs-NOESY experiments (see appendix 3).

^{13}C NMR (D_2O, 125.03 MHz): δ (ppm) 153.80 (s, NCN), 127.22 (s, NCH), 117.34 (s, NCN), 47.53 (s, NCH_2), 42.26 (s, CH β to N), 34.82 (s, NCH_3), 29.16 (s, ^{i}Pr CH), 27.28 (s, CH_2 γ to N), 19.59 (s, ^{i}Pr CH_3), 16.48 (s, ^{i}Pr CH_3).

High Resolution ESI_{pos}-MS (MeCN): found 165.1385 (calc 165.1392 dev: -4.2 ppm).

Anal. Calc for $C_{10}H_{17}N_2Br$ (Mw = 245.16): C, 48.99; H, 6.99; N, 11.43. Found: C, 48.77; H, 6.95; N, 11.38.

2.4 Bibliography and notes

1. Crudden, C. M.; Allen, D. P., *Coord. Chem. Rev.* **2005,** 248, 2247-2273.
2. McGuinness, D. S.; Saendig, N.; Yates, B. F.; Cavell, K. J., *J. Am. Chem. Soc.* **2001,** 123, 4029-4040.
3. Cavell, K. J.; McGuinness, D. S., *Coord. Chem. Rev.* **2004,** 248, 671-679.
4. Bacciu, D.; Cavell, K. J.; Fallis, I. A.; Ooi, L.-l., *Angew. Chem. Int. Ed.* **2005,** 44, 5282-5284.
5. Graham, D. C.; Cavell, K. J.; Yates, B. F., *Dalton. Trans.* **2005**, 1093-1100.
6. McGuinness, D. S.; Cavell, K. J.; Yates, B. F.; Skelton, B. W.; White, A. H., *J. Am. Chem. Soc.* **2001,** 123, 8317-8328.
7. Hawkes, K. J.; McGuinness, D. S.; Cavell, K. J.; Yates, B. F., *Dalton. Trans.* **2004**, 2505-2513.
8. Clement, N. D.; Cavell, K. J.; Jones, C.; Elsevier, C. J., *Angew. Chem. Int. Ed.* **2004,** 43, 1277-1279.
9. McGuinness, D. S.; Cavell, K. J.; Yates, B. F., *Chem. Commun.* **2001**, 355-356.
10. Clement, N. D.; Cavell, K. J., *Angew. Chem. Int. Ed.* **2004,** 43, 3845-3847.
11. Dupont, J.; Spencer, J., *Angew. Chem. Int. Ed.* **2004,** 43, 5296-5297.
12. Xu, L.; Chen, W.; Xiao, J., *Organometallics* **2000,** 19, 1123-1127.
13. McLachlan, F.; Mathews, C. J.; Smith, P. J.; Welton, T., *Organometallics* **2003,** 22, 5350-5357.
14. Aggarwal, V. K.; Emme, I.; Mereu, A., *Chem. Commun.* **2002**, 1612-1613.
15. Duin, M. A.; Clement, N. D.; Cavell, K. J.; Elsevier, C. J., *Chem. Commun.* **2003**, 400-401.
16. Viciano, M.; Mas-Marzá, E.; Poyatos, M.; Sanaú, M.; Crabtree, R. H.; Peris, E., *Angew. Chem. Int. Ed.* **2005,** 44, 444-447.
17. Ott, L. S.; Cline, M. L.; Deetlefs, M.; Seddon, K. R.; Finke, R. G., *J. Am. Chem. Soc.* **2005,** 127, 5758-5759.
18. Chianese, A. R.; Kovacevic, A.; Zeglis, B. M.; Faller, J. W.; Crabtree, R. H., *Organometallics* **2004,** 23, 2461-2468.
19. Lebel, H.; Janes, M. K.; Charette, A. B.; Nolan, S. P., *J. Am. Chem. Soc.* **2004,** 126, 5046-5047.
20. Clarke, M. J.; Taube, H., *J. Am. Chem. Soc.* **1975,** 97, 1397-1403.
21. Sini, G.; Eisenstein, O.; Crabtree, R. H., *Inorg. Chem.* **2002,** 41, 602-604.
22. Tan, K. L.; Bergman, R. G.; Ellman, J. A., *J. Am. Chem. Soc.* **2002,** 124, 3202-3203.
23. Sanderson, M. D.; Kamplain, J. W.; Bielawski, C. W., *J. Am. Chem. Soc.* **2006,** 128, 16514-16515.
24. Doris, K., *Angew. Chem. Int. Ed.* **2007,** 46, 3405-3408.
25. Ruiz, J.; Perandones, B. F., *J. Am. Chem. Soc.* **2007,** 129, 9298-9299.
26. Wilson, R. M.; Thalji, R. K.; Bergman, R. G.; Ellman, J. A., *Org. Lett.* **2006,** 8, 1745-1747.
27. Wiedemann, S. H.; Lewis, J. C.; Ellman, J. A.; Bergman, R. G., *J. Am. Chem. Soc.* **2006,** 128, 2452-2462.
28. Wiedemann, S. H.; Ellman, J. A.; Bergman, R. G., *J. Org. Chem.* **2006,** 71, 1969-1976.
29. Lewis, J. C.; Wu, J. Y.; Bergman, R. G.; Ellman, J. A., *Angew. Chem. Int. Ed.* **2006,** 45, 1589-1591.
30. Colby, D. A.; Bergman, R. G.; Ellman, J. A., *J. Am. Chem. Soc.* **2006,** 128, 5604-5605.
31. Thalji, R. K.; Ahrendt, K. A.; Bergman, R. G.; Ellman, J. A., *J. Org. Chem.* **2005,** 70, 6775-6781.
32. Wiedemann, S. H.; Bergman, R. G.; Ellman, J. A., *Org. Lett.* **2004,** 6, 1685-1687.
33. Tan, K. L.; Ellman, J. A.; Bergman, R. G., *J. Org. Chem.* **2004,** 69, 7329-7335.
34. Lewis, J. C.; Wiedemann, S. H.; Bergman, R. G.; Ellman, J. A., *Org. Lett.* **2004,** 6, 35-38.

35. Tan, K. L.; Vasudevan, A.; Bergman, R. G.; Ellman, J. A.; Souers, A. J., *Org. Lett.* **2003,** 5, 2131-2134.
36. Tan, K. L.; Bergman, R. G.; Ellman, J. A., *J. Am. Chem. Soc.* **2002,** 124, 13964-13965.
37. the Rh(III) hydride is probably generated by protonation of the Rh(I) NHC intermediate. This might explain why the reaction does not proceed if PCy_3 alone is used as the source of ligand.
38. Lewis, J. C.; Bergman, R. G.; Ellman, J. A., *J. Am. Chem. Soc.* **2007,** 129, 5332-5333.
39. Sheldon, R., *Chem. Commun.* **2001**, 2399-2407.
40. Wasserscheid, P.; Keim, W., *Angew. Chem. Int. Ed.* **2000,** 39, 3772-3789.
41. Chiappe, C.; Pieraccini, D., *J. Phys. Org. Chem.* **2005,** 18, 275-297.
42. Jain, N.; Kumar, A.; Chauhan, S.; Chauhan, S. M. S., *Tetrahedron* **2005,** 61, 1015-1060.
43. Zeitler, K., *Angew. Chem. Int. Ed.* **2005,** 44, 7506-7510.
44. Normand, A. T.; Hawkes, K. J.; Clement, N. D.; Cavell, K. J.; Yates, B. F., *in press, Organometallics.*
45. see ref 44 for computational details.
46. Tolman, C. A., *J. Am. Chem. Soc.* **1970,** 92, 2953-2956.
47. Tolman, C. A., *J. Am. Chem. Soc.* **1970,** 92, 2956-2965.
48. Tolman, C. A., *Chem. Rev.* **1977,** 77, 313-348.
49. Crabtree, R. H., *The organometallic chemistry of the transition metals.* 3rd ed.; Wiley: New York, 2000.
50. Diez-Gonzalez, S.; Nolan, S. P., *Coord. Chem. Rev.* **2007,** 251, 874-883.
51. Dorta, R.; Stevens, E. D.; Scott, N. M.; Costabile, C.; Cavallo, L.; Hoff, C. D.; Nolan, S. P., *J. Am. Chem. Soc.* **2005,** 127, 2485-2495.
52. Hillier, A. C.; Sommer, W. J.; Yong, B. S.; Petersen, J. L.; Cavallo, L.; Nolan, S. P., *Organometallics* **2003,** 22, 4322-4326.
53. Louie, J.; Gibby, J. E.; Farnworth, M. V.; Tekavec, T. N., *J. Am. Chem. Soc.* **2002,** 124, 15188-15189.
54. Ogoshi, S.; Ueta, M.; Oka, M.-A.; Kurosawa, H., *Chem. Commun.* **2004**, 2732-2733.
55. Campeau, L.-C.; Thansandote, P.; Fagnou, K., *Org. Lett.* **2005,** 7, 1857-1860.
56. Graham, D. C.; Cavell, K. J.; Yates, B. F., *Dalton. Trans.* **2006**, 1768-1775.
57. some of the results obtained by Mrs Yen could not be reproduced; notably compound **3h** was isolated and fully characterised despite her failure to do so.
58. rearrangement is unnecessary in this case, as the required conformation can be achieved for olefin insertion.
59. the product was not isolated. Conversion was determined by ^{1}H NMR of the crude reaction mixture.
60. Ni, B.; Garre, S.; Headley, A. D., *Tetrahedron Lett.* **2007,** 48, 1999-2002.
61. Kan, H.-C.; Tseng, M.-C.; Chu, Y.-H., *Tetrahedron* **2007,** 63, 1644-1653.
62. reaction conditions: 0.7 mmol of **2a**, 5 % of Ni $(COD)_2$, 5.5 % of ligand, 20 hours, 50 to 90 °C in DMF.
63. Noyori, R., *Angew. Chem. Int. Ed.* **2002,** 41, 2008-2022.
64. Ohta, T.; Takaya, H.; Kitamura, M.; Nagai, K.; Noyori, R., *J. Org. Chem.* **1987,** 52, 3174-3176.
65. Bergman made the same hypothesis when developing his reaction, see ref. 33. However only the use of Brønsted acids proved successful in this case.
66. N. C. Clement and K. J. Cavell, unpublished results.
67. K. J. Hawkes and B. F. Yates, unpublished results.
68. Smith, V. C. M.; Aplin, R. T.; Brown, J. M.; Hursthouse, M. B.; Karalulov, A. I.; Malik, K. M. A.; Cooley, N. A., *J. Am. Chem. Soc.* **1994,** 116, 5180-5189.
69. Gottlieb, H. E.; Kotlyar, V.; Nudelman, A., *J. Org. Chem.* **1997,** 62, 7512-7515.

70. Anthony J. Arduengo, I.; Krafczyk, R.; Schmutzler, R.; Craig, H. A.; Goerlich, J. R.; Marshall, W. J.; Unverzagt, M., *Tetrahedron* **1999,** 55, 14523-14534.
71. Schunn, R. A., *Inorganic Syntheses* **1974,** 15, 5-9.
72. Normand, A. T.; Yen, S. K.; Stasch, A.; Cavell, K. J.; Huynh, H. V.; Hor, T. S. A., *manuscript in preparation.*

3 Chapter three: Synthesis and Characterisation of Cationic π-allyl Mixed Phosphine-NHC Pd(II) Complexes

3.1 Background

Cationic palladium(II) π-allyl complexes have attracted considerable attention over the years,[1-6] mainly due to their reactivity towards nucleophiles, which makes them excellent catalysts for the so-called Tsuji-Trost reaction (***Figure 1***).[7-14]

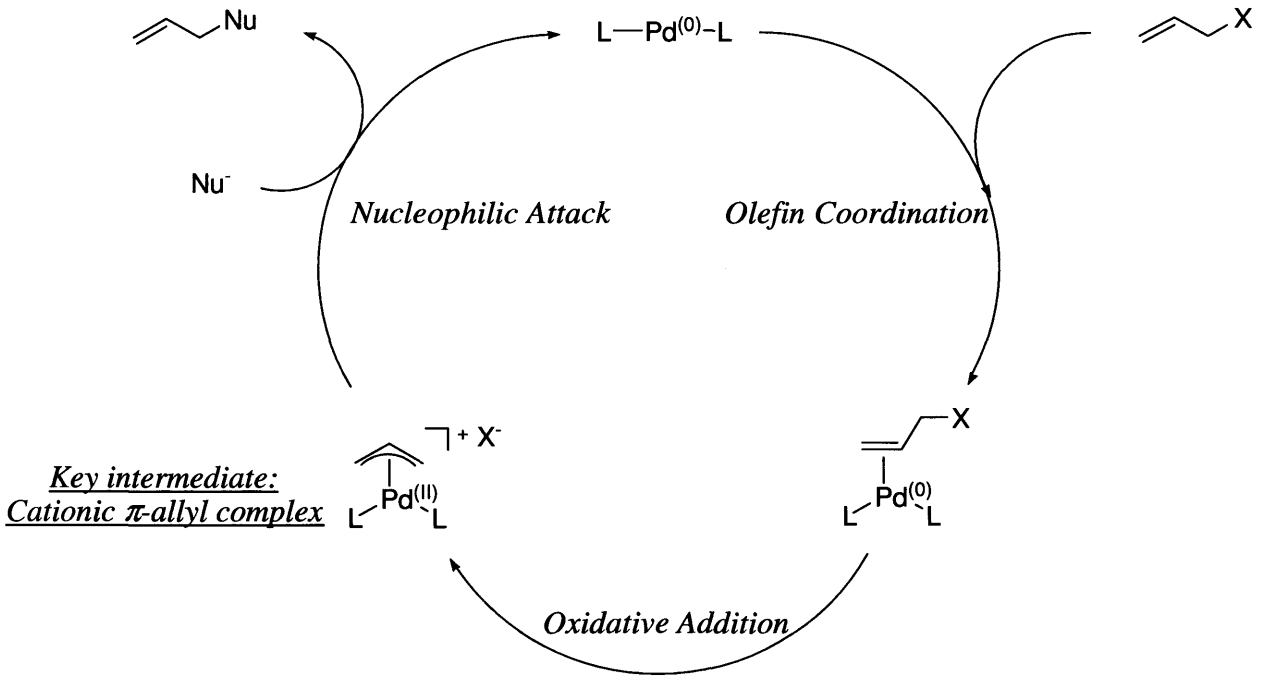

Figure 1: *"textbook" mechanism of the Pd-catalysed allylic alkylation (Tsuji-Trost) reaction*

Transition metal allyl complexes can exist in two coordination modes, η^1 (acting as an anionic, or X, 2e ligand) and η^3 (acting as a mixed, or LX, 4e ligand). An interesting feature of such compounds is their tendency to undergo η^3-η^1-η^3 rearrangements (***Scheme 1***):

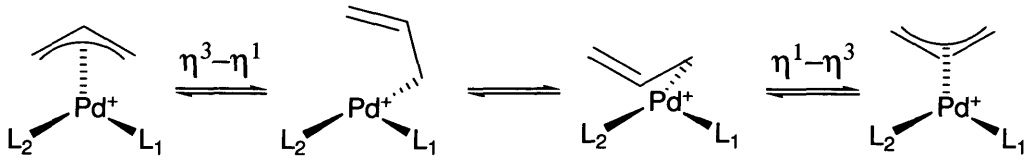

Scheme 1: *η^3-η^1-η^3 rearrangement in cationic Pd(II) complexes*

This behaviour can be observed directly by NOESY spectroscopy in the case of complexes bearing a chiral chelating bis(phosphine) ligand (see Chapter 3.2).[15, 16] Allyl decoordination occurs under steric or electronic control and may happen exclusively *trans* to either L_1 or L_2. It is followed by either rotation around the Pd-C, or the C-C bond of the allyl.[13, 14, 17, 18] It is worth noting that a recent computational study suggested cationic η^1-allyl palladium complexes are feasible intermediates in palladium catalyzed reactions,[19] and that an example of a neutral η^1-allyl complex with a bidentate P,N ligand has been isolated by Helmchen (***Figure 2***):[20]

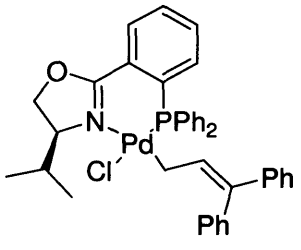

Figure 2: *isolated η^1-allyl complex*[20]

NHC-containing Pd(II) π-allyl complexes have been known for some time (***Figure 3***). They have mainly been developed by Nolan as telomerisation and cross-coupling catalysts, and have shown unprecedented catalytic activity in their latest generation (***Scheme 2***).[21-24]

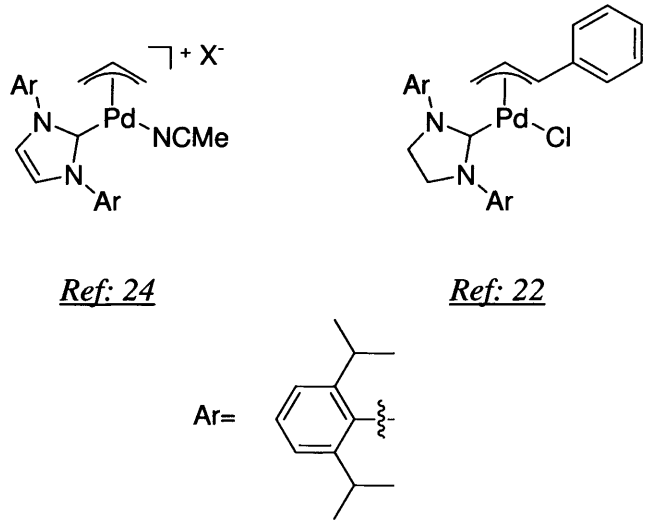

Ref: 24 *Ref: 22*

Figure 3: *previously reported examples of Pd(II) NHC π-allyl complexes*

Such complexes were reported to be air and moisture stable. They are also stable towards reductive elimination of 2-propenylimidazolium,[23] which raises the question as to whether they undergo η^3-η^1-η^3 rearrangement at all.

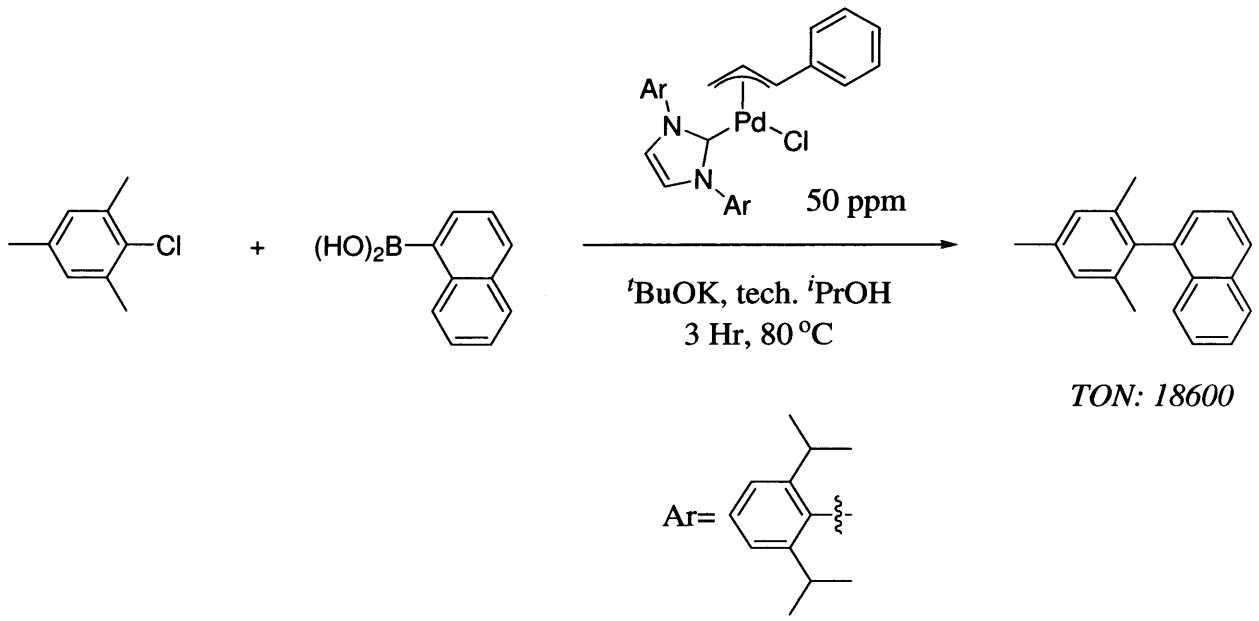

Scheme 2: *highly efficient Suzuki-Miyaura coupling of challenging substrates with a Pd(II) NHC π-allyl complex.*[22]

It would be interesting to selectively prevent or trigger reductive elimination in complexes where either L_1 or L_2 is an NHC (***Figure 4***). This goal is in line with previous (Nicolas Clement and David McGuinness[25-29]) and current work within the group (this PhD project, see Chapter 2), as in the case of L_1= tertiary phosphine and L_2= NHC, reductive elimination would generate "monoligated"[30] phosphine-Pd(0) complexes (***Figure 4***). Such species are believed to be the active catalysts in the Pd-catalysed coupling reaction of azolium salts with olefins (see Chapter 2).

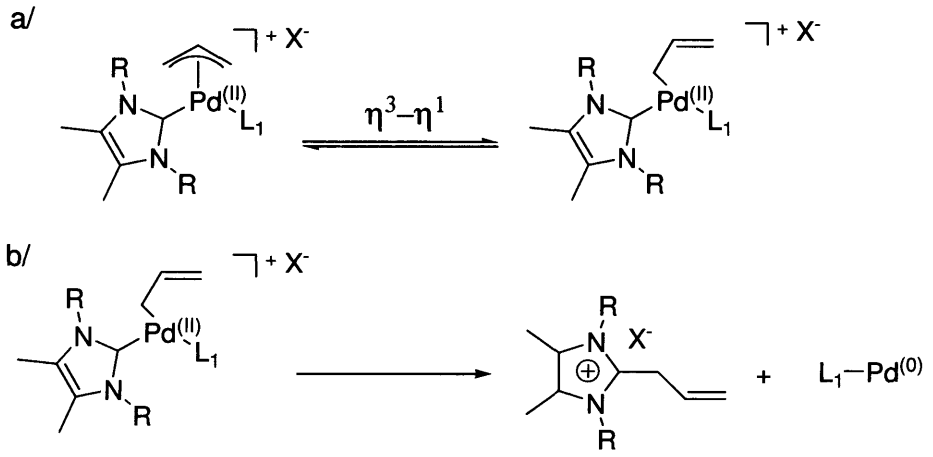

Figure 4: *hypothetical reductive elimination of 2-propenylimidazolium from a Pd-π-allyl complex following* η^3-η^1 *rearrangement.*

So-called monoligated Pd(0) species have attracted attention due to their supposed involvement in a number of Pd-catalysed reactions,[31-33] and their generation by activation of mixed phosphine/NHC Pd(II) complexes was deemed an interesting prospect. In the case of Nolan's work (***Scheme 2***), a monoligated NHC-Pd(0) intermediate is likely to be the active catalyst, and as a result the precatalyst has to be activated by the base present in the reaction medium, *i.e.* ^{t}BuOK.[22, 23] It would be a decisive advantage if one could use a preacatalyst without the need for an external activator. This would represent a major step towards a "universal cross-coupling catalyst", a concept recently introduced by Organ with the PEPPSI-IPr complex (***Figure 5***).[34, 35 36]

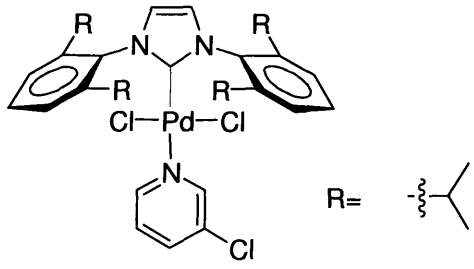

Figure 5: *PEPPSI-IPr precatalyst*

In this chapter a general synthetic route is presented for this new family of Pd(II) π-allyl complexes containing both a phosphine and a carbene ligand. The results of investigations of their solid-state and solution structures will also be presented (by X-ray diffraction and 2D NMR spectroscopy: HSQC and NOESY).

3.2 Synthesis of compounds of general formula [Pd(π-allyl)(NHC)(L)]BF_4.

The synthesis of title compounds [Pd(π-allyl)(NHC)(L)]BF_4 was initially planned according to *Scheme 3*:

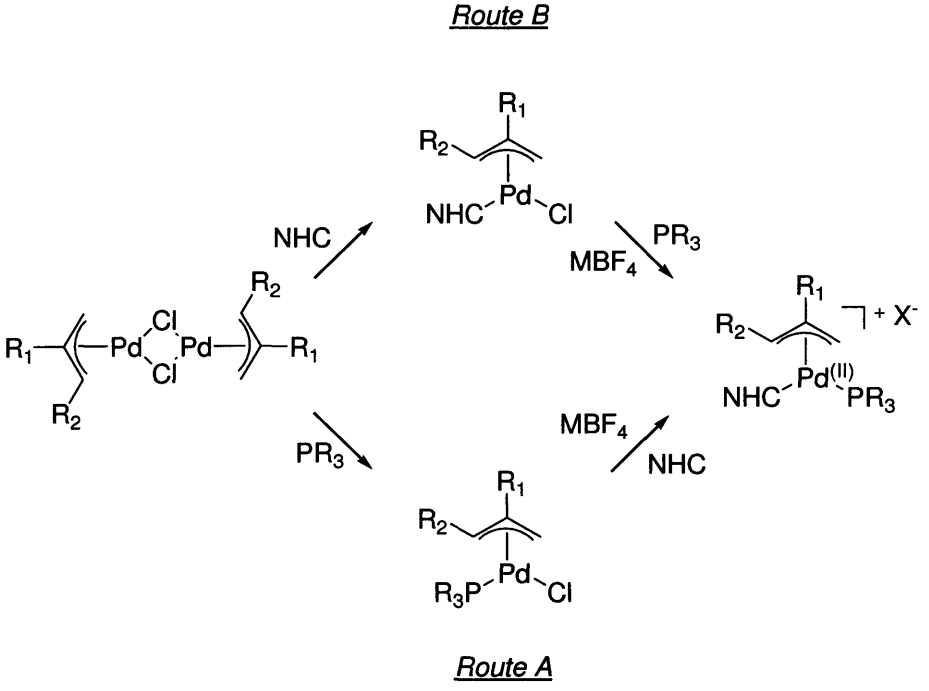

Scheme 3: *possible routes for the synthesis of compounds of general formula [Pd(π-allyl)(NHC)(L)]BF_4*

Both routes (*i.e.* A or B) seemed reasonable, as the intermediate chloro complexes have been isolated as air stable solids for a variety of phosphines and carbenes.[1, 24, 37, 38] Removal of the Cl ligand in the second step (and its replacement by either a phosphine or an NHC) could be envisaged by the action of MBF_4 (where M=Ag, Na or Tl). This type of ligand substitution reaction is well documented for π-allyl Pd complexes.[1, 2, 37, 39] With this general scheme in hand, a range of ligands was identified (***Figure 6***).

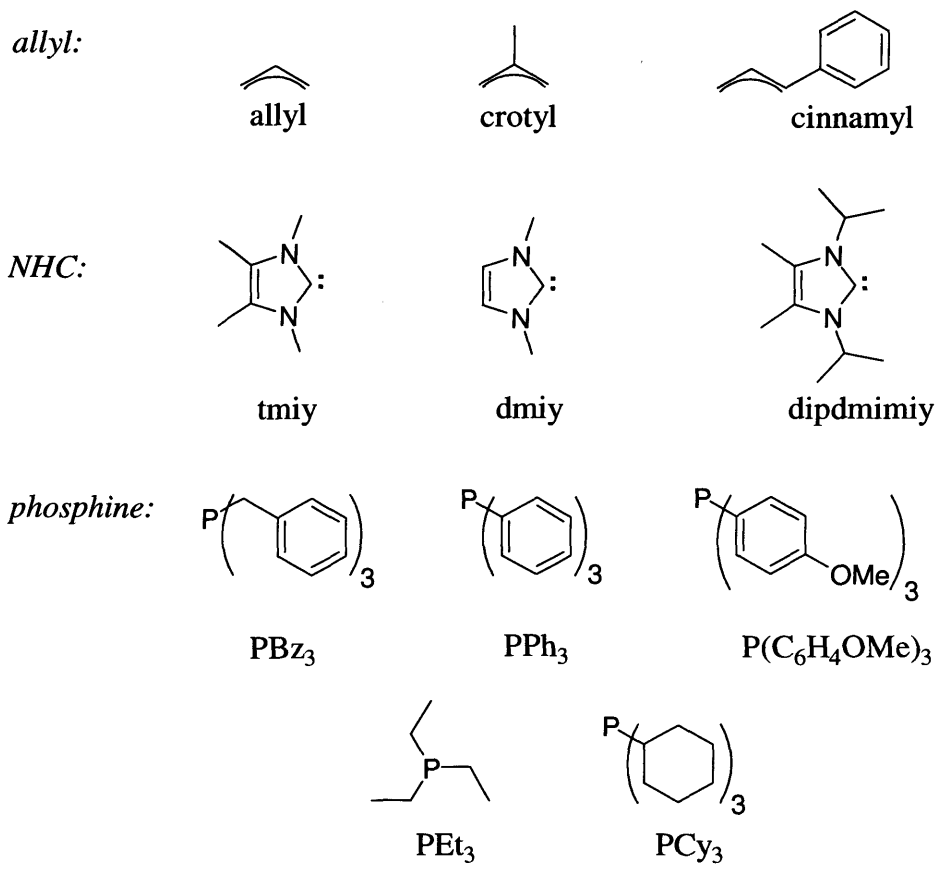

Figure 6: *selected ligands*

The NHCs investigated in this study were selected because of their low steric bulk compared to IMes or IPr. This feature was expected to influence the reductive elimination behaviour of the final Pd(II) π-allyl complexes. The choice of phosphine ligands was mainly guided by their commercial availability. A Tolman map (see chapters 1 and 2) of these ligands is plotted in ***Figure 7***:[40]

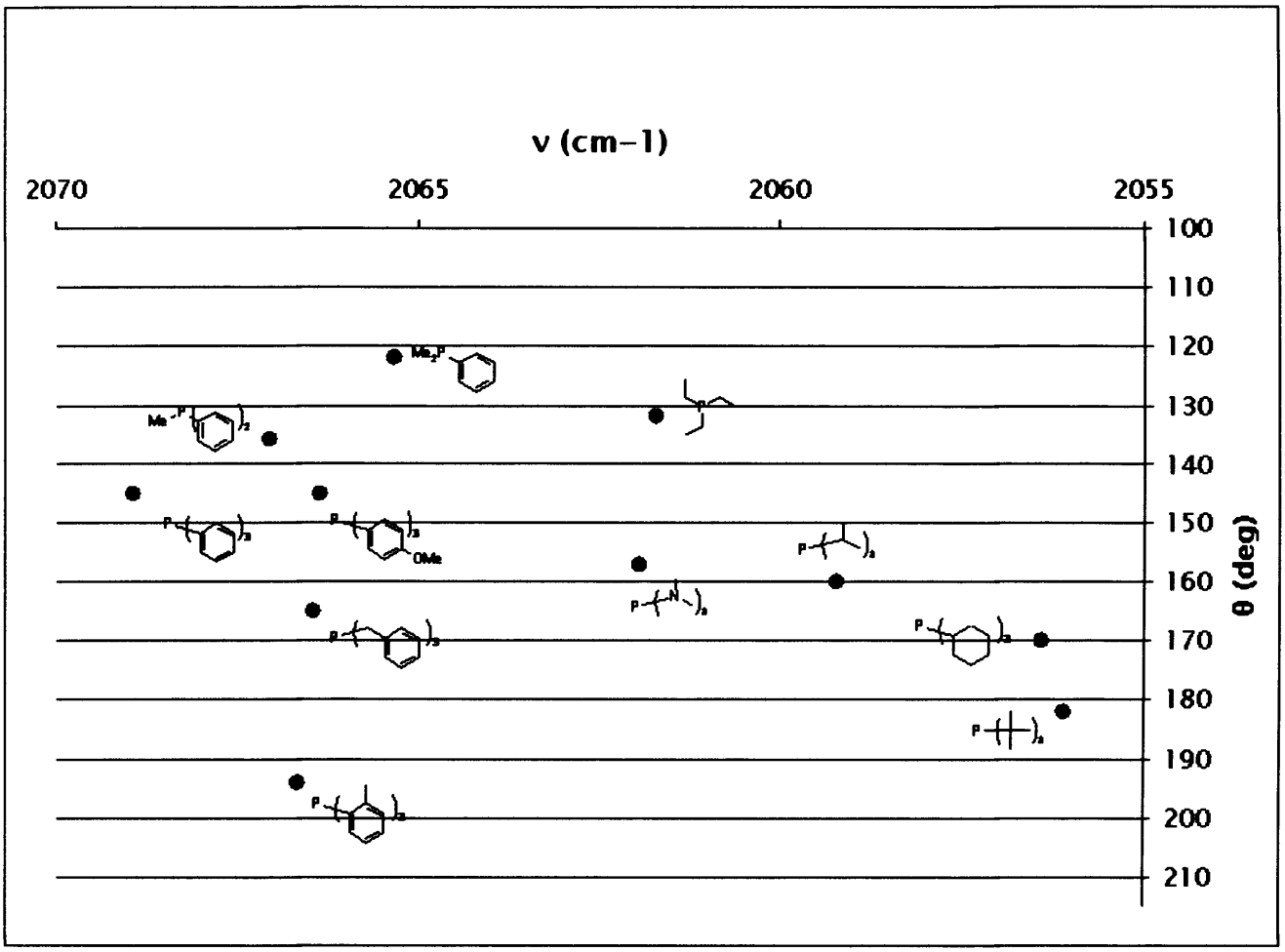

Figure 7: *Tolman map*[40] *of a selection of commercially available phosphines*

The synthesis of complexes containing PPh_3 (θ= 145 °, ν= 2068.9 cm^{-1}), PBz_3 (θ= 165 °, ν= 2066.4 cm^{-1}), and $P(C_6H_4OMe)_3$ (θ= 145 °, ν= 2066.3 cm^{-1}) was particular interesting, as this triad allows for the independent comparison of the effects of steric parameter θ ($P(C_6H_4OMe)_3$ *vs* PBz_3) and electronic parameter ν (PPh_3 *vs* $P(C_6H_4OMe)_3$), on the structure and reactivity of the final complexes.

Known compounds [Pd(π-allyl)(Cl)(PCy_3)] were synthesised according to route A (***Scheme 4***):

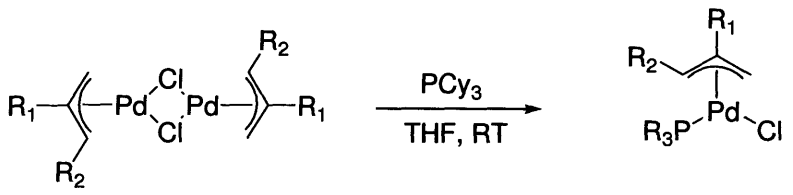

R_1= H	R_2= H	**5a**	81 %
R_1= Me	R_2= H	**6a**	81 %
R_1= H	R_2= Ph	**7a**	75 %

Scheme 4: *synthesis of [Pd(π-allyl)(Cl)(PCy_3)]*

This route is essentially the same as reported procedures,[38] but the use of THF instead of DCM gave better results as decomposition was observed in some cases with DCM.[41] The desired compounds were obtained in good yields.

The second step in the preparation of [Pd(π-allyl)(NHC)(PCy_3)]BF_4 following route A is the abstraction of Cl^- followed by coordination of an NHC. Despite repeated attempts, the complexes could not be obtained in pure form. The reactions invariably resulted in mixtures containing, in addition to the target complexes, cationic bis-carbene complexes (identified on the basis of ^1H and ^{31}P NMR spectroscopy and ESI/MS) and decomposition products probably resulting from the nucleophilic attack of NHCs on the allyl ligands (***Scheme 5***):

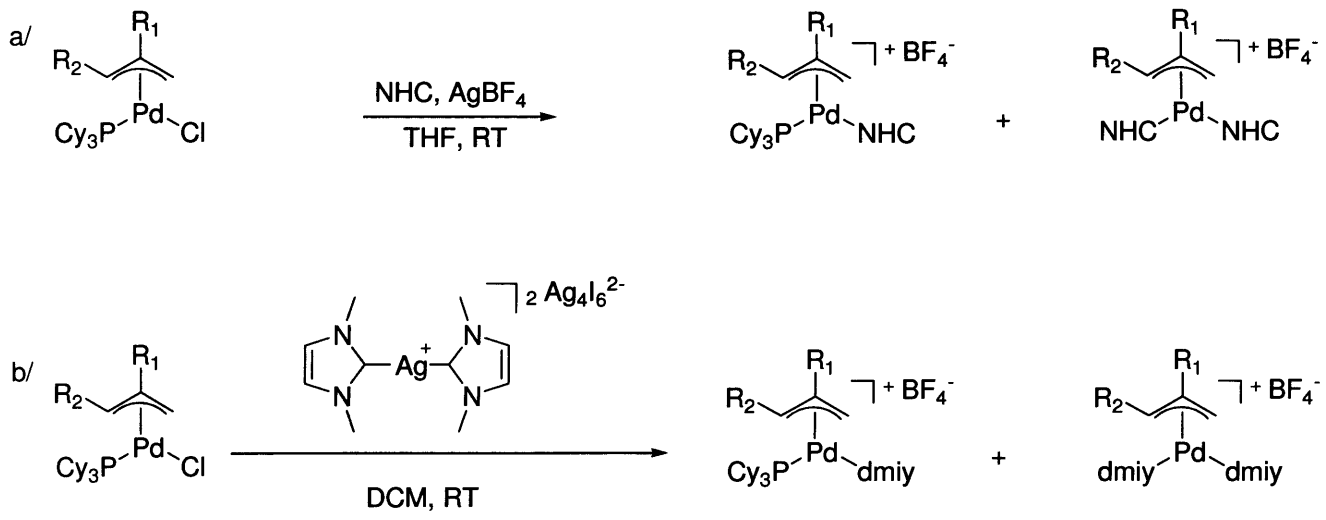

Scheme 5: *attempted synthesis of [Pd(π-allyl)(NHC)(PCy$_3$)]BF$_4$*

Although the decomposition products could be separated in the cases of allyl and crotyl, the bis-carbene complexes have, in most cases, similar solubility profiles to the mixed complexes, and it was not possible to separate them. The only exception was complex **6b** (NHC= tmiy, R_1= Me, R_2= H). In this case, the bis-carbene complex could be separated from the desired compound due to their respective solubilities in THF. In addition, compound **5b** (R_1= R_2= H, NHC= dmiy, PR_3= PCy_3), prepared by using carbene transfer agent $[Ag(dmiy)_2]_2Ag_4I_6$, although obtained as a mixture of desired compound and bis-carbene complex, could be crystallised on a small scale and gave crystals suitable for X-ray diffraction. These compounds are shown in ***Figure 8***. It was apparent that route A was not a viable synthetic approach, hence Route B was investigated (***Scheme 6***).

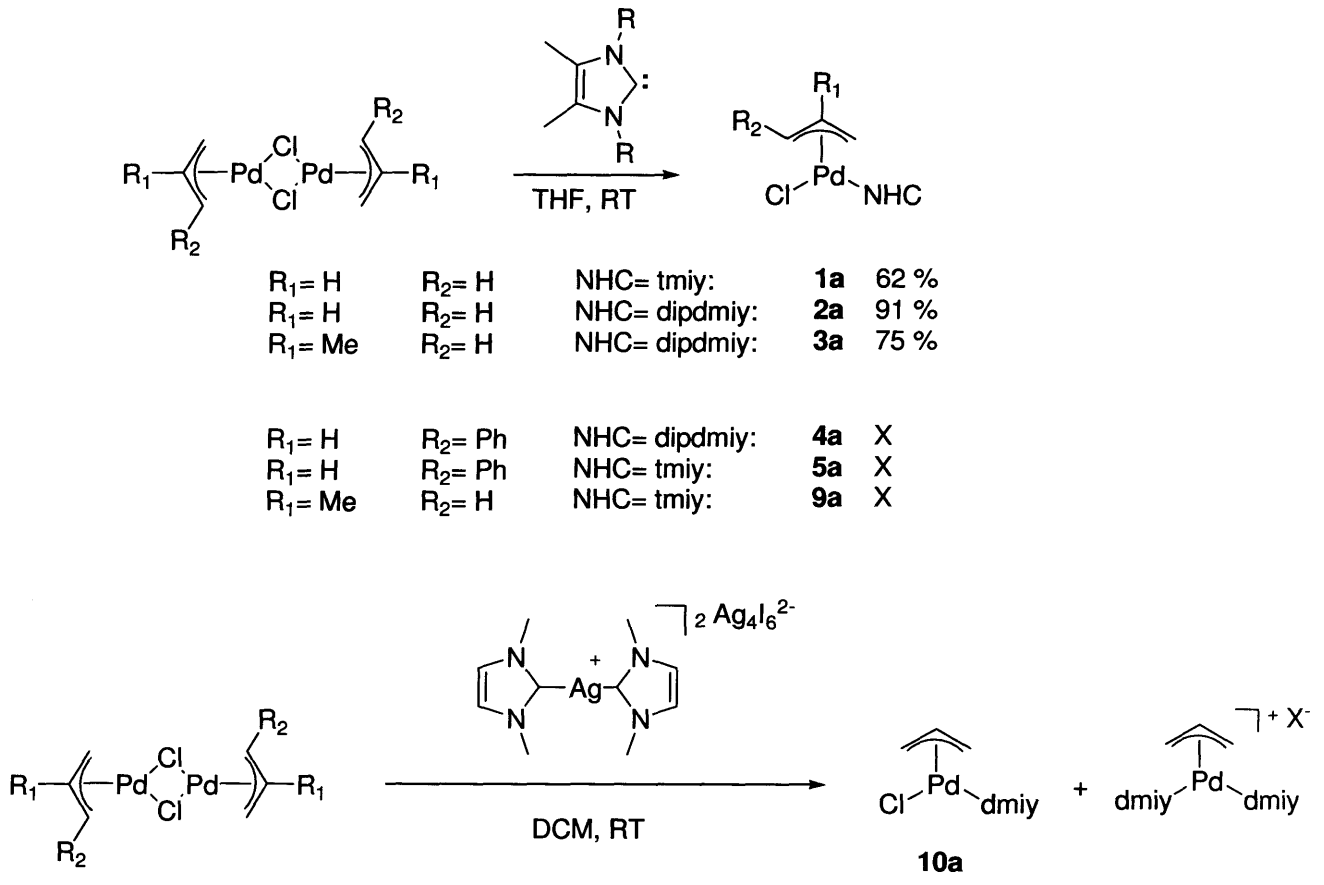

Scheme 6: *synthesis of [Pd(π-allyl)(Cl)(NHC)]*

Compounds **1a**, **2a** and **3a** were obtained as air stable yellow solids slowly decomposing over time at room temperature (**3a** and **2a** are stable over weeks in the solid state whereas **1a** decomposes to Pd black in one week).

Surprisingly, it was impossible to obtain pure cinnamyl complexes **4a** and **5a** because the reactions invariably resulted in a mixture of products. However, an impure sample of **4a** was successfully recrystallised from DCM/hexane on a small scale and crystals suitable for X-ray diffraction were obtained (see section **3.3**). A mixture of products was also obtained in the case of **9a**. Nolan[22] and others[37, 42, 43] have reported similar compounds with bulky NHCs, therefore the higher reactivity (possibly due to their more compact nature) of tmiy and dipdmiy towards electrophiles must account for these results (the same procedure as that of Nolan was used in this work). The synthesis of **10a**

via the reaction of $[Pd(\pi\text{-allyl})Cl]_2$ with $[Ag(dmiy)_2]_2Ag_4I_6$ (carbene transfer agent)[44] resulted in a mixture of the desired compound and cationic *bis*(carbene)allylpalladium(II) (***Scheme 6***).

The synthesis of cationic complexes from these precursors was then attempted (***Scheme 7***).

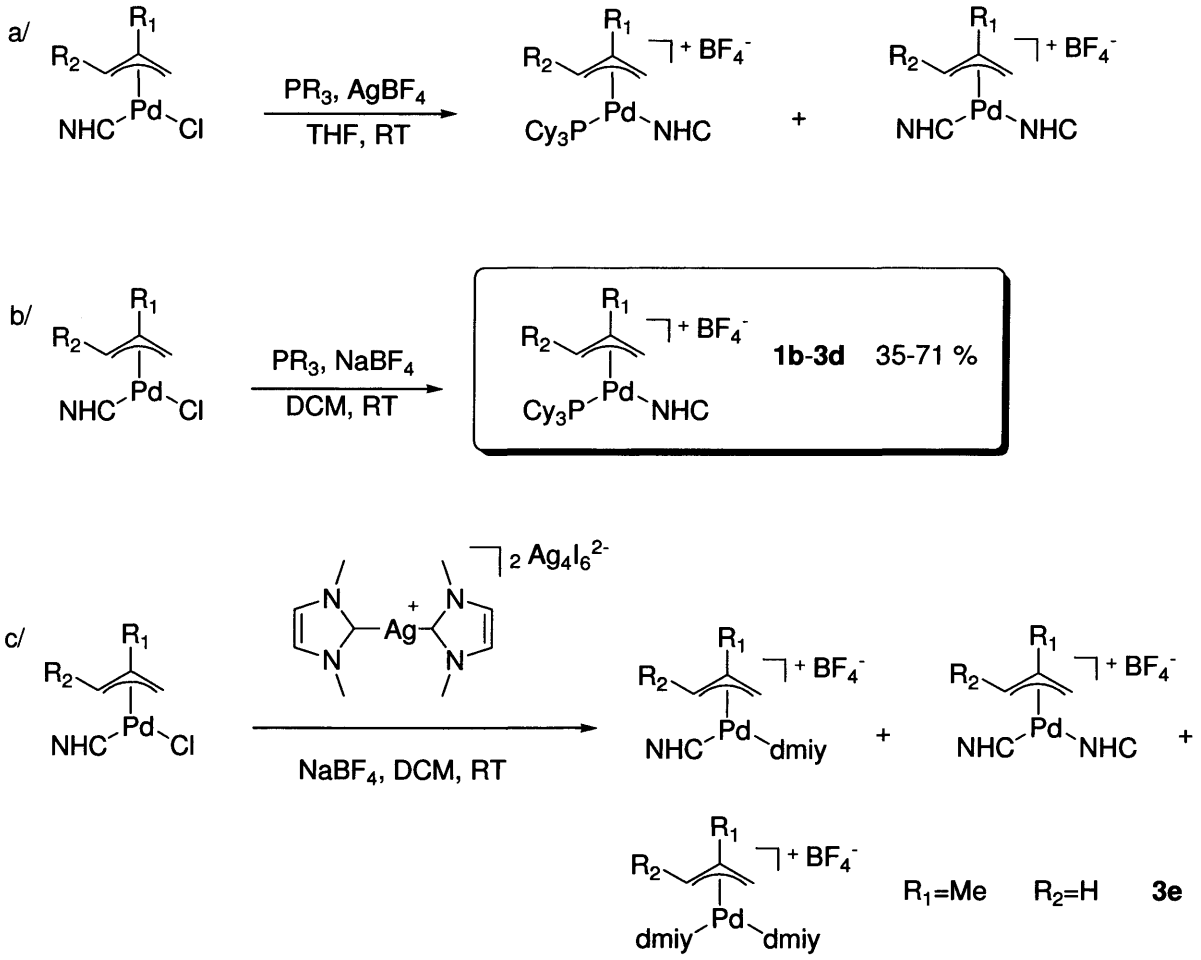

Scheme 7: *attempted synthesis of [Pd(π-allyl)(NHC)(L)]BF_4 from [Pd(π-allyl)(Cl)(NHC)]*

The reaction of neutral precursors with $AgBF_4$ led to carbene ligand scrambling (***Scheme 7*** a and c), and it became clear that Ag(I) salts were not a viable option.

A few reports have appeared in the literature on the sometimes unexpected reactivity of silver carbene transfer agents. While the present chapter was being written, Porschke reported the synthesis of NHC-Pd π-allyl complexes containing weakly cordinating ligands such as BF_4^- or TfO^- from the

corresponding chloro precursors.[43] The authors found that the NHC in the chloro complexes reacted with an excess of Ag(I) salt to give [Ag(NHC)(Y)] (where Y= BF_4^-...). The steric bulk of the NHCs employed in their study apparently prevented the formation of cationic bis-carbene complexes but it is likely that in the present work the formation of a silver-NHC complex would be followed by carbene transfer to Pd. In addition, Clyburne reported the unexpected transfer of Ag and Cl from [Ag(Cl)(IMes)] to osmium carbonyl clusters.[45]

Compound **3e** was crystallised from a sample of an impure cationic complex (***Scheme 7*** c), and a crystal structure was obtained, thus unambiguously confirming the nature of the impurity (see Chapter 3.3). In addition, treating **1a** with free IMes in the presence of $AgBF_4$ resulted in a complex mixture of products which could not readily be separated, although compound **1g**, [Pd(η^3-C_3H_5)(IMes)(tmiy)]BF_4 crystallised on small scale and gave crystals suitable for X-ray diffraction, see Chapter 3.3).

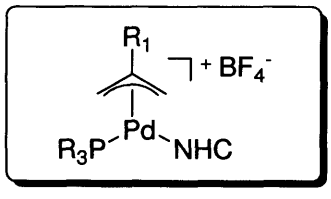

R_1= H, NHC= tmiy:		R_1= H, NHC= dipdmiy:		R_1= Me, NHC= dipdmiy:	
PR_3= PCy_3 :	**1b**	PR_3=PCy_3:	**2b**	PR_3= PCy_3 :	**3b**
PR_3= $P(C_6H_4OMe)_3$:	**1c**	PR_3=$P(C_6H_4OMe)_3$:	**2c**	PR_3= $P(C_6H_4OMe)_3$:	**3c**
PR_3= PPh_3:	**1d**	PR_3=PPh_3:	**2d**	PR_3= PEt_3:	**3d**
PR_3= PBz_3:	**1e**	PR_3= PEt_3:	**2e**		
PR_3= PEt_3:	**1f**				
		R_1= Me, NHC= tmiy:			
		PR_3= PCy_3 :	**6b**		

Figure 7: *prepared compounds of general formula [Pd(π-allyl)(NHC)(PR_3)]BF_4*

$AgBF_4$ was dismissed and the use of $NaBF_4$ was considered instead. This method afforded the desired compounds **1b-3d** in fair to good yields, without generating any of the bis-carbene complex.[46] Thus, a new family of cationic Pd(II) π-allyl complexes has been prepared (***Figure 7***).

Atoms in these compounds are named according to ***Figure 8***:

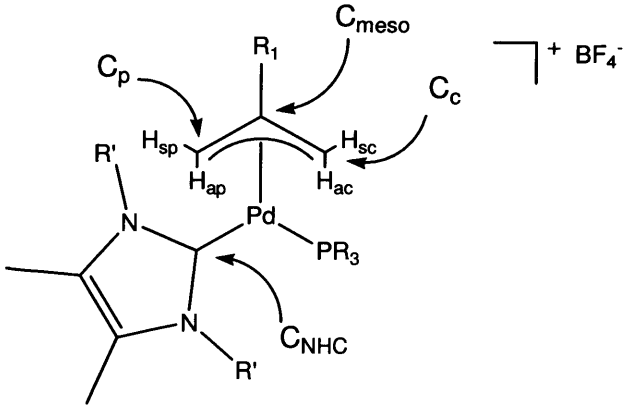

Figure 8: *naming of H and C atoms in compounds of general formula [Pd(π-allyl)(NHC)(PR₃)]BF₄.*

In the case of neutral compounds of general formula $[Pd(\eta^3\text{-}C_3H_5)(X)(L)]$, the carbon atom trans to X is referred to as C_X, and the carbon atom trans to L is referred to as C_L.

3.3 X-ray diffraction studies

For the majority of compounds, crystals suitable for X-ray diffraction were grown by slow evaporation of CH_2Cl_2 solutions of the complexes into hexane, or diffusion of Et_2O into THF solutions of the compounds.[47] The structures of these crystals were elucidated by single crystal X-ray diffraction and POV-Ray projections are presented in ***Figure 9*** to ***Figure 13***. Crystallographic data for these structures can be found in the CD-ROM enclosed with the present thesis.

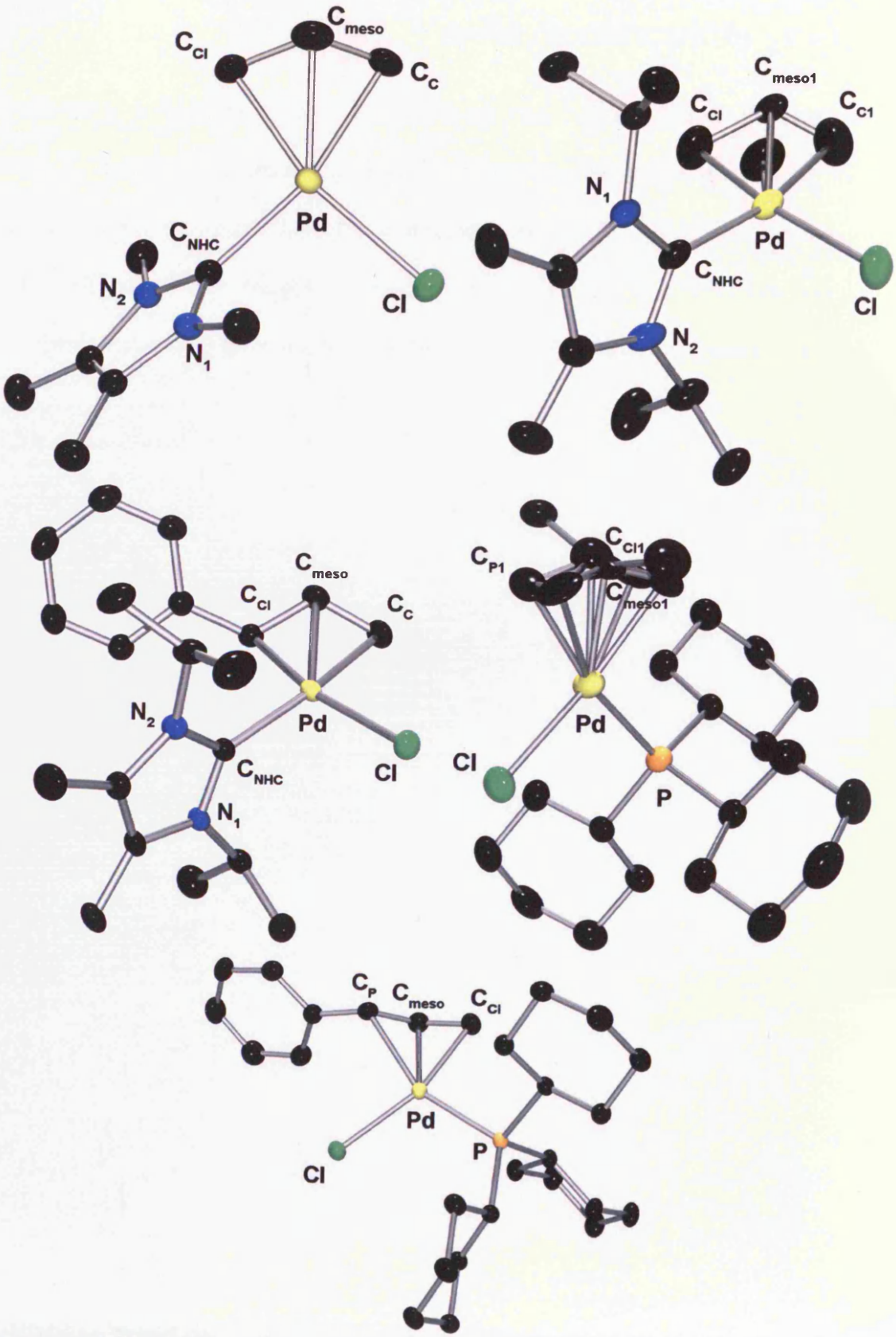

Figure 9: *POV-Ray projections of complexes of general formula [Pd(π-allyl)(Cl)(L)]*

Solvent molecules as well as hydrogen atoms and, in the case of cationic complexes BF_4 anions, have been omitted from these projections for clarity. Thermal ellipsoids are drawn at the 50 % probability level.

In this chapter, two additional structures (**8a** and **8b**, see ***Figure 10***), which are interesting for comparison purposes, are presented. Compound **8a** is only the second example of an iodo Pd(II) π-allyl structure to be reported,[48] although **8a** and other analogues (containing P^tBu_3, P^iPr_3 and PPh_3) have been used in two patents as efficient Suzuki and Heck cross coupling catalysts.[49, 50]

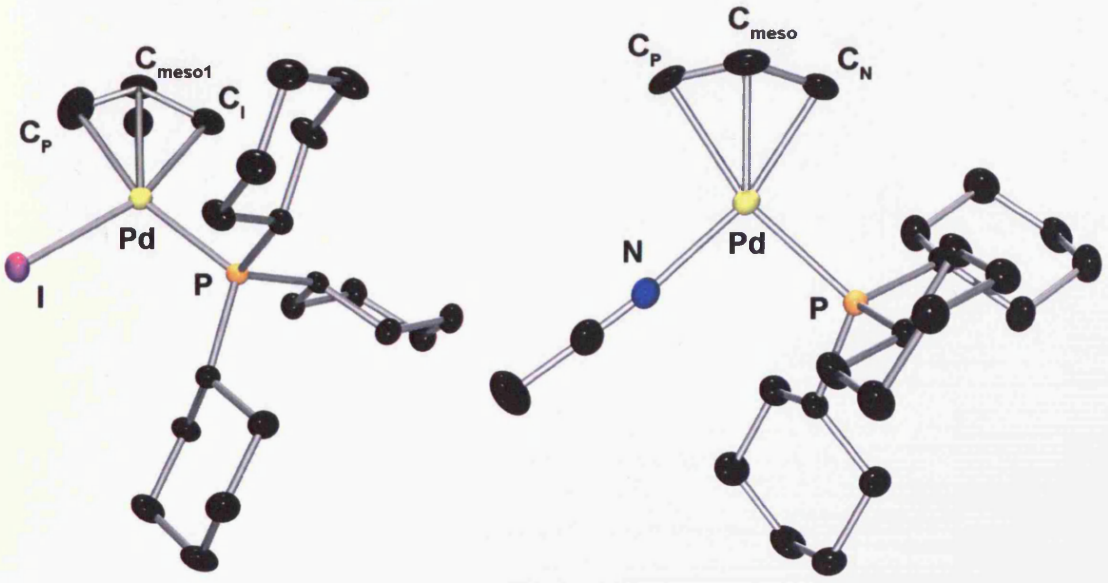

Figure 10: *POV-Ray projections of* $[Pd(\eta^3\text{-}C_3H_5)(I)(PCy_3)]$ ***8a*** *and* $[Pd(\eta^3\text{-}C_3H_5)(MeCN)(PCy_3)]BF_4$ ***8b***

Where present, the more compact allyl group η^3-C_3H_5 is disordered (disorder was refined anisotropically), with the notable exception of **1a** and **8b**. Also, **5b** contains one disordered CH_2Cl_2 molecule per unit cell (refined isotropically). The crotyl ligand in **6a** is disordered (refined anisotropically). The unit cell of two complexes bearing a tmiy ligand contains 2 independent molecules (**1b**-1, **1b**-2; **6b**-1, **6b**-2). [51]

Relevant bond distances and angles (around Pd and *intra*-ligands) are presented in ***Tables 1*** to ***8***. Least-square planes were calculated for the allyl ligand,[52] the mean coordination plane[53] and the NHC ring.[54] Acute interplanar angles Φ_1 and Φ_2 between those planes were calculated, as shown in ***Figure 14***. These angles were calculated using the PLATON suite of programs (with the LSPL and CALC GEOM commands).

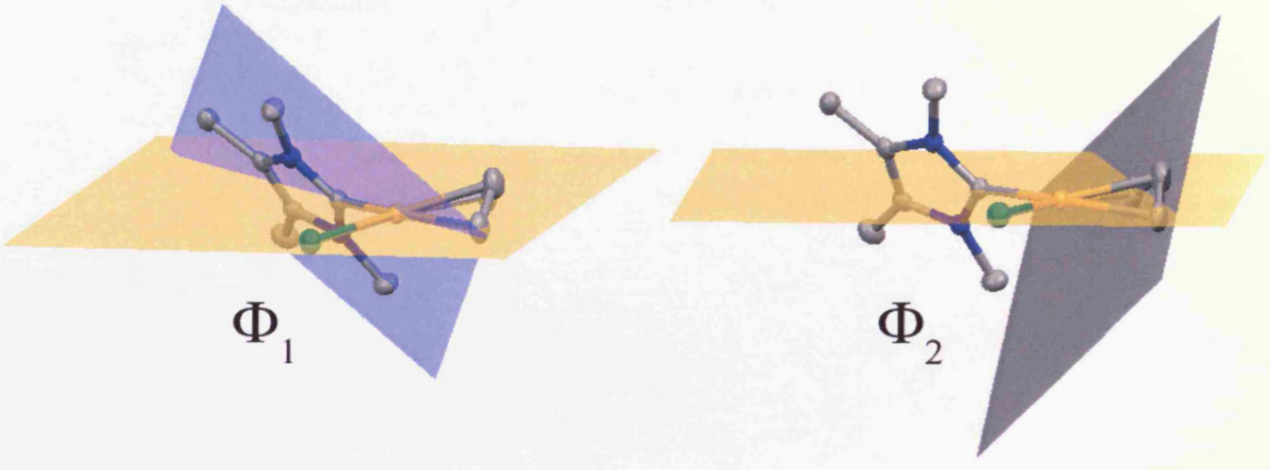

Figure 14: *least-square planes calculated to determine acute angles Φ_1 and Φ_2 between the carbene ring (blue) or the allyl group (black) and the mean coordination plane (gold)*

3.3.1 Neutral complexes of general formula [Pd(π-allyl)(X)(L)]

Neutral complexes generally display little variation in their geometries. The distances and angles of previously reported structures **5a**,[9] **9a**,[23] **10a**,[23] **11a**,[55] **12a**[22] and **13a**[48] (***Figure 15***) are included in ***Tables 1*** to ***4*** for comparison. The main structural features of these complexes are:

- A pseudo-square planar geometry. Only **7a** and **13a** significantly differ from this arrangement with X-Pd-L angles of 105.20 ° and 108.03 ° respectively (***Table 3***).
- A Φ_2 value of about 65 ° with respect to the coordination plane, and the three carbon atoms of the allyl forming a C_X-C_{meso}-C_L angle of 120 ° on average. Notable exceptions to these

average values are phosphine-containing complexes **5a** and **8a**: they display even more tilted π-allyl goups (Φ_2 values of 59.7(13) ° and 55.3(14) ° respectively), and wider C_X-C_{meso}-C_L angles (129.6(10) ° and 135.1(9) °).

- A roughly perpendicular orientation of the NHC with respect to the coordination plane, most probably to minimize steric interactions. This tendency increases both with the size of the NHC and that of the π-allyl. Thus, Φ_1 values range from 60.10(12) (**1a**) to 89.22(10) (**4a**).[56]

Compound	Pd-L	Pd-X	Pd-C_L	Pd-C_{meso}	Pd-C_X
[Pd(η^3-C_3H_5)(Cl)(tmiy)] **1a**	2.046(3)	2.3985(10)	2.200(3)	2.131(3)	2.107(3)
[Pd(η^3-C_3H_5)(Cl)(dipdmiy)] **2a**	2.042(4)	2.3752(9)	2.199(5)	2.140(8)	2.097(4)
[Pd(η^3-C_3H_4Ph)(Cl)(dipdmiy)] **4a**	2.043(2)	2.3699(6)	2.202(2)	2.1476(19)	2.1300(19)
[Pd(η^3-C_3H_5)(Cl)(ICy)] **9a**[23]	*2.072(2)*	*2.4191(8)*	*2.236(4)*	*2.178(3)*	*2.137(5)*
[Pd(η^3-C_3H_5)(Cl)(I^{t}Bu)] **10a**[23]	*2.062(2)*	*2.3897(8)*	*2.175(3)*	*2.125(3)*	*2.096(3)*
[Pd(η^3-C_4H_7)(Cl)(I^{t}Bu)] **11a**[55]	*2.062(3)*	*2.3782(13)*	*2.157(5)*	*2.163(4)*	*2.121(4)*
[Pd(η^3-C_3H_4Ph)(Cl)(IPr)] **12a**[22]	*2.040(9)*	*2.348(3)*	*2.282(11)*	*2.139(11)*	*2.084(12)*
[Pd(η^3-C_3H_5)(Cl)(PCy_3)] **5a**[9]	*2.3045(16)*	*2.3689(18)*	*2.190(8)*	*2.115(10)*	*2.112(7)*
[Pd(η^3-C_4H_7)(Cl)(PCy_3)] **6a**	2.3022(11)	2.3616(11)	2.177(7)	2.121(12)	2.110(7)
[Pd(η^3-C_3H_4Ph)(Cl)(PCy_3)] **7a**	2.2991(6)	2.3734(7)	2.3198(18)	2.1608(18)	2.1074(19)
[Pd(η^3-C_3H_5)(I)(PCy_3)] **8a**	2.3096(8)	2.6386(3)	2.187(4)	2.131(8)	2.135(3)
[Pd(η^3-C_3H_5)(I)(P*)] **13a**[48]	*2.304(2)*	*2.639(1)*	*2.193(7)*	*2.157(7)*	*2.142(7)*

Table 1: *bond distances (Å) around Pd for complexes of general formula [Pd(π-allyl)(X)(L)]*

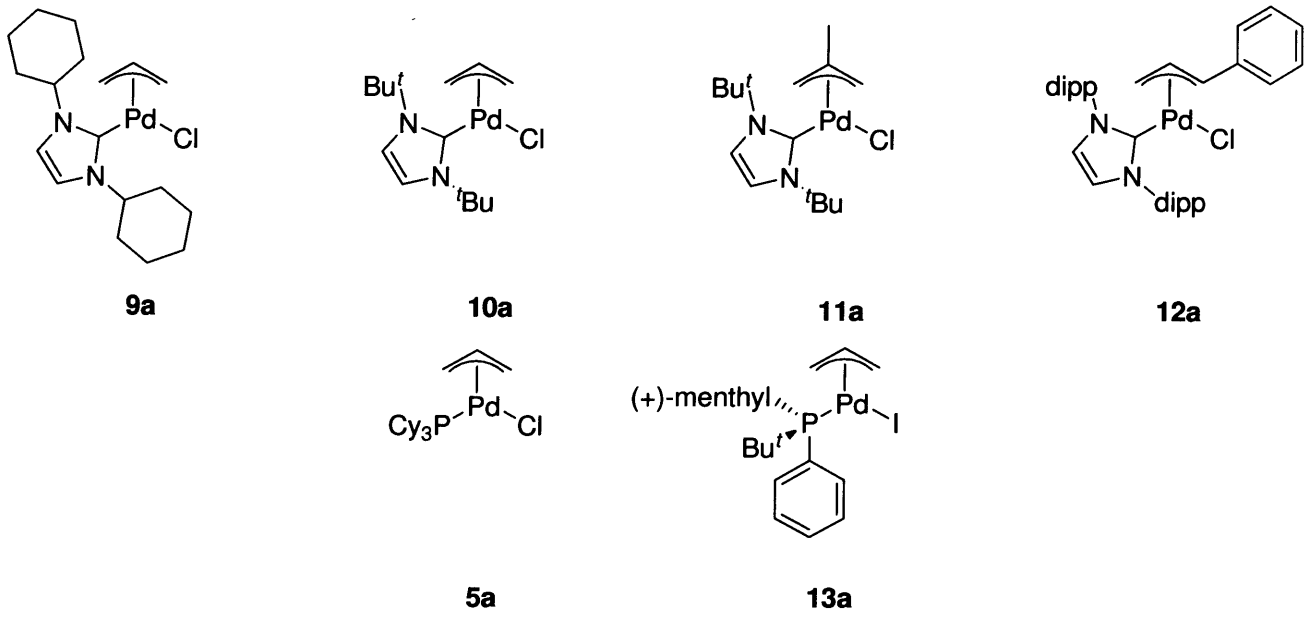

Figure 15: *previously reported neutral structures of general formula [Pd(π-allyl)(X)(L)]*

Compound	C_X-C_{meso}	C_L-C_{meso}	N_1-C_{NHC}	N_2-C_{NHC}
[Pd(η^3-C_3H_5)(Cl)(tmiy)] **1a**	1.401(5)	1.349(5)	1.348(3)	1.355(3)
[Pd(η^3-C_3H_5)(Cl)(dipdmiy)] **2a**	1.469(11)	1.236(10)	1.348(4)	1.345(4)
[Pd(η^3-C_3H_4Ph)(Cl)(dipdmiy)] **4a**	1.429(3)	1.386(3)	1.354(2)	1.353(2)
[Pd(η^3-C_3H_5)(Cl)(ICy)] **9a**[23]	*1.413(6)*	*1.419(6)*	*1.388(4)*	*1.383(4)*
[Pd(η^3-C_3H_5)(Cl)(I^{t}Bu)] **10a**[23]	*1.382(4)*	*1.359(5)*	*1.380(4)*	*1.357(4)*
[Pd(η^3-C_4H_7)(Cl)(I^{t}Bu)] **11a**[55]	*1.422(6)*	*1.385(6)*	*1.369(5)*	*1.362(4)*
[Pd(η^3-C_3H_4Ph)(Cl)(IPr)] **12a**[22]	*1.380(16)*	*1.389(15)*	*1.368(11)*	*1.376(11)*
[Pd(η^3-C_3H_5)(Cl)(PCy_3)] **5a**[9]	*1.403(15)*	*1.266(17)*	*NA*	*NA*
[Pd(η^3-C_4H_7)(Cl)(PCy_3)] **6a**	1.404(14)	1.367(14)	NA	NA
[Pd(η^3-C_3H_4Ph)(Cl)(PCy_3)] **7a**	1.419(3)	1.386(3)	NA	NA
[Pd(η^3-C_3H_5)(I)(PCy_3)] **8a**	1.402(11)	1.198(11)	NA	NA
[Pd(η^3-C_3H_5)(I)(P*)] **13a**[48]	*1.38(1)*	*1.36(1)*	*NA*	*NA*

Table 2: *other bond distances (Å) for complexes of general formula [Pd(π-allyl)(X)(L)]*

- Distances between Pd and the NHC ligands are much shorter than distances between Pd and the phosphines (on average 2.04 Å against 2.30 Å), perhaps reflecting the strength of the Pd-NHC bond compared to the Pd-phosphine bond.[57] However the covalent radius of phosphorus (110 pm) is higher than that of carbon (77 pm).
- Distances between Pd and the carbon atom *trans* to NHCs or the phosphine (Pd-C_L; 2.20 Å on average for NHCs, 2.19 Å for PCy_3) are longer than distances between Pd and the carbon atom *trans* to Cl (Pd-C_X), owing to the strong electron donating ability of NHCs and PCy_3. Likewise, the allyl C-C bonds *trans* to L (L= NHC or PCy_3) are shorter than the C-C bonds *trans* to Cl, although absolute values vary from one complex to the other (***Tables 1*** and ***2***).

Compound	X-Pd-L	L-Pd-C_X	C_X-Pd-C_L	C_L-Pd-X
[Pd(η^3-C_3H_5)(Cl)(tmiy)] **1a**	96.82(7)	97.29(11)	67.85(12)	97.97(8)
[Pd(η^3-C_3H_5)(Cl)(dipdmiy)] **2a**	92.93(10)	97.11(18)	68.2(2)	101.73(15)
[Pd(η^3-C_3H_4Ph)(Cl)(dipdmiy)] **4a**	94.76(6)	96.99(8)	68.59(8)	99.72(7)
[Pd(η^3-C_3H_5)(Cl)(ICy)] **9a**[23]	*94.28(9)*	*98.10(16)*	*68.38(18)*	*98.88(12)*
[Pd(η^3-C_3H_5)(Cl)(I^{t}Bu)] **10a**[23]	*96.34(12)*	*98.78(14)*	*68.34(13)*	*96.40(10)*
[Pd(η^3-C_4H_7)(Cl)(I^{t}Bu)] **11a**[55]	*91.54(9)*	*102.89(15)*	*68.04(18)*	*97.32(13)*
[Pd(η^3-C_3H_4Ph)(Cl)(IPr)] **12a**[22]	*94.9(3)*	*102.3(4)*	*66.8(4)*	*96.3(3)*
[Pd(η^3-C_3H_5)(Cl)(PCy_3)] **5a**[9]	*97.94(6)*	*98.2(2)*	*68.3(3)*	*95.5(2)*
[Pd(η^3-C_4H_7)(Cl)(PCy_3)] **6a**	96.49(4)	98.7(2)	68.0(3)	96.04(19)
[Pd(η^3-C_3H_4Ph)(Cl)(PCy_3)] **7a**	105.20(3)	91.17(6)	66.68(7)	97.01(6)
[Pd(η^3-C_3H_5)(I)(PCy_3)] **8a**	100.41(2)	98.17(11)	67.60(16)	97.73(13)
[Pd(η^3-C_3H_5)(I)(P*)] **13a**[48]	*108.03(4)*	*95.2(2)*	*66.8(3)*	*90.2(2)*

Table 3: *angles (°) around Pd for complexes of general formula [Pd(π-allyl)(X)(L)]*

Compound	C_X-C_{meso}-C_L	N_1-C_{NHC}-N_2	Φ_1	Φ_2
[Pd(η^3-C_3H_5)(Cl)(tmiy)] **1a**	121.9(3)	104.6(2)	61.10(12)	66.5(4)
[Pd(η^3-C_3H_5)(Cl)(dipdmiy)] **2a**	125.9(8)	105.8(3)	77.25(18)	62.2(9)
[Pd(η^3-C_3H_4Ph)(Cl)(dipdmiy)] **4a**	120.3(2)	105.46(16)	89.22(10)	66.6(2)
[Pd(η^3-C_3H_5)(Cl)(ICy)] **9a**[23]	*120.5(4)*	*104.9(2)*	*74.10(16)*	*64.7(4)*
[Pd(η^3-C_3H_5)(Cl)(I^{t}Bu)] **10a**[23]	*122.2(3)*	*105.06(17)*	*84.95(14)*	*64.3(4)*
[Pd(η^3-C_4H_7)(Cl)(I^{t}Bu)] **11a**[55]	*117.1(4)*	*104.8(3)*	*89.19(15)*	*64.8(4)*
[Pd(η^3-C_3H_4Ph)(Cl)(IPr)] **12a**[22]	*120.8(10)*	*102.5(7)*	*83.6(4)*	*68.7(13)*
[Pd(η^3-C_3H_5)(Cl)(PCy_3)] **5a**[9]	*129.6(10)*	*NA*	*NA*	*59.7(13)*
[Pd(η^3-C_4H_7)(Cl)(PCy_3)] **6a**	119.8(11)	NA	NA	65.3(11)
[Pd(η^3-C_3H_4Ph)(Cl)(PCy_3)] **7a**	120.85(17)	NA	NA	70.71(19)
[Pd(η^3-C_3H_5)(I)(PCy_3)] **8a**	135.1(9)	NA	NA	55.3(14)
[Pd(η^3-C_3H_5)(I)(P*)] **13a**[48]	*121.9(4)*	*NA*	*NA*	*65.5(7)*

Table 4: *other angles (°) for complexes of general formula [Pd(π-allyl)(X)(L)]*

3.3.1.1 Cationic complexes of general formula [Pd(π-allyl)(L)(L')]BF_4

There are noticeable differences in bond distances (***Tables 5*** to ***8***) between the complexes, but it appears that none can be easily rationalised.

Some parameters hardly vary at all from one structure to the other. Thus, distances Pd-C_{NHC}, N_1-C_{NHC}, N_2-C_{NHC} and angles N_1-C_{NHC}-N_2, are equal or very close within standard deviation limits. Because these parameters are most likely to be affected by the electronic nature of the NHC, it suggests that carbene ligands in the investigated series have very similar electronic properties.[57, 58] This result is not surprising in itself since dmiy, tmiy and dipdmiy all bear alkyl subsituents on the nitrogen atoms.

Other parameters are somewhat more variable, such as distances Pd-C_C (varying from 2.103 Å for **8b** to 2.32 Å for **1b**$_1$), C_P-C_{meso} (from 1.1977 Å for **1c** to 1.405 Å for **6b**-2), Pd-P (from 2.3154 Å for **6b**-2 to 2.3358 Å for **1b**-1) and angles C_P-C_{meso}-C_C (from 117.1 ° for **6b**-2 to 128.4 ° for **5b**).

The main structural features of these cationic complexes are:

- A pseudo-square planar geometry.
- A Φ_2 angle of just above 65 °, with the notable exceptions of **1b**-1 (70.14 °), **2b** (59.8 °) and **1c** (39.5 °). Interestingly, **1b** and **1c** were found to be active in the arylation of Pd-bound NHCs described in chapter 4.
- In a similar fashion to neutral complexes, C_X-C_{meso}-C_L angles are close to 120 ° on average. Some structures (**1c**, **5b**, **2b** and **2d**) significantly deviate from this value though, with wider C_P-C_{meso}-C_C angles (138.3 °, 128.40 °, 131.3(6) ° and 127.8 ° respectively). The reasons for this behaviour remain obscure.
- Compared to neutral complexes, the perpendicular orientation of the NHC ligand is even more pronounced with a 85 ° average value of Φ_1, most probably to accommodate the larger phosphine ligand. This geometry is likely to be the one adopted in solution, as indicated by NOESY studies. Bis-carbene complexes **3e** and **1g** show different geometries to adapt to different steric requirements. Thus, the two dmiy rings in **3e** sit at angles of 74.69 ° and 72.67 ° with respect to the coordination plane, making them almost parallel as a result (2.02 °). **1g** on the other hand, displays an arrangement which allows the tmiy ring to be almost parallel with one of the mesityl groups of IMes.[59] Finally, **1c** displays a reduced value for Φ_1, at 71.48 °. This is probably due to the reduced congestion of the complex. Indeed, PPh_3 and tmiy are both compact ligands.
- As observed in neutral complexes, C-C bonds *trans* to NHCs (C_C-C_{meso}) are shorter than C-C bonds *trans* to phosphines (C_P-C_{meso}), although the difference is sometimes negligible (*e.g.* **6b**-2, 1.405 Å *vs* 1.410 Å) and distances vary between complexes (***Table 6***). The only

exception is **3d**, with C_{meso}-C_C being longer (1.394(10) Å) than C_{meso}-C_P (1.382(11). In this case, the compact nature of PEt_3 (compared to dipdmiy) might be responsible for this observation.

- Pd-C_C and Pd-C_P distances on the other hand can be alternatively longer, shorter or equal within standard deviation limits (***Table 5***).

Compound	Pd-C_{NHC}	Pd-P	Pd-C_c	Pd-C_{meso}	Pd-C_P
$[Pd(\eta^3\text{-}C_3H_5)(dmiy)(PCy_3)]BF_4$ **5b**	2.042(4)	2.3198(11)	2.169(6)	2.150(6)	2.216(16)
$[Pd(\eta^3\text{-}C_3H_5)(tmiy)(PPh_3)]BF_4$ **1c**	2.056(3)	2.3079(9)	2.168(4)	2.177(14)	2.167(6)
$[Pd(\eta^3\text{-}C_3H_5)(tmiy)(PCy_3)]BF_4$ **1b**-1	2.034(3)	2.3358(10)	2.32(3)	2.180(9)	2.17(2)
$[Pd(\eta^3\text{-}C_3H_5)(tmiy)(PCy_3)]BF_4$ **1b**-2	2.035(3)	2.3277(10)	2.220(10)	2.163(6)	2.197(12)
$[Pd(\eta^3\text{-}C_3H_5)(tmiy)(PBz_3)]BF_4$ **1e**	2.057(3)	2.3073(9)	2.181(4)	2.151(10)	2.181(4)
$[Pd(\eta^3\text{-}C_3H_5)(dipdmiy)(PCy_3)]BF_4$ **2b**	2.062(2)	2.3167(7)	2.182(3)	2.131(7)	2.178(3)
$[Pd(\eta^3\text{-}C_3H_5)(dipdmiy)P(C_6H_4OMe)_3]BF_4$ **2d**	2.050(5)	2.3000(14)	2.165(6)	2.099(10)	2.147(6)
$[Pd(\eta^3\text{-}C_3H_5)(MeCN)(PCy_3)]BF_4$ **8b**[a]	2.085(2)	2.3106(6)	2.103(3)	2.144(3)	2.213(3)
$[Pd(\eta^3\text{-}C_3H_5)(tmiy)(IMes)]BF_4$ **1g**[b]	2.061(3)	2.041(3)	2.24(2)	2.122(7)	2.213(8)
$[Pd(\eta^3\text{-}C_4H_7)(dmiy)_2]BF_4$ **3e**[c]	2.051(4)	2.046(4)	2.145(4)	2.179(4)	2.159(5)
$[Pd(\eta^3\text{-}C_4H_7)(tmiy)(PCy_3)]BF_4$ **6b**-1	2.045(2)	2.3181(10)	2.176(2)	2.181(2)	2.174(3)
$[Pd(\eta^3\text{-}C_4H_7)(tmiy)(PCy_3)]BF_4$ **6b**-2	2.045(2)	2.3154(8)	2.176(2)	2.180(2)	2.167(3)
$[Pd(\eta^3\text{-}C_4H_7)(dipdmiy)(PCy_3)]BF_4$ **3b**	2.054(6)	2.3191(18)	2.185(6)	2.168(7)	2.155(7)
$[Pd(\eta^3\text{-}C_4H_7)(dipdmiy)(PEt_3)]BF_4$ **3d**	2.047(6)	2.2971(19)	2.153(7)	2.141(7)	2.158(8)

Table 5: *bond distances (Å) around Pd for complexes of general formula [Pd(π-allyl)(L)(L')]BF_4.* [a] *MeCN replaces NHC.* [b] *IMes replaces PR_3.* [c] *2nd dmiy replaces PR_3*

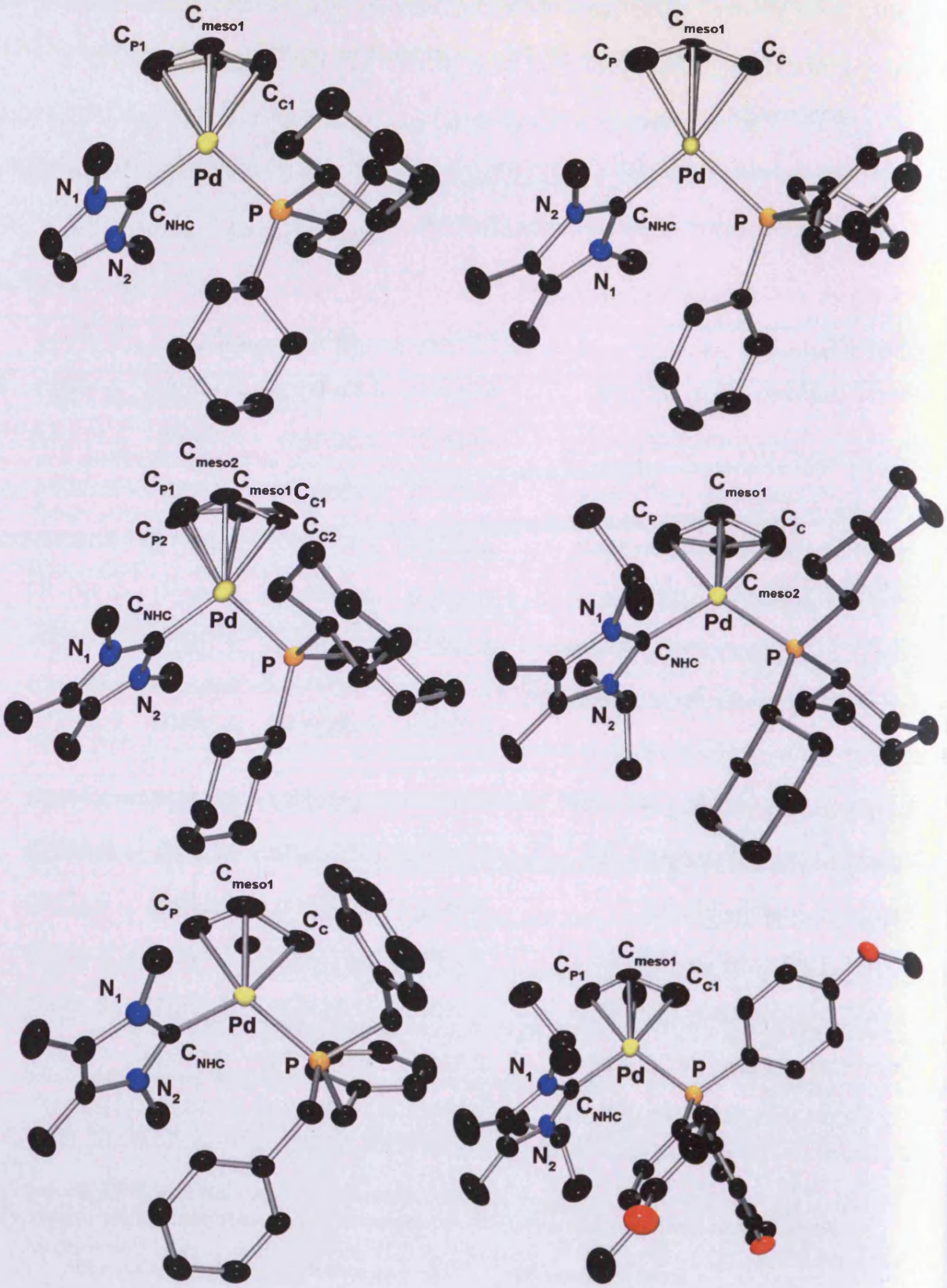

Figure 11: *POV-Ray projections of complexes of general formula* $[Pd(\eta^3\text{-}C_3H_5)(NHC)(PR_3)]BF_4$

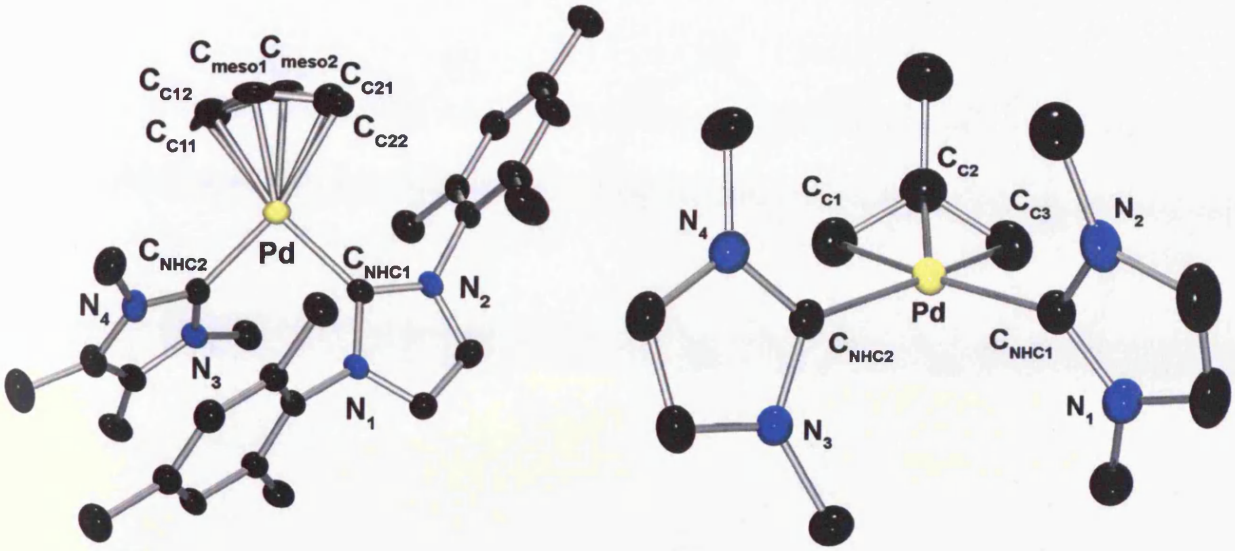

Figure 12: *POV-Ray projections of complexes of general formula [Pd(π-allyl)(NHC)(NHC')]BF_4*

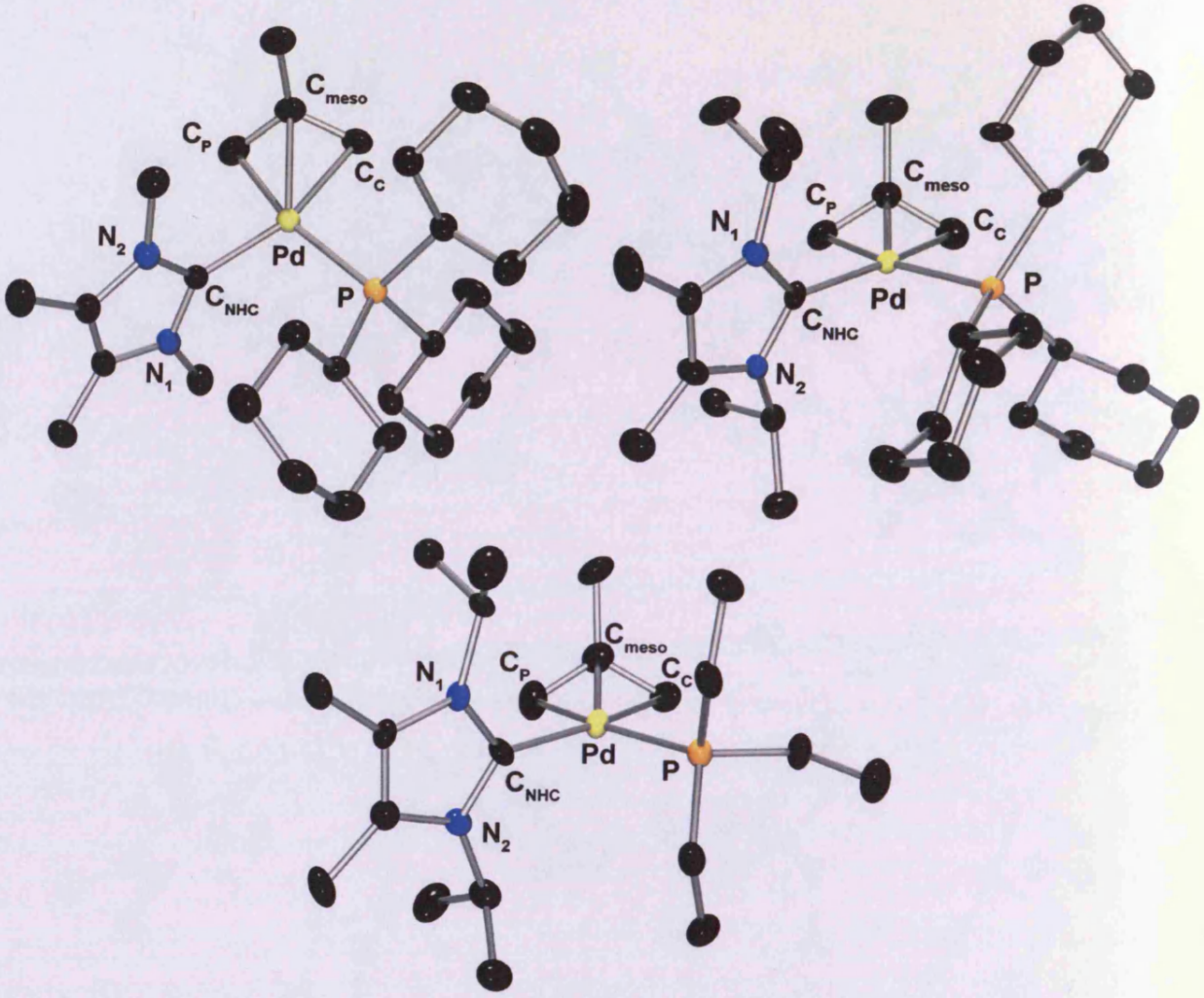

Figure 13: *POV-Ray projections of complexes of general formula* $[Pd(\eta^3\text{-}C_4H_7)(NHC)(PR_3)]BF_4$

Compound	C_P-C_{meso}	C_C-C_{meso}	N_1-C_{NHC}	N_2-C_{NHC}
$[Pd(\eta^3\text{-}C_3H_5)(dmiy)(PCy_3)]BF_4$ **5b**	1.285(14)	1.390(11)	1.353(5)	1.354(5)
$[Pd(\eta^3\text{-}C_3H_5)(tmiy)(PPh_3)]BF_4$ **1c**	1.198(16)	1.374(16)	1.351(5)	1.355(4)
$[Pd(\eta^3\text{-}C_3H_5)(tmiy)(PCy_3)]BF_4$ **1b**-1	1.371(16)	1.391(16)	1.355(4)	1.350(4)
$[Pd(\eta^3\text{-}C_3H_5)(tmiy)(PCy_3)]BF_4$ **1b**-2	1.403(11)	1.426(10)	1.353(4)	1.354(4)
$[Pd(\eta^3\text{-}C_3H_5)(tmiy)(PBz_3)]BF_4$ **1e**	1.247(13)	1.524(14)	1.336(5)	1.351(4)
$[Pd(\eta^3\text{-}C_3H_5)(dipdmiy)(PCy_3)]BF_4$ **2b**	1.297(8)	1.382(8)	1.349(3)	1.353(3)
$[Pd(\eta^3\text{-}C_3H_5)(dipdmiy)P(C_6H_4OMe)_3]BF_4$ **2d**	1.275(14)	1.421(14)	1.346(6)	1.348(6)
$[Pd(\eta^3\text{-}C_3H_5)(MeCN)(PCy_3)]BF_4$ **8b**[a]	1.362(4)	1.397(4)	NA	NA
$[Pd(\eta^3\text{-}C_3H_5)(tmiy)(IMes)]BF_4$ **1g**[b]	1.412(10)	1.369(15)	1.359(4)/ 1.351(4)	1.365(4)/ 1.350(4)
$[Pd(\eta^3\text{-}C_4H_7)(dmiy)_2]BF_4$ **3e**[c]	1.397(7)	1.400(6)	1.346(5)/ 1.352(5)	1.347(5)/ 1.349(5)
$[Pd(\eta^3\text{-}C_4H_7)(tmiy)(PCy_3)]BF_4$ **6b**-1	1.398(4)	1.405(4)	1.352(3)	1.352(3)
$[Pd(\eta^3\text{-}C_4H_7)(tmiy)(PCy_3)]BF_4$ **6b**-2	1.405(4)	1.410(3)	1.356(3)	1.351(3)
$[Pd(\eta^3\text{-}C_4H_7)(dipdmiy)(PCy_3)]BF_4$ **3b**	1.385(10)	1.397(10)	1.363(9)	1.367(8)
$[Pd(\eta^3\text{-}C_4H_7)(dipdmiy)(PEt_3)]BF_4$ **3d**	1.394(10)	1.382(11)	1.379(8)	1.334(9)

Table 6: *other bond distance (Å) for complexes of general formula [Pd(π-allyl)(L)(L')]BF_4.* [a] *MeCN replaces NHC.* [b] *IMes replaces PR_3.* [c] *2nd dmiy replaces PR_3*

Compound	P-Pd-C_{NHC}	C_{NHC}-Pd-C_P	C_p-Pd-C_c	C_c-Pd-P
$[Pd(\eta^3\text{-}C_3H_5)(dmiy)(PCy_3)]BF_4$ **5b**	99.16(11)	95.7(4)	66.6(4)	98.76(19)
$[Pd(\eta^3\text{-}C_3H_5)(tmiy)(PPh_3)]BF_4$ **1c**	97.40(10)	99.38(19)	67.4(2)	95.84(12)
$[Pd(\eta^3\text{-}C_3H_5)(tmiy)(PCy_3)]BF_4$ **1b**-1	101.36(10)	97.6(5)	65.5(7)	95.4(5)
$[Pd(\eta^3\text{-}C_3H_5)(tmiy)(PCy_3)]BF_4$ **1b**-2	101.21(9)	95.1(3)	67.9(4)	95.6(2)
$[Pd(\eta^3\text{-}C_3H_5)(tmiy)(PBz_3)]BF_4$ **1e**	100.52(9)	94.45(15)	67.35(17)	97.68(12)
$[Pd(\eta^3\text{-}C_3H_5)(dipdmiy)(PCy_3)]BF_4$ **2b**	100.93(7)	95.50(11)	68.09(12)	95.44(9)
$[Pd(\eta^3\text{-}C_3H_5)(dipdmiy)P(C_6H_4OMe)_3]BF_4$ **2d**	97.69(12)	96.7(2)	68.3(3)	97.3(2)
$[Pd(\eta^3\text{-}C_3H_5)(MeCN)(PCy_3)]BF_4$ **8b**[a]	97.35(6)	97.31(9)	67.48(10)	97.79(7)
$[Pd(\eta^3\text{-}C_3H_5)(tmiy)(IMes)]BF_4$ **1g**[b]	95.76(12)	105.5(3)	66.9(6)	91.7(5)
$[Pd(\eta^3\text{-}C_4H_7)(dmiy)_2]BF_4$ **3e**[c]	96.95(16)	99.17(18)	67.56(19)	96.03(16)
$[Pd(\eta^3\text{-}C_4H_7)(tmiy)(PCy_3)]BF_4$ **6b**-1	99.50(7)	94.54(11)	67.01(11)	99.07(8)
$[Pd(\eta^3\text{-}C_4H_7)(tmiy)(PCy_3)]BF_4$ **6b**-2	98.74(7)	94.74(10)	67.15(11)	98.74(7)
$[Pd(\eta^3\text{-}C_4H_7)(dipdmiy)(PCy_3)]BF_4$ **3b**	100.72(19)	95.4(3)	66.7(3)	96.99(18)
$[Pd(\eta^3\text{-}C_4H_7)(dipdmiy)(PEt_3)]BF_4$ **3d**	98.24(18)	96.2(3)	67.1(3)	98.3(2)

Table 7: *angles around Pd (°) for complexes of general formula* $[Pd(\pi\text{-allyl})(L)(L')]BF_4$. [a] *MeCN replaces NHC.* [b] *IMes replaces* PR_3. [c] 2^{nd} *dmiy replaces* PR_3

Compound	C_p-C_{meso}-C_c	N_1-C_{NHC}-N_2	Φ_1	Φ_2
$[Pd(\eta^3\text{-}C_3H_5)(dmiy)(PCy_3)]BF_4$ **5b**	128.40(13)	104.5(3)	80.6(3)	63.5(16)
$[Pd(\eta^3\text{-}C_3H_5)(tmiy)(PPh_3)]BF_4$ **1c**	138.3(13)	104.2(3)	71.48(18)	39.5(17)
$[Pd(\eta^3\text{-}C_3H_5)(tmiy)(PCy_3)]BF_4$ **1b**-1	124.0(2)	104.3(3)	87.8(5)	70.14(19)
$[Pd(\eta^3\text{-}C_3H_5)(tmiy)(PCy_3)]BF_4$ **1b**-2	121.3(10)	104.8(3)	89.6(2)	68.5(11)
$[Pd(\eta^3\text{-}C_3H_5)(tmiy)(PBz_3)]BF_4$ **1e**	120.7(9)	106.0(3)	83.33(17)	69.0(12)
$[Pd(\eta^3\text{-}C_3H_5)(dipdmiy)(PCy_3)]BF_4$ **2b**	131.3(6)	105.7(2)	80.01(12)	59.8(7)
$[Pd(\eta^3\text{-}C_3H_5)(dipdmiy)P(C_6H_4OMe)_3]BF_4$ **2d**	127.8(11)	105.7(4)	84.2(2)	65.3(13)
$[Pd(\eta^3\text{-}C_3H_5)(MeCN)(PCy_3)]BF_4$ **8b**[a]	120.7(3)	NA	NA	67.0(3)
$[Pd(\eta^3\text{-}C_3H_5)(tmiy)(IMes)]BF_4$ **1g**[b]	123.9(12)	103.9(3)/ 104.9(3)	36.3(3)/ 69.5(3)	69.7(14)
$[Pd(\eta^3\text{-}C_4H_7)(dmiy)_2]BF_4$ **3e**[c]	117.7(4)	104.8(4)/ 104.2(3)	74.7(3)/ 72.6(2)	64.0(5)
$[Pd(\eta^3\text{-}C_4H_7)(tmiy)(PCy_3)]BF_4$ **6b**-1	117.9(2)	104.80(19)	82.24(11)	67.6(3)
$[Pd(\eta^3\text{-}C_4H_7)(tmiy)(PCy_3)]BF_4$ **6b**-2	117.1(2)	104.5(2)	83.32(12)	68.5(3)
$[Pd(\eta^3\text{-}C_4H_7)(dipdmiy)(PCy_3)]BF_4$ **3b**	118.2(6)	104.6(6)	80.6(3)	67.4(8)
$[Pd(\eta^3\text{-}C_4H_7)(dipdmiy)(PEt_3)]BF_4$ **3d**	118.2(7)	104.8(5)	84.3(3)	68.6(8)

Table 8: *other angles (°) for complexes of general formula [Pd(π-allyl)(L)(L')]BF_4.* [a] *MeCN replaces NHC.* [b] *IMes replaces PR_3.* [c] *2nd dmiy replaces PR_3*

3.4 Solution structure

3.4.1 1D NMR spectroscopy

Whilst X-ray crystallography provides extremely direct and useful information about the solid-state structure of metal complexes, NMR spectroscopy remains a powerful tool for the investigation of their behaviour in solution. In addition to the routine identification of the product(s) of a reaction, the combination of 1D and 2D techniques can provide chemists with very detailed information (including dynamic equiibria) about the structures they study.[1, 12, 60-62]

The assignment of chemical shifts for [Pd(π-allyl)(NHC)(PR_3)]BF_4 complexes was partially obtained by the combination of 1D ^{1}H, ^{13}C and ^{31}P NMR spectroscopy. Relevant chemical shifts are presented in ***Tables 9*** and ***10***. Atoms are named according to ***Figure 8*** as previously.

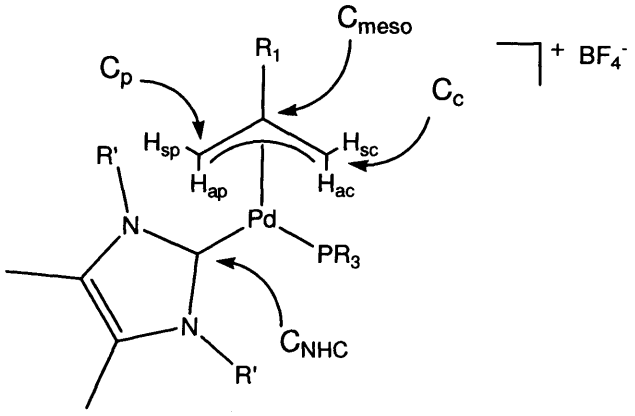

Compounds	R_1	H_{sp}	H_{sc}	H_{ap} (J_{HP} in Hz)	H_{ac}
1b	H 5.24	4.07	4.10	2.80 (8.9)	2.58
1c	H 5.58	4.29	3.99	3.06 (NA)	2.91
1d	H 5.52	4.22	3.92	3.00 (10.3)	2.85
1e	H 4.99	3.94	3.04-3.14[a]	2.65 (10.3)	2.08
1f	H 5.31	4.12	3.93	2.83 (9.4)	2.66
2b	H 5.20	4.09-4.15[a]	4.09-4.15[a]	2.72 (8.8)	2.58
2c	H 5.53	4.22-4.30[a]	3.76	2.98 (8.8)	2.87
2d	H 5.50	4.21	3.71	2.94 (9.9)	2.84
2e	H 5.28	4.13	3.90	2.75 (9.5)	2.65
3b	CH_3 1.74	3.87-3.91[a]	3.87-3.91[a]	2.62 (8.8)	2.47
3c	CH_3 1.87	3.86	3.43	2.77-2.85 (NA)[b]	2.77-2.85
3d	CH_3 1.75	3.90	3.63	2.63 (9.5)	2.52
6b	CH_3 1.77	3.84	3.87	2.59 (8.8)	2.49

Table 9: *selected ^1H NMR data for [Pd(π-allyl)(NHC)(PR_3)]BF_4 complexes (in d_2-DCM).Chemical shift, δ, is in ppm. [a] Overlap with other peaks. [b] Overlap with H_{ac} prevented the determination of J_{HP}*

Compounds	C_{meso} (J_{CP} in Hz)	C_p (J_{CP} in Hz)	C_c	C_{NHC} (J_{CP} in Hz)	P
1b	119.88 (4.5)	66.50 (27.9)	61.28[a]	173.15 (16.3)	42.01
1c	121.59 (5.5)	65.84 (30.9)	68.88	171.90 (16.8)	26.25
1d	121.35 (5.5)	65.23 (31.4)	68.08	172.84 (21.3)	22.36
1e	121.21 (6.0)	66.01 (29.9)	64.45	171.83 (19.9)	26.09
1f	121.13 (5.0)	66.13 (28.9)	61.72	172.39 (18.9)	20.41
2b	119.37 (4.0)	66.72 (27.9)	60.79	173.35 (15.0)	41.39
2c	121.02 (6.0)	66.17 (30.9)	69.87[a]	170.75 (18.9)	23.88
2d	120.78 (5.0)	65.68 (30.9)	69.08	171.32 (17.0)	19.99
2e	120.64 (5.0)	67.09 (29.9)	61.49	171.24 (18.9)	20.41
3b	133.66 (4.0)	66.83 (28.9)	60.91	174.27 (16.0)	42.40
3c	135.62 (5.0)	64.83 (31.9)	68.76	171.21 (18.0)	21.89
3d	134.99 (5.0)	66.47 (30.9)	61.34	172.21 (18.9)	21.59
6b	134.11 (4.0)	66.05 (28.9)	61.22	174.18 (16.0)	43.17

Table 10: *selected ^{13}C and ^{31}P NMR data for [Pd(π-allyl)(NHC)(PR_3)]BF_4 complexes (in d_2-DCM).Chemical shift, δ, in ppm.* [a] *A very small P-C coupling was seen in ^{13}C NMR spectrum*

The presence of a phosphine ligand in these compounds induces visible $^3J_{HP}$ and $^2J_{CP}$ coupling in ^1H and $\{^1H\}^{13}C$ spectra for hydrogen and carbon atoms *trans* to P. This feature of phosphine-containing Pd(II) π-allyl complexes has been reported previously.[1] In addition, $^3J_{HH}$ coupling between H_{meso} and H_{anti} allows the complete assignment of chemical shifts of carbon and hydrogen atoms in π-allyl ligands.

It is interesting to compare the electron donating ability and bulk of the phosphines used with the ^{1}H and the ^{13}C chemical shifts of the π-allyl ligands. Overall, there is no clear-cut correlation between the Tolman parameters (θ and ν) of the phosphine ligands and the NMR data. Interestingly however, the chemical shift of the π-allyl carbon atom *trans* to the NHC is quite sensitive to the nature of the phosphine, ranging from 60.79 ppm (**2b**) to 69.87 ppm (**2c**) whilst the chemical shifts of the carbon atom *trans* to PR_3 only ranges from 64.83 ppm (**3c**) to 67.09 ppm (**2e**). This result is counter-intuitive as one would expect the carbon atoms *trans* to PR_3 to be more affected than the *cis* ones if electronic effects dominated. On the other hand steric effects are more likely to affect substituents *cis* to PR_3. However, the fact that **2b** (containing PCy_3) and **2e** (PEt_3) have very close chemical shifts for C_c indicates that steric effects alone cannot be used to rationalise the range of chemical shifts.

Interestingly, phosphines with aromatic substituents (**1c**, **1d**, **2c**, **2d**) all induce a marked downfield chemical shift at the *cis* carbon atoms, thus inverting the pattern observed for other phosphines. These observations are crucial because they bring yet more evidence that phosphine ligands cannot simply be described by their Tolman parameters, as the nature of substituents (*e.g.* alkyl or aryl) plays a part in the properties of transition metal complexes and their catalytic activity. Previous work tentatively classified phosphines into pure σ-donor and σ-donor/π-acceptor categories,[63] but the phosphines employed in this work all belong to the pure σ-donor group, therefore this criterion is not useful in this case. Moreover, studies by Orpen have shown discrepancies between observed and expected (on the basis of Tolman parameters) catalytic activity: thus, whilst bulky triarylphosphites form efficient catalysts in the rhodium-catalysed hydroformylation of alkenes, bulky perfluoroarylphosphines with similar ν and θ parameters are very poor ligands in this reaction.[64]

3.4.2 2D solution NMR

NOESY has been widely applied to the structure elucidation of complex organic molecules,[65] and more rarely so to organometallic species.[60, 66] However, work by Pregosin has shown that this NMR technique can successfully be applied to Pd(II) π-allyl complexes with two purposes: gaining structural information, and observing chemical exchange occuring at the allyl ligand.[6, 13, 15-18, 67] An elegant example of the application of NOESY to the observation of dynamic allyl exchange in a chiral bis-phosphine complex is shown in ***Figure 16***:

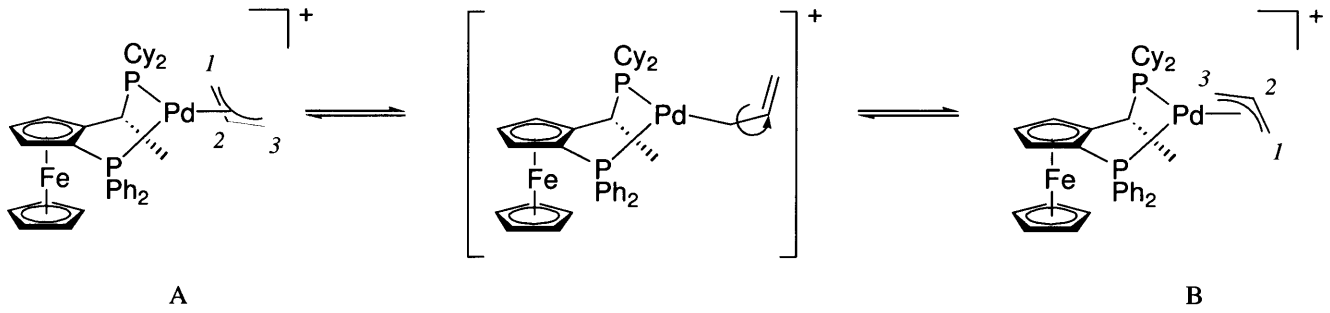

Figure 16: *dynamic behavior of a π-allyl bis-phosphine Pd(II) complex as observed by NOES.*[17]

Diastereoisomers A and B are both present in solution, and negative-phase cross-peaks between these compounds reveal selective exchange between allyl hydrogens *trans* to PPh_2, (*i.e.* decoordination occurs under steric control exclusively *cis* to the bulky PCy_2 moiety).

Cross peaks in NOESY are caused by spatial proximity (NOE effect, positive phase) and chemical exchange (negative phase, the diagonal is also negative phase). Importantly, both effects can superimpose and cancel each other. COSY-type signals caused by *J*-coupling are observed too but their pattern is quite distinctive and they are easily identified.[62] As an illustration, ***Figure 17*** shows a section of the NOESY spectrum of **2c**: circled cross-peaks 7 and 8 arise from ^3J- coupling between hydrogen atoms of the isopropyl group of dipdmiy. Other circled cross-peaks indicate spatial proximity between hydrogens.

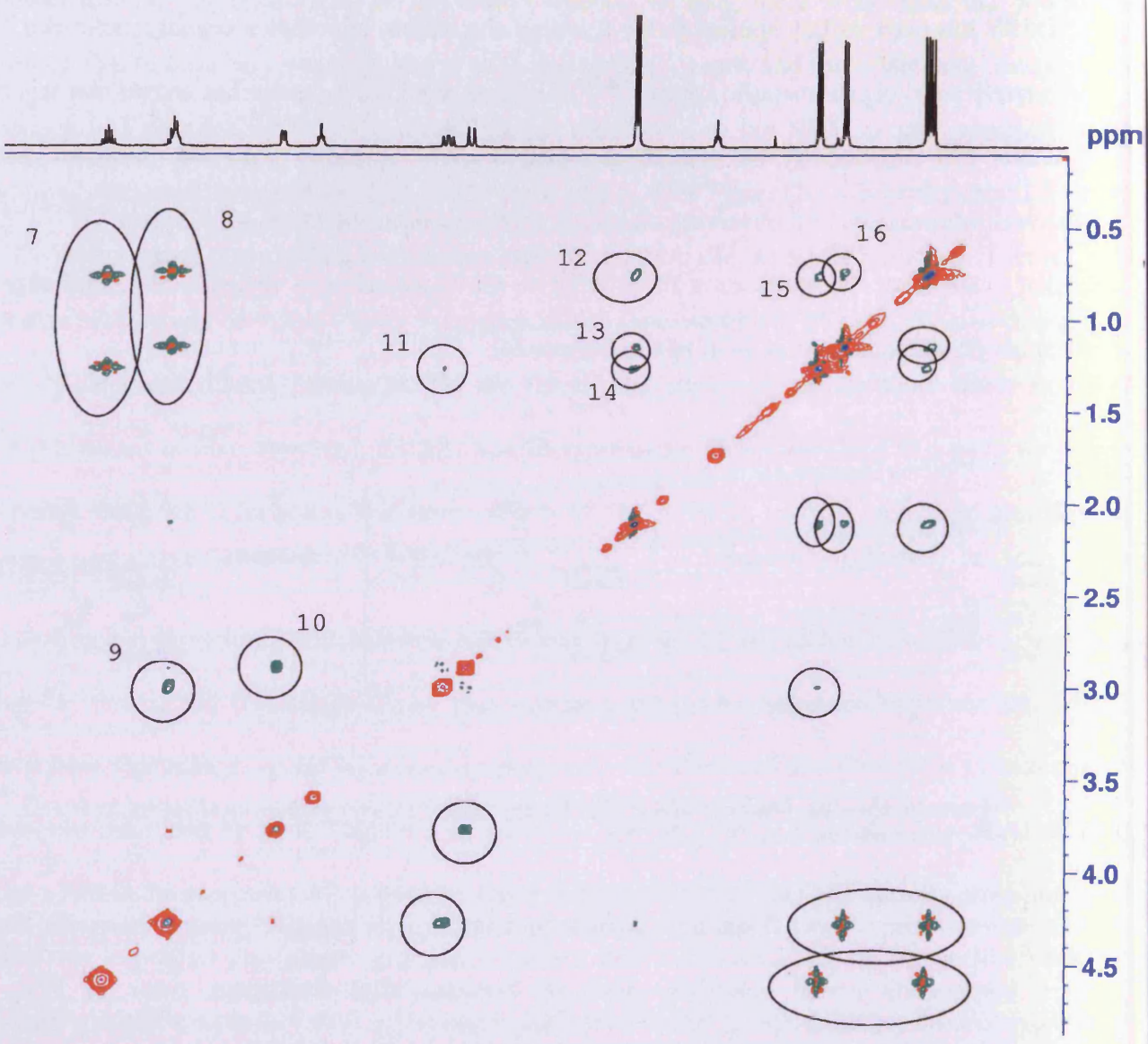

Figure 17: *example of NOESY spectrum (**2c**)*

X-ray diffraction studies (see section 3.2) show that NHCs adopt a perpendicular orientation with respect to the coordination plane in the solid state. It was thus interesting to confirm this preference in solution. This section presents studies pertaining to compounds **2c**, **2d** and **3c**. These complexes bear a dipdmiy ligand and a phosphine ligand with three aromatic substituents. Complexes bearing either a phosphine with alkyl substituents or a more compact NHC (dmiy, tmiy) did not show any

cross-peak between the phosphine and the NHC, thus precluding absolute assignment of NMR signals. Atoms in **2c**, **2d** and **3c** are named according to ***Figure 18***:

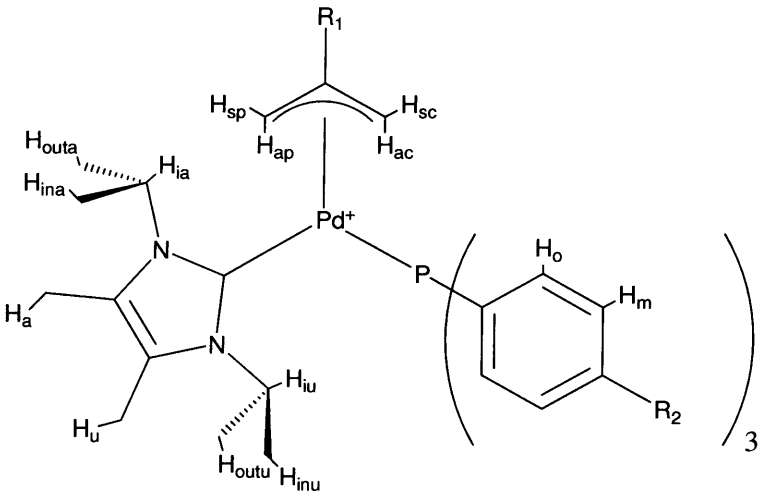

Figure 18: *nomenclature for complexes studied by NOESY*

NHC ligands are divided in four quadrants: above and under the coordination plane (a and u), towards or away from palladium (in and out). Hydrogens on the allyl are named as previously, and hydrogens on the phosphine are named according to their position relative to the phosphorus atom (*ortho*, o; *meta*, m; *para*, p).

Tables 11, ***12*** and ***13*** summarise the NOESY spectrum of **2c**, **2d** and **3c** respectively. Coloured areas indicate cross-peaks (red cells indicate cross-peaks used to determine relative *under/above* assignment, green cells indicate those used for absolute *in/out* assignment and orange cells indicate missing peaks in **2c** and **2d** compared to **3c**), and numbers correspond to circled areas on the spectrum (see appendices 3, 4 and 5).

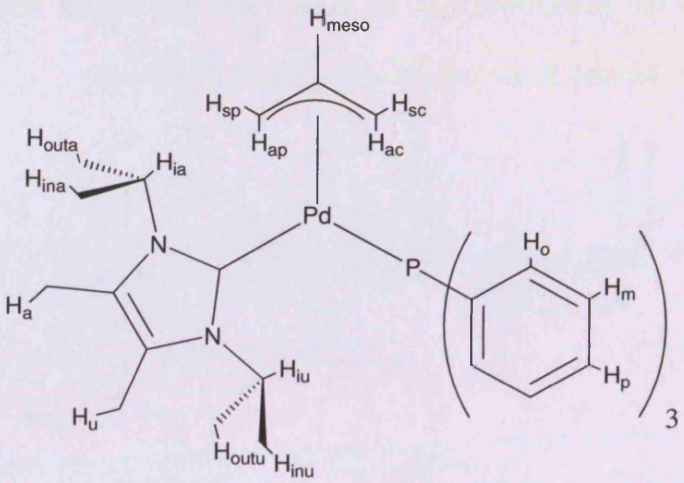

2c	δ(ppm)	H_o	H_m	H_p	H_{meso}	H_{iu}	H_{ia}	H_{sp}	H_{sc}	H_{ap}	H_{ac}	H_u	H_a	H_{outu}	H_{outa}	H_{inu}	H_{ina}
H_o	6.96[a]								3		2					1	
H_m	7.31[a]																
H_p	7.42[a]																
H_{meso}	5.53							4	5		6						
H_{iu}	4.57													7		7	
H_{ia}	4.26[a]														8		8
H_{sp}	4.26[a]				4					9							
H_{sc}	3.76	3			5						10						
H_{ap}	2.98							9						11			
H_{ac}	2.87	2			6				10								
H_u	2.10													14		12	
H_a	2.09														13		12
H_{outu}	1.25					7				11		14				15	
H_{outa}	1.13						8						13				16
H_{inu}	0.74	1				7						12		15			
H_{ina}	0.72						8						12		16		

Table 11: *Summary of NOESY data for* **2c**.[a] *multiplet centre*

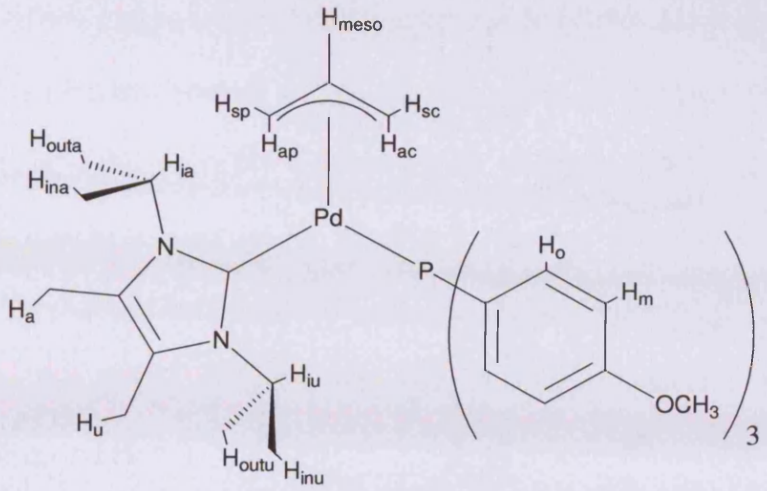

2d	δ(ppm)	H_o	H_m	CH_3[b]	H_{meso}	H_{iu}	H_{ia}	H_{sp}	H_{sc}	H_{ap}	H_{ac}	H_u	H_a	H_{outu}	H_{outa}	H_{inu}	H_{ina}
H_o	6.86								2		3					1	
H_m	6.81			4													
CH_3[b]	3.74		4														
H_{meso}	5.5							4	5		6						
H_{iu}	4.60													8		8	
H_{ia}	4.30												10		9		9
H_{sp}	4.21				5					11					9		
H_{sc}	3.71	2			6						12						
H_{ap}	2.94							11						13			
H_{ac}	2.84	3			7				12								
H_u	2.12													16		14	
H_a	2.10						10								15		14
H_{outu}	1.27					8				13		16				17	
H_{outa}	1.15						9	9					15				18
H_{inu}	0.82	1				8						14		17			
H_{ina}	0.78						9						14		18		

Table 12: *Summary of NOESY data for* ***2d****.*[a] *multiplet centre.*[b] *methoxy*

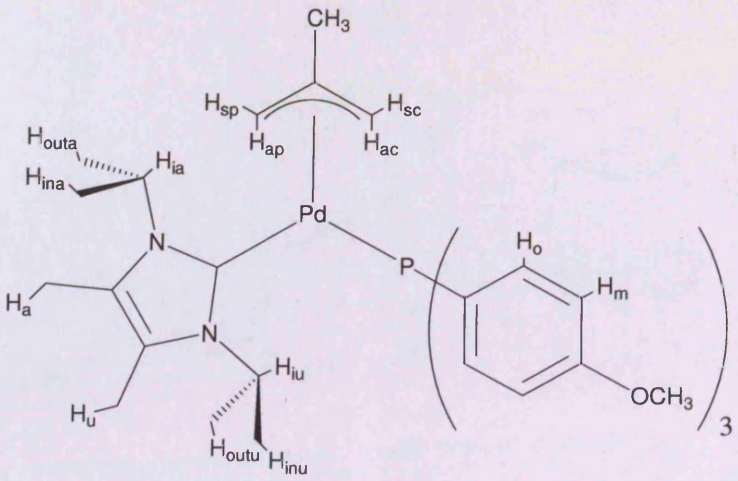

3c	δ(ppm)	H_o	H_m	CH_3^b	CH_3^c	H_{iu}	H_{ia}	H_{sp}	H_{sc}	H_{ap}	H_{ac}	H_u	H_a	H_{outu}	H_{outa}	H_{inu}	H_{ina}
H_o	6.89[a]			5	2				4		3					1	1
H_m	6.82[a]			6													
CH_3^b	3.74	5	6														
CH_3^c	1.87	2						11	13	15					22		21
H_{iu}	4.60													7		7	
H_{ia}	4.35														8		8
H_{sp}	3.96				11					12					10		
H_{sc}	3.43	4			13						14						
H_{ap}	2.81[a]				15			12						16			
H_{ac}	2.81[a]	3							14								
H_u	2.13													20		18	
H_a	2.11														19		17
H_{outu}	1.26				7					16		20				24	
H_{outa}	1.20				22		8	10					19				23
H_{inu}	0.84	1			7							18		24			
H_{ina}	0.75	1			21		8						17		23		

Table 13: *Summary of NOESY data for* ***3c****.*[a] *multiplet centre.* [b] *methoxy.* [c] *crotyl* CH_3

The relative *under/above* assignment of NMR signals for **3c** (***Table 13***) is given by cross peaks 7, 18, 20, 24 (red cells) between protons u (H_u, H_{iu}, H_{outu}, H_{inu}). Interestingly, no cross-peak are observed between H_{iu} and H_u, probably because H_{iu} is pointing away from the carbene methyl towards Pd. A similar pattern is observed for protons a. Absolute assignment stems from key inter-ligand cross-peaks 1 (protons *in* and H_o), 10 (H_{sp}/H_{outa}), 16 (H_{ap}/H_{outu}), 22 (H_{outa}/crotyl CH_3) and 21 (H_{ina}/crotyl CH_3). The fact that H_o interacts with both *in* methyls indicates that dipdmiy retains a perpendicular orientation in solution.

2c and **2d** (***Tables 11*** and ***12***) have essentially the same NOESY pattern as **3c**. The only significant differences are the absence of cross-peaks between R_1 (H_{meso}) and H_{ina} and H_{outa} as a consequence of replacing CH_3 by a hydrogen, and the absence of cross-peaks between H_o and H_{ina} and between H_{sp} and H_{outa} (orange cells). In addition, **2d** displayed a small NOE effect between H_a and H_{ia} (blue cells), but nothing between H_u and H_{iu}. Other key cross-peaks are observed, confirming the assignment obtained for **3c**.

As mentioned above, NOESY can be applied to the observation of chemical exchange (it is then sometimes referred to as EXSY). No negative-phase signals were observed between *in* and *out* protons of dipdmiy, suggesting that there is no free rotation around the Pd-C bond. Finally, no evidence of chemical exchange was found at the allyl in **2c**, **2d** and **3c** under the chosen experimental conditions (298 K, in CD_2Cl_2, 300 ms evolution time). However, because *syn* and *anti* protons show cross-peaks due to proximity, chemical exchange would be difficult to see unless it outweighed (or at least significantly competed with) NOE effects. One way to investigate this would be to perform NOESY experiments at variable temperature and evolution time: changes in cross-peak intensity would indicate that chemical exchange is occuring.

HSQC spectra (see appendices 3, 4 and 5)) allow correlation of ^1H and ^{13}C NMR chemical shifts. Thus, the combination of HSQC and NOESY results in complete ^1H and ^{13}C NMR assignment for

2c, **2d** and **3c**. ***Table 14*** lists selected chemical shifts for these compounds. Mean value and standard deviation for each set of data are provided.

Upon inspection, ***Table 14*** reveals that ^{13}C chemical shifts are most affected by (and thus a good indicator of) the nature of the phosphine and allyl ligands. C_{ia} is more affected than C_{iu}, probably as a consequence of varying R_1 from H to CH_3. Also, C_{inu} and C_{ina} are more affected than C_{outu} and C_{outa} respectively: this observation is consistent with the fact that C_{inu} and C_{ina} are closer to the phosphine, and should be more affected by it.

	H_{iu}	H_{ia}	C_{iu}	C_{ia}	H_{outu}	H_{outa}	C_{outu}	C_{outa}	H_{inu}	H_{ina}	C_{inu}	C_{ina}
2c	4.57	4.26[a]	55.47	54.46	1.25	1.13	22.84	22.59	0.74	0.72	20.90	21.09
2d	4.60	4.30	55.43	54.38	1.27	1.15	22.86	22.63	0.82	0.78	21.24	21.06
3c	4.60	4.35	55.21	54.91	1.26	1.20	22.75	22.57	0.84	0.75	21.07	20.88
mean	4.59	4.33	55.37	54.58	1.26	1.16	22.82	22.60	0.80	0.75	21.07	21.01
std dev	0.02	0.04	0.14	0.29	0.01	0.04	0.06	0.03	0.05	0.03	0.17	0.11

Table 14: *^1H and ^{13}C chemical shifts for **2c**, **2d** and **3c**.[a] multiplet centre*

3.5 Conclusion

A new family of cationic Pd(II) complexes of general formula $[Pd(\pi\text{-allyl})(NHC)(PR_3)]BF_4$ has been described. The range of phosphines that can be incorporated into this type of complex appears to be virtually unlimited. By contrast, the choice of π-allyl and NHC ligands is still restricted, owing to the variable stability of the intermediate complexes [Pd(π-allyl)(Cl)(NHC)]. The structures of some of those complexes were investigated by X-ray crystallography and NMR spectroscopy (including NOESY). Despite the relatively large range of compounds in this study, trends between stereoelectronic properties of phosphines and spectroscopic data of the Pd complexes are difficult to establish, pointing to the limited usefulness of Tolman parameters as accurate descriptors of the chemical properties of phosphine-based metal complexes.

3.6 Experimental Section

3.6.1 General procedures

All manipulations involving air sensitive compounds were performed under argon atmosphere, using standard Schlenk line techniques or in a nitrogen atmosphere MBRAUN UNILAB glovebox with less than 1 ppm water and O_2 (where free NHCs, phosphines and Pd π-allyl dimers were stored). Solvents were dried using appropriate drying agents (CaH_2 for CH_2Cl_2, sodium/benzophenone for THF, Et_2O and hexane). The following compounds were prepared according to literature procedures: $[Ag(dmiy)_2]_2Ag_4I_6$,[68] tmiy and dipdmiy.[69] $[Pd(\eta^3\text{-}C_3H_5)(Cl)]_2$, $[Pd(\eta^3\text{-}C_4H_7)(Cl)]_2$ and $[Pd(\eta^3\text{-}C_3H_4C_6H_5)(Cl)]_2$ were prepared using a slight modification of known literature procedures (using non-degassed H_2O as solvent and no carbon monoxide).[4] NMR spectra were recorded at 298 K on a Bruker Avance 500 MHz with a multinuclear gradient probe. Chemical shift values are given relative to residual solvent peak,[70] *i.e.* for CD_2Cl_2 5.23 ppm for ^1H NMR and 54.00 ppm for ^{13}C NMR. ^{31}P chemical shifts are given relative to H_3PO_4 (capillary tube filled with an aqueous solution of H_3PO_4 in CD_2Cl_2). NOESY spectra were recorded in degassed CD_2Cl_2 with a gradient duration of 300 ms. ESI/MS were perfomed on a WATERS LCT Premier XE instrument, with a source temperature of 80 °C, a desolvation temperature of 200 °C, a capillary voltage of 3500 V and a cone voltage of 100 V. X-ray diffraction data were obtained on a Kappa Nonius CCD diffractometer equipped with an Oxford cryogenic system to maintain the crystals at 150 K. Structure solution and refinement were performed by Dr. Andreas Stasch, Dr. Li-Ling Ooi, or the author as indicated in the text. Microanalyses were performed by Warwick Analytical Services.

3.6.2 Synthesis of compounds of general formula [Pd(π-allyl)(X)(L)]

3.6.2.1 Synthesis of tetramethylimidazol-2-ylidenepalladium allyl chloride 1a

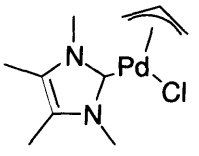

1a

Tetramethylimidazol-2-ylidene (tmiy; 182 mg, 1.47 mmol, 2.1 eq.) was dissolved in 5 mL THF. This solution was syringed into a 5 mL THF suspension of $[Pd(\eta^3\text{-}C_3H_5)Cl]_2$ (256 mg, 0.70 mmol, 1 eq) at -10 °C. The resulting brown solution was warmed to 0 °C for about 15 min. It was then cooled down to -70 °C. A yellow precipitate formed, the solution was filtered out and the solid rinsed with 4 mL of a 1:1 mixture of THF and Et_2O. The collected mass was collected 280 mg (62 %), and the batch number was AN/396/A. Slowly degrades at room temperature, precluding microanalysis and ESI/MS.

^1H NMR (CD_2Cl_2, 500.13 MHz, 298 K): δ (ppm) 5.35 (m, 1H, H_{meso} overlapping with solvent signal), 4.13 (d, 1H, H_{syn} *trans* to Cl, $^3J_{HsynHmeso}$= 7.7 Hz), 3.66 (s, 6H, NCH_3), 3.37(d, 1H, H_{syn} *trans* to tmiy, $^3J_{HsynHmeso}$= 6.6 Hz), 3.20 (d, 1H, H_{anti} *trans* to Cl, $^3J_{HantiHmeso}$ = 13.6 Hz), 2.42 (d, 1H, H_{anti} *trans* to tmiy, $^3J_{HantiHmeso}$ = 11.7 Hz), 2.10 (s, 6H, carbene CH_3).

^{13}C NMR (CD_2Cl_2, 125.76 MHz, 298 K): δ (ppm) 176.09 (s, PdC), 125.33 (s, NC), 114.61 (s, C_{meso}), 71.52 (s, C_{term} anti to Cl), 47.23 (s, C_{term} anti to tmiy), 35.18 (s, NCH_3), 8.91 (s, carbene CH_3).

X-ray diffraction data were collected, solved and refined by Dr. Andreas Stasch.

3.6.2.2 Synthesis of 1,3-diisopropyl-4,5-dimethylimidazol-2-ylidenepalladium allyl chloride 2a

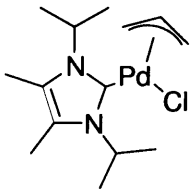

2a

1,3-diisopropyl-4,5-dimethylimidazol-2-ylidene (dipdmiy; 260 mg, 1.40 mmol, 2.05 eq) was dissolved in 2.5 mL THF. This solution was syringed into a 2.5 mL THF suspension of $[Pd(\eta^3\text{-}C_3H_5)Cl]_2$ (250 mg, 0.68 mmol, 1 eq) at -70 °C. The yellow solution was stirred for 25 min, then warmed to room temperature and evaporated. The residue was triturated with a 1:1 mixture of Et_2O and hexane, filtered through a sintered glass filter and vacuum dried. The collected mass was 456 mg (91%) and the batch number was AN/460/A. Yellow solid, decomposes over time at room temperature. This compound was previously described in a patent but no analytical data was reported.

^{1}H NMR (CD_2Cl_2, 500.13 MHz, 298 K): δ (ppm) 5.25-5.35 (two overlapping m overlapping with residual solvent peak, 2H, isopropyl CH and H_{meso}), 4.85 (m, 1H, isopropyl CH), 4.07 (d, H_{syn} *trans* to Cl, $^3J_{HsynHmeso}$= 7.5 Hz), 3.34 (d, 1H, H_{syn} *trans* to tmiy, $^3J_{HsynHmeso}$= 6.6 Hz), 3.18 (d, 1H, H_{anti} *trans* to Cl, $^3J_{HantiHmeso}$=13.6 Hz), 2.33 (d, 1H, H_{anti} *trans* to tmiy, $^3J_{HantiHmeso}$= 11.7 Hz), 2.12-2.20 (two overlapping s, 6H, carbene CH_3), 1.40-1.60 (two overlapping m, 12H, isopropyl CH_3).

^{13}C NMR (CD_2Cl_2, 125.76 MHz, 298 K): δ (ppm) 176.00 (s, PdC), 126.24 (s, NC), 125.62 (s, NC), 114.28 (s, C_{meso}), 70.83 (s, C_{term} anti to Cl), 54.32 (s, isopropyl CH), 53.07 (s, isopropyl CH), 48.23 (s, C_{term} anti to tmiy), 22.88 (s, isopropyl CH_3), 22.61 (s, isopropyl CH_3), 10.50 (s, carbene CH_3), 10.33 (s, carbene CH_3).

Anal. Calcd for $C_{14}H_{25}N_2ClPd$ (MW= 363.24): C, 46.40; H, 6.96; N, 7.73. Found: C, 45.79; H, 6.82; N, 7.55.

X-ray diffraction data were collected, solved and refined by Dr. Li-Ling Ooi.

3.6.2.3 Synthesis of 1,3-diisopropyl-4,5-dimethylimidazol-2-ylidenepalladium crotyl chloride 3a

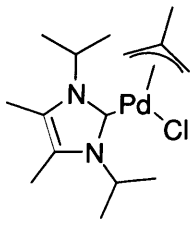

3a

1,3-diisopropyl-4,5-dimethylimidazol-2-ylidene (dipdmiy; 191 mg, 1.03 mmol, 2.05 eq) was dissolved in 2 mL THF. This solution was syringed into a 4 mL THF suspension of $[Pd(\eta^3\text{-}C_4H_7)Cl]_2$ (162 mg, 0.41 mmol, 1 eq) at -55 °C. The yellow solution was stirred for 30 min, then warmed to room temperature and evaporated. The residue was triturated with a 1:1 mixture of Et_2O and hexane, filtered through a sintered glass filter and vacuum dried. The collected mass was 237 mg (75%) and the batch number was AN/455/A. Yellow solid, slowly degrades at room temperature.

^1H NMR (CD_2Cl_2, 500.13 MHz, 298 K): δ (ppm) 5.26 (m, 1H, isopropyl CH), 5.00 (m, 1H, isopropyl CH), 3.87 (d, H_{syn} *trans* to Cl, $^4J_{HsynHsyn}$= 2.9 Hz), 3.15 (m, 1H, H_{syn} *trans* to tmiy), 3.04 (s, 1H, H_{anti} *trans* to Cl), 2.26 (d, 1H, H_{anti} *trans* to tmiy, $^2J_{HantiHsyn}$ = 0.9 Hz), 2.18-2.17 (two overlapping s, 6H, carbene CH_3), 1.97 (s, 3H, crotyl CH_3), 1.40-1.60 (two overlapping m, 12H, isopropyl CH_3).

^{13}C NMR (CD_2Cl_2, 125.76 MHz, 298 K): δ (ppm) 176.89 (s, PdC), 126.07 (s, NC), 125.58 (s, NC), 113.16 (s, C_{meso}), 88.78 (s, C_{term} anti to Cl), 54.32 (s, isopropyl CH), 53.07 (s, isopropyl CH), 43.57 (s, C_{term} anti to tmiy), 23.16 (s, isopropyl CH_3), 22.86 (s, isopropyl CH_3), 22.63 (s, isopropyl CH_3), 22.40 (s, isopropyl CH_3), 17.31 (s, crotyl CH_3), 10.55 (s, carbene CH_3), 10.36 (s, carbene CH_3).

High Resolution ESI_{pos}-MS (MeCN): $[M\text{-}Cl+MeCN]^+$ found 382.1479 (calc. 382.1474, dev: 1.3 ppm)

Anal. Calcd for $C_{15}H_{27}N_2ClPd$ (MW= 377.26): C, 48.53; H, 7.52; N, 7.99. Found: C, 47.86; H, 7.24 N, 7.45.

No X-ray diffraction data were obtained.

3.6.2.4 Synthesis of tricyclohexylphosphinepalladium allyl chloride 5a

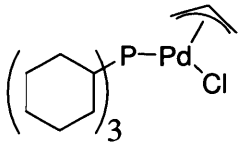

5a

Tricyclohexylphosphine (PCy_3; 767 mg, 2.73 mmol, 1 eq) was dissolved in 20 mL of DCM. This solution was canulated over 5 min to a solution of $[Pd(\eta^3\text{-}C_3H_5)Cl]_2$ (500 mg, 1.37 mmol, 0.5 eq) in 20 mL of DCM. The solution became paler. When the addition was complete, the solution was stirred 30 min, evaporated under reduced pressure and triturated with hexane to afford a yellow solid. The solid was rinsed with hexane. The collected mass was 1.02 g (81 %) and the batch number was AN/329/A. Found identical to literature.[38]

3.6.2.5 Synthesis of tricyclohexylphosphinepalladium crotyl chloride 6a

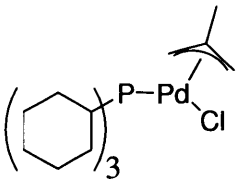

6a

Tricyclohexylphosphine (PCy_3; 712 mg, 2.54 mmol, 1.0 eq) was dissolved in 5 mL of DCM. This solution was canulated over 5 min to a solution of $[Pd(\eta^3\text{-}C_4H_7)Cl]_2$ (500 mg, 1.37 mmol, 0.5 eq) in 5 mL of DCM. The solution became paler. When the addition was complete, the solution was stirred 10 min, evaporated under reduced pressure and triturated with hexane to afford a yellow solid. The solid was rinsed with hexane. The collected mass was 986 mg (81 %) and the batch number was AN/343/A. Found identical to literature.[38]

X-ray diffraction data were collected, solved and refined by Dr. Andreas Stasch.

3.6.2.6 Synthesis of tricyclohexylphosphinepalladium cinnamyl chloride 7a

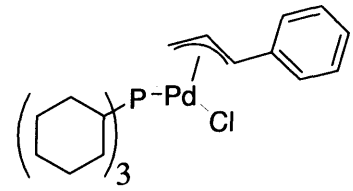

7a

Tricyclohexylphosphine (PCy_3; 832 mg, 2.97 mmol, 1.03 eq) was dissolved in 10 mL of DCM. This solution was canulated over 5 min to a solution of $[Pd(\eta^3\text{-}C_4H_6C_6H_5)Cl]_2$ (750 mg, 1.45 mmol, 0.5 eq) in 10 mL of DCM. The solution became paler. When the addition was complete, the solution was stirred 30 min, evaporated under reduced pressure and triturated with hexane to afford a yellow solid. The solid was rinsed with hexane. The collected mass was 1186 mg (75 %) and the batch number was AN/343/A. Found identical to literature.[38]

X-ray diffraction data were collected, solved and refined by Dr. Andreas Stasch.

3.6.2.7 Synthesis of tricyclohexylphosphinepalladium allyl iodide 8a

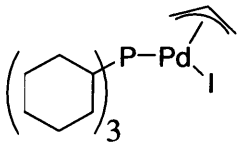

8a

Tricyclohexylphosphinepalladium allyl chloride 5a (144 mg, 0.31 mmol, 1.0 eq) and sodium iodide (466 mg, 3.11 mmol, 10 eq) were suspended in 5 mL of DCM for 18 hr. The reaction mixture was filtered through Celite®, evaporated, and the residue was triturated in hexane to afford the title compound. Yellow powder, the collected mass was 112 mg (65 %) and the batch number was AN/488/A. This compound was reported in a patent but no analytical data were given.[50]

^{1}H NMR (CD_2Cl_2, 500.13 MHz, 298 K): δ (ppm) 5.16 (m, 1H, H_{meso}), 4.53 (m, 1H, H_{syn} *trans* to PCy_3), 3.91 (m, 1H, H_{syn} *trans* to I), 3.12 (dd, 1H, H_{anti} *trans* to PCy_3, $^{3}J_{HantiHmeso}$= 13.5 Hz, J_{PHanti}= 9.0 Hz), 2.75 (d, 1H, H_{anti} *trans* to I, $^{3}J_{HantiHmeso}$= 12.3 Hz), 2.15 (m, 3H, PCH), 1.13-1.87 (m, 30H, PCy_3 cyclohexyl).

^{13}C NMR (CD_2Cl_2, 125.76 MHz, 298 K): δ (ppm) 115.27 (d, C_{meso}, J_{PC}= 5.0 Hz), 75.66 (d, C_{term} *trans* to PCy_3, J_{PC}= 29.9 Hz), 60.64 (d, C_{term} *trans* to I, J_{PC}= 2.0 Hz), 36.01 (d, PCH, J_{PC}= 18.9 Hz), 30.87 (s, CH_2), 28.10 (d, CH_2, J_{PC}= 3.0 Hz), 28.01 (d, CH_2, J_{PC}= 3.0 Hz), 26.93 (s, CH_2).

^{31}P{^{1}H} NMR (CD_2Cl_2, 202.46 MHz, 298 K): δ (ppm) 39.68.

High Resolution ESI_{pos}-MS (MeCN): $[M\text{-}I+MeCN]^+$ found 466.1994 (calc. 466.2017, dev: -4.9 ppm)

Anal calcd. For $C_{21}H_{38}PPdI$ (MW= 554.82): C, 45.46; H, 6.90; P, 5.58. Found: C, 45.21; H, 6.85; P, 5.86.

X-ray diffraction data were collected, solved and refined by Dr. Li-Ling Ooi.

3.6.3 Synthesis of compounds of general formula [Pd(π-allyl)(L)(L')]BF_4

3.6.3.1 Synthesis of tricycloxexylphosphine acetonitrilepalladium allyl tetrafluoroborate 8b

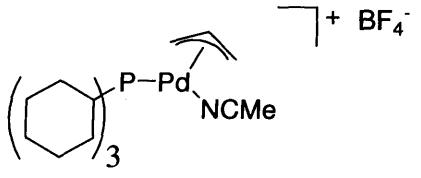

8b

$AgBF_4$ (42 mg, 0.22 mmol, 1 eq) and [Pd(η^3-C_3H_5)(Cl)(PCy_3)] **5a** (100 mg, 0.22 mmol, 1 eq) were stirred in dry acetonitrile (5 mL) under argon for 1 hour. The suspension was then filtered through Celite® and the filtrate was concentrated to about 1 mL by evaporation. Dry Et_2O was then added to precipitate the product and the resulting powder was dried under vacuum. The collected mass was 111mg (91 %) and the batch number was AN/368/A.

^{1}H NMR (CD_2Cl_2, 500.13 MHz, 298 K): δ (ppm) 5.51 (m, 1H, H_{meso}), 4.95 (m, 1H, H_{syn} *trans* to PCy_3), 3.70 (dd, 1H, H_{anti} *trans* to PCy_3, $^3J_{HantiHmeso}$= 14.4 Hz, J_{PHanti}= 8.4 Hz), 3.48 (m, 1H, H_{syn} *trans* to MeCN), 2.69 (d, 1H, H_{anti} *trans* to MeCN, $^3J_{HantiHmeso}$= 11.8 Hz), 2.34 (s, 3H, MeCN), 1.86-1.96 (m, 3H, PCH), 1.12-1.85 (m, 30H, PCy_3 cyclohexyl).

^{13}C NMR (CD_2Cl_2, 125.76 MHz, 298 K): δ (ppm) 120.51 (bs, C_{meso}), 84.71 (d, C_{term} *trans* to PCy_3, J_{PC}= 21.9 Hz), 52.36 (s, C_{term} *trans* to MeCN), 35.32 (d, , PCH, J_{PC}= 18.9 Hz), 30.85(s, CH_2), 30.70 (s, CH_2), 28.07 (d, CH_2, J_{PC}= 2.0 Hz), 27.99 (d, CH_2, J_{PC}= 2.0 Hz), 26.72 (s, CH_2), 3.57 (s, MeCN CH_3). The signal for the carbon atom of CN in acetonitrile was not seen.

X-ray diffraction data were collected, solved and refined by Dr. Andreas Stasch.

3.6.3.2 Synthesis of tricyclohexylphosphine tetramethyl-imidazol-2-ylidenepalladium allyl tetrafluoroborate 1b

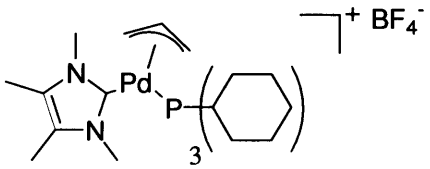

1b

A mixture of tetramethylimidazol-2-ylidenepalladium allyl chloride **1a** (230 mg, 1.07 mmol, 1.0 eq) and sodium tetrafluoroborate (334 mg, 3.21 mmol, 3.0 eq) was suspended in 2.5 mL of DCM.. Tricyclohexylphosphine (329 mg, 1.17 mmol, 1.1 eq) was added as a 2.5 mL solution in DCM over 5 min. The reaction mixture was stirred at room temperature for 3 hr then filtered through Celite®, and the solution was evaporated and triturated with Et_2O. The resulting brown-red powder was further purified by successive washes with small amounts of hot THF to yield a white powder. The collected mass was 230 mg and the batch number was AN478/A. A further 115 mg was obtained from the THF liquors (combined yield 47%).

^{1}H NMR (CD_2Cl_2, 500.13 MHz, 298 K): δ (ppm) 5.24 (m overlapping with solvent signal, 1H, H_{meso}), 4.10 (overlapped m, 1H, H_{syn} *trans* to tmiy), 4.07 (overlapped m, 1H, H_{syn} *trans* to PCy_3), 3.47 (s, 3H, NCH_3), 3.30 (s, 3H, NCH_3), 2.80 (dd, 1H, H_{anti} *trans* to PCy_3, $^3J_{HantiHmeso}$= 13.8 Hz, J_{PHanti}= 8.9 Hz), 2.58 (d, 1H, H_{anti} *trans* to tmiy, $^3J_{HantiHmeso}$= 13.2 Hz), 2.09 (s, 3H, carbene CH3), 2.07 (s, 3H, carbene CH3), 1.80 (m, 3H, PCH), 1.60-1.75 (m, 15H, PCy_3 cyclohexyl), 1.00-1.23 (m, 15H, PCy_3 cyclohexyl). Signals were assigned on the basis of a gs-HSQC experiment. A gs-COSY experiment showed coupling between H_{meso} and both H_{syn}, but it was impossible to resolve the spectrum in order to obtain coupling constants.

^{13}C NMR (CD_2Cl_2, 125.76 MHz, 298 K): δ (ppm) 173.15 (d, PdC, J_{PC}= 16.3 Hz), 127.95 (s, NC), 127.74 (s, NC), 119.88 (d, C_{meso}, J_{PC}= 4.5 Hz), 66.50 (d, C_{term} *trans* to PCy_3, J_{PC}= 27.9 Hz), 61.28 (s, C_{term} *trans* to tmiy), 36.85 (d, PCH, J_{PC}= 18.9 Hz), 36.26 (s, NCH_3), 36.01 (s, NCH_3), 30.94 (s, CH_2),

30.64 (s, CH_2), 27.95 (s, CH_2), 27.86 (s, CH_2), 26.65 (s, CH_2), 9.43 (s, carbene CH_3), 9.37 (s, carbene CH_3).

$^{31}P\{^1H\}$ NMR (CD_2Cl_2, 202.46 MHz, 298 K): δ (ppm) 42.88.

High Resolution ESI_{pos}-MS (MeCN): found 551.2729 (calc. 551.2746, dev: -3.2 ppm)

Anal calcd. For $C_{28}H_{50}N_2PPdBF_4$ (MW= 638.28): C, 52.64; H, 7.89; N, 4.39. Found: C, 52.78; H, 7.78; N, 4.15.

X-ray diffraction data.was collected, solved and refined by Dr. Andreas Stasch.

3.6.3.3 Synthesis of triphenylphosphine tetramethylimidazol-2-ylidenepalladium allyl tetrafluoroborate 1c

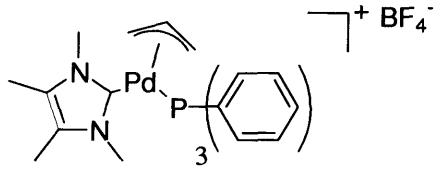

1c

A mixture of tetramethylimidazol-2-ylidenepalladium allyl chloride **1a** (125 mg, 0.41 mmol, 1.0 eq) and sodium tetrafluoroborate (131 mg, 1.27 mmol, 3.0 eq) was suspended in 2.5 mL of DCM.. Triphenylphosphine (113 mg, 0.43 mmol, 1.1 eq) was added as a 2.5 mL solution in DCM over 5 min. The reaction mixture turned from pink to yellow to orange. It was stirred at room temperature for 2.5 hr then filtered through Celite®, evaporated and purified by trituration with THF, followed by successive washes with small amounts of hot THF. White powder, the collected mass was 108 mg (42 %) and the batch number was AN/475/A.

^1H NMR (CD_2Cl_2, 500.13 MHz, 298 K): δ (ppm) 7.39-7.44 (m, 3H, H_{arom} para to P), 7.28-7.34 (m, 6H, H_{arom} meta to P), 7.06-7.12 (m, 6H, H_{arom} ortho to P), 5.58 (m, 1H, H_{meso}), 4.29 (m, 1H, H_{syn} *trans* to PPh_3), 3.99 (d, 1H, H_{syn} *trans* to tmiy, $^3J_{HsynHmeso}$= 7.3 Hz), 3.09 (s, 3H, NCH_3), 3.06 (m overlapping with NCH_3 signal, 1H, H_{anti} *trans* to PPh_3,), 2.95 (s, 3H, NCH_3), 2.91 (d, 1H, H_{anti} *trans*

to tmiy, $^{3}J_{HantiHmeso}$= 13.2 Hz), 1.90 (s, 6H, carbene CH_3). Signals were assigned on the basis of gs-HSQC and gs-NOESY experiments (appendix 3).

^{13}C NMR (CD_2Cl_2, 125.76 MHz, 298 K): δ (ppm) 171.90 (d, PdC, J_{PC}= 16.8 Hz), 133.79 (d, C_{arom} ortho to P, J_{PC}= 13.0 Hz), 132.12 (d, PC_{arom}, J_{PC}= 43.9 Hz), 131.67 (d, C_{arom} para to P, J_{PC}= 3.0 Hz), 129.52 (d, C_{arom} meta to P, J_{PC}= 11.0 Hz), 127.78 (s, NC), 127.62 (s, NC), 121.59 (d, C_{meso}, J_{PC}= 5.5 Hz), 68.88 (d, C_{term} *trans* to tmiy), 65.84 (s, C_{term} *trans* to PPh_3, J_{PC}= 30.9 Hz), 35.39 (s, NCH_3), 35.24 (s, NCH_3), 9.29 (s, carbene CH_3).

$^{31}P\{^{1}H\}$ NMR (CD_2Cl_2, 202.46 MHz, 298 K): δ (ppm) 26.12.

High Resolution ESI_{pos}-MS (MeCN): found 531.1332 (calc. 531.1343 dev: -2.1 ppm)

Anal calcd. For $C_{28}H_{32}N_2PPdBF_4$ (MW= 620.14): C, 54.18; H, 5.20; N, 4.52. Found: C, 54.01; H, 5.11; N, 4.34.

X-ray diffraction data were collected, solved and refined by Dr. Li-Ling Ooi.

3.6.3.4 Synthesis of tris(4-methoxyphenyl)phosphine tetramethylimidazol-2-ylidenepalladium allyl tetrafluoroborate 1d

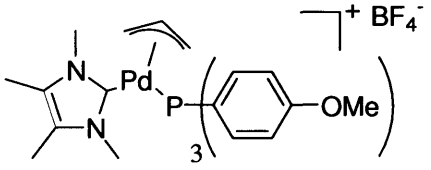

1d

A mixture of tetramethylimidazol-2-ylidenepalladium allyl chloride **1a** (125 mg, 0.41 mmol, 1.0 eq) and sodium tetrafluoroborate (131 mg, 1.27 mmol, 3.0 eq) was suspended in 2.5 mL of DCM.. Tris(4-methoxyphenyl)phosphine (140 mg, 0.43 mmol, 1.1 eq) was added as a 2.5 mL solution in DCM over 5 min. No change of colour was observed. The reaction mixture was stirred at room temperature for 2.5 hr then filtered through Celite®, evaporated and purified by trituration with Et_2O, then 3:1 Et_2O/THF mixtures to give a yellow oil, turning back to a powder after drying and

triturating with Et_2O). Yellow powder, soluble in THF, the collected mass was 145 mg (50 %) and the batch number was AN/475/B.

^1H NMR (CD_2Cl_2, 500.13 MHz, 298 K): δ (ppm) 6.93-6.98 (m, 6H, H_{arom}), 6.77-6.81 (m, 6H, H_{arom}), 5.52 (m, 1H, H_{meso}), 4.22 (m, 1H, H_{syn} *trans* to $P(C_6H_4OMe)_3$), 3.92 (d, 1H, H_{syn} *trans* to tmiy, $^3J_{HsynHmeso}$= 7.3 Hz), 3.72 (s, 9H, OCH_3), 3.10 (s, 3H, NCH_3), 3.00 (dd, 1H, H_{anti} *trans* to $P(C_6H_4OMe)_3$, $^3J_{HantiHmeso}$= 13.5 Hz, J_{PHsyn}= 10.3 Hz), 2.95 (s, 3H, NCH_3), 2.85 (d, 1H, H_{anti} *trans* to tmiy, $^3J_{HantiHmeso}$= 13.4 Hz), 1.90 (s, 6H, carbene CH_3). Signals were assigned on the basis of gs-HSQC and gs-NOESY experiments (appendix 3).

^{13}C NMR (CD_2Cl_2, 125.76 MHz, 298 K): δ (ppm) 172.84 (d, PdC, J_{PC}= 21.3 Hz), 162.40 (d, $C_{arom}O$, J_{PC}= 2.0 Hz), 135.21 (d, C_{arom}, J_{PC}= 15.0 Hz), 127.56 (s, NC), 127.40 (s, NC), 123.57 (d, PC, J_{PC}= 48.9 Hz), 121.35 (d, C_{meso}, J_{PC}= 5.5 Hz), 115.00 (d, C_{arom}, J_{PC}= 11.5 Hz), 68.08 (s, C_{term} *trans* to tmiy), 65.23 (d, C_{term} *trans* to $P(C_6H_4OMe)_3$, J_{PC}= 31.4 Hz), 56.05 (s, OCH_3), 35.44 (s, NCH_3), 35.27 (s, NCH_3), 9.33 (s, carbene CH_3).

$^{31}P\{^1H\}$ NMR (CD_2Cl_2, 202.46 MHz, 298 K): δ (ppm) 22.23.

High Resolution ESI_{pos}-MS (MeCN): found 621.1632 (calc. 621.1660 dev: -4.5 ppm)

Anal calcd. For $C_{31}H_{38}N_2O_3PPdBF_4$ (MW= 710.17): C, 52.38; H, 5.39; N, 3.99. Found: C, 51.00; H, 5.27; N, 4.09. These values are not satisfactory due to the solubility of **1d** in THF, causing minor impurities to remain in the sample.

No X-ray diffraction data were obtained.

3.6.3.5 Synthesis of tribenzylphosphine tetramethylimidazol-2-ylidenepalladium allyl tetrafluoroborate 1e

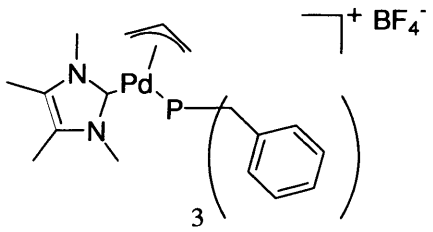

1e

A mixture of tetramethylimidazol-2-ylidenepalladium allyl chloride **1a** (125 mg, 0.41 mmol, 1.0 eq) and sodium tetrafluoroborate (131 mg, 1.27 mmol, 3.0 eq) was suspended in 2.5 mL of DCM.. Tribenzylphosphine (131 mg, 0.43 mmol, 1.1 eq) was added as a 2.5 mL solution in DCM over 5 min. The reaction mixture turned from pink to yellow. It was stirred at room temperature for 2.5 hr then filtered through Celite®, evaporated and purified by trituration with THF, followed by successive washes with small amounts of hot THF. White powder, the collected mass was 167 mg (62 %) and the batch number was AN/475/C.

^{1}H NMR (CD_2Cl_2, 500.13 MHz, 298 K): δ (ppm) 7.21-7.25 (m, 9H, H_{arom}), 6.96-7.00 (m, 6H, H_{arom}), 4.99 (m, 1H, H_{meso}), 3.94 (m, 1H, H_{syn} *trans* to PBz_3), 3.04-3.14 (two overlapping m, 7H, PCH_2 and H_{syn} *trans* to tmiy), 3.02 (s, 3H, NCH_3), 2.82 (s, 3H, NCH_3), 2.65 (dd, H_{anti} *trans* to PBz_3, $^3J_{HantiHmeso}$= 13.3 Hz, J_{PHanti}= 10.3 Hz), 2.08 (d, 1H, H_{anti} *trans* to tmiy, $^3J_{HantiHmeso}$= 13.4 Hz), 1.98 (s, 3H, CCH_3), 1.97 (s, 3H, CCH_3). Signals were assigned on the basis of gs-HSQC and gs-NOESY experiments (appendix 3).

^{13}C NMR (CD_2Cl_2, 125.76 MHz, 298 K): δ (ppm) 171.83 (d, PdC, J_{PC}= 19.9 Hz), 134.59 (d, C_{arom}, J_{PC}= 3.0 Hz), 130.28 (d, C_{arom}, J_{PC}= 5.0 Hz), 129.46 (d, C_{arom}, J_{PC}= 2.0 Hz), 127.87 (d, C_{arom}, J_{PC}= 3.0 Hz), 127.77 (s, NC), 127.58 (s, NC), 121.21 (d, C_{meso}, J_{PCmeso}= 6.0 Hz), 66.01 (s, C_{term} *trans* to PBz_3, J_{PC}= 29.9 Hz), 64.45 (d, C_{term} *trans* to tmiy), 35.42 (d, PCH_2, J_{PC}= 17.0 Hz), 35.27 (s, NCH_3), 34.99 (s, NCH_3), 9.36 (s, carbene CH_3), 9.34 (s, carbene CH_3).

$^{31}P\{^{1}H\}$ NMR (CD_2Cl_2, 202.46 MHz, 298 K): δ (ppm) 25.96.

High Resolution ESI_{pos}-MS (MeCN): found 575.1779 (calc. 575.1807 dev: -4.9 ppm)

Anal calcd. For $C_{31}H_{38}N_2PPdBF_4$ (MW= 662.18): C, 56.18; H, 5.78; N, 4.23. Found: C, 56.05; H, 5.76; N, 4.20.

X-ray diffraction data were collected, solved and refined by Dr. Li-Ling Ooi.

3.6.3.6 Synthesis of triethylphosphine tetramethylimidazol-2-ylidenepalladium allyl tetrafluoroborate 1e

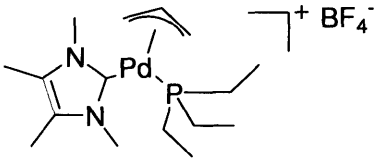

1f

A mixture of tetramethylimidazol-2-ylidenepalladium allyl chloride **1a** (140 mg, 0.46 mmol, 1.0 eq) and sodium tetrafluoroborate (142 mg, 1.37 mmol, 3.0 eq) was suspended in 3.0 mL of DCM.. Triethylphosphine (d=0.81, 70µl, 0.48 mmol, 1.05 eq) was added neat by microsyringe over 2 min. The reaction mixture was stirred at room temperature for 3 hr then filtered through Celite®, evaporated and purified by trituration with hexane, followed by trituration in 1:3 mixtures of THF/Et_2O (forms an oil which turned back into powdery material after drying and triturating with hexane). Yellow-green powder, soluble in THF, forms an oil when washed with Et_2O. The collected mass was 111 mg (51 %) and the batch number was AN/446/A.

^{1}H NMR (CD_2Cl_2, 500.13 MHz, 298 K): δ (ppm) 5.31 (m, 1H, H_{meso}), 4.12 (m, 1H, H_{syn} *trans* to PEt_3), 3.93 (d, 1H, H_{syn} *trans* to tmiy, $^{3}J_{HsynHmeso}$= 7.5 Hz), 3.46 (s, 3H, NCH_3), 3.29 (s, 3H, NCH_3), 2.83 (dd, H_{anti} *trans* to PEt_3, $^{3}J_{HantiHmeso}$= 13.7 Hz, J_{PHanti}= 9.4 Hz), 2.66 (d, 1H, H_{anti} *trans* to tmiy, $^{3}J_{HantiHmeso}$= 13.4 Hz), 2.08 (s, 3H, CCH_3), 2.06 (s, 3H, carbene CH_3), 1.61 (m, 6H, PCH_2), 0.94 (m, 9H, CH_3).

^{13}C NMR (CD_2Cl_2, 125.76 MHz, 298 K): δ (ppm) 172.39 (d, PdC, J_{PC}= 18.9 Hz), 127.73 (s, NC), 127.54 (s, NC), 121.13 (d, C_{meso}, J_{PCmeso}= 5.0 Hz), 66.13 (s, C_{term} *trans* to PEt_3, J_{PC}= 28.9 Hz), 61.72 (d, C_{term} *trans* to tmiy), 35.82 (s, NCH_3), 35.59 (s, NCH_3), 19.10 (d, PCH_2, J_{PC}= 24.9 Hz), 9.37 (s, carbene CH_3), 8.53 (s, CH3).

$^{31}P\{^1H\}$ NMR (CD_2Cl_2, 202.46 MHz, 298 K): δ (ppm) 21.38.

High Resolution ESI_{pos}-MS (MeCN): found 389.1328 (calc. 389.1338 dev: -2.6 ppm)

Anal calcd. For $C_{16}H_{32}N_2PPdBF_4$ (MW= 476.14): C, 40.32; H, 6.77; N, 5.88; P, 6.51. Found: C, 39.91; H, 6.70; N, 5.91; P, 6.25.

No X-ray diffraction data were obtained.

3.6.3.7 Synthesis of tricyclohexylphosphine 1,3-diisopropyl-4,5-dimethylimidazol-2-ylidenepalladium allyl tetrafluoroborate 2b

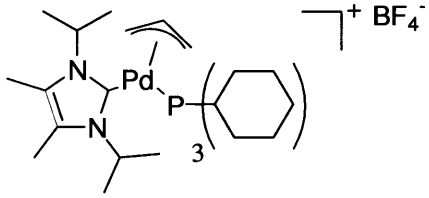

2b

A mixture of 1,3-diisopropyl-4,5-dimethylimidazol-2-ylidenepalladium allyl chloride **2a** (249 mg, 0.67 mmol, 1.0 eq) and sodium tetrafluoroborate (214 mg, 2.06mmol, 3.0 eq) was suspended in 3 mL of DCM. Tricyclohexylphosphine (212 mg, 0.75 mmol, 1.1 eq) was added as a 3 mL solution in DCM over 5 min. The reaction mixture was stirred at room temperature for 4.5 hr then filtered through Celite®, evaporated and triturated with Et_2O. The resulting powder was taken in hot THF and cooled to -80 °C for 30 min. The resulting precipitate was filtered, rinsed with Et_2O and dried under vacuum. White powder, the collected mass was 160 mg (35 %) and the batch number was AN/421/D.

^1H NMR (CD_2Cl_2, 500.13 MHz, 298 K): δ (ppm) 5.20 (m overlapping with solvent signal, 1H, H_{meso}), 4.61 (m, 1H, isopropyl CH), 4.36 (m, 1H, isopropyl CH), 4.09-4.15 (two overlapped m, 2H,

H_{syn} *trans* to dipdmiy and PCy_3), 2.72 (dd, 1H, H_{anti} *trans* to PCy_3, $^3J_{HantiHmeso}$= 13.5 Hz, J_{PHanti}= 8.8 Hz), 2.58 (d, 1H, H_{anti} *trans* to tmiy, $^3J_{HantiHmeso}$= 13.2 Hz), 2.18 (s, 3H, carbene CH_3), 2.15 (s, 3H, carbene CH_3), 1.86 (m, 3H, PCH), 1.61-1.75 (m, 15H, PCy_3 cyclohexyl), 1.49 (d, 3H, isopropyl CH_3, $^3J_{HH}$= 7.2 Hz), 1.39 (d, 3H, isopropyl CH_3, $^3J_{HH}$= 7.2 Hz), 1.30 (d, 3H, isopropyl CH_3, $^3J_{HH}$= 7.0 Hz), 1.24 (overlapped d, 3H, isopropyl CH_3, $^3J_{HH}$= 7.0 Hz), 1.02-1.30 (overlapped m, 9H, PCy_3 cyclohexyl). Signals were assigned on the basis of gs-NOESY and gs-HSQC experiments (appendix 3).

^{13}C NMR (CD_2Cl_2, 125.76 MHz, 298 K): δ (ppm) 173.35 (d, PdC, J_{PC}= 15.0 Hz), 128.37 (s, NC), 128.02 (s, NC), 119.37 (d, C_{meso}, J_{PC}= 4.0 Hz), 66.72 (d, C_{term} *trans* to PCy_3, J_{PC}= 27.9 Hz), 60.79 (s, C_{term} *trans* to tmiy), 55.16 (s, isopropyl CH), 54.71 (s, isopropyl CH), 36.57 (d, PCH, J_{PC}= 18.9 Hz), 30.81 (s, CH_2), 30.64 (s, CH_2), 30.56 (s, CH_2), 27.94 (s, CH_2), 27.92 (s, CH_2),), 27.85 (s, CH_2), 27.84 (s, CH_2), 26.58 (s, CH_2), 23.23 (s, isopropyl CH_3), 22.82 (s, isopropyl CH_3), 21.71 (s, isopropyl CH_3), 21.51 (s, isopropyl CH_3), 10.92 (s, carbene CH_3), 10.90 (s, carbene CH_3).

$^{31}P\{^1H\}$ NMR (CD_2Cl_2, 202.46 MHz, 298 K): δ (ppm) 41.26.

High Resolution ESI_{pos}-MS (MeCN): found 605.3354 (calc. 605.3378, dev: -4.0 ppm)

Anal calcd. For $C_{32}H_{58}N_2PPdBF_4$ (MW= 638.28): C, 55.30; H, 8.41; N, 4.03. Found: C, 55.10; H, 8.30; N, 3.94.

X-ray diffraction data were collected, solved and refined by the author, with the guidance of Dr. D. J. Beetstra.

3.6.3.8 Synthesis of triphenylphosphine 1,3-diisopropyl-4,5-dimethylimidazol-2-ylidenepalladium allyl tetrafluoroborate 2c

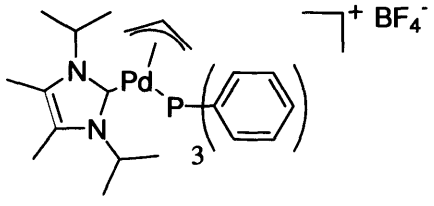

2c

A mixture of 1,3-diisopropyl-4,5-dimethylimidazol-2-ylidenepalladium allyl chloride **2a** (200 mg, 0.54 mmol, 1.0 eq) and sodium tetrafluoroborate (169 mg, 1.63 mmol, 3.0 eq) was suspended in 3 mL of DCM.. Triphenylphosphine (150 mg, 0.57 mmol, 1.1 eq) was added as a 3.0 mL solution in DCM over 3 min. The reaction mixture was stirred at room temperature for 2.5 hr then filtered through Celite®, evaporated and purified by trituration Et_2O, a 3:1 mixture of Et_2O/THF and finally with THF. White powder, the collected mass was 262 mg (71 %) and the batch number was AN/462/A.

^1H NMR (CD_2Cl_2, 500.13 MHz, 298 K): δ (ppm) 7.39-7.44 (m, 3H, H_{arom} para to P), 7.28-7.34 (m, 6H, H_{arom} meta to P), 6.94-7.00 (m, 6H, H_{arom} ortho to P), 5.53 (m, 1H, H_{meso}), 4.57 (m, 1H, isopropyl CH), 4.22-4.30 (two overlapped m, 2H, isopropyl CH and H_{syn} *trans* to PPh_3), 3.76 (dm, 1H, H_{syn} *trans* to tmiy, $^3J_{HsynHmeso}$= 7.3 Hz), 2.98 (dd, 1H, H_{anti} *trans* to PPh_3, $^3J_{HantiHmeso}$= 13.4 Hz, J_{PHanti}= 9.9 Hz), 2.87 (d, 1H, H_{anti} *trans* to tmiy, $^3J_{HantiHmeso}$= 13.4 Hz), 2.10 (s, 3H, CCH_3), 2.09 (s, 3H, CCH_3), 1.25 (d, 3H, isopropyl CH_3, $^3J_{HH}$= 7.0 Hz), 1.13 (d, 3H, isopropyl CH_3, $^3J_{HH}$= 7.0 Hz), 0.74 (d, 3H, isopropyl CH_3, $^3J_{HH}$= 7.2 Hz), 0.72 (d, 3H, isopropyl CH_3, $^3J_{HH}$= 7.2 Hz). Signals were assigned on the basis of gs-NOESY and gsHSQC experiments (appendix 3).

^{13}C NMR (CD_2Cl_2, 125.76 MHz, 298 K): δ (ppm) 170.75 (d, PdC, J_{PC}= 18.9 Hz), 133.81 (d, C_{arom}, J_{PC}= 13.0 Hz), 132.10 (d, PC_{arom}, J_{PC}= 42.9 Hz), 131.72 (d, C_{arom}, J_{PC}= 2.0 Hz), 129.66 (d, C_{arom}, J_{PC}= 11.0 Hz), 128.50 (s, NC), 127.95 (s, NC), 121.02 (d, C_{meso}, J_{PC}= 6.0 Hz), 69.87 (d, C_{term} *trans* to dipdmiy, J_{PC}= 2.0 Hz), 66.17 (d, C_{term} *trans* to PPh_3, J_{PC}= 30.9 Hz), 55.47 (s, isopropyl CH), 54.46 (s, isopropyl CH), 22.84 (s, isopropyl CH_3), 22.59 (s, isopropyl CH_3), 21.09 (s, isopropyl CH_3), 20.90 (s, isopropyl CH_3), 10.62 (s, carbene CH_3), 10.52 (s, carbene CH_3).

$^{31}P\{^1H\}$ NMR (CD_2Cl_2, 202.46 MHz, 298 K): δ (ppm) 23.75.

High Resolution ESI_{pos}-MS (MeCN): found 587.1948 (calc. 587.1969 dev: -3.6 ppm)

Anal calcd. For $C_{32}H_{40}N_2PPdBF_4$ (MW= 676.20): C, 56.79; H, 5.96; N, 4.14; P, 4.58. Found: C, 55.89; H, 6.03; N, 3.78; P, 4.36.

No X-ray diffraction data were obtained.

3.6.3.9 Synthesis of tris(4-methoxyphenyl)phosphine 1,3-diisopropyl-4,5-dimethylimidazol-2-ylidenepalladium allyl tetrafluoroborate 2d

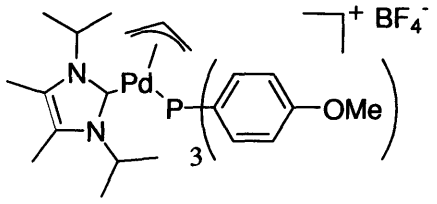

2d

A mixture of 1,3-diisopropyl-4,5-dimethylimidazol-2-ylidenepalladium allyl chloride **2a** (250 mg, 0.69 mmol, 1.0 eq) and sodium tetrafluoroborate (214 mg, 2.06 mmol, 3.0 eq) was suspended in 5 mL of DCM.. Tris(4-methoxyphenyl)phosphine (255 mg, 0.78 mmol, 1.05 eq) was added as a 5 mL solution in DCM over 1 min. The reaction mixture turned from yellow to colourless and finally to orange (after 30 min). It was stirred at room temperature for 5 hr then filtered through Celite®, evaporated and purified by trituration with Et_2O, followed by washing with hot THF. White powder, the collected mass was 290 mg (56 %) and the batch number was AN/449/A.

^{1}H NMR (CD_2Cl_2, 500.13 MHz, 298 K): δ (ppm) 6.83-6.90 (m, 6H, H_{arom} ortho to P), 6.79-6.83 (m, 6H, H_{arom} meta to P), 5.50 (m, 1H, H_{meso}), 4.60 (m, 1H, isopropyl CH), 4.30 (m, 2H, isopropyl CH), 4.21 (m, 1H, H_{syn} *trans* to $P(C_6H_4OMe)_3$), 3.74 (s, 9H, OCH_3), 3.71 (overlapped m, 1H, H_{syn} *trans* to dipdmiy), 2.94 (dd, 1H, H_{anti} *trans* to $P(C_6H_4OMe)_3$, $^3J_{HantiHmeso}$= 13.5 Hz, J_{PHanti}= 9.9 Hz), 2.84 (d, 1H, H_{anti} *trans* to tmiy, $^3J_{HantiHmeso}$= 13.4 Hz), 2.12 (s, 3H, carbene CH_3), 2.10 (s, 3H, carbene CH_3), 1.27 (d, 3H, isopropyl CH_3, $^3J_{HH}$= 7.2 Hz), 1.15 (d, 3H, isopropyl CH_3, $^3J_{HH}$= 7.0 Hz), 0.82 (d, 3H, isopropyl CH_3, $^3J_{HH}$= 7.2 Hz), 0.78 (d, 3H, isopropyl CH_3, $^3J_{HH}$= 7.0 Hz). Signals were assigned on the basis of gs-HSQC and gNOESY experiments (appendix 3).

^{13}C NMR (CD_2Cl_2, 125.76 MHz, 298 K): δ (ppm) 171.32 (d, PdC, J_{PC}= 17.0 Hz), 162.40 (bs, $C_{arom}O$), 135.23 (d, C_{arom} ortho to P, J_{PC}= 15.0 Hz), 128.39 (s, NC), 127.81 (s, NC), 123.65 (d, PC,

J_{PC}= 48.9 Hz), 120.78 (d, C_{meso}, J_{PC}= 5.0 Hz), 115.16 (d, C_{arom} meta to P, J_{PC}= 11.0 Hz), 69.08 (s, C_{term} *trans* to tmiy), 65.68 (d, C_{term} *trans* to $P(C_6H_4OMe)_3$, J_{PC}= 30.9 Hz), 56.05 (s, OCH_3), 55.43 (s, isopropyl CH), 54.38 (s, isopropyl CH), 22.86 (s, isopropyl CH_3), 22.63 (s, isopropyl CH_3), 21.24 (s, isopropyl CH_3), 21.06 (s, isopropyl CH_3), 10.68 (s, carbene CH_3), 10.59 (s, carbene CH_3).

$^{31}P\{^1H\}$ NMR (CD_2Cl_2, 202.46 MHz, 298 K): δ (ppm) 19.86.

High Resolution ESI_{pos}-MS (MeCN): found 679.2287 (calc. 679.2281 dev: 0.9 ppm).

Anal calcd. For $C_{35}H_{46}N_2O_3PPdBF_4$ (MW= 738.23): C, 54.81; H, 6.05; N, 3.66; P, 4.04. Found: C, 54.66; H, 6.00; N, 3.60; P, 3.97.

X-ray diffraction data were collected, solved and refined by Dr. Li-Ling Ooi.

3.6.3.10 Synthesis of triethylphosphine 1,3-diisopropyl-4,5-dimethylimidazol-2-ylidenepalladium allyl tetrafluoroborate 2e

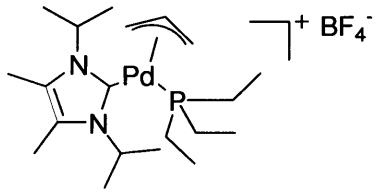

2e

A mixture of 1,3-diisopropyl-4,5-dimethylimidazol-2-ylidenepalladium allyl chloride **2a** (250 mg, 0.69 mmol, 1.0 eq) and sodium tetrafluoroborate (214 mg, 2.06 mmol, 3.0 eq) was suspended in 5 mL of DCM.. Triethylphosphine (d=0.81, 105µl, 0.72 mmol, 1.05 eq) was added neat by microsyringe over 2 min. The reaction mixture was stirred at room temperature for 3 hr then filtered through Celite®, evaporated and purified by trituration with Et_2O. Yellow-green powder, the collected mass was 193 mg (53 %) and the batch number was AN/447/A2.

^1H NMR (CD_2Cl_2, 500.13 MHz, 298 K): δ (ppm) 5.28 (m, 1H, H_{meso}), 4.58 (m, 1H, isopropyl CH), 4.31 (m, 1H, isopropyl CH), 4.13 (m, 1H, H_{syn} *trans* to PEt_3), 3.90 (d, 1H, H_{syn} *trans* to dipdmiy, $^3J_{HsynHmeso}$= 6.9 Hz), 2.75 (dd, H_{anti} *trans* to PEt_3, $^3J_{HantiHmeso}$= 13.0 Hz, J_{PHanti}= 9.5 Hz), 2.65 (d, 1H, H_{anti} *trans* to tmiy, $^3J_{HantiHmeso}$= 13.2 Hz), 2.17 (s, 3H, carbene CH_3), 2.14 (s, 3H, carbene CH_3), 1.65

(m, 6H, PCH_2), 1.45 (d, 3H, isopropyl CH_3, $^3J_{HH}$= 7.3 Hz), 1.34 (overlapped d, 3H, isopropyl CH_3, $^3J_{HH}$= 6.9 Hz), 1.33 (overlapped d, 3H, isopropyl CH_3, $^3J_{HH}$= 6.9 Hz), 1.25 (d, 3H, isopropyl CH_3, $^3J_{HH}$= 7.3 Hz) 0.95 (m, 9H, PEt_3 CH_3).

^{13}C NMR (CD_2Cl_2, 125.76 MHz, 298 K): δ (ppm) 171.24 (d, PdC, J_{PC}= 18.9 Hz), 128.22 (s, NC), 127.58 (s, NC), 120.64 (d, C_{meso}, J_{PCmeso}= 5.0 Hz), 67.09 (s, C_{term} *trans* to PEt_3, J_{PC}= 29.9 Hz), 61.49 (d, C_{term} *trans* to dipdmiy), 55.13 (s, isopropyl CH), 54.16 (s, isopropyl CH), 22.76 (s, isopropyl CH_3), 22.55 (s, isopropyl CH_3), 22.16 (s, isopropyl CH_3), 19.41 (d, PCH_2, J_{PC}= 24.9 Hz), 10.75 (s, carbene CH_3), 10.66 (s, carbene CH_3), 8.57 (s, PEt_3 CH_3).

$^{31}P\{^1H\}$ NMR (CD_2Cl_2, 202.46 MHz, 298 K): δ (ppm) 20.28.

High Resolution ESI_{pos}-MS (MeCN): found 445.1945 (calc. 445.1964 dev: -4.3 ppm)

Anal calcd. For $C_{20}H_{40}N_2PPdBF_4$ (MW= 532.20): C, 45.10; H, 7.57; N, 5.26; P, 5.82. Found: C, 44.77; H, 7.56; N, 5.19; P, 6.10.

No X-ray diffraction data were obtained.

3.6.3.11 Synthesis of tricyclohexylphosphine 1,3-diisopropyl-4,5-dimethylimidazol-2-ylidenepalladium crotyl tetrafluoroborate 3b

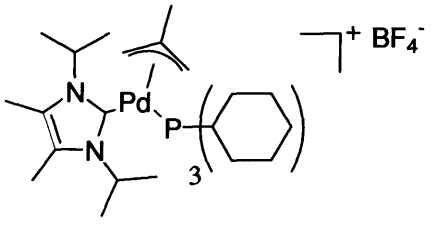

3b

A mixture of 1,3-diisopropyl-4,5-dimethylimidazol-2-ylidenepalladium crotyl chloride **3a** (136 mg, 0.36 mmol, 1.0 eq) and sodium tetrafluoroborate (112 mg, 1.08 mmol, 3.0 eq) was suspended in 2.5 mL of DCM.. Tricyclohexylphosphine (106 mg, 0.38 mmol, 1.08 eq) was added as a 2.5 mL solution in DCM over 15 min. The yellow reaction mixture turned pale. It was stirred at room temperature for 2.5 hr then filtered through Celite®, evaporated and purified by trituration with

Et_2O, then a 3:1 mixture of Et_2O/THF. White solid, the collected mass was 140 mg (60 %) and the batch number was AN/423/A2.

^1H NMR (CD_2Cl_2, 500.13 MHz, 298 K): δ (ppm) 4.64 (m, 1H, isopropyl CH), 4.38 (m, 1H, isopropyl CH), 3.87-3.91 (two overlapped m, 2H, H_{syn} *trans* to dipdmiy and PCy_3), 2.62 (d, 1H, H_{anti} *trans* to PCy_3, J_{PHanti}= 8.8 Hz), 2.47 (s, 1H, H_{anti} *trans* to tmiy), 2.17 (s, 3H, carbene CH_3), 2.16 (s, 3H, carbene CH_3), 1.83 (m, 3H, PCH), 1.74 (overlapped s, 3H, crotyl CH_3), 1.60-1.79 (overlapped m, 15H, PCy_3 cyclohexyl), 1.47 (d, 3H, isopropyl CH_3, $^3J_{HH}$= 7.2 Hz), 1.41 (d, 3H, isopropyl CH_3, $^3J_{HH}$= 7.2 Hz), 1.29 (overlapped d, 3H, isopropyl CH_3, $^3J_{HH}$= 5.5 Hz), 1.27 (overlapped d, 3H, isopropyl CH_3, $^3J_{HH}$= 5.5 Hz), 1.02-1.32 (overlapped m, 9H, PCy_3 cyclohexyl).

^{13}C NMR (CD_2Cl_2, 125.76 MHz, 298 K): δ (ppm) 174.27 (d, PdC, J_{PC}= 16.0 Hz), 133.66 (d, C_{meso}, J_{PC}= 4.0 Hz), 128.10 (s, NC), 128.03 (s, NC), 66.83 (d, C_{term} *trans* to PCy_3, J_{PC}= 28.9 Hz), 60.91 (s, C_{term} *trans* to tmiy), 55.08 (s, isopropyl CH), 54.77 (s, isopropyl CH), 36.37 (d, PCH, J_{PC}= 18.0 Hz), 30.79 (s, CH_2), 30.58 (s, CH_2), 27.92 (d, CH_2, J_{CP}= 3.0 Hz), 27.83 (d, CH_2, J_{CP}= 3.0 Hz), 26.61 (s, CH_2), 23.63 (s, crotyl CH_3), 23.14 (s, isopropyl CH_3), 22.94 (s, isopropyl CH_3), 21.60 (s, isopropyl CH_3), 21.44 (s, isopropyl CH_3), 10.93 (s, carbene CH_3), 10.87 (s, carbene CH_3).

$^{31}P\{^1H\}$ NMR (CD_2Cl_2, 202.46 MHz, 298 K): δ (ppm) 42.27.

High Resolution ESI_{pos}-MS (MeCN): found 619.3504 (calc.619.3534, dev: -4.8 ppm)

Anal calcd. For $C_{33}H_{60}N_2PPdBF_4$ (MW= 709.04): C, 55.90; H, 8.53; N, 3.95; P, 4.37. Found: C, 55.64; H, 8.57; N, 3.88; P, 4.46.

X-ray diffraction data were collected, solved and refined by Dr. Li-Ling Ooi.

3.6.3.12 Synthesis of tris(4-methoxyphenyl)phosphine 1,3-diisopropyl-4,5-dimethylimidazol-2-ylidenepalladium crotyl tetrafluoroborate 3c

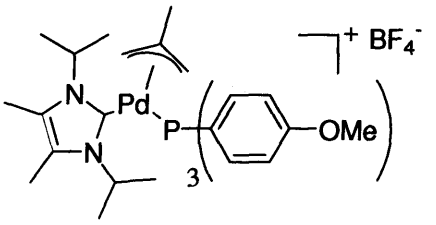

3c

A mixture of 1,3-diisopropyl-4,5-dimethylimidazol-2-ylidenepalladium crotyl chloride **3a** (190 mg, 0.50 mmol, 1.0 eq) and sodium tetrafluoroborate (165 mg, 1.57 mmol, 3.0 eq) was suspended in 5 mL of DCM.. Tris(4-methoxyphenyl)phosphine (172 mg, 0.53 mmol, 1.05 eq) was added as a 2 mL solution in DCM over 5 min. The reaction mixture gradually turned from a paler to a darker yellow . It was stirred at room temperature for 3 hr then filtered through Celite®, evaporated and purified by trituration with Et_2O, followed by a 2:1 mixture of Et_2O/THF. White powder, the collected mass was 258 mg (65 %) and the batch number was AN/452/B.

^{1}H NMR (CD_2Cl_2, 500.13 MHz, 298 K): δ (ppm) 6.78-6.85 (m, 6H, H_{arom} *meta* to P), 6.85-6.92 (m, 6H, H_{arom} *ortho* to P), 4.60 (m, 1H, isopropyl CH), 4.35 (m, 2H, isopropyl CH), 3.96 (m, 1H, Hsyn *trans* to $P(C_6H_4OMe)_3$), 3.74 (s, 9H, OCH_3), 3.43 (bs, 1H, H_{syn} *trans* to dipdmiy), 2.77-2.85 (overlapped dd and s, 2H, H_{anti} *trans* to $P(C_6H_4OMe)_3$ and dipdmiy), 2.13 (s, 3H, carbene CH_3), 2.11 (s, 3H, carbene CH_3), 1.87 (s, 3H, crotyl CH_3), 1.26 (d, 3H, isopropyl CH_3, $^3J_{HH}$= 6.9 Hz), 1.20 (d, 3H, isopropyl CH_3, $^3J_{HH}$= 6.9 Hz), 0.84 (d, 3H, isopropyl CH_3, $^3J_{HH}$= 6.9 Hz), 0.75 (d, 3H, isopropyl CH_3, $^3J_{HH}$= 7.3 Hz). Signals were assigned on the basis of gs-HSQC and gs-NOESY experiments (appendix 3).

^{13}C NMR (CD_2Cl_2, 125.76 MHz, 298 K): δ (ppm) 171.21 (d, PdC, J_{PC}= 18.0 Hz), 162.37 (s, $C_{arom}O$), 135.62 (d, C_{meso}, J_{PC}= 5.0 Hz), 135.18 (d, C_{arom}, J_{PC}= 15.0 Hz), 128.06 (s, NC), 127.96 (s, NC), 123.65 (d, PC, J_{PC}= 46.9 Hz), 115.10 (d, C_{arom}, J_{PC}= 11.0 Hz), 68.76 (s, C_{term} *trans* to dipdmiy), 64.83 (d, C_{term} *trans* to $P(C_6H_4OMe)_3$, J_{PC}= 31.9 Hz), 56.04 (s, OCH_3), 55.21 (s, isopropyl CH),

54.91 (s, isopropyl CH), 24.07 (s, crotyl CH_3), 22.75 (s, isopropyl CH_3), 22.57 (s, isopropyl CH_3), 21.07 (s, isopropyl CH_3), 20.88 (s, isopropyl CH_3), 10.69 (s, carbene CH_3), 10.64 (s, carbene CH_3).

$^{31}P\{^1H\}$ NMR (CD_2Cl_2, 202.46 MHz, 298 K): δ (ppm) 21.76.

High Resolution ESI_{pos}-MS (MeCN): found 693.2451 (calc. 693.2437 dev: 2.0 ppm).

Anal calcd. For $C_{35}H_{46}N_2O_3PPdBF_4$ (MW= 738.23): C, 55.37; H, 6.20; N, 3.59. Found: C, 54.94; H, 6.34; N, 3.55.

3.6.3.13 Synthesis of triethylphosphine 1,3-diisopropyl-4,5-dimethylimidazol-2-ylidenepalladium crotyl tetrafluoroborate 3d

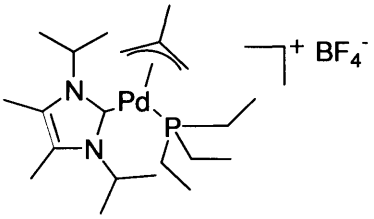

3d

A mixture of 1,3-diisopropyl-4,5-dimethylimidazol-2-ylidenepalladium crotyl chloride **3a** (200 mg, 0.53 mmol, 1.0 eq) and sodium tetrafluoroborate (165 mg, 1.57 mmol, 3.0 eq) was suspended in 5 mL of DCM.. Triethylphosphine (d=0.81, 81µl, 0.56 mmol, 1.05 eq) was added neat by microsyringe over 5 min. The colour of the yellow reaction mixture gradually faded away. It was stirred at room temperature for 3 hr then filtered through Celite®, evaporated and purified by trituration with Et_2O. A solution of the compound in hot THF was layered with hexane followed by cooling to -80 °C. Grey powder, the collected mass was 197 mg (68 %) and the batch number was AN/452/A2.

^1H NMR (CD_2Cl_2, 400.13 MHz): δ (ppm) 4.57 (m, 1H, isopropyl CH), 4.32 (m, 1H, isopropyl CH), 3.90 (m, 1H, H_{syn} *trans* to PEt_3), 3.63 (m, 1H, H_{syn} *trans* to dipdmiy), 2.63 (d, H_{anti} *trans* to PEt_3, J_{PHanti}= 9.5 Hz), 2.52 (s, 1H, H_{anti} *trans* to tmiy), 2.16 (s, 3H, carbene CH_3), 2.15 (s, 3H, carbene CH_3), 1.75 (s, 3H, crotyl CH_3), 1.63 (m, 6H, PCH_2), 1.43 (d, 3H, isopropyl CH_3, $^3J_{HH}$= 7.0 Hz), 1.37

(overlapped d, 3H, isopropyl CH_3, $^3J_{HH}$= 7.0 Hz), 1.32 (d, 3H, isopropyl CH_3, $^3J_{HH}$= 7.0 Hz), 1.28 (d, 3H, isopropyl CH_3, $^3J_{HH}$= 7.0 Hz) 0.95 (m, 9H, PEt_3 CH_3).

^{13}C NMR (CD_2Cl_2, 125.03 MHz): δ (ppm) 172.21 (d, PdC, J_{PC}= 18.9 Hz), 134.99 (d, C_{meso}, J_{PCmeso}= 5.0 Hz), 127.96 (s, NC), 127.76 (s, NC), 66.47 (s, C_{term} *trans* to PEt_3, J_{PC}= 30.9 Hz), 61.34 (d, C_{term} *trans* to dipdmiy), 55.05(s, isopropyl CH), 54.59 (s, isopropyl CH), 24.19 (s, crotyl CH_3), 22.70 (s, isopropyl CH_3), 22.52 (s, isopropyl CH_3), 22.15 (s, isopropyl CH_3), 22.06 (s, isopropyl CH_3), 19.36 (d, PCH_2, J_{PC}= 24.9 Hz), 10.81 (s, carbene CH_3), 10.77 (s, carbene CH_3), 8.66 (s, PEt_3 CH_3).

$^{31}P\{^1H\}$ NMR (CD_2Cl_2, 202.46 MHz, 298 K): δ (ppm) 21.46.

High Resolution ESI_{pos}-MS (MeCN): found 457.2110 (calc. 457.2126 dev: -3.5 ppm)

Anal calcd. For $C_{21}H_{42}N_2PPdBF_4$ (MW= 546.21): C, 46.13; H, 7.74; N, 5.12; P, 5.66. Found: C, 45.99; H, 7.76; N, 4.97; P, 5.66.

X-ray diffraction data were collected, solved and refined by this author, with the guidance of Dr. D. J. Beetstra.

3.6.3.14 Synthesis of tricyclohexylphosphine tetramethylimidazol-2-ylidene palladium crotyl tetrafluoroborate 6b

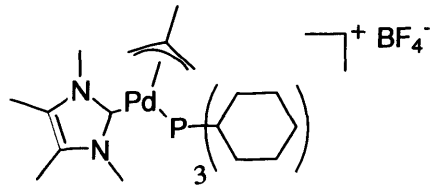

6b

A mixture of tricyclohexylpalladium crotyl chloride **6a** (442 mg, 0.93 mmol, 1.0 eq) and silver tetrafluoroborate (189 mg, 0.93 mmol, 1.0 eq) was suspended in 4.0 mL THF in a Schlenk tube under argon. Tetramethylimidazol-2-ylidene (1115 mg, 0.93 mmol, 1.0 eq) was added as a 4 mL solution in THF over 1 min. The reaction mixture was stirred at room temperature for 1 hr then evaporated, taken in DCM and filtered through Celite®, evaporated and triturated with Et_2O. The

resulting powder was taken in hot THF and filtered, the solution evaporated and triturated with Et_2O to afford a white powder. The collected mass was 150 mg (25 %) and the batch number was AN/457/A2.

^1H NMR (CD_2Cl_2, 500.13 MHz, 298 K): δ (ppm) 3.87 (m, 1H, H_{syn} *trans* to tmiy), 3.84 (m, 1H, H_{syn} *trans* to PCy_3), 3.46 (s, 3H, NCH_3), 3.32 (s, 3H, NCH_3), 2.59 (d, 1H, H_{anti} *trans* to PCy_3, J_{PHanti}= 8.8 Hz), 2.49 (s, 1H, H_{anti} *trans* to tmiy), 2.08 (s, 3H, carbene CH_3), 2.07 (s, 3H, carbene CH_3), 1.77 (overlapped s, 3H, crotyl CH_3), 1.59-1.83 (overlapped m, 18H, PCy_3 cyclohexyl), 1.47 (d, 3H, isopropyl CH_3, $^3J_{HH}$= 7.2 Hz), 1.41 (d, 3H, isopropyl CH_3, $^3J_{HH}$= 7.2 Hz), 1.00-1.24 (overlapped m, 15H, PCy_3 cyclohexyl).

^{13}C NMR (CD_2Cl_2, 125.03 MHz): δ (ppm) 174.18 (d, PdC, J_{PC}= 16.0 Hz), 134.11 (s, C_{meso}, J_{PC}= 4.0 Hz), 127.85 (s, NC), 127.74 (s, NC), 66.05 (d, C_{term} *trans* to PCy_3, J_{PC}= 28.9 Hz), 61.22 (s, C_{term} *trans* to tmiy), 36.71 (d, PCH, J_{PC}= 18.9 Hz), 36.31 (s, NCH_3), 36.29 (s, NCH_3), 31.06 (s, CH_2), 30.74 (s, CH_2), 27.99 (d, CH_2, J_{CP}= 2.0 Hz), 27.91 (d, CH_2, J_{CP}= 3.0 Hz), 26.72 (d, CH_2, J_{CP}= 2.0 Hz), 24.32 (s, crotyl CH_3), 9.44 (s, carbene CH_3), 9.41 (s, carbene CH_3).

$^{31}P\{^1H\}$ NMR (CD_2Cl_2, 202.46 MHz, 298 K): δ (ppm) 43.04.

High Resolution ESI_{pos}-MS (MeCN): found 565.2912 (calc.565.2903, dev: 1.6 ppm)

Anal calcd. For $C_{29}H_{52}N_2PPdBF_4$ (MW= 652.93): C, 53.35; H, 8.03; N, 4.29; P, 4.74. Found: C, 52.89; H, 7.95; N, 4.17; P, 5.00.

X-ray diffraction data were collected, solved and refined by Dr. Andreas Stasch.

3.6.3.15 Synthesis of tricyclohexylphosphine dimethylimidazol-2-ylidene palladium allyl tetrafluoroborate 5b

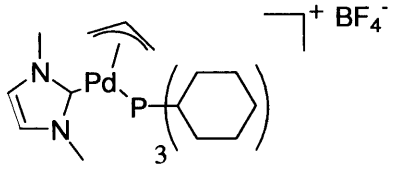

5b

A mixture of tricyclohexylpalladium allyl chloride **5a** (400 mg, 0.86 mmol, 2.1 eq), dmiy transfer agent $[(C_5H_8N_2)_2Ag]_2Ag_4I_6$ (375 mg, 0.41 mmol, 1.0 eq) and silver tetrafluoroborate (176 mg, 0.90 mmol, 2.2 eq) was suspended in 15 mL THF in a schlenk under argon. The reaction mixture was stirred at room temperature for 1 hr then filtered through Celite®, evaporated and triturated with Et_2O. The resulting powder containing about 10% of bis-carbene complex was taken in DCM. THF was added to this solution, the resulting solid was removed by filtration and the mother liquors concentrated to afford a white solid, containing residual bis-carbene complex (about 5%, judged by integration of the N-methyl signals in ^1H NMR). The cllected mas was 250 mg, and the batch number was AN/322/E.

^1H NMR (CD_2Cl_2, 500.13 MHz, 298 K): δ (ppm) 7.13 (d, 1H, carbene CH, $^3J_{HH}$= 1.8 Hz), 7.11 (d, 1H, carbene CH, $^3J_{HH}$= 1.8 Hz), 5.26 (m overlapping with solvent signal, 1H, H_{meso}), 4.09-4.14 (two overlapped m, 2H, H_{syn}), 3.62 (s, 3H, NCH_3), 3.45 (s, 3H, NCH_3), 2.82 (dd, 1H, H_{anti} *trans* to PCy_3, $^3J_{HantiHmeso}$= 13.3 Hz, J_{PHanti}= 8.5 Hz), 2.60 (d, 1H, H_{anti} *trans* to tmiy, $^3J_{HantiHmeso}$= 13.2 Hz), 1.80 (m, 3H, PCH), 1.59-1.75 (m, 15H, PCy_3 cyclohexyl), 0.97-1.21 (m, 15H, PCy_3 cyclohexyl).

^{13}C NMR (CD_2Cl_2, 125.03 MHz): δ (ppm) 124.16 (s, NC), 123.99 (s, NC), 119.52 (s, C_{meso}, J_{PC}= 4.5 Hz), 66.38 (d, C_{term} *trans* to PCy_3, J_{PC}= 27.4 Hz), 60.89(s, C_{term} *trans* to tmiy), 38.08 (s, NCH_3), 37.90 (s, NCH_3), 36.45 (d, PCH, J_{PC}= 18.9 Hz), 30.45 (s, CH_2), 30.17 (s, CH_2), 27.38 (s, CH_2), 27.29 (s, CH_2), 26.05 (d, CH_2, J_{CP}= 1.5 Hz). No PdC signal was observed, probably due to insufficient sample concentration.

$^{31}P\{^1H\}$ NMR (CD_2Cl_2, 202.46 MHz, 298 K): δ (ppm) 42.53.

High Resolution ESI_{pos}-MS (MeCN): found 523.2451 (calc.523.2433, dev: 3.4 ppm)

X-ray diffraction data were collected, solved and refined by Dr. Andreas Stasch.

3.7 Bibliography and notes

1. Aakermark, B.; Krakenberger, B.; Hansson, S.; Vitagliano, A., *Organometallics* **1987,** 6, 620-628.
2. Torralba, M. C.; Campo, J. A.; Heras, J. V.; Bruce, D. W.; Cano, M., *Dalton Trans.* **2006**, 3918-3926.
3. Johns, A. M.; Tye, J. W.; Hartwig, J. F., *J. Am. Chem. Soc.* **2006,** 128, 16010-16011.
4. Auburn, P. R.; Mackenzie, P. B.; Bosnich, B., *J. Am. Chem. Soc.* **1985,** 107, 2033-2046.
5. Bastero, A.; Bella, A. F.; Fernández, F.; Jansat, S.; Claver, C.; Gómez, M.; Muller, G.; Ruiz, A.; Font-Bardía, M.; Solans, X., *Eur. J. Inorg. Chem.* **2007**, 132-139.
6. Schott, D.; Pregosin, P. S.; Veiros, L. F.; Calhorda, M. J., *Organometallics* **2005,** 24, 5710-5717.
7. Consiglio, G.; Waymouth, R. M., *Chem. Rev.* **1989,** 89, 257-276.
8. Fairlamb, I. J. S.; Lloyd-Jones, G. C.; Vyskocil, Š.; Kocovský, P., *Chem. Eur. J.* **2002,** 8, 4443-4453.
9. Faller, J. W.; Sarantopoulos, N., *Organometallics* **2004,** 23, 2179-2185.
10. Trost, B. M.; Crawley, M. L., *Chem. Rev.* **2003,** 103, 2921-2944.
11. Trost, B. M.; Van Vranken, D. L., *Chem. Rev.* **1996,** 96, 395-422.
12. Pregosin, P. S.; Salzmann, R., *Coord. Chem. Rev.* **1996,** 155, 35-68.
13. Abbenhuis, H. C. L.; Burckhardt, U.; Gramlich, V.; Koellner, C.; Pregosin, P. S.; Salzmann, R.; Togni, A., *Organometallics* **1995,** 14, 759-766.
14. Sprinz, J.; Kiefer, M.; Helmchen, G.; Reggelin, M.; Huttner, G.; Walter, O.; Zsolnai, L., *Tetrahedron Lett.* **1994,** 35, 1523-1526.
15. Dotta, P.; Kumar, P. G. A.; Pregosin, P. S., *Magn. Res. Chem.* **2002,** 40, 653-658.
16. Albinati, A.; Ammann, C.; Pregosin, P. S., *Organometallics* **1990,** 9, 1826-1833.
17. Breutel, C.; Pregosin, P. S.; Salzmann, R.; Togni, A., *J. Am. Chem. Soc.* **1994,** 116, 4067-4068.
18. Herrmann, J.; Pregosin, P. S.; Salzmann, R.; Albinati, A., *Organometallics* **1995,** 14, 3311-3318.
19. García-Iglesias, M.; Buñuel, E.; Cárdenas, D. J., *Organometallics* **2006,** 25, 3611-3618.
20. Kollmar, M.; Helmchen, G., *Organometallics* **2002,** 21, 4771-4775.
21. Navarro, O.; Marion, N.; Mei, J.; Nolan, S. P., *Chem. Eur. J.* **2006,** 12, 5142-5148.
22. Marion, N.; Navarro, O.; Mei, J.; Stevens, E. D.; Scott, N. M.; Nolan, S. P., *J. Am. Chem. Soc.* **2006,** 128, 4101-4111.
23. Viciu, M. S.; Navarro, O.; Germaneau, R. F.; Kelly, R. A. III.; Sommer, W.; Marion, N.; Stevens, E. D.; Cavallo, L.; Nolan, S. P., *Organometallics* **2004,** 23, 1629-1635.
24. Viciu, M. S.; Zinn, F. K.; Stevens, E. D.; Nolan, S. P., *Organometallics* **2003,** 22, 3175-3177.
25. Graham, D. C.; Cavell, K. J.; Yates, B. F., *Dalton Trans.* **2006**, 1768-1775.
26. Graham, D. C.; Cavell, K. J.; Yates, B. F., *Dalton Trans.* **2005**, 1093-1100.
27. Cavell, K. J.; McGuinness, D. S., *Coord. Chem. Rev.* **2004,** 248, 671-679.
28. McGuinness, D. S.; Saendig, N.; Yates, B. F.; Cavell, K. J., *J. Am. Chem. Soc.* **2001,** 123, 4029-4040.
29. Clement, N. D.; Cavell, K. J., *Angew. Chem. Int. Ed.* **2004,** 43, 3845-3847.
30. the term "monoligated" is somewhat inaccurate, as it is likely that 2-propenylimidazolium would bind, albeit weakly, to the Pd(0) phosphine complex.
31. Christmann, U.; Vilar, R., *Angew. Chem. Int. Ed.* **2005,** 44, 366-374.
32. Ahlquist, M.; Norrby, P.-O., *Organometallics* **2007,** 26, 550-553.

33. Galardon, E.; Ramdeehul, S.; Brown, J. M.; Cowley, A.; Hii, K. K.; Jutand, A., *Angew. Chem. Int. Ed.* **2002,** 41, 1760-1763.
34. Organ, M. G.; Avola, S.; Dubovyk, I.; Hadei, N.; Kantchev, E. A. B.; O'Brien, C. J.; Valente, C., *Chem. Eur. J.* **2006,** 12, 4749-4755.
35. O'Brien, C. J.; Kantchev, E. A. B.; Valente, C.; Hadei, N.; Chass, G. A.; Lough, A.; Hopkinson, A. C.; Organ, M. G., *Chem. Eur. J.* **2006,** 12, 4743-4748.
36. PEPPSI- pyridine-enhanced precatalyst preparation, stabilisation and initiation.
37. Ding, Y.; Goddard, R.; Pörschke, K.-R., *Organometallics* **2005,** 24, 439-445.
38. DiRenzo, G. M.; White, P. S.; Brookhart, M., *J. Am. Chem. Soc.* **1996,** 118, 6225-6234.
39. Carturan, G.; Biasiolo, M.; Daniele, S.; Mazzocchin, G. A.; Ugo, P., *Inorg. Chim. Acta.* **1986,** 119, 19-24.
40. Tolman, C. A., *Chem. Rev.* **1977,** 77, 313-348.
41. this appears to be due to the unreliable quality of dry DCM used in the lab. ^{31}P NMR of PCy_3 in d_2-DCM straight from the bottle revealed several peaks, whereas the same batch of PCy_3 was found to be >95 % pure in dry C_6D_6.
42. Roland, S.; Audouin, M.; Mangeney, P., *Organometallics* **2004,** 23, 3075-3078.
43. Chernyshova, E. S.; Goddard, R.; Porschke, K. R., *Organometallics* **2007,** 26, 3236-3251.
44. Green, M. J.; Cavell, K. J.; Skelton, B. W.; White, A. H., *J. Organomet. Chem.* **1998,** 554, 175-179.
45. Cooke, C. E.; Ramnial, T.; Jennings, M. C.; Pomeroy, R. K.; Clyburne, J. A. C., *Dalton Transactions* **2007**, 1755-1758.
46. The synthesis of known $[Pd(\eta^3\text{-}C_3H_5)(PCy_3)_2]BF_4$ from **5a** was also attempted, but the reaction mainly yielded allyltricyclohexylphosphonium cation and almost no desired compound. This is most probably the result of nucleophilic attack of free PCy_3 onto the allyl ligand and indicates that NHC ligands are probably far better at labilising the chloro ligand (and slow down the nucleophilic attack on the allyl).
47. some compounds did not crystallise, others gave thin microcrystals unsuitable for X-ray crystallography.
48. Bayersdorfer, R.; Ganter, B.; Englert, U.; Keim, W.; Vogt, D., *J. Organomet. Chem.* **1998,** 552, 187-194.
49. Tinkl, M.; Hafner, A. WO 9947474, 1999.
50. Tinkl, M.; Hafner, A. WO 2001016057, 2001.
51. only one molecule is depicted in the case of **1b** and **6b** although both molecules appear in the tables.
52. comprising the three carbon atoms coordinated to Pd.
53. comprising Pd and the four atoms sitting at the corners of the pseudo-square.
54. comprising the three carbon and two nitrogen atoms of the imidazol-2-ylidene ring.
55. Navarro, O.; Oonishi, Y.; Kelly, R. A.; Stevens, E. D.; Briel, O.; Nolan, S. P., *J. Organomet. Chem.* **2004,** 689, 3722-3727.
56. Cl is relatively small but the fact that smaller NHCs significantly deviate from this orientation points to a steric rather than electronic preference.
57. Dorta, R.; Stevens, E. D.; Scott, N. M.; Costabile, C.; Cavallo, L.; Hoff, C. D.; Nolan, S. P., *J. Am. Chem. Soc.* **2005,** 127, 2485-2495.
58. Diez-Gonzalez, S.; Nolan, S. P., *Coord. Chem. Rev.* **2007,** 251, 874-883.
59. the angle between the two least squares planes is 9.72(17) °.
60. Viviente, E. M.; Pregosin, P. S.; Schott, D., NMR spectroscopy and homogeneous catalysis. In *Mechanisms in homogeneous catalysis*, Heaton, B., Ed. Wiley-VCH: Weinheim, 2005; pp 1-80.
61. Brown, J. M., *J. Organomet. Chem.* **2004,** 689, 4006-4015.
62. Berger, S.; Braun, S., *200 and More NMR Experiments: A Practical Course*. Wiley-VCH: Weinheim, 2004.

63. Rahman, M. M.; Liu, H. Y.; Eriks, K.; Prock, A.; Giering, W. P., *Organometallics* **1989,** 8, 1-7.
64. Clarke, M. L.; Ellis, D.; Mason, K. L.; Orpen, A. G.; Pringle, P. G.; Wingad, R. L.; Zaher, D. A.; Baker, R. T., *Dalton Trans.* **2005**, 1294-1300.
65. Neuhaus, D.; Williamson, M. P., *The Nuclear Overhauser Effect in Structural and Conformational Analysis.* 2nd ed.; Wiley-VCH: Weinheim, 2000.
66. Pregosin, P. S.; Wombacher, F., *Magn. Res. Chem.* **1991,** 29, S106-S117.
67. Filipuzzi, S.; Pregosin, P. S.; Albinati, A.; Rizzato, S., *Organometallics* **2006,** 25, 5955-5964.
68. Chen, W.; Liu, F., *J. Organomet. Chem.* **2003,** 673, 5-12.
69. Kuhn, N.; Kratz, T., *Synthesis* **1993**, 561-562.
70. Gottlieb, H. E.; Kotlyar, V.; Nudelman, A., *J. Org. Chem.* **1997,** 62, 7512-7515.

4 Chapter Four: Unusual Reactivity of Pd(II) Complexes Leading to C-C Bond Formation

This chapter describes the reactivity and catalytic activity of some of the [Pd(π-allyl)(NHC)(PR_3)]BF_4 compounds described in chapter 3, and more particularly complex **1b** (***Figure 1***):

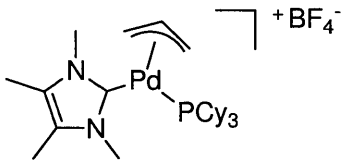

1b

Figure 1: *main compound studied in this chapter*

Complex **1b** and related compounds were originally synthesised with the aim of developing a family of air-stable Pd(II) precatalysts that could be used in the Pd-catalysed alkenylation of azolium salts and other Pd-catalysed coupling reactions (see chapter 3). It was thought that these complexes would undergo an activation reaction to yield a "monoligated" Pd(0) active catalyst (***Scheme 1***):

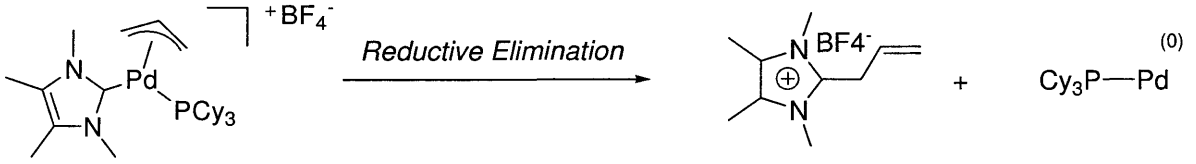

Scheme 1: *activation of a Pd(II) precatalyst yielding active monoligated Pd*

4.1 Background: frontiers in Pd chemistry

4.1.1 Monoligated Pd: a new paradigm in Pd catalysis

In the past 30 to 40 years, the development of Pd-catalysed cross-coupling reactions has transformed synthetic chemistry.[1, 2] Nowadays, so called Heck,[3-7] Suzuki,[8] Sonogashira[9] and Buchwald[10-12] reactions (***Scheme 2***) are extremely useful components of the chemists' toolbox. The exact mechanism of these reactions varies depending on the source of Pd ($Pd_2(dba)_3$, $Pd(OAc)_2$, $PdCl_2$...) and other experimental parameters (nature of the base...), and there is a wealth of literature on this topic.[13-20] However, a general "textbook mechanism" is usually invoked (***Figure 2***):

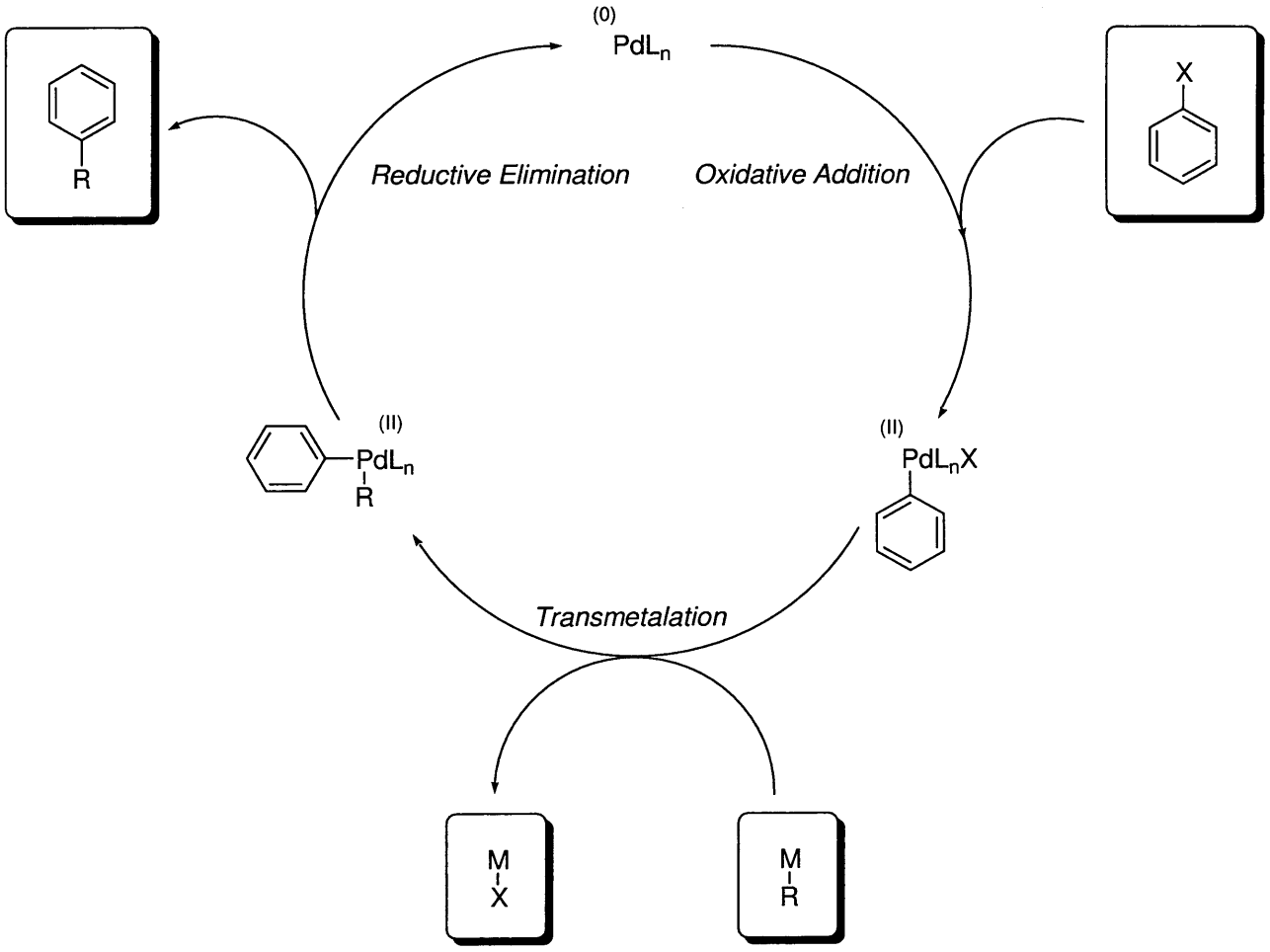

Figure 2: *"textbook mechanism" of Pd-catalysed coupling reactions*

Heck:

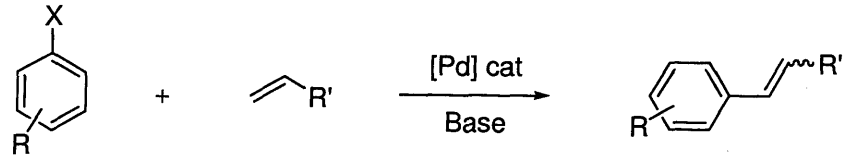

Suzuki:

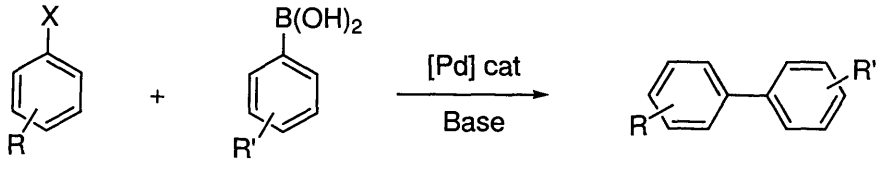

Sonogashira:

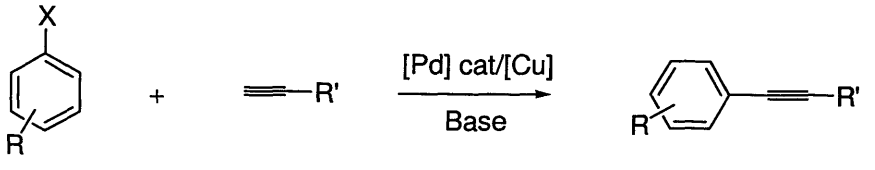

Buchwald:

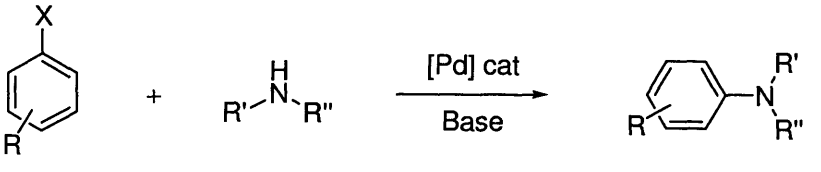

X= halide, OTf... Base: K_2CO_3, K_3PO_4, ^tBuOK, NEt_3...

Scheme 2: *Pd-catalysed coupling of aryl electrophiles with nucleophiles*

According to the mechanism in ***Figure 2***, three main steps form the catalytic cycle: oxidative addition, transmetalation and reductive elimination. This is a typical Pd(0)/Pd(II) sequence.

To date, most research efforts have focused on oxidative addition because it is thought to be the rate determining step in the case of aryl chlorides, which are cheaper and more readily available than other aryl halides.[21-24] The development of Pd catalysts using bulky, electron-rich phosphines or NHCs has enabled excellent progress in the coupling of aryl chlorides.[22, 25]

The success of these ligands is thought to be due to the fact that they generate reactive "monoligated" Pd species under the reaction conditions.[26] An important aspect of this chemistry has been the concomitant development of well-defined Pd precatalysts containing one ligand per Pd atom. For example, Nolan has developed a range of Pd(II) NHC precatalysts **2-5** for this purpose,[27-30] whilst Beller reported monophosphine and monocarbene Pd(0) complexes **6-9** (***Figure 3***).[31-34]

It is worth noting that the activity of **6** in cross-coupling reactions is quite low,[33] whereas it is extremely efficient in butadiene telomerisation.[28] This is due to the fact that the reactive Pd-L fragment is deactivated by the chelating dvds ligand (dimethylvinyldisiloxane): in telomerisation, **6** is activated by displacement of dvds by butadiene. This highlights the fact that the design of the Pd source in Pd-catalysed reactions is of paramount importance. One must be able to generate (activation) and maintain (stabilisation) significant amounts of catalytically active species in order to obtain good TONs.

Besides the important improvements in Pd-catalysed reactions since the development of Pd-L precatalysts, studies confirm that Pd-L pathways are operating in stoichiometric processes as well. At least two detailed experimental studies show that stoichiometric oxidative addition of aryl halides goes via 12-electron PdL rather than 14-electron PdL_2 species (see chapter 1 for an example).[21, 35]

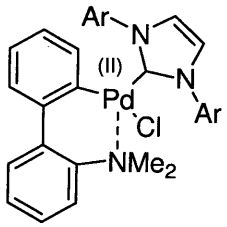

2

Ref. 30

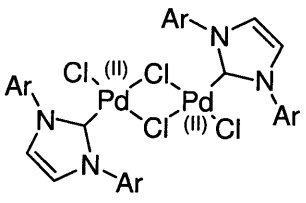

3

Ref. 31

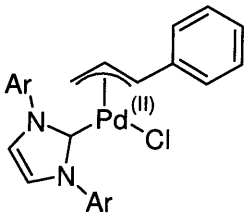

4

Ref. 27

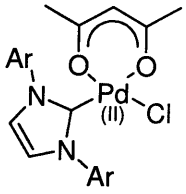

5

Ref. 28

Ar= 2,6-diisopropylphenyl

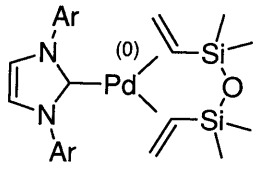

6

Ref. 34

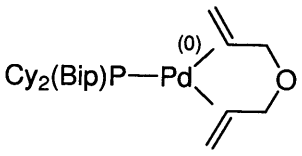

7

Ref. 36

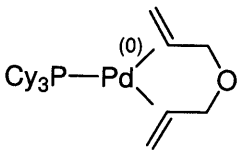

8

Ref. 36

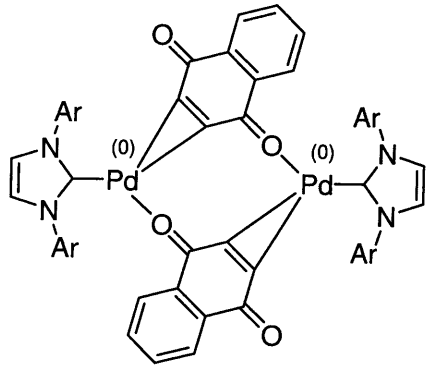

9

Ref. 35

Ar= 2,4,6-trimethylphenyl

Figure 3: *Pd-L precatalysts developed by Nolan and Beller*

Although monoligated Pd has been invoked as the active catalytic species in a number of reactions for some time,[22, 35, 36] there had been no theoretical work on this matter until recently. However, Norrby investigated the oxidative addition of phenyl iodide to Pd(0) and concluded that oxidative addition is more likely to go *via* monoligated Pd(0) than the usually postulated 14-electron PdL_2 (L=phosphine).[37] Work on the oxidative addition of aryl chlorides came to the same conclusions.[24] This is consistent with the idea that coordinatively unsaturated metal fragments are expected to be more reactive towards oxidative addition (see chapter 1). Thus, ligands such as IMes, IPr, or P^tBu_3 are doubly beneficial: they both favour coordinative unsaturation because of their steric bulk, and give high electronic density to Pd(0), thus facilitating oxidative addition.

Overall, there is now considerable evidence showing that monoligated Pd is the active catalytic species in Pd-catalysed reactions going *via* Pd(0)/Pd(II) cycles. This is a general phenomenon, and its recognition should help develop other catalytic reactions in the future. More particularly, this chapter will describe an application of the concept of monoligated Pd to the design of more efficient catalysts.

4.1.2 C-H functionalisation: a new generation of Pd-catalysed reactions

Now that the reactions described in the previous section enter the dawn of a new era, *i.e.* their routine application to large-scale processes,[6, 7, 12, 38] a new generation of Pd-catalysed reactions is emerging. The development of these new methodologies is largely driven by the increasing need for atom-economical transformations.[39] Traditional methodologies rely on aryl halides and organometallics to form new C-C bonds, which generates waste. So-called C-H bond functionalisation is both more direct and less wasteful. C-H functionalisation can be catalysed by a variety of metals, and a number of reviews have been published on this topic.[40-42] In the following, selected examples using Pd are discussed.

4.1.2.1 Direct intramolecular arylation of arenes

Replacement of the organometallic partner in cross-coupling reactions affords new opportunities for the synthesis of complex molecules in a minimum number of steps.[43-45] Not only is this methodology more atom-economical and potentially easier to work-up (it generates HX instead of MX), but targeting C-H instead of C-M bonds means functional group tolerance issues are much less critical.

As shown in ***Scheme 3***, the intramolecular version of this methodology bears considerable potential for the synthesis of polycyclic molecules. In this case, the success of the strategy lies in the proximity of C-H and C-X bonds and the favoured formation of a 5- or 6-membered cycle.

The mechanism of direct intramolecular arylation has been investigated in detail by Fagnou[43, 44, 46] (experimentally) and Echavarren[47, 48] (experimentally and by DFT calculations). It is thought that the reaction proceeds by oxidative addition of the aryl halide to Pd(0), metalation of the arene, and finally reductive elimination. In a recent study, Echavarren concluded that the metalation step is assisted by the base present in the reaction media,[47, 48] consistent with independent studies by

MacGregor on the palladation of arenes by $Pd(OAc)_2$.[49] On the other hand, Fagnou suggested an electrophilic palladation step followed by deprotonation.[43]

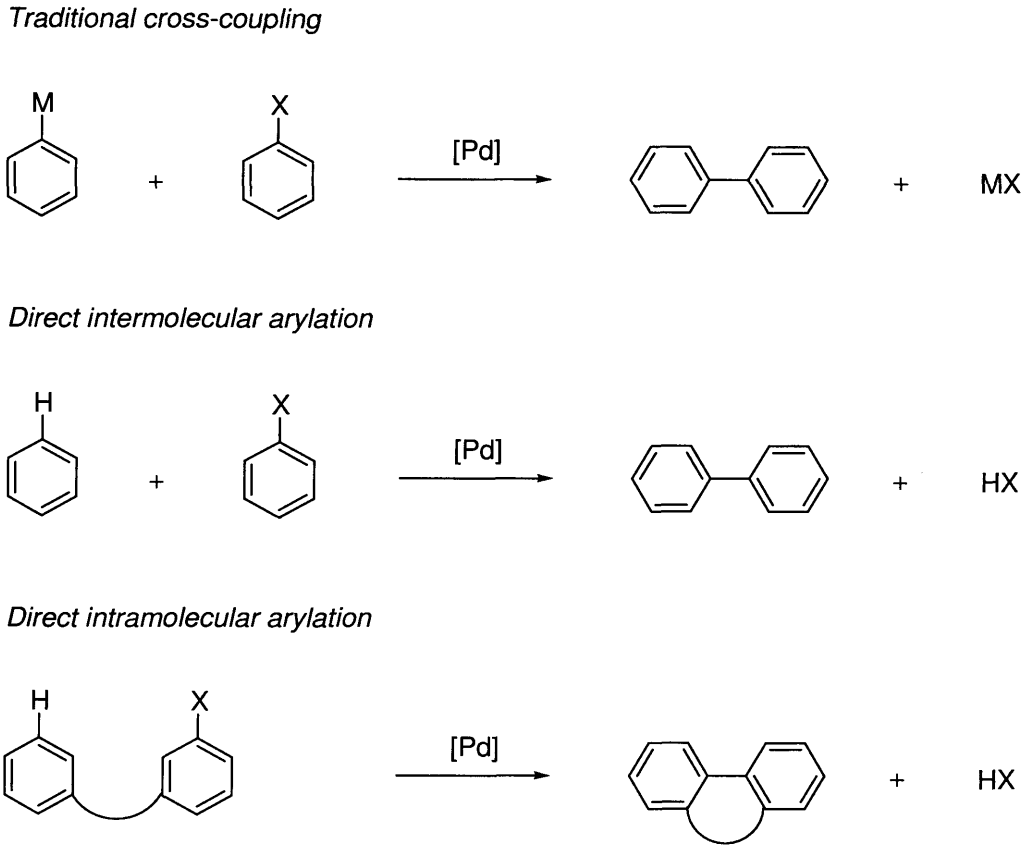

Scheme 3: *comparison of traditional and direct cross-coupling methodologies*

Scheme 4 shows the application of direct intramolecular arylation to the synthesis of antitumor compounds of the carbazole family by Fagnou[43] and Bedford.[45] These examples illustrate how direct arylation nicely complements other well-established cross-coupling methodologies, since aryl chlorides (the least reactive compounds in traditional cross-coupling reactions) are more reactive than aryl bromides or iodides.[43, 44] Carbazoles **11** and **13** are thus synthesised in two sequences:

starting from commercially available compounds; a Buchwald amination selectively affords the tethered chloro derivatives **10** and **12**, which are then cyclised by C-H functionalisation.

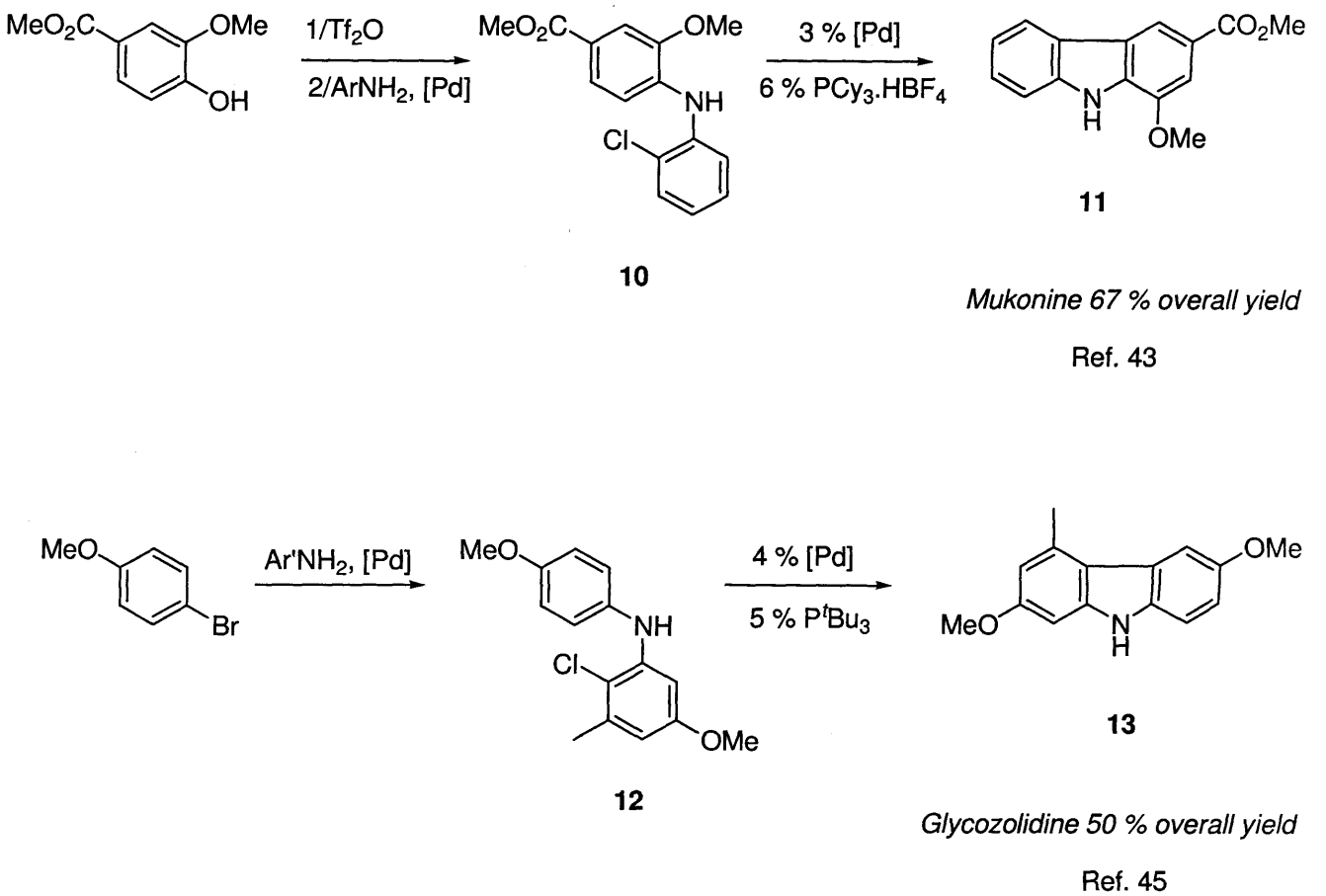

Scheme 4: *synthesis of antitumour compounds by direct intramolecular arylation*

Catalytic aryl coupling is obviously an area of great interest, and there are many possible ways of tackling the problem of $C(sp^2)$-$C(sp^2)$ bond formation. A recent review by Catellani (which includes the reactions discussed in this section) focused on the progress in this field.[50]

4.1.2.2 Direct functionalisation of N-heterocycles

In chapter 2, the Rh-catalysed alkenylation of N-heterocycles was discussed.[51-63] It is also possible to directly arylate N-heterocycles, in a similar fashion to the reaction of arenes. This methodology is of considerable interest since heterocycles are notoriously challenging substrates for cross-coupling reactions.[12, 44, 64-67] The groups of Sanford[68, 69] and Sames[70-76] have investigated the Pd-catalysed direct arylation of indoles, pyrroles and azoles, with sometimes spectacular results. However, Sames has since retracted a number of key papers on this topic,[73, 75-78] thus casting serious doubts on the veracity of his results. Other groups have reported the Pd-catalysed direct arylation of various heterocycles [44, 50, 79-81]

In a recent paper, Sanford reported the Pd-catalysed arylation of indoles with I(III) aryl reagents (***Scheme 5***). The reaction proceeds at room temperature, in contrast with the usually harsher conditions required by these C-H functionalisation methodologies.[69]

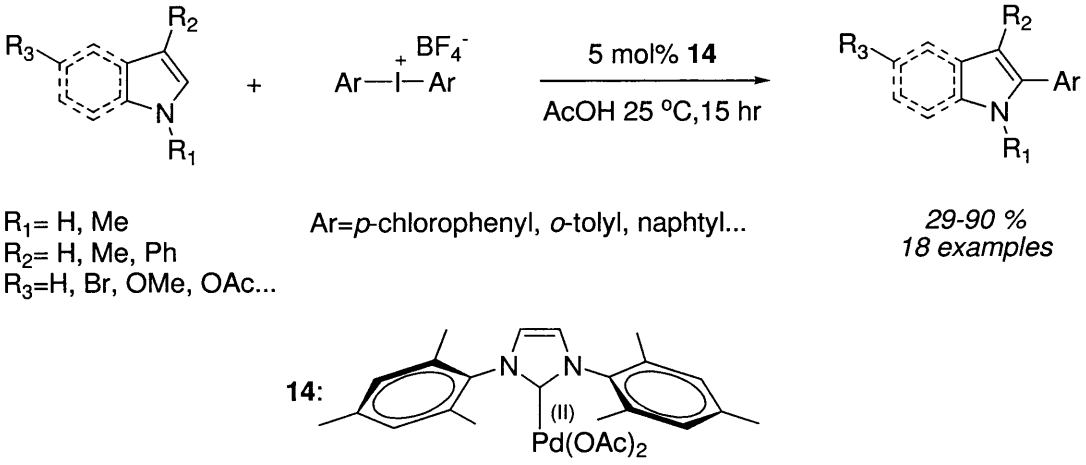

Scheme 5: *Pd-catalysed direct arylation of indoles*

Complex **14** (another example of Pd-L precatalyst) was found to give very interesting activities with a variety of substrates. Interestingly, this reaction seems to proceed by a Pd(II)/Pd(IV) cycle.

According to Sanford, palladation of the indole heterocycle yields an electron-rich σ-indole NHC Pd(II) intermediate which undergoes oxidative addition of the I(III) reagent and finally reductive elimination. This claim is backed by stoichiometric studies of C-H activation/oxygenation reactions conducted by the same group (see following section).[82]

4.1.3 Pd(IV) or not Pd(IV) ? The importance of transmetalation processes

Most of Pd chemistry is that of the 0, +I and +II oxidation states. This is in stark contrast with Pt, for which the +IV oxidation state is common.[83] In 1975 however, the first organometallic Pd(IV) compound **15** (***Figure 4***) was reported,[84] and Canty reported the first alkyl Pd(IV) **16** in 1986.[85] Other examples have been reported more recently such as **17** (by Sanford)[82] and **18** (by Malinakova)[86]:

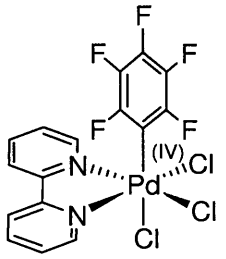

15

Ref. 84

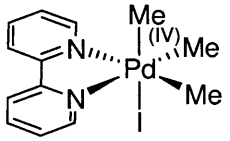

16

Ref. 85

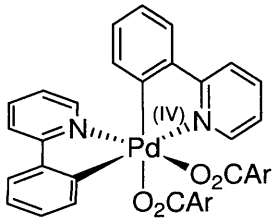

Ar=*p*-nitrophenyl

17

Ref. 82

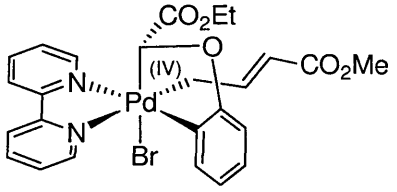

18

Ref. 86

Figure 4: *examples of isolated Pd(IV) compounds*

A feature of stable Pd(IV) complexes such as **15-18** is the stabilisation of the octahedral geometry by rigid and planar chelating ligands such as bipyridine (bipy, in complexes **15**, **16** and **18**) or phenanthroline. Pd(IV) compounds are otherwise unstable and readily decompose by reductive elimination.[83] *However, their very existence suggests that they are feasible intermediates in catalytic reactions.*

4.1.3.1 Genuine examples of Pd(IV) intermediates in Pd-catalysed reactions

Complex **17** is a very close model compound to the Pd(IV) intermediate postulated by Sanford in the directed C-H oxygenation of arylpyridines (***Scheme 6***):[82, 87, 88]

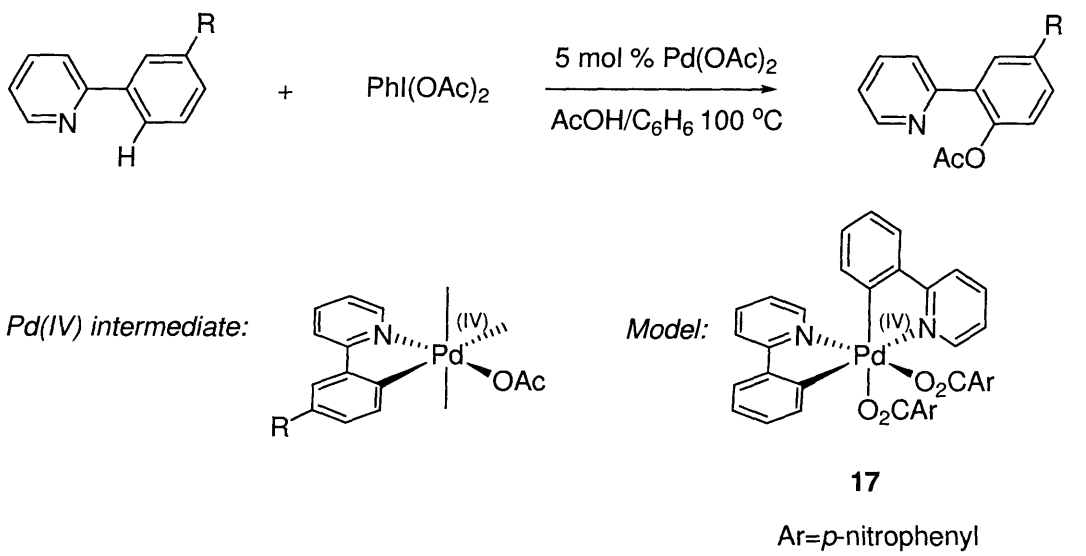

Scheme 6: *C-H functionalisation of pyridines via a Pd(IV) intermediate*

Importantly, complex **17** is prepared from I(III) carboxylate compounds analogous to those used in the catalytic reaction. Moreover, **17** and related compounds have also been shown to decompose by reductive elimination to yield carboxylated arylpyridines.[82] Thus, there is solid evidence for the intermediacy of Pd(IV) in this example. Another such example is the Pd-catalysed synthesis of

benzoxepines and benzopyrans reported by Malinakova. In this case, the postulated intermediate (**18**, ***Figure 4***) was isolated.[86]

Because of their instability, which constitutes a common feature with catalytic intermediates,[13, 89, 90] Pd(IV) compounds are sometime invoked as intermediates in the absence of any other explanation. A well-known example is Herrmann's palladacycles for the Heck reaction: a Pd(II)/Pd(IV) mechanism was initially proposed,[91] before work by Beletskaya and others provided much more solid evidence that these catalysts actually act as Pd(0) reservoirs.[5, 92]

In the following, examples of catalytic and stoichiometric reactions which *could* go *via* Pd(IV) intermediates but for which there is strong evidence for another mechanism (*i.e.* transmetalation) are discussed. These examples are directly relevant to the results presented in this chapter, and actually helped shape the proposed mechanism of the Pd-mediated arylation of NHCs described in section **4.4**.

4.1.3.2 Inter- Pd(II) transmetalation: the Pd(IV) illusion

4.1.3.2.1 Reaction of trans-[Pd(Ar)$_2$L$_2$] with MeI and PhI

In 1986, Yamamoto reported the reaction of *trans*-Pd(*m*-tolyl)$_2$L$_2$ **19** (where L=PEt$_2$Ph) with MeI to give *trans*-Pd(*m*-tolyl)IL$_2$ **20** and *m*-xylene in 75 % yield on the one hand, and *trans*-PdMeIL$_2$ **21** and 3,3'-bitolyl in 25 % yield on the other (***Scheme 7***).[93]

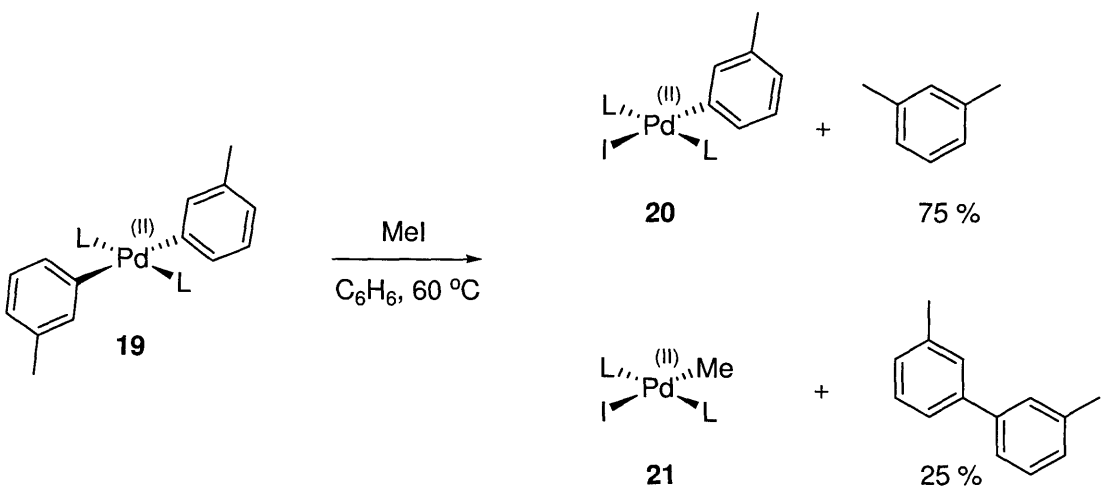

Scheme 7: *reaction of a Pd(II) complex with MeI*

The formation of **20** appears *at first sight* to result from a Pd(II)/Pd(IV) oxidative addition/reductive elimination sequence involving MeI (work by Canty has shown that Pd(II) undergoes oxidative addition with MeI to yield Pd(IV) species[85]). The formation of **21** on the other hand, would occur by a classic Pd(0)/Pd(II) sequence involving reductive elimination of 3,3'-bitolyl from **19** followed by oxidative addition of MeI to the 14-electron PdL$_2$ complex.

However, Yamamoto elegantly demonstrated that this reaction does not involve Pd(IV), but rather proceeds by aryl/Me exchange between **19'** and **21** (***Scheme 8***):

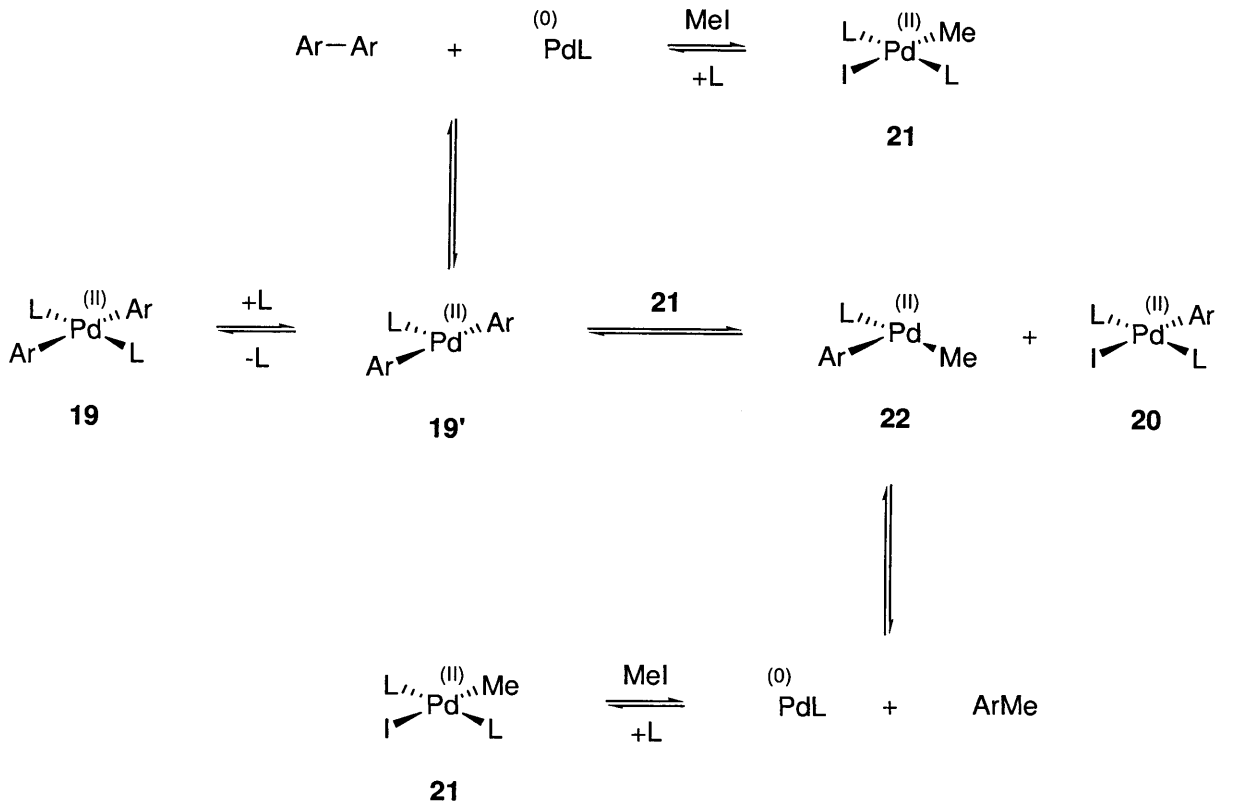

Scheme 8: *aryl/Me transfer mechanism in the reaction of* ***19*** *with MeI*

Importantly, the reaction is accelerated by the addition of **21**, consistent with the autocatalytic process suggested by the S-shaped kinetic plots (see section **4.2.3.3** for similar plots). Also, the presence of additional phosphine was found to inhibit the reaction, in agreement with the mechanism shown in ***Scheme 8***. Indeed, the formation of **19'** (and hence, the whole proces) would be expected to be slowed down by additional phosphine. Finally, deuterium labeling studies showed that the incorporation of deuterium in the products of the reaction agreed with the predicted distribution.[93]

In another study, Yamamoto reported that the reaction of **19** with the *m*-tolyl analogue of **21** gave similar results, thus demonstrating that the transmetalation reaction was not limited to alkyl ligands.[94]

The exact nature of the intermediate in the transmetalation step could not be elucidated. Yamamoto suggested a binuclear Pd complex with a 5-coordinate Pd atom (**23**),[93, 94] but a binuclear complex with one less phosphine (**24**) can also be envisaged (***Scheme 9***).

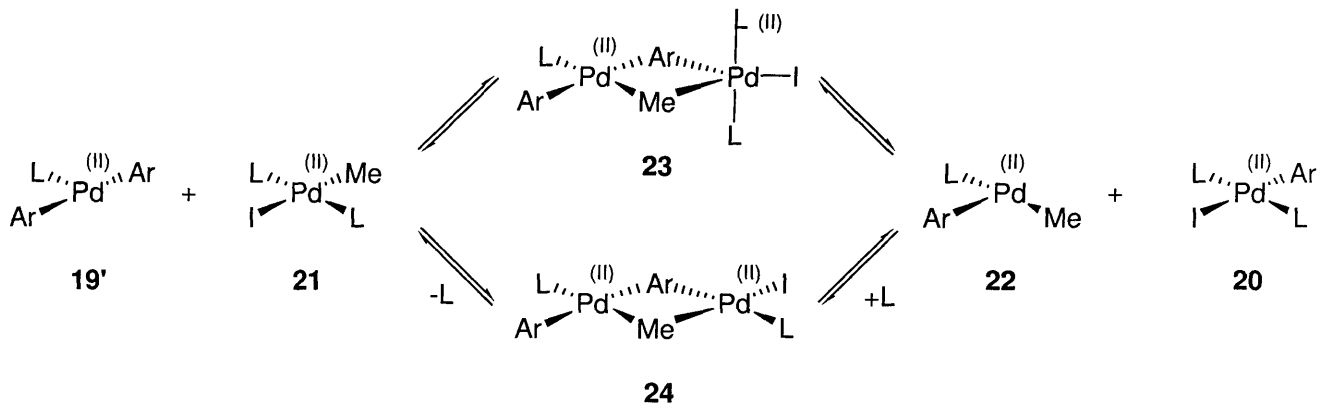

Scheme 9: *possible intermediates in the reaction of* ***19*** *with MeI*

4.1.3.2.2 *Transmetalation processes involving Pd(II) complexes of tmiy*

In 1999, Cavell reported compound **25**, a Pd(0) complex of tmiy stabilised by π-acid maleic anhydride. The oxidative addition of PhI to **25** was expected to yield Pd(II) complex **26**. However, the formation of **26** was not observed. Instead, the reaction resulted in Pd(II) complex **27**, together with biphenyl, Pd black and 2-phenyl-1,3,4,5-tetramethylimidazolium iodide [$\mathbf{PI_1}$]I (***Scheme 10***).[95]

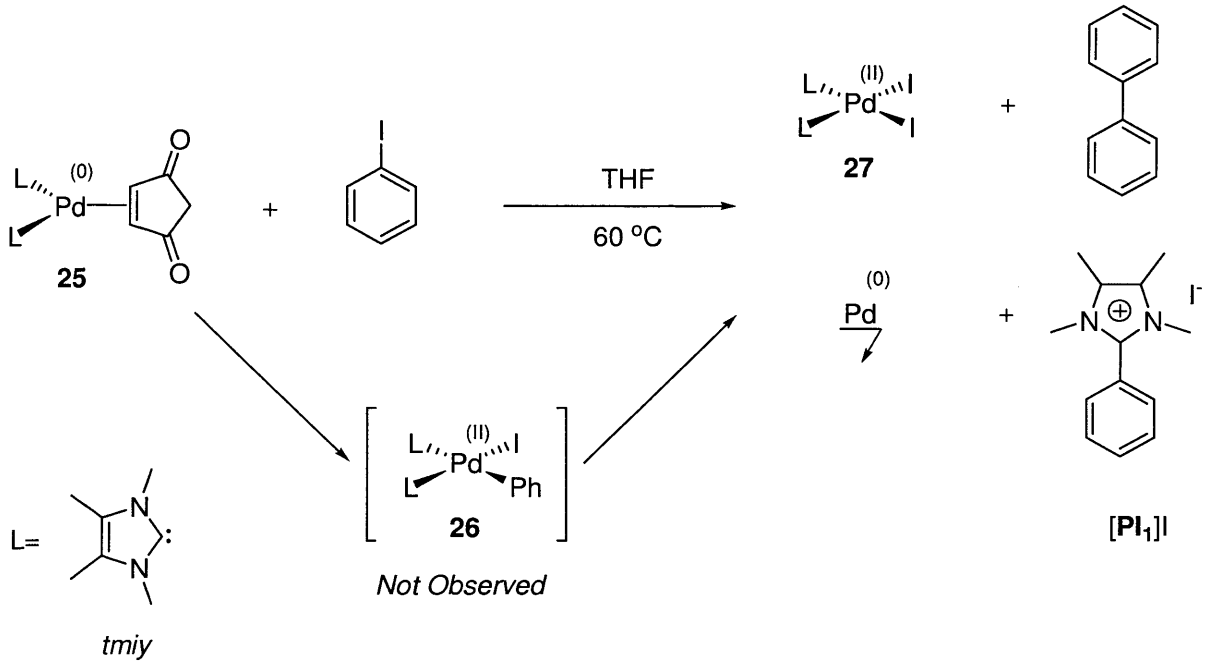

Scheme 10: *reaction of a Pd(0) NHC complex with PhI yielding an imidazolium salt*

This was the first time reductive elimination of a phenylimidazolium ($\mathbf{PI^+}$) cation from a Pd(II) NHC aryl complex was observed (Grushin reported a similar reaction in 2003[96]). The formation of $\mathbf{PI_1^+}$ from **26** is not surprising since reductive elimination of Pd(II) alkyl NHC species had been observed previously. Moreover, a stable analogue of **26** with *p*-nitrophenyl as the aryl ligand was obtained from the reaction of **25** with 4-iodonitrobenzene, indicating that such species actually formed. However, the formation of biphenyl is somewhat more puzzling. Indeed, for biphenyl to

form, a diaryl Pd complex is required. Such an intermediate can either be a Pd(II) species such as **29** (formed by transmetalation of **26** with another Pd(II) aryl species such as **28**), or a Pd(IV) species such as **30** (***Scheme 11***).

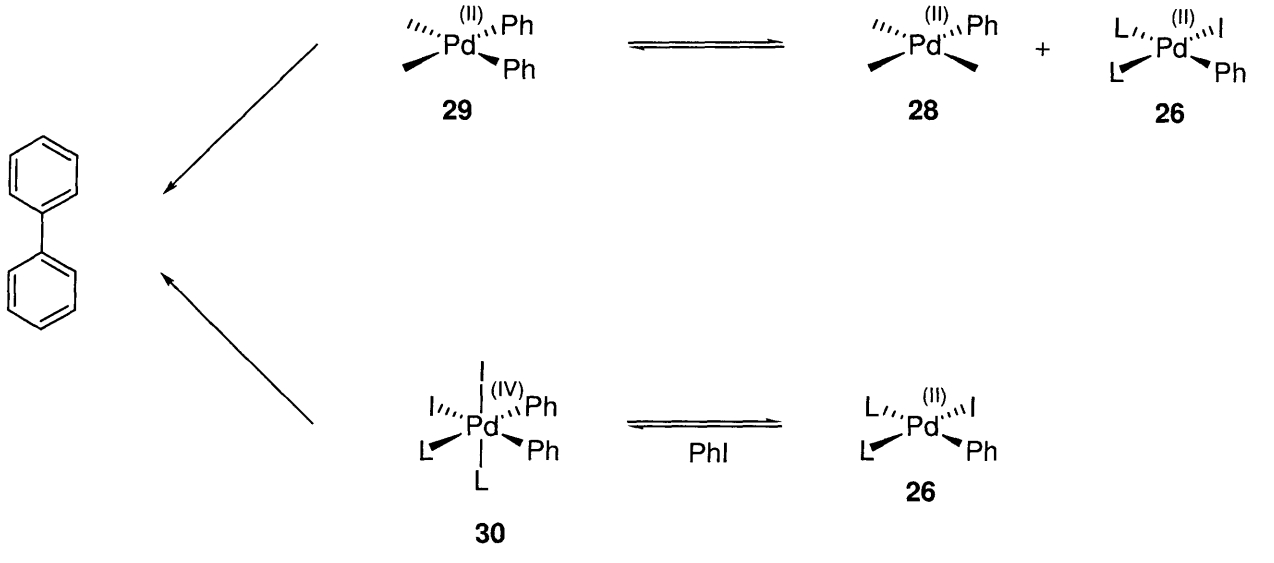

Scheme 11: *possible intermediates in the reaction of* ***25*** *with PhI*

Whilst the formation of **30** would likely result in the same products as those observed, no Pd(IV) species were detected and the authors concluded that, in light of Yamamoto's work, a transmetalation route was more likely. The exact nature of the Pd(II) intermediates was not investigated though. The authors pointed out that dissociation of a tmiy ligand in a similar fashion to the phosphine dissociation observed by Yamamoto was unlikely.

Very recently, Cavell reported the unexpected behaviour of a series of Pd(II) methyl NHC complexes (**31**). These compounds were expected to decompose to give reactive $Pd(0)L_2$ fragments, thus providing a useful source of analogues of Whiteside's compound (***Scheme 12***):[97]

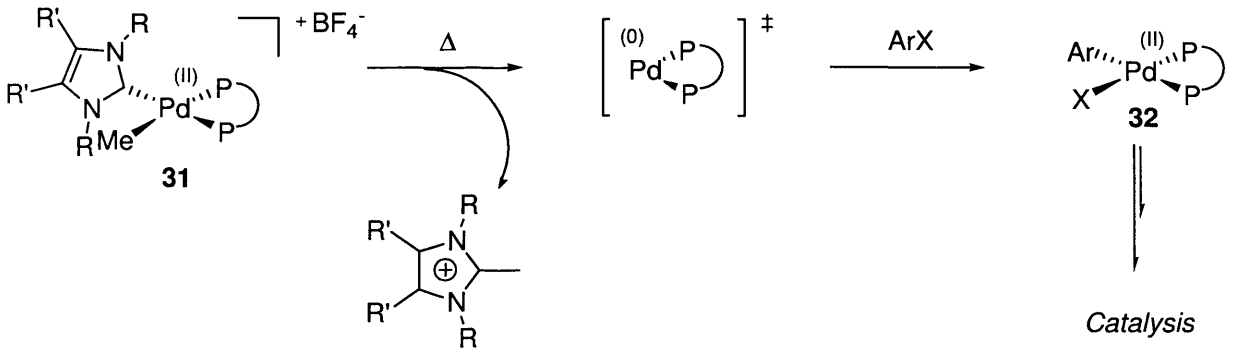

Scheme 12: decomposition of Pd(II) methyl NHC complexes yielding reactive Pd(0)L_2 fragments

However, the reaction of these compounds with aryl halides did not give the expected Pd(II) complexes **32**. Mixtures were obtained in which a number of Pd(II) bis(phosphine) compounds (**32-35**) were identified (***Scheme 13***).

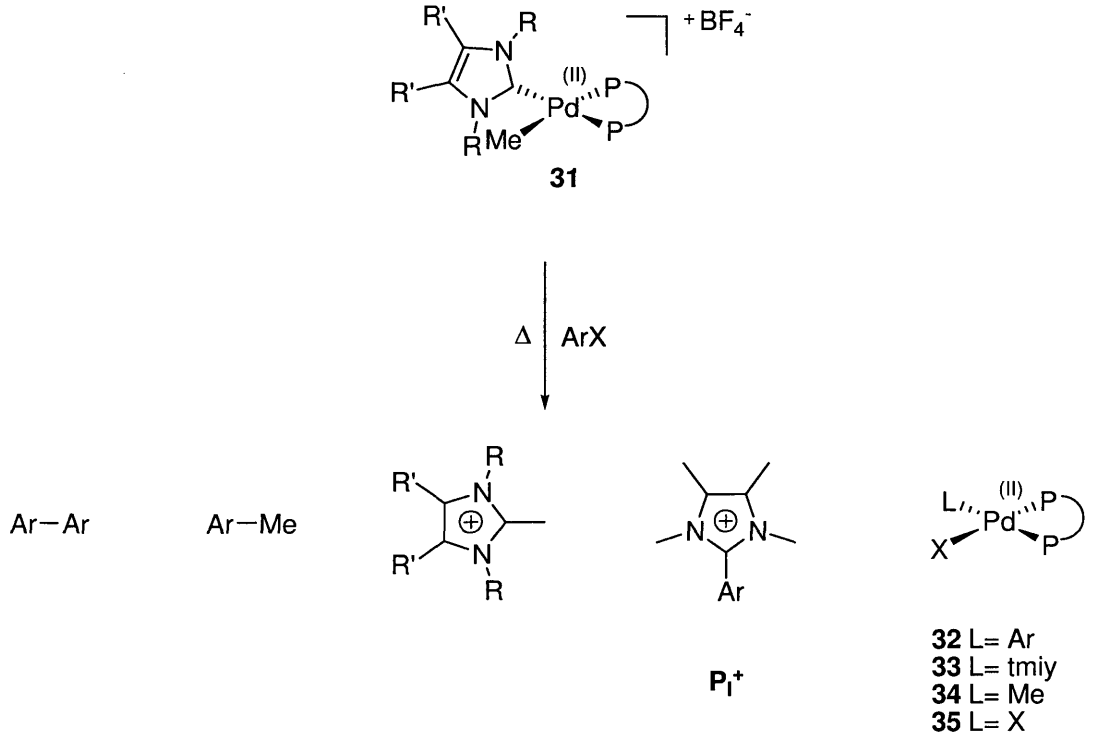

Scheme13: reaction of Pd(II) methyl NHC complexes with ArX

In addition to the expected pentamethylimidazolium cation, $\mathbf{P_I}^+$ cations, toluenes and biaryls were observed. (***Scheme 13***). The authors suggested a multi-step sequence of transmetalation reactions to explain the observed product distribution. Indeed, the presence of **35** and biphenyls cannot be explained by a Pd(IV) mechanism.

Interestingly, the reaction of **31'** with **32'** was monitored by ^{31}P NMR spectroscopy and the two major products detected were **33'** and **34'**, *suggesting that NHCs remain tightly bound to the metal and do not take part in the transmetalation reactions* (***Scheme 14***). Whilst this control experiment does not provide definitive evidence for the inertness of Pd-bound tmiy towards transmetalation, it is an important observation (see section **4.2**).

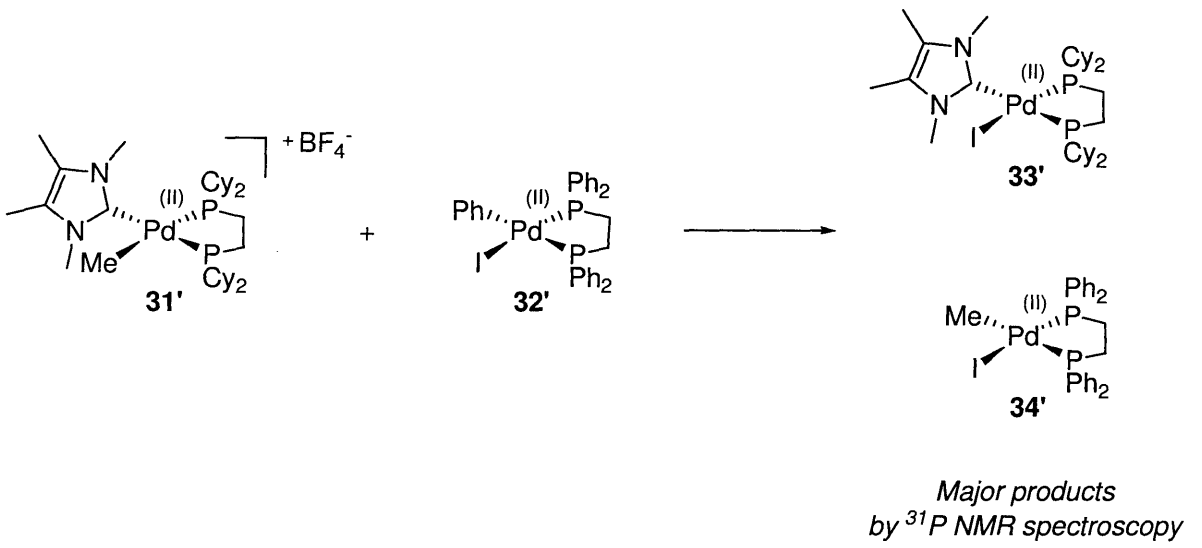

Scheme 14: *reaction of two Pd(II) complexes*

The examples discussed above demonstrate the importance of transmetalation processes in stoichiometric reactions. It is obviously much easier to obtain conclusive experimental data (such as kinetic plots) for these reactions than in the case of catalytic processes *apparently* going *via* Pd(IV) intermediates. In this case, *in silico* studies can greatly help mechanism elucidation.

4.1.3.2.3 Transmetalation in catalytic C-H functionalisation

In 1992, Dyker reported the Pd-catalysed formation of substituted 6H-dibenzo[b,d]pyrans from iodoanisoles (see ***Scheme 15*** for an example):[98]

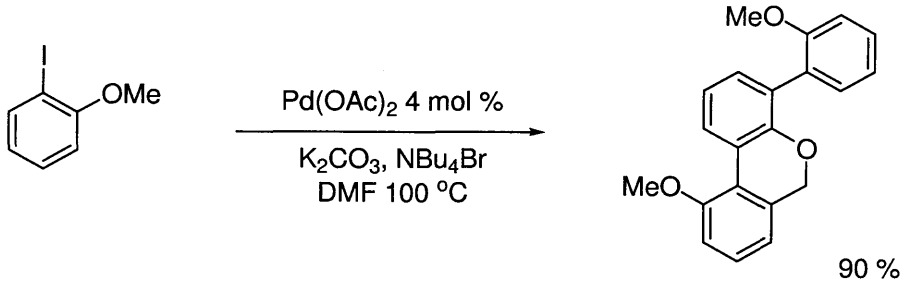

Scheme 15: *Pd-catalysed domino reaction of 2-iodoanisole*

Clearly, this reaction involves activation of the C-H bond of a methoxy group and Dyker postulated the intermediacy of palladacycles **37** in this reaction. These would form by oxidative addition of iodoanisoles to Pd(0) followed by base-mediated metalation of the methyl group, as shown in ***Scheme 16***:

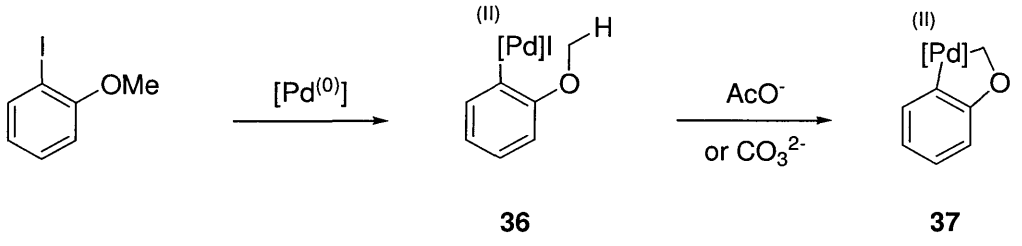

Scheme 16: *palladacycles intermediates in the Pd-catalysed domino reaction of 2-iodoanisole*

Further studies of this reaction confirmed this hypothesis, as summarised in a study by Echavarren of the mechanism of this reaction.[99]

In his original paper, Dyker claimed that **37** underwent oxidative addition of a second aryl iodide, thus yielding Pd(IV) intermediates **38** which would then reductively eliminate to yield palladated compounds **39** (***Scheme 17***). From these intermediates, the reaction would continue, eventually yielding 6H-dibenzo[b,d]pyrans products.[98]

Obviously, in light of the examples discussed above, another mechanism involving transmetalation between palladacycles **37** and the oxidative addition product of iodoanisoles (**36**) to Pd(0) is possible (***Scheme 17***).

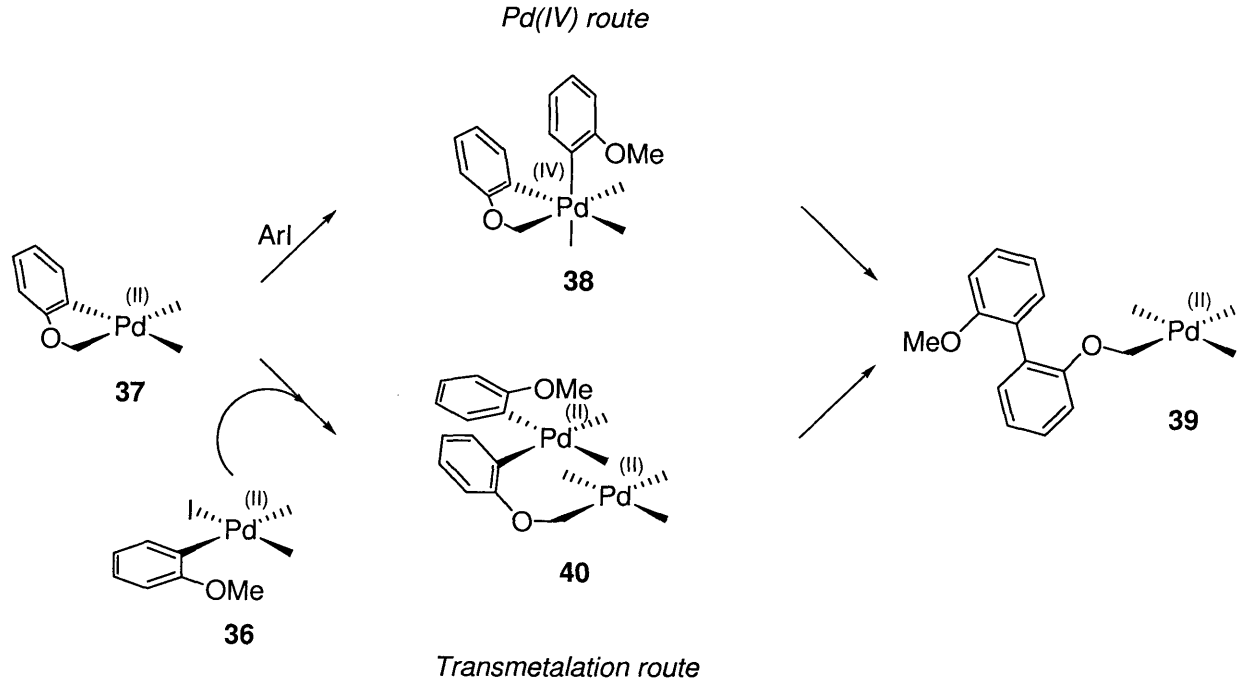

Scheme 17: *possible routes for the arylation of palladacycles 37*

This mechanism was proposed and investigated by Echavarren.[99] DFT calculations evaluated both routes and indicated that this type of reaction (*i.e.* the arylation of palladacycles) was more likely to proceed by a transmetalation sequence than *via* Pd(IV) intermediates. This example illustrates the benefit of using computational methods to evaluate the different possible mechanisms of a reaction involving transient intermediates such as **38** or **40**.

4.2 Results and discussion

4.2.1 Catalytic activity of $[Pd(\eta^3\text{-}C_3H_5)(tmiy)(PCy_3)]BF_4$

The Pd-catalysed intermolecular alkenylation of azolium salts was described in chapter 2. Several phosphines and NHCs were tested to generate Pd(0) catalysts *in situ*, and it was found that PCy_3 gave the best results. One of the features of this reaction is the strong inhibiting effect of excess phosphine, suggesting that monoligated Pd(0) is the active catalyst. This prompted the use of well-defined Pd complexes bearing PCy_3 (***Figure 5***):

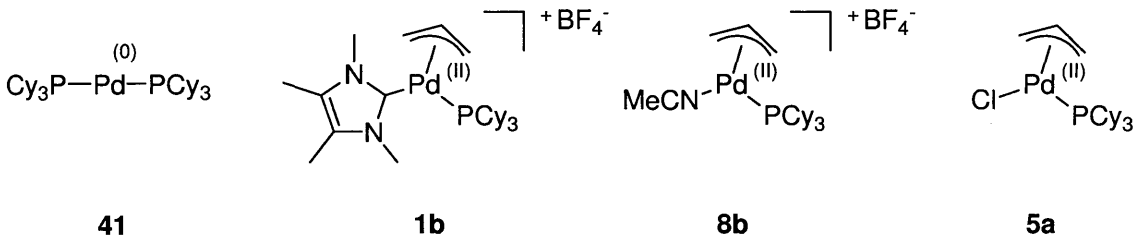

41 **1b** **8b** **5a**

Figure 5: *well-defined Pd complexes tested in catalysis*

The synthesis of compounds **1b**, **8b** and **5a** has been described in chapter 3, and **41** was prepared according to a literature procedure.[100] The activity of those complexes in the coupling of 1-propyl-3-methylimidazolium bromide ([pmim]Br) with ethylene was compared with that of the *in situ* system using $Pd(dba)_2/PCy_3$ (***Table 1***):

Table 1: *selected results for the Pd-catalysed coupling of ethylene and [pmim]Br*[a]

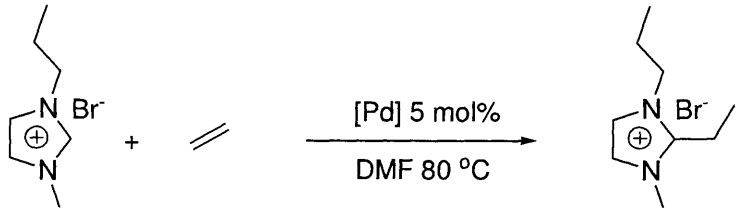

Entry	Catalyst	Conv. (%)
1	$Pd(dba)_2/PCy_3$ 1:1	26
2	**5a**	0
3	**8b**	0
4	**41**	61
5	**1b**	81

[a] Reagents and conditions : 1-propyl-3-methylimidazolium bromide [pmim]Br 0.73 mmol, [Pd] 5 mol%, DMF 3 mL, C_2H_4 1 bar, 80 °C, 24 hr. Based on the average of two runs

The best *in situ* catalyst found previously gave a modest 26 % conversion at 5 mol% Pd loading (entry 1). Using *bis*(tricycloxexylphosphine)palladium(0) **41** resulted in noticeable improvement (entry 4), consistent with the expectation that **41** would lose a phosphine upon heating, thus generating a reactive Pd-L fragment. In a study of the activity of *bis*(phosphine)palladium(0) complexes in the Heck reaction, Brown reported that aryl halides oxidatively add to **41** at room temperature without prior phosphine dissociation. Complexes bearing more bulky ligands such as P^tBu_3 were found to react after dissociation.[101] At 80 °C however, **41** is likely to be involved in a dissociation equilibrium. Finally, **1b** showed very good activity in the reaction of [pmim]Br with ethylene (entry 5), indicating that the unique structure of this complex might effectively generate monoligated Pd(0). Importantly, **5a** and **8b** were completely inactive (entries 2-3), showing that the activity of **1b** is neither due to the allyl ligand nor to its cationic nature. These extremely encouraging results prompted a deeper investigation of the activation mechanism of **1b**.

4.2.2 Activation of $[Pd(\eta^3\text{-}C_3H_5)(tmiy)(PCy_3)]BF_4$

4.2.2.1 Possible activation pathways

Although complex **1b** and related compounds were originally designed to decompose to Pd-L upon reductive elimination, their exact activation mechanism under reaction conditions remains an interesting question. As shown in ***Scheme 18***, the generation of Pd(0) species from **1b** could either occur by reductive elimination following decoordination of the allyl ligand, or by intermolecular nucleophilic attack on the allyl moiety.

Activation by allyl decoordination

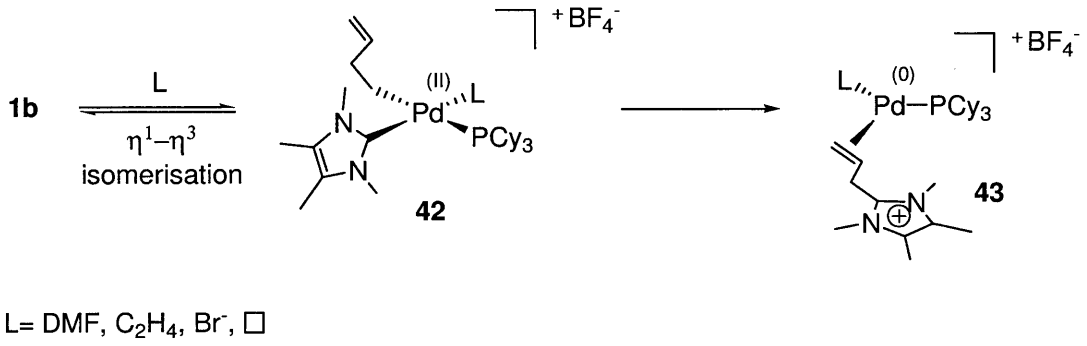

Activation by nucleophilic attack

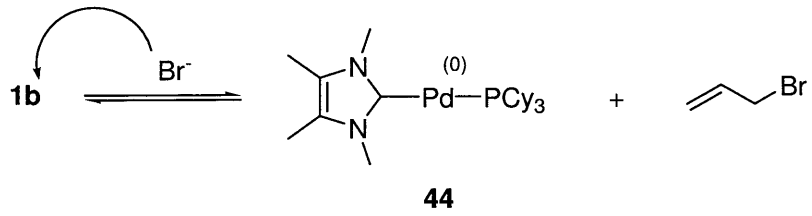

Scheme 18: *activation of* ***1b*** *under reaction conditions*

The η^1-η^3 isomerisation sequence generates a free coordination site; therefore it could be triggered by a coordinating species present in the reaction medium, such as ethylene, a bromide ion from

[pmim]Br or the solvent. It is also possible that **42** exist as a transient 3-coordinate species if reductive elimination presents a small activation energy.[102] In any case, the resulting Pd(0) species **42** only contains one firmly bound ligand (*i.e.* PCy_3).

Since Pd(II) π-allyl complexes are prone to nucleophilic attack (see chapter 3), one could also envisage an alternative activation mechanism in which a bromide ion provided by [pmim]Br would reversibly generate allyl bromide and **43**. This intermediate would then enter the catalytic cycle by oxidative addition of the imidazolium cation, much like the mixed $[Ni(dmiy)(PMe)_3]$ system studied computationally by Hawkes and Yates (see chapter 2).[103]

4.2.2.2 Behaviour of $[Pd(\eta^3\text{-}C_3H_5)(tmiy)(PCy_3)]BF_4$ under reaction conditions

To find which of these scenarios was more likely, the behaviour of **1b** in the presence of the different components of the catalytic reaction was investigated. Thus, **1b** was heated in DMF on its own, in the presence of ethylene or [pmim]Br. Reaction mixtures were analysed by ^1H and ^{31}P NMR spectroscopy and low resolution electrospray mass spectrometry (ESI/MS). The relevant spectra are included in appendix 5.

- When **1b** was heated in DMF for 5 hours (***Scheme 19***), no change was observed either visually or in the ^1H and ^{31}P NMR spectra. ESI/MS showed little change, with only a very small signal corresponding to 2-propenyl-1,3,4,5-tetramethylimidazolium (**A**) present (m/z= 165.1), the main signal being that of **1b** (m/z= 551.3). A control ESI/MS experiment on **1b** showed no other signal than that of **1b**, showing that the degradation of **1b** is not an artefact caused by the electrospray. However it is unlikely that the activation of **1b** would be caused solely by thermal activation under the reaction conditions.

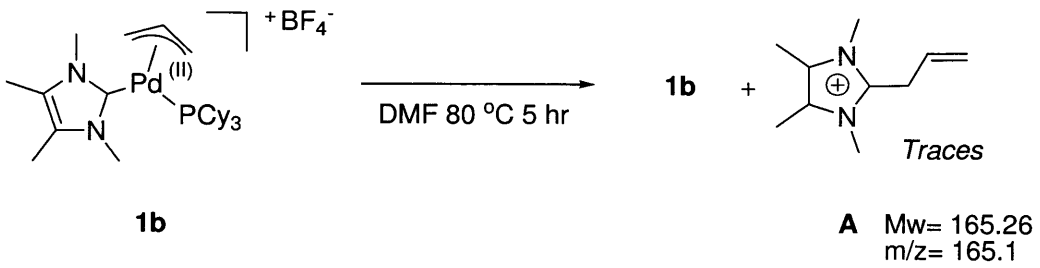

Scheme 19: *thermal stability of* ***1b***

- When **1b** was heated in DMF under 1 bar of ethylene (***Scheme 20***), the solution turned brown very quickly, and some Pd black was observed. Interestingly, the ^{31}P NMR spectrum did not change, although a set of signals consistent with the presence of **A** was observed by ^{1}H NMR.[104] The ratio of **A** to **1b** was 1.5 to 10. The ESI/MS spectrum on the other hand changed dramatically, with a strong signal corresponding to **A** (m/z=165.1). These results are consistent with ethylene triggering the activation of **1b** as shown in ***Scheme 18***.

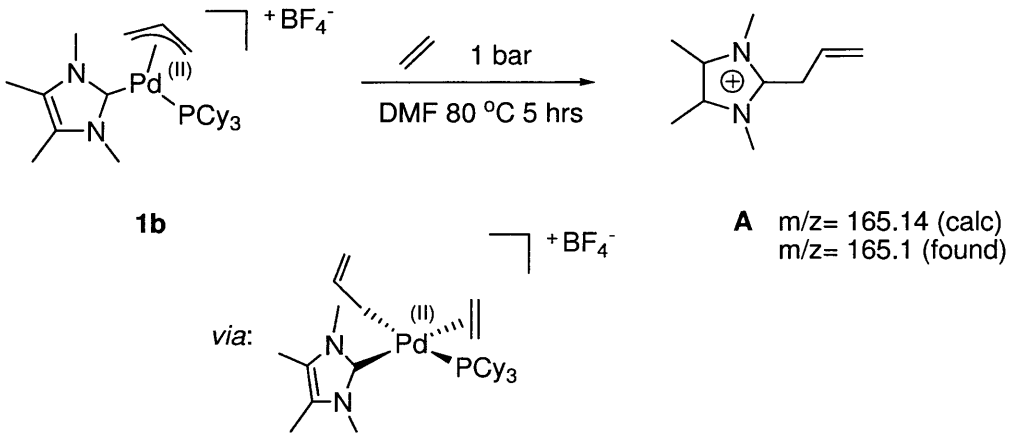

Scheme 20: *activation of* ***1b*** *with ethylene*

- Finally, when **1b** was heated in DMF in the presence of 2 eq of [pmim]Br (***Scheme 21***) a yellow solution was obtained. The resulting ^{1}H and ^{31}P NMR spectra were very complex, but ^{31}P NMR indicated that most of **1b** had been consumed. Signals observed by ESI/MS include that of **A** (the main peak) and a peak consistent with allyltricyclohexylphosphonium **B** (m/z= 321.3). The only significant set of peaks containing Pd was that of **1b**. It is difficult to establish whether the formation of **B** results from nucleophilic attack of PCy_3 on allyl bromide or **1b**, or even reductive elimination from **1b** (***Scheme 22***).

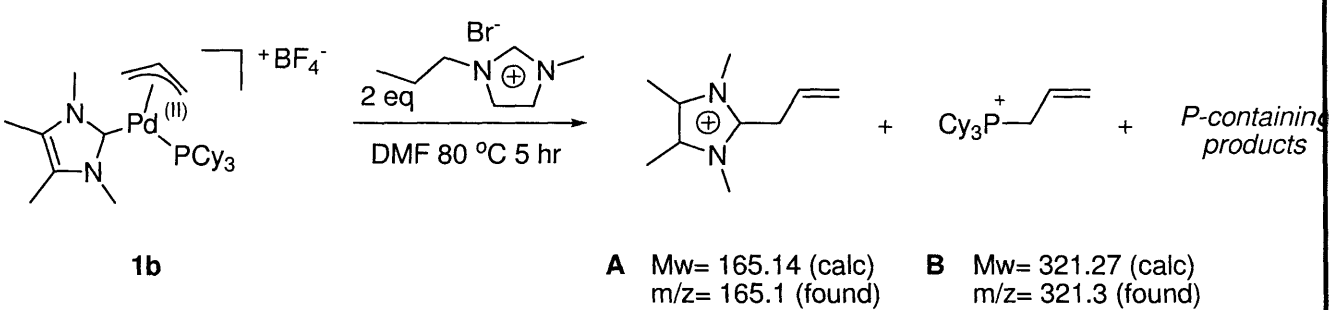

1b

A Mw= 165.14 (calc)
m/z= 165.1 (found)

B Mw= 321.27 (calc)
m/z= 321.3 (found)

Scheme 21: *activation of* ***1b*** *by [pmim]Br*

These results indicate that **1b** could be activated by ethylene or bromide-mediated η^1-η^3 isomerisation of the allyl ligand. Depending on the nature of the ligand, this would generate η^1-allyl intermediates **42** or **42'**. In the presence of bromide, a phosphonium salt is generated, indicating that this ion could play a significant role in catalyst deactivation.

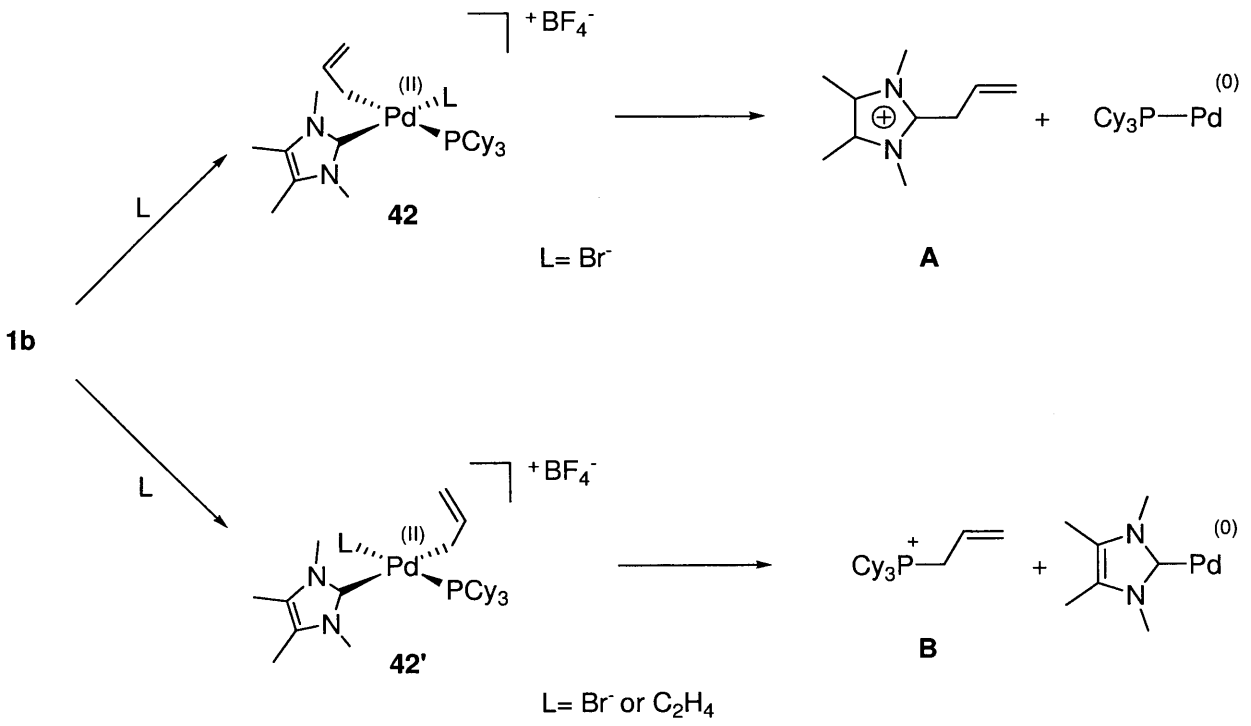

Scheme 22: *generation of A or B by reductive elimination*

4.2.3 Pd-mediated arylation of NHCs

4.2.3.1 Serendipitous discovery of the reactivity of $[Pd(\eta^3\text{-}C_3H_5)(tmiy)(PCy_3)]BF_4$ towards phenyl iodide

The studies described in the previous section confirmed the initial hypothesis that **1b** was probably reduced to Pd(0) under the conditions used in catalysis. However, as exemplified by the reaction with [pmim]Br (***Scheme 21***), the resulting Pd(0) species could not be identified because of its reactivity, causing multiple side-reactions to occur (see ESI/MS and ^{31}P NMR spectra in appendix 5). On the other hand it was expected that any Pd-L fragment would immediately react with aryl iodides, generating 3-coordinate Pd(II) complex **C**, possibly as dimer $\mathbf{C_2}$ (***Scheme 23***). Hartwig has reported similar compounds resulting from the oxidative addition of PhBr to Pd(0) in the presence of 1 eq. of phosphine.[105]

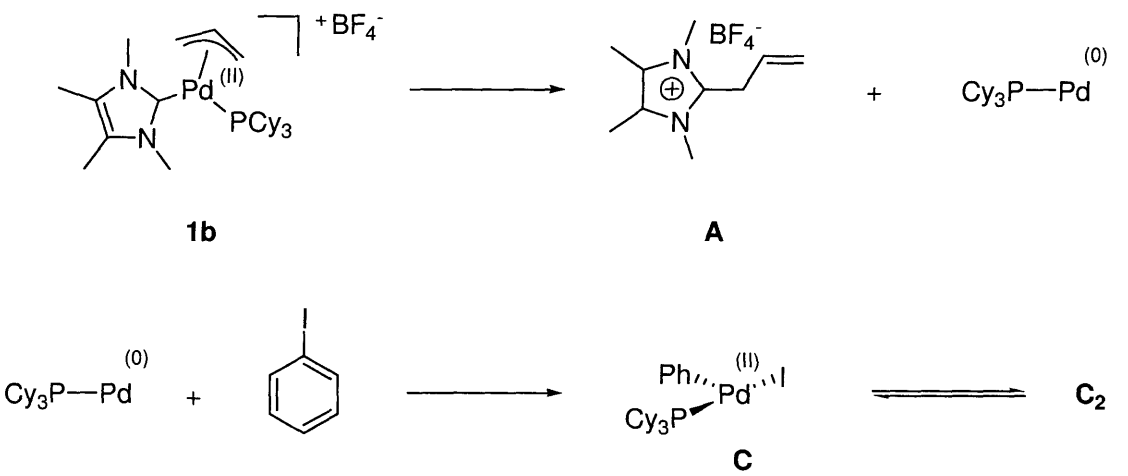

Scheme 23: *expected outcome of the reaction of* ***1b*** *with phenyl iodide*

Species such as **C** or $\mathbf{C_2}$, if isolated, would provide solid evidence that the catalytic activity of **1b** is due to its tendency to generate monoligated Pd(0) fragments.

Thus, **1b** was reacted with phenyl iodide (PhI) in DMF at 80 °C (***Scheme 24***):

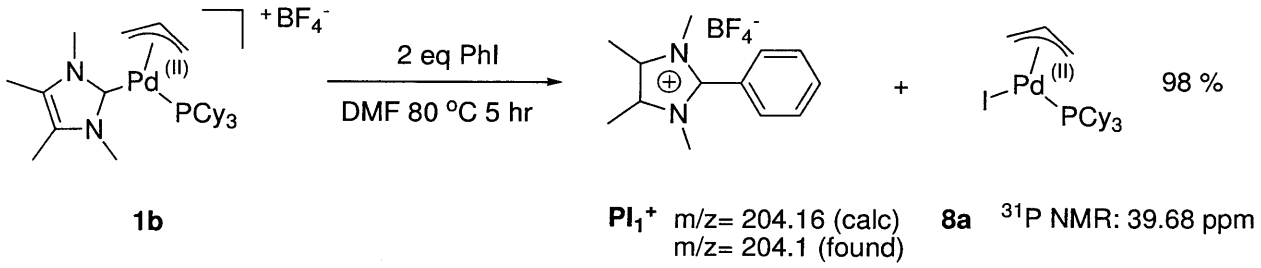

Scheme 24: *reaction of **1b** with phenyl iodide*

Surprisingly, neither **C** nor $\mathbf{C_2}$ were found in the reaction mixture. Instead, ^{1}H and ^{31}P NMR spectroscopy and ESI/MS all confirmed the almost complete conversion of **1b** to phenylimidazolium tetrafluoroborate $[\mathbf{PI_1}]BF_4$ and **8a** (see appendix 5).

Compound **8a** was prepared independently from the corresponding chloro derivative (see experimental part of chapter 3). Its ^{1}H (in particular the H_{meso} signal at 5.16 ppm) and ^{31}P (39.68 ppm) signals were observed, and the ESI/MS spectrum showed a set of peaks centered on m/z= 468.2 corrseponding to the $[\mathbf{8a}\text{-I+MeCN}]^+$ ion.

Due to the small scale on which the experiment was performed, it was not possible to isolate $[\mathbf{PI_1}]BF_4$, and attempts at independently preparing it using a reported procedure for similar compounds failed.[106] However $[\mathbf{PI_1}]I$ has been reported previously,[95] and the ^{1}H signals corresponding to $\mathbf{PI_1}^+$ were observed. In addition, ESI/MS of the reaction mixture showed a very strong signal corresponding to $\mathbf{PI_1}^+$ (m/z= 204.1).

The ^{31}P NMR spectrum of the reaction mixture indicated that, in addition to **1b** and **8a**, another P-containing compound was present in very small amounts (signal at 21.68 ppm). In addition, the ESI/MS spectrum revealed the presence of **A** (m/z= 165.1) and a peak at m/z=357.3, consistent with the presence of phenyltricyclohexylphosphonium **D** (***Figure 6***). However, the additional signal in

the ^{31}P NMR spectrum is unlikely to be due to **D**: work by Marks on phosphonium salts indicates that the signal for **D** should be close to -40 ppm.[107]

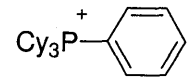

D

m/z= 357.27 (calc)
m/z= 357.3 (found)

Figure 6: *trace compound detected by ESI/MS in the reaction of* ***1b*** *with PhI*

This unexpected reaction is surprisingly selective (the ^{1}H NMR spectrum of the crude reaction mixture only shows **1b**, **8a** and $\mathbf{PI_1}^+$), and although it requires stoichiometric amounts of Pd, it provides an effective route to 2-arylimidazolium salts. Therefore, it bears synthetic potential and its scope and mechanism were investigated further.

4.2.3.2 Scope of the arylation of NHCs

To investigate the scope of the Pd-mediated arylation of NHCs, this reaction was run using different electrophiles or analogues of **1b** as described in chapter 3.

4.2.3.2.1 Reaction of $[Pd(\eta^3\text{-}C_3H_5)(tmiy)(PCy_3)]BF_4$ with electrophiles

It was of interest to determine whether the reactivity of **1b** was limited to aryl iodides. Thus, other aryl halides were tested in this reaction, together with methyl iodide (MeI) and an I(III) reagent, $[(C_6H_5)_2I]BF_4$ (**45**). The latter has been used by Sanford as a source of $C_6H_5^+$ in Pd-catalysed reactions (see ***Scheme 5***).[68, 69] The reactions were run in CD_2Cl_2 and analysed by ^{1}H and ^{31}P NMR spectroscopy and ESI/MS. Results are presented in ***Table 2***.

Table 2: *reaction of* ***1b*** *with electrophiles*[a]

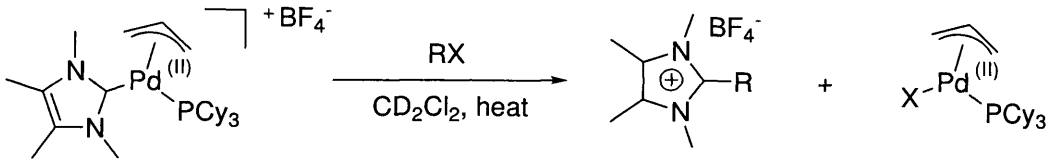

Entry	R-X	Temp (°C)	Time (hr)	Conv (%)[b]
1	PhI (5 eq)[c]	70	9	97
2	*p*-$C_6H_4(NO_2)I$ (2 eq)	60	18.5	12
3	*p*-$C_6H_4(NO_2)I$ (2 eq)	70	20	68
4	PhCl (2 eq)	100	26.5	traces[d]
5	PhBr (2 eq)	70	16	20
6	PhBr (2 eq)	80	25	82
7	**45** (3 eq)	70	0.5	53
8	**45** (3 eq)	80	0.5	100
9	MeI (4 eq)	85	19.5	traces[d]

[a] Reagents and conditions: **1b** (entries 2-9: 0.016 mmol, entry 1: 0.0200 mmol); RX, x eq; CD_2Cl_2 650 µL; sealed NMR tube. [b] Calculated by ^1H NMR spectroscopy. [C] 1.5 eq of *p*-xylene was used as an internal reference, see experimental section . [d] Detected by ESI/MS

The reactivity of **1b** towards aryl halides follows the classical trend I>Br>>Cl (entries 1-6). In the case of aryl chlorides (entry 4), hardly any product is observed even at elevated temperatures. This trend is reminiscent of that observed in other Pd(0)/Pd(II) catalytic reactions, where aryl chlorides are very challenging substrates.[90]

Interestingly, *p*-iodonitrobenzene is less reactive than iodobenzene (entries 1 and 3). This reactivity pattern suggests that in the case of aryl iodides, reductive elimination (*i.e.* the C-C bond forming step) is the rate determining step of the whole process, regardless of the exact mechanism of the reaction (see chapter 1).[108]

The use of the I(III) reagent **45** dramatically improved reaction rates (entries 7-8): at 70 °C, the reaction is about 9 times faster than with PhI (entry 1). Compound **45** is a convenient source of Ph^+ that can react with Pd(II) to yield Pd(IV) species. However, the fact that MeI hardly reacts with **1b**, even at elevated temperatures (entry 9), casts serious doubts on the assumption that this reaction goes *via* Pd(IV) intermediates.

4.2.3.2.2 Reaction of $[Pd(\eta^3\text{-}C_3H_5)(NHC)(PR_3)]BF_4$ with p-iodonitrobenzene

The reaction of **1b** analogues bearing a different phosphine or NHC ligand was investigated next (***Table 3***). The electrophile chosen for this study was *p*-iodonitrobenzene because being a solid, it is easier to weigh accurately in small quantities.

Table 3: *reaction of **1b** analogues with p-$C_6H_4(NO_2)I$* [a]

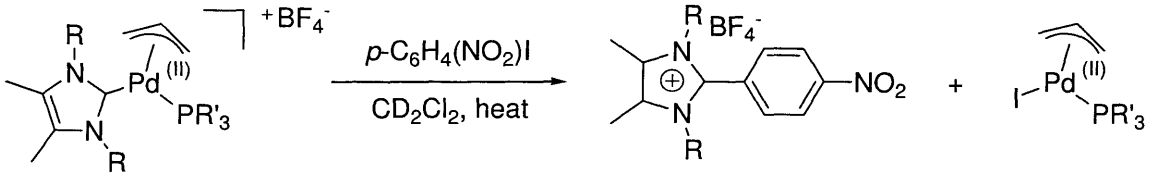

Entry (compound)	NHC	PR'$_3$	Temp (°C)	Time (hr)	Conv (%)[b]
1 (**1b**)	tmiy	PCy_3	70	20	68
2[c] (**1c**)	tmiy	PPh_3	70	15	100
3[c] (**1e**)	tmiy	PBz_3	70	15	traces[d]
4[c] (**1f**)	tmiy	PEt_3	70	15	traces[d]
5 (**2b**)	dipdmiy	PCy_3	85	19.5	traces[d]
6 (**2b**)	dipdmiy	PCy_3	107	21.5	10
7 (**2c**)	dipdmiy	PPh_3	70	18.5	traces[d]

[a] Reagents and conditions : [Pd] (entries 1 and 5-7: 0.016 mmol, entries 2-4: 0.0200 mmol); *p*-$C_6H_4(NO_2)I$ (entries 1 and 5-7: 2 eq, entries 2-4: 5 eq); CD_2Cl_2 650 µL; sealed NMR tube. [b] Calculated by ^1H NMR spectroscopy. [C] 1.5 eq of *p*-xylene was used as an internal reference. [d] Detected by ESI/MS

Table 3 reveals interesting trends. Using complexes bearing tmiy as an NHC, it appears that **1c** (PR'_3= PPh_3) is the most reactive complex (entry 2). Using more basic and bulky PBz_3 (**1e**, entry 3) inhibits the reaction. However, increasing phosphine basicity and bulk even more (**1b**, entry 1) restores some activity, although not to the level observed with **1c**. Finally, the use of **1f**, a complex bearing compact and basic PEt_3, also inhibits the reaction. The apparent lack of consistency of these results actually points to a complex, multi-step sequence rather than a simpler oxidative addition/reductive elimination going via a Pd(IV) intermediate. In the latter case, one would expect reductive elimination to be a facile process, owing to the instability of Pd(IV) complexes.[83] Therefore a compact, electron donating phosphine such as PEt_3 (in **1c**) would be expected to be the best ligand to promote the reaction.

Changing the NHC on the other hand gave less surprising results. The bulkier dipdmiy (present in **2b** and **2c**, which contain phosphines previously found to promote the reaction) inhibited the reaction even at elevated temperatures (entries 5-7).

Overall, these results indicate that the Pd-mediated arylation of NHCs is quite sensitive to the nature of the NHC and the phosphine ligands borne by the Pd complex. On the other hand, a variety of electrophiles (aryl halides and bromides, I(III) arylating reagents) seem to be successfully coupled.

A kinetic study was next conducted, to shed more light on the mechanism of the reaction. Although investigations of the scope of the reaction indicated that a Pd(II)/Pd(IV) sequence was probably not operating, it was hoped that kinetic data would yield conclusive results as to the type of Pd intermediates involved.

4.2.3.3 Mechanism of the reaction of $[Pd(\eta_3\text{-}C_3H_5)(tmiy)(PCy_3)]BF_4$ with aryl iodides

4.2.3.3.1 Kinetic study

The reaction of **1b** with *p*-iodonitrobenzene in deuterated solvents was followed by ^1H NMR spectroscopy. For comparison, the reaction was also run with phenyl iodide in d_2-DCM (***Graph 1***, see experimental section for the detailed procedure). A 5-fold excess of aryl iodide was used in order to have a pseudo-constant concentration of that reactant (equation (1)).

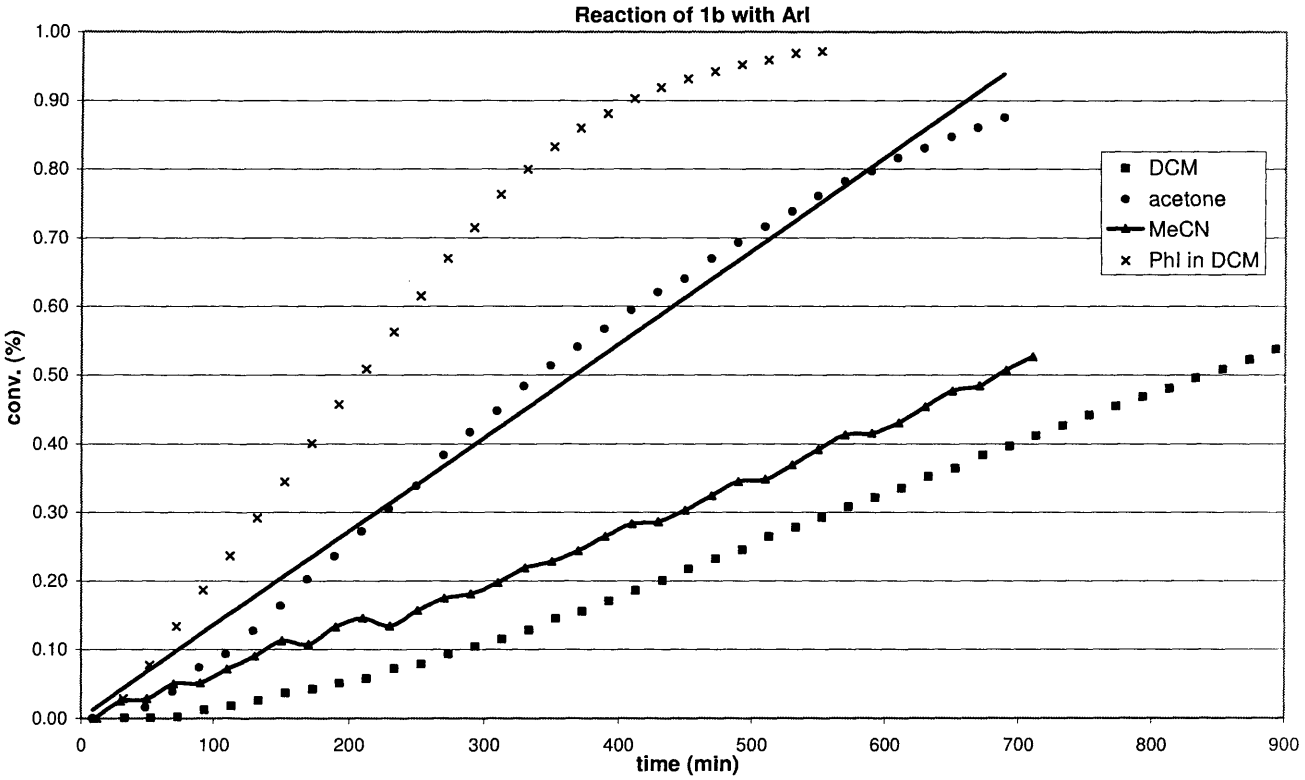

Graph 1: *kinetic plots of the reaction of* ***1b*** *with ArI*

As expected from the scope studies, the reaction with PhI is considerably faster than with *p*-iodonitrobenzene. From ***Graph 1***, it is apparent that the reaction does not follow simple kinetics. The

curves representing the conversion of **1b** as a function of time are S-shaped, indicating that the reaction begins with an initiation phase; in other words the reaction is autocatalytic, in a similar way to the reaction described by Yamamoto (see discussion in section **4.1.3.2.1**). This is especially visible for the reaction in d_6-acetone (a straight line has been drawn in ***Graph 1*** to highlight this).

The reaction in d_3-MeCN displayed interesting kinetics: at first, it appeared that the plot was of poor quality. However, the source NMR spectra were fine (and a second run gave very close results), and closer inspection of the curve in ***Graph 1*** revealed that the observed wobble was periodic. Indeed, from 300-400 min reaction time onwards, the reaction seems to accelerate then stop with a frequency of about 80 min. This behaviour was not observed in other solvents or with phenyl iodide.

Another interesting aspect of these plots is the relative reaction rates according to the solvent. Thus, the reaction rate decreases in the order: d_6-acetone (polarity index 5.1), d_3-MeCN (polarity index 5.8) and d_2-DCM (polarity index 3.1). Therefore, there is no correlation between solvent polarity and reaction rate. However, nitriles are good ligands for Pd(II), much more so than ketones or deuterated solvents (for example, $[Pd(MeCN)_2Cl_2]$ and $[Pd(PhCN)_2Cl_2]$ are common sources of Pd(II)).[109] As will be seen in the next section, the electron donating abilities of d_3-MeCN probably explain both the relative reaction rate in this solvent and the observed unsteady kinetics.

Finally, the kinetics of the reaction at high conversions were found to be first order in **1b** (see appendix 6). The pseudo first-order rate constants k' were extracted from the plots of ln[**1b**]= f(t) according to equation (3).

$$\frac{d[\mathbf{1b}]}{dt} = k \cdot [\mathbf{1b}] \cdot [\mathrm{ArX}]^n \approx k' \cdot [\mathbf{1b}] \quad (1)$$

$$[\mathbf{1b}]_t = [\mathbf{1b}]_0 \cdot e^{-k' \cdot t} \quad (2)$$

$$-\ln[\mathbf{1b}]_t = C + k' \cdot t \quad (3)$$

Table 4: *pseudo first-order rate constants for the reaction of* ***1b*** *with ArI*

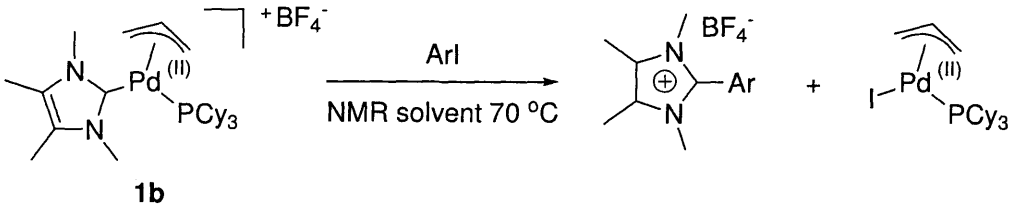

1b

Entry	ArI	Solvent	k' (10^{-3}.mol^{-1}.L^{-1}.s^{-1})
1	*p*-$C_6H_4(NO_2)I$	d_2-DCM	1.2
2	*p*-$C_6H_4(NO_2)I$	d_3-MeCN	1.4
3	*p*-$C_6H_4(NO_2)I$	d_6-acetone	4.4
4	PhI	d_2-DCM	8.8

4.2.3.3.2 Comparison of possible mechanisms with experimental data

Pd(IV) mechanism

As discussed above, it is doubtful that the Pd-mediated arylation of NHCs, exemplified by the reaction of **1b** with ArI, proceeds by an oxidative addition/reductive elimination sequence involving Pd(IV) (***Scheme 25***):

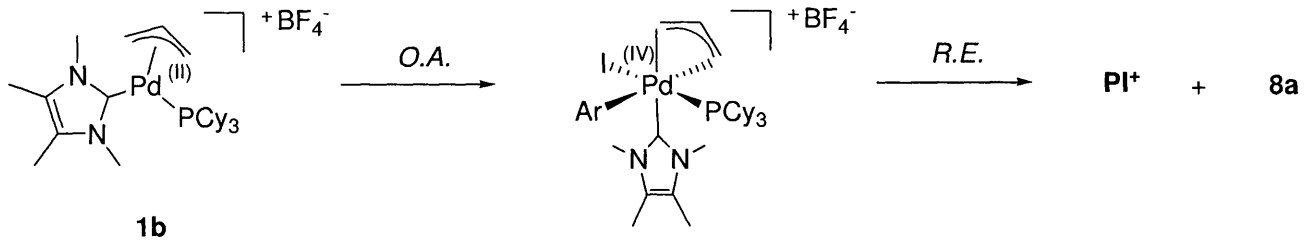

1b

Scheme 25: *Pd(II)/Pd(IV) mechanism*[110]

This mechanism cannot operate for several reasons:

- Firstly, if such a pathway was operating, MeI would react with **1b**. Indeed, MeI has been shown to readily react with Pd(II) to give Pd(IV).[83, 85] This is not the case here, even at elevated temperatures (see section **4.2.3.2.1**); therefore this reaction only takes place with aryl halides.
- Secondly, Pd(IV) formation usually follows an S_N2 mechanism. If this was the rate-determining step of the whole sequence (which is consistent with the high reactivity of Pd(IV) and would explain the lack of spectroscopic evidence for any such species), one would expect a first-order dependence of the reaction rate on the concentration of **1b** throughout the whole reaction.
- Thirdly, a Pd(IV) mechanism is not consistent with the widely different reactivities of **1b-1e**, for the reasons discussed in section **4.2.3.2.2**.
- Finally, as pointed out by Echavarren, even though Pd(IV) aryl complexes exist, "there is no clear-cut experimental evidence for the oxidative addition of $C(sp^2)$-X electrophiles to Pd(II) complexes".[99] Such species are thus formed by indirect methods, or using I(III) arylating reagents.[68, 82-84] Complex **1b** reacts with I(III) reagent **45**, but it also reacts with ArI and ArBr electrophiles.

Concerted σ-bond metathesis mechanism

Early on in the scope studies, it became apparent that a Pd(IV) mechanism was unlikely. In particular, the fact that MeI does not react with **1b** casts serious doubts on this hypothesis. This selectivity for aryl over methyl indicated that an alternative mechanism involving the aryl ligand's π electrons might operate. This mechanism would proceed by a so-called σ-bond metathesis,[90] facilitated by the overlap between the aryl's π-system and the NHC's partially filled p_π orbital (***Scheme26***):

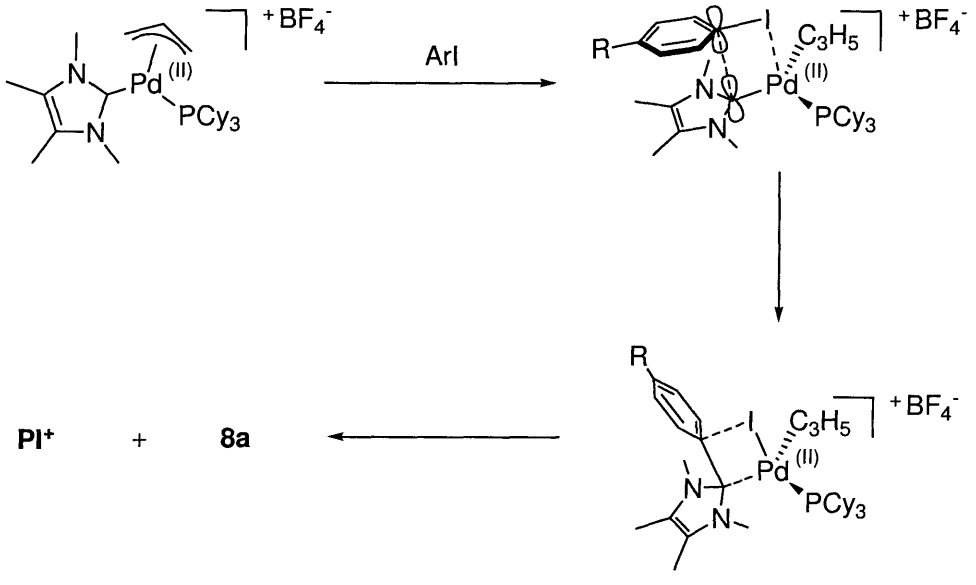

Scheme 26: *alternative σ-bond metathesis mechanism*

This mechanism, if operating, would be an extremely rare occurrence in Pd chemistry.[111] It would explain the lower reactivity of dipdmiy compared with tmiy (see section **4.4.2.2**), and the inertness of MeI. However, the reaction rate would be expected to display first-order dependence on the concentration of **1b** throughout the reaction. Therefore, although this mechanism cannot be disproved with as much confidence as the Pd(IV) mechanism, another pathway is probably operating.

Ligand transfer mechanism

In section **4.1.3.2**, some examples of C-C bond forming processes *apparently* going *via* Pd(IV) intermediates but *actually* involving one or several transmetalation steps between Pd(II) centres have been discussed.

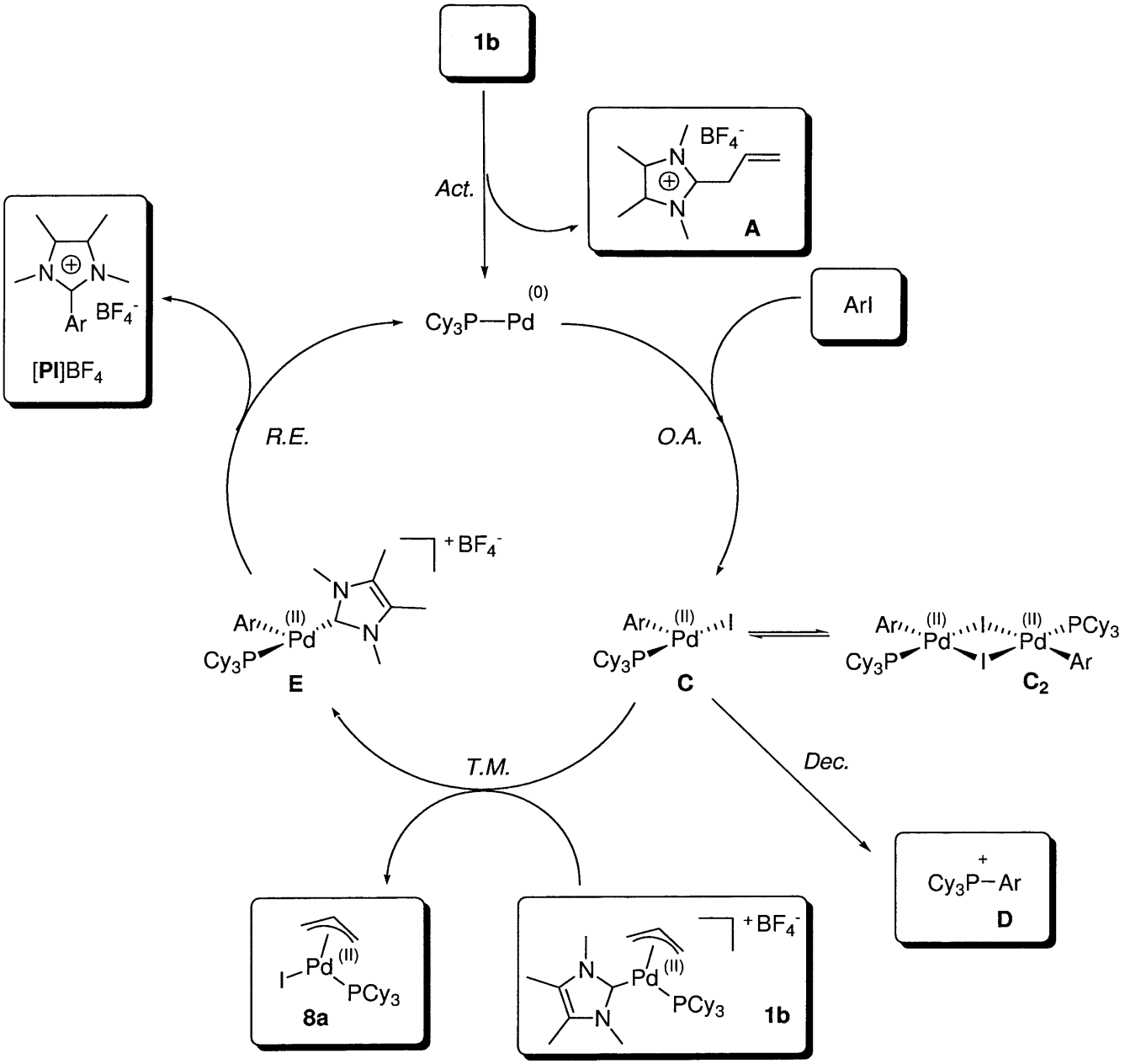

Figure 7: proposed mechanism involving transmetalation between Pd(II) centres[112]

Bearing in mind those examples, the mechanism showed in ***Figure 7*** is proposed for the Pd-mediated arylation of NHCs. This mechanism is backed by several pieces of experimental evidence. It is useful to discuss this sequence step by step:

- First, the *activation* of the Pd(II) allyl NHC complex (*e.g.* **1b**) is likely to provide an entry into the catalytic cycle. It was shown previously (see section **4.3**) that **1b** can decompose to **A**, and this compound was found in trace amounts in reaction mixtures.
- Secondly, *oxidative addition* of the monoligated Pd(0) fragment would generate T-shaped Pd(II) aryl complex **C**, possibly equilibrating as a dimer $\mathbf{C_2}$. This intermediate may be expected to thermally *decompose* to Pd black and **D** (the decomposition of aryl phosphine Pd(II) complexes to give phosphonium salts analoguous to **D** has been studied in detail by Grushin[113]). Importantly, **D** was identified by ESI/MS in reaction mixtures (see section **4.4.1**).
- The central step to the whole sequence is the *transmetalation* between **C** and **1b**, yielding 3-coordinate Pd(II) aryl NHC complex **E** and **8a**. The possible mechanisms for this reaction are discussed in the following.
- Finally, *reductive elimination* of $\mathbf{PI^+}$ from **E** would regenerate the monoligated Pd(0) species. This step is likely to be retarded by coordinating solvents such as nitriles, as the resulting 4-coordinate Pd(II) intermediate would be more stable than **E**. It is also likely that the transmetalation step would be retarded for the same reasons, and this would explain why the reaction of **1b** with *p*-iodonitrobenzene is faster in d_6-acetone than in d_3-MeCN, as one of these steps is likely to be the rate determining one.

Importantly, this mechanism is not invalidated by the kinetic data as the observed initiation phase is consistent with the activation step of the mechanism in ***Figure 7***.

The exact nature of the transmetalation step is obviously very difficult to predict with the existing experimental evidence. At the time of writing, DFT calculations were being conducted by D. J. Willock at Cardiff University. It is hoped that this computational work will yield results that will help clarify the mechanism of this step. There are two different pathways for this step: aryl/allyl exchange, and NHC/halide exchange. Two possible transition states corresponding to these scenarios are shown in ***Figure 8***:

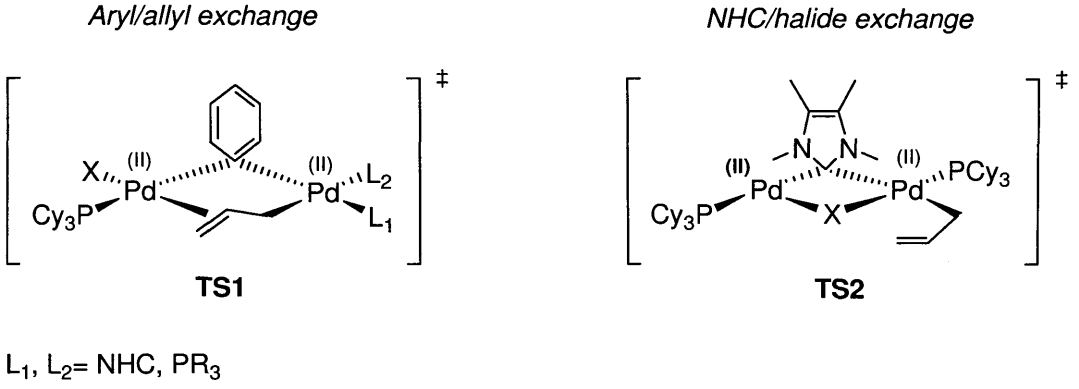

Figure 8: *possible transition states for the transmetalation step*

Obviously, the implications of **TS1** and **TS2** are very important:

If transmetalation involves the NHC and the halide ligands (**TS2**), this would be the first example of NHC transfer between two Pd complexes. However, such a process is less likely than aryl/allyl exchange, because the reaction was found to proceed much faster with the I(III) arylating agent **45** than with aryl iodides. The absence of halide in **TS2** would probably be destabilising, and thus retard, not accelerate the reaction.[114] Moreover the examples of ligand exchanges in Pd(II) NHC complexes discussed in section **4.1.3.2.2** are not thought to involve the NHC.[97]

A mechanism involving aryl/allyl exchange as in **TS1** appears somewhat more likely. Firstly, the ability of the allyl ligand to switch to η_1-bonding mode is expected to help bring the two Pd complexes close to each other (**TS2** also shows a σ-bound allyl, but it is possible to imagine a

5-coordinate Pd atom with a π-bound allyl). Secondly, the inhibiting effect of d_3-MeCN compared to d_6-acetone would be explained by this structure, as it requires a free coordination site on **C**.

4.2.3.3.3 Further studies validating a ligand transfer mechanism

The mechanism shown in ***Figure 7*** involves intermediates which, if introduced independently into the reaction mixture, should promote the reaction. Thus, an example of compound $\mathbf{C_2}$ was prepared according to ***Scheme 27***:

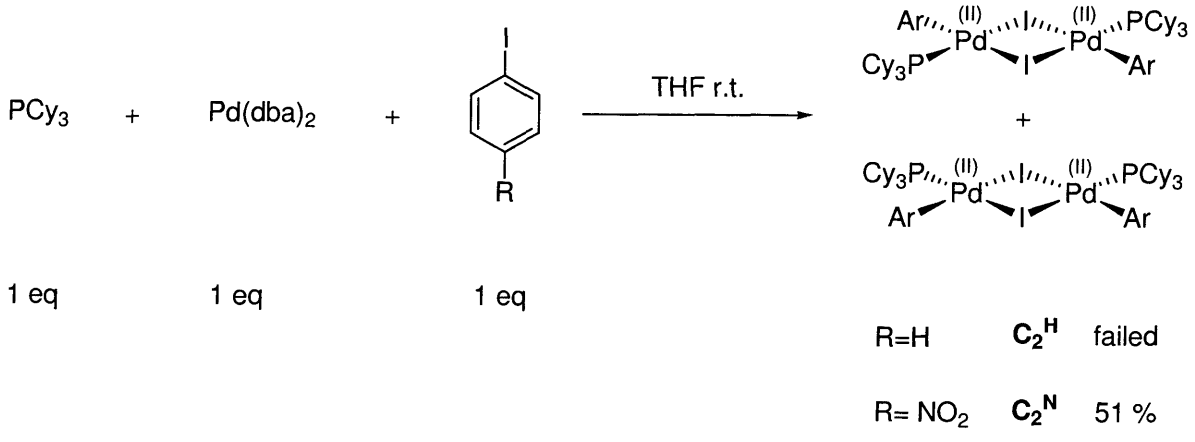

Scheme 27: *synthesis of dimeric Pd(II) compound* C_2^N

Complex $\mathbf{C_2^N}$ was conveniently prepared in moderate yield from $Pd(dba)_2$ as an air-stable solid. It was isolated as a 1:2.6 mixture of the *cis* and *trans* isomers.[115] Its analogue $\mathbf{C_2^H}$ could not be purified despite repeated attempts.

The reaction of **1b** with *p*-iodonitrobenzene in the presence of 5 % of $\mathbf{C_2^N}$ in d_2-DCM was monitored by ^{1}H NMR spectroscopy. The kinetic plot of this reaction (compared to the plot without $\mathbf{C_2^N}$) is shown in ***Graph 2:***

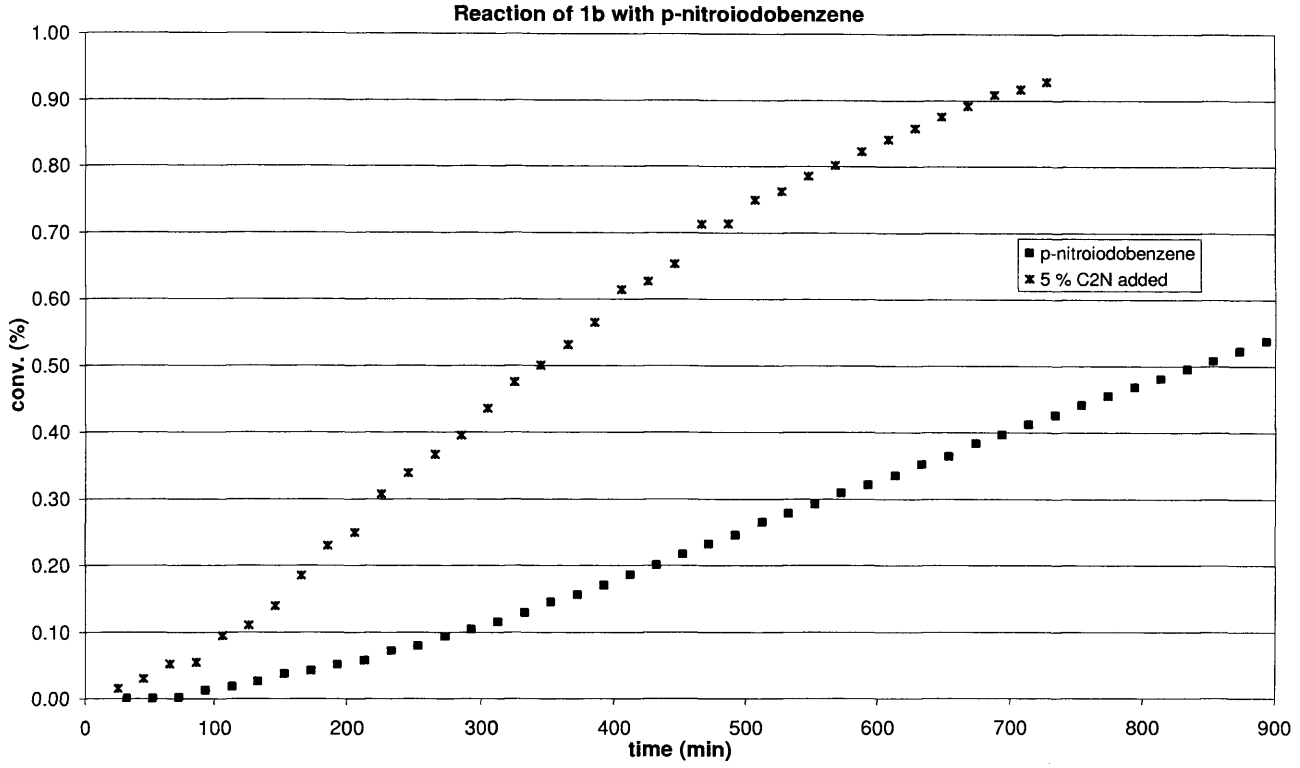

Graph 2: *kinetic plot of the reaction of* ***1b*** *with p-iodonitrobenzene with and without* C_2^N

This plot clearly shows the accelerating effect of the addition of C_2^N on the reaction rate. The value of the extracted rate constant k' at high conversion ($6.5\ 10^{-3} mol^{-1}.s^{-1}$) is more than 5 times higher than that of the reaction without C_2^N. From this plot it can be concluded that C_2^N acts as a reservoir of active species for the reaction. It is very likely (although not totally certain) that this species is C^N.

Interestingly, the plot of the reaction in the presence of C_2^N is still S-shaped. This could be due to the low solubility of C_2^N in d_2-DCM, causing a gradual increase over time of the concentration of the active species C^N.

To verify that the accelerating effect of C_2^N is actually due to the release of a catalytically active intermediate, two stoichiometric control experiments were run with C_2^N on the one hand, and **46** on the other. Similar complexes to **46** and C_2^N have been shown by Grushin to decompose to

phosphonium salts.[113] If, for example, phosphonium salt **D** had an active role in the reaction, the reaction of **1b** with **46** should be possible.

Compound **46** was prepared using a similar procedure to that used for the synthesis of $\mathbf{C_2^N}$ (2 eq of PCy_3 were used for **46**). Then, 1 eq of **1b** was reacted with 1 eq of either $\mathbf{C_2^N}$ or **46** in d_2-DCM (***Scheme 28***):

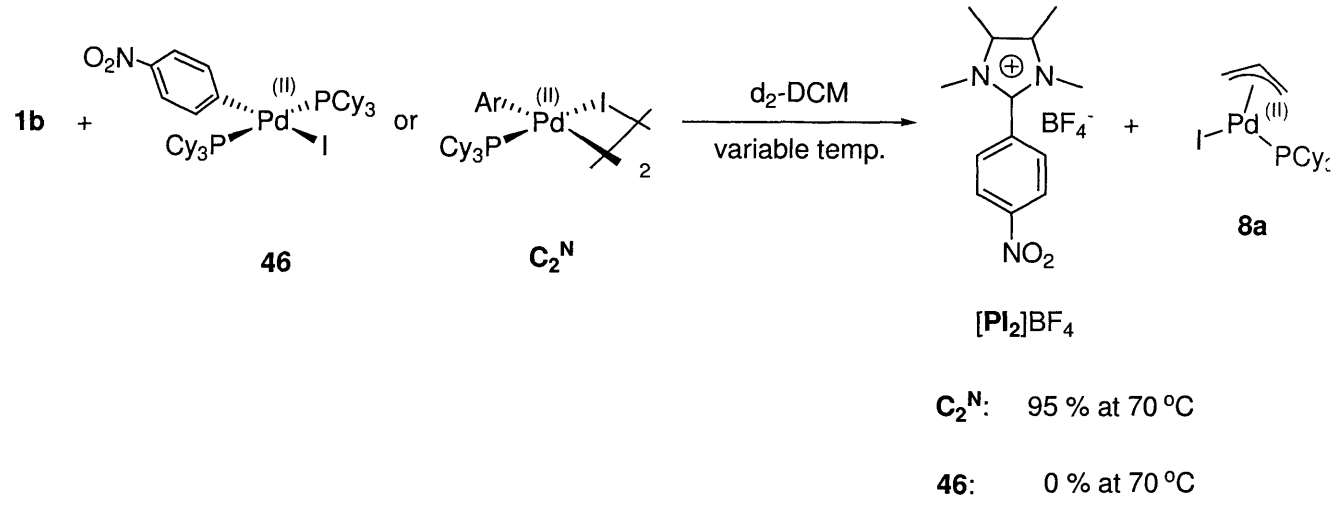

Scheme 28: *stoichiometric reaction of* ***1b*** *with Pd(II) aryl complexes*

Whilst the reaction of **1b** with $\mathbf{C_2^N}$ started at 40 °C (the reaction of **1b** with *p*-iodonitrobenzene was found to start around 60 °C) and was almost complete after 16 hours at 70 °C (see appendix 5 for ^1H and ^{31}P NMR spectra),[116] no reaction was observed with **46** in the 40-70 °C temperature range. Thus, it would seem that $\mathbf{C_2^N}$ is effectively acting as a reservoir of active species, unlike **46** in which extra phosphine totally inhibits the reaction.

Finally, compound **47** was synthesised to model the reductive elimination behaviour of **E**. This compound is conveniently prepared in moderate yield from $\mathbf{C_2^N}$ and carbene transfer agent **48** (***Scheme 29***):

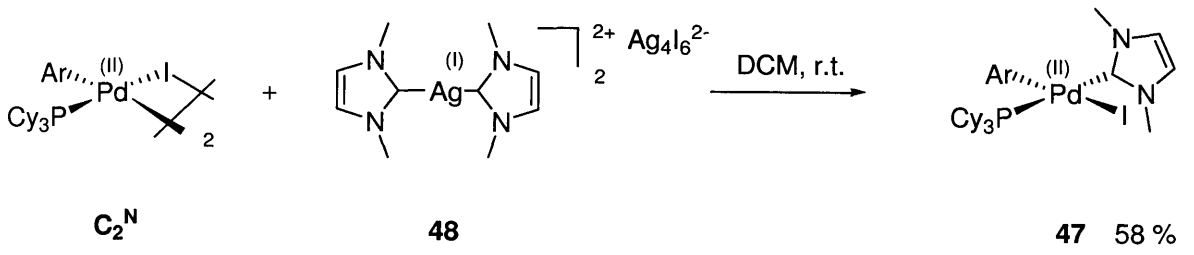

C_2^N **48** **47** 58 %

Scheme 29: *synthesis of* ***47****, a model for intermediate* ***E***

Compound **47** was found to be variably stable. At room temperature, it decomposes to $\mathbf{PI_1}^+$ over weeks (identified by ^{1}H NMR spectroscopy and ESI/MS). However when mixed with an excess of $AgBF_4$ in d_3-MeCN (in an attempt to generate **49**), it immediately decomposes to several products including $\mathbf{PI_2}^+$ and nitrophenyltricyclohexyphosphonium (both identified by ESI/MS, see appendix 5). The use of Ag^+ to promote the decomposition probably causes NHC and phosphine scrambling between Ag(I) and Pd(II), thus complicating the analysis of the reaction mixture. However this experiment demonstrates that compounds very similar to **E** do decompose to $\mathbf{PI_2}^+$, and that this decomposition is much faster for coordinatively unsaturated compounds (***Scheme 30***):

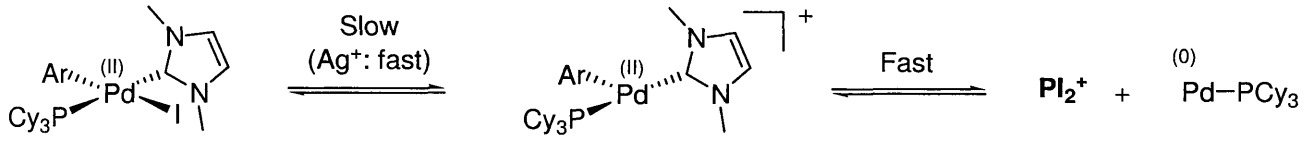

47 *weeks* **49** *seconds*

Scheme 30: *decomposition of* ***47***

It is worth noting that **47** and related compounds could provide a useful entry into catalytic cycles by decomposing to monoligated Pd(0).

4.2.3.4 Towards the direct arylation of imidazolium salts

One of the features of the arylation of NHCs described in section **4.4.3** is that it is both catalytic and stoichiometric in Pd. If one could regenerate the Pd (II) NHC starting material (such as **1b**) from the Pd(II) halo product (such as **8a**), one would obtain a fully catalytic reaction. An obvious way of tackling this problem would be to use an imidazolium salt and a base, as shown in ***Scheme 31***:

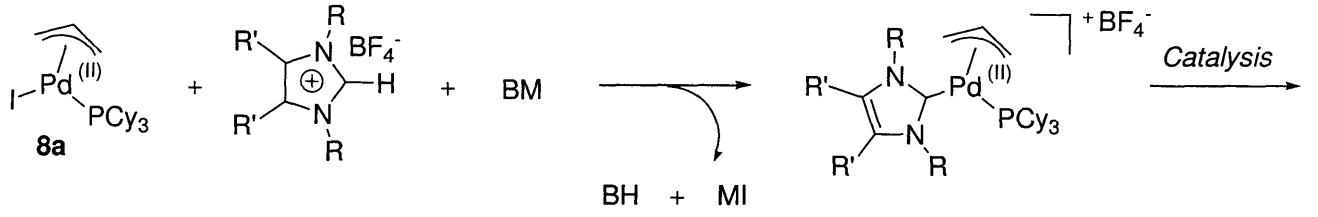

Scheme 31: *regeneration of Pd(II) NHC starting material from* ***8a***

If this strategy proved successful, the direct arylation of imidazolium salts would be achieved, as shown in ***Scheme 32***:

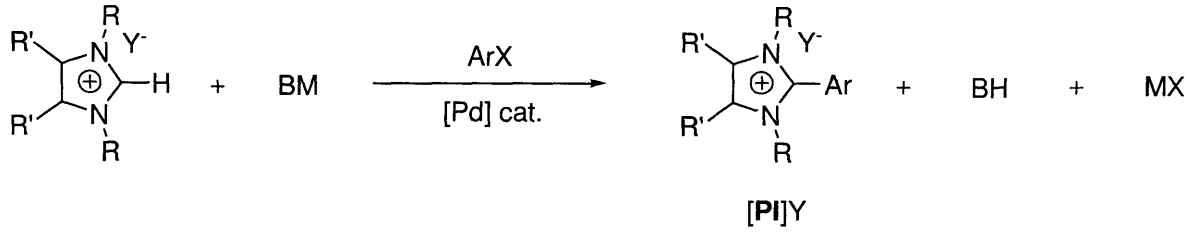

Scheme 32: *Pd-catalysed arylation of imidazolium salts*

Obviously, this reaction would be of great interest, as 2-arylimidazolium salts [**PI**]Y are interesting targets, for example as precursors for "abnormal" NHC complexes.[117] It has been shown in section **4.1.2** how direct C-H functionalisation is an advantageous methodology.

Unfortunately, attempts at using combinations of base and imidazolium salts failed to give any appreciable amounts of 2-arylimidazolium products. These attempts are summarised in ***Table 5***:

Table 5: *attempted direct arylation of imidazolium salts*[a]

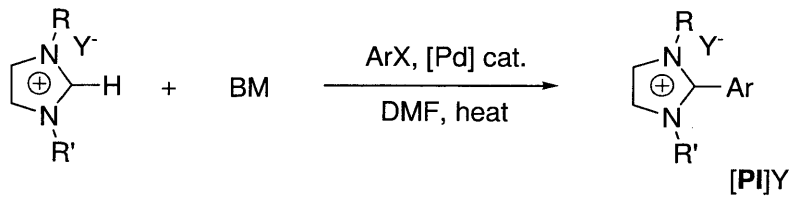

R= Me R'=Me Y^-= I^- [dmim]I

R= Me R'=Pr Y^-= BF_4^- [pmim]BF_4

Entry	Salt	Base	ArX
1	[dmim]I	Cs_2CO_3	PhI
2	[dmim]I	Cs_2CO_3	*p*-$C_6H_4(COCH_3)Br$
3	[dmim]I	Cs_2CO_3	PhBr
4	[dmim]I	Cs_2CO_3	PhCl
5	[pmim]BF_4	Cs_2CO_3	**45** ($[(C_6H_5)_2I]BF_4$)
6	[pmim]BF_4	Cs_2CO_3	*p*-$C_6H_4(NO_2)I$
7	**48** ([dmim]I + Ag_2O)[b]		*p*-$C_6H_4(NO_2)I$

[a]Reagents and conditions : imidazolium salt (0.16 mmol), base (entries 1-6: 3 eq), **1b** (10 mol%), ArX (1.2 eq), DMF (entries 1-4: 3 mL, entries 5-7: 2 mL), 80 °C, 24 hours. [b]: 1 eq of **48** (prepared separately, 0.08 mmol) was used.

Using **1b** as a catalyst and a variety of aryl electrophiles, no [**PI**]Y product was identified by ^1H NMR spectroscopy. ESI/MS analysis of the crude reaction mixtures only revealed traces of product.

The use of carbene transfer agent **48** also proved unsuccessful, indicating that this reagent probably does not transfer dmiy to the Pd(II) iodo product **8a**. This is not unexpected considering the stoichiometric reaction of **48** with $\mathbf{C_2}^N$ (see ***Scheme 29***). Indeed, assuming intermediate **C** is

produced (following activation of **1b** and oxidative addition of the aryl iodide, see ***Figure 7***), the carbene transfer agent probably reacts to yield **47**, which is too stable to react further (***Scheme 33***):

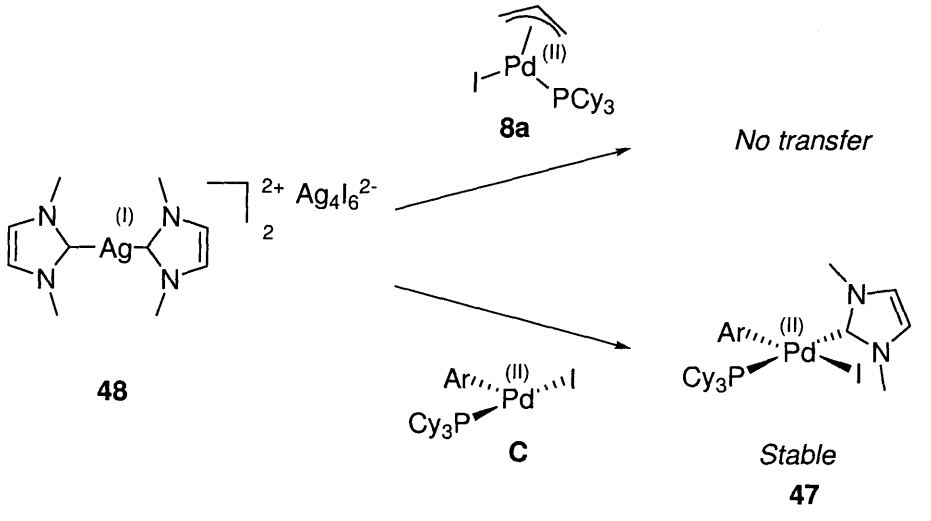

Scheme 33: *in situ NHC transfer to Pd(II) under reaction conditions*

The enhanced reactivity of **C** compared to **8a** is a major obstacle to the successful catalytic arylation of imidazolium salts. However, it has been shown that the loss of the iodide ligand in **47** caused rapid decomposition of this compound. Therefore, if one could generate **49** by transferring an NHC to a Pd(II) aryl complex in the absence of halide, this problem would be solved. The use of an I(III) arylating reagent such as **45** in combination with a source of NHC (such as an imidazolium salt and a base, or a carbene transfer agent such as **48**) and a source of Pd(0) such as $Pd(dba)_2$ (with or without additional ligand) might give the expected 2-aylimidazolium product (***Scheme 34***):

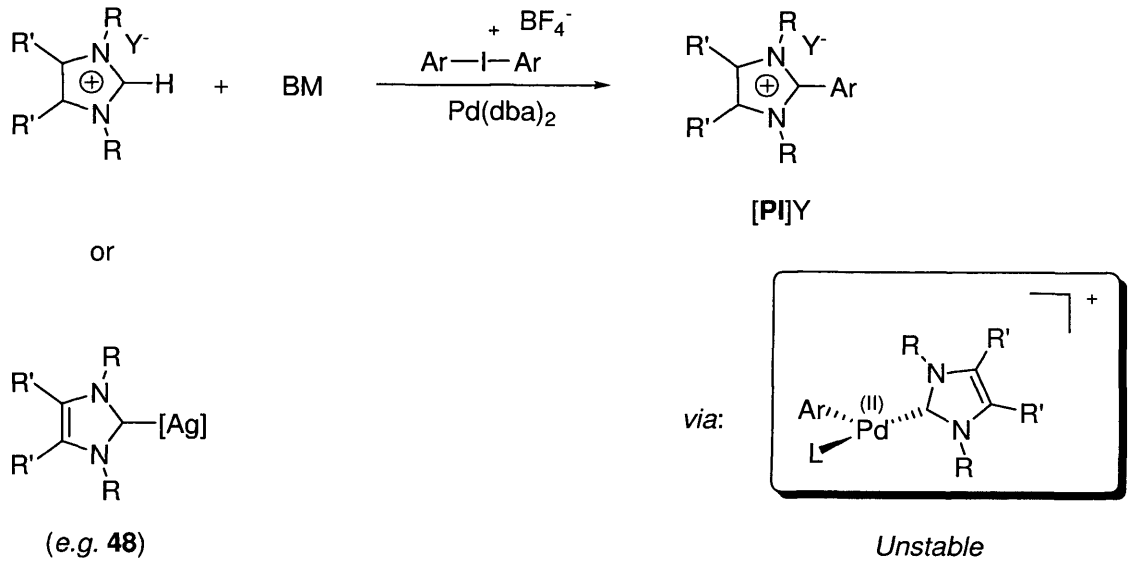

Scheme 34: *alternative reaction scheme for the direct arylation of imidazolium salts*

Thus, **48** was reacted with **45** in the presence of 5 mol% of $Pd(dba)_2$. The reaction was conducted with or without additional phosphine (PPh_3 or PCy_3, 1 eq), and a control experiment was run without Pd (***Scheme 35***):

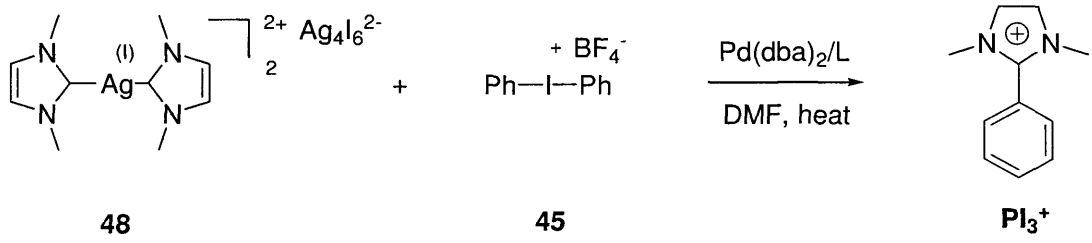

Scheme 35: *attempted arylation of **48** with **45***

Whilst the reaction without Pd did not show any evidence for the formation of $\mathbf{PI_3^+}$ (by ^1H NMR spectroscopy or ESI/MS), the reaction in the presence of $Pd(dba)_2$ showed significant amounts of this product by ESI/MS, although the ^1H NMR spectra were very messy (see appendix 5 for ESI/MS spectra). This is an encouraging result and indicates that this strategy might be successful.

4.3 Conclusion

The catalytic activity of $[Pd(\eta^3\text{-}C_3H_5)(tmiy)(PCy_3)]BF_4$ (**1b**) in the alkenylation of azolium salts was explored and it was found that this compound was an efficient catalyst. There is strong evidence that the activation mechanism of **1b** is reductive elimination to yield a monoligated Pd(0) intermediate, as expected from the structure of this complex.

The reaction of **1b** with electrophiles gave unexpected results, *i.e.* the Pd-mediated arylation of the NHC on **1b**. The mechanism of this reaction was investigated in detail and it appears that this process does not proceed *via* a Pd(II)/Pd(IV) sequence nor σ-bond metathesis, but that it probably involves ligand transfer between two Pd(II) centres.

The scope of this reaction was also investigated and it was found that it is not limited to aryl iodides, and that aryl bromides and I(III) arylating reagents could be used as well. This reaction is stoichiometric in Pd, but the Pd-containing product is a Pd(II) compound; therefore its recycling is in theory possible. However, attempts at developing a direct arylation procedure for imidazolium salts failed, although the results obtained indicate that this goal might be reached in a not-so-distant future.

4.4 Experimental Section

4.4.1 General procedures

All manipulations involving air sensitive compounds were performed under argon atmosphere, using standard Schlenk line techniques or in a nitrogen atmosphere MBRAUN UNILAB glovebox with less than 1 ppm water and O_2. Solvents were dried using appropriate drying agents (CaH_2 for CH_2Cl_2, sodium/benzophenone for THF, Et_2O and hexane). DMF was purchased from Aldrich and stored in a Young's Schlenk tube over 4 Å molecular sieves. Ethylene (research grade) was purchased from BOC gases. NMR spectra were recorded at 298 K on a Bruker Avance 500 MHz with a multinuclear gradient probe. Chemical shift values are given relative to residual solvent peak, *i.e.* 5.23 ppm for ^1H NMR and 54.00 ppm for ^{13}C NMR in CD_2Cl_2. ^{31}P chemical shifts are given relative to H_3PO_4 (capillary tube filled with an aqueous solution of H_3PO_4 in CD_2Cl_2). NOESY spectra were recorded in degassed CD_2Cl_2 with a gradient duration of 300 ms. ESI/MS were perfomed on a WATERS LCT Premier XE instrument, with a source temperature of 80 °C, a desolvation temperature of 200 °C, a capillary voltage of 3500 V and a cone voltage of 100 V. Microanalyses were performed by Warwick Analytical Services.

4.4.2 Procedures for the catalytic activity and reactivity of 1b

4.4.2.1 Procedure for the Pd-catalysed coupling of ethylene and [pmim]Br

A 60 mL Young's Schlenk tube was charged with the Pd catalyst (0.037 mmol, 5 mol%), or $Pd(dba)_2$ (0.037 mmol, 5 mol%) and PCy_3 (0.040 mmol, 5.5 mol%), and the substrate (0.73 mmol, 1 eq) in a glove box. DMF was then syringed under a flow of ethylene into the reaction vessel and the orange/yellow solution was heated to 80 °C. The vessel was then pressurised with 1 bar of ethylene and closed. The solution was stirred for 24 hours. The solvent was then removed *in vacuo* and the residue dissolved in d_6-DMSO and submitted for ^1H NMR spectroscopy.

4.4.2.2 Procedure for the studies of the activation of 1b

1b (10 mg, 0.016 mmol) was dissolved in 1 mL DMF. The appropriate reagent was added (phenyl iodide or 1-propyl-3-methylimidazolium bromide, 2 eq) and the reaction mixture was heated to 80 °C under Ar or ethylene (1 bar). After 5 hours, the solvent was removed *in vacuo* and the crude reaction mixture was analysed by ^{1}H and ^{31}P NMR spectroscopy and ESI/MS.

4.4.2.3 Procedure for the scope study

Accurately weighed (to 1 mg) amounts of Pd complex (for **1b** 10mg, 0.016 mmol) and electrophile (generally 2 eq, 0.032 mmol) were placed into a Young's NMR tube. Then, CD_2Cl_2 (650 μL) was injected, and the tube was heated to the indicated temperature (generally 70 °C) in an oil bath. The samples were submitted for ^{1}H and ^{31}P NMR spectroscopy and ESI/MS without further treatment.

4.4.2.4 Procedure for the kinetic study

All manipulations were carried out in air. Accurately weighed (to 0.01 mg) amounts of **1b** (about 12.78 mg, 0.02000 mmol), aryl iodide (5 eq, 0.1000 mmol) and *p*-xylene (3.00 μL, 1.5 eq, 0.300 mmol) were placed into a Young's NMR tube. When $\mathbf{C_2^N}$ was used, 1.34 mg (0.00105 mmol, 5.3 mol%) was introduced in the tube. Then, deuterated solvent (650 μl) was injected, and the tube was sealed and stored at -18 °C for 36 hr (typically, the samples were prepared on Friday afternoons and run on Sunday mornings). The tube was then placed in a Bruker Avance 500 MHz spectrometer thermostatted at 343 K. Spectra were recorded at 20 min intervals using 4 scans with a 30 ° pulse, an acquisition delay of 6.55 s and a d_1 delay of 1.00 s. Disappearance of the starting material was measured by comparing integration of the methyl groups on *p*-xylene (the reference) to that of the methyl groups on tmiy in **1b**.

4.4.2.5 Procedure for the stoichiometric reaction of 1b with C_2^N and 46

Accurately weighed (to 1 mg) amounts of **1b** (10mg, 0.016 mmol) and Pd(II) aryl complex (1 eq, 0.016 mmol) were placed into a Young's NMR tube. Then, d_2-DCM (650 μL) was injected, and the tube was heated in an oil bath to 40 °C for 3 hours, then to 70 °C for 16 hours. Samples were submitted for ^1H and ^{31}P NMR spectroscopy and ESI/MS after each temperature plateau.

4.4.2.6 Procedure for the attempted direct arylation of NHCs catalysed by 1b

A vessel was charged with an imidazolium salt (0.73 mmol, 1 eq), Cs_2CO_3 (2.2 mmol, 3 eq) and **1b** (0.073 mmol, 10 mol%). Alternatively, carbene transfer agent **48** (0.37 mmol, 0.5 eq) was used with 10 mol% of **1b**. DMF was added (2 to 3 mL), and the aryl electrophile was syringed or added in one portion (0.87 mmol, 1.2 eq). The reaction mixture was heated to 80 °C for 24 hours. The solvent was removed *in vacuo* and the crude reaction mixture was submitted for ^1H NMR spectroscopy and ESI/MS.

4.4.2.7 Procedure for the attempted arylation of Ag-bound dmiy catalysed by $Pd(dba)_2$

A vessel was charged with carbene transfer agent **48** (0.56 mmol, 1eq), I(III) arylating agent **45** (0.56 mmol, 1 eq), $Pd(dba)_2$ (0.028 mmol, 5 mol%) and a phosphine (PCy_3 or PPh_3, 0.028 mmol, 5 mol%). DMF (5 mL) was added and the reaction mixture was heated to 95 °C for 24 hours. The solvent was removed *in vacuo* and the crude reaction mixture was submitted for ^1H NMR spectroscopy and ESI/MS.

4.4.3 Synthesis of phosphine aryl Pd(II) complexes

4.4.3.1 Synthesis of *cis* and *trans* *bis*(iodo-4-nitrophenyl-(tricyclohexylphosphine)palladium (II)) C_2^N

trans

cis

C_2^N

Tricyclohexylphosphine (421 mg, 1.5 mmol, 1 eq) and $Pd(dba)_2$ (863 mg, 1.5 mmol, 1 eq) were dissolved in 16 mL of THF and stirred under argon at room temperature for 5 min. 4-nitro-iodobenzene (374 mg, 1.5 mmol, 1 eq) was added in one portion and the reaction mixture was stirred for 1 hr. A pale brick-red precipitate gradually appeared. The suspension was filtered in air, rinsed with THF, acetone and Et_2O. The collected mass was 504 mg (51%) and the batch number was AN/562/A. This compound was found to be a 1:2.6 mixture of *cis* and *trans* isomers in $CDCl_3$ at 298 K.

^1H NMR ($CDCl_3$, 500.13 MHz): δ (ppm) 7.83 (d, 2H, *meta* aromatic CH, major isomer, $^3J_{HH}$= 8.6 Hz), 7.76 (d, 2H, *meta* aromatic CH, minor isomer, $^3J_{HH}$= 8.7 Hz), 7.70 (d, 2H, *ortho* aromatic CH, major isomer, overlapping with minor isomer *ortho* CH , $^3J_{HH}$= 8.6 Hz), 7.68 (d, 2H, *ortho* aromatic CH, minor isomer, overlapping with major isomer *ortho* CH), 1.87-1.97 (m, 6H, PCy_3 CH_2), 1.73-1.84 (m, 9H, overlapped PCy_3 CH and CH_2), 1.67-1.72 (m, 6H, PCy_3 CH_2), 1.20-1.32 (m, 6H, PCy_3 CH_2), 0.93-1.07 (m, 6H, PCy_3 CH_2).

^{13}C NMR ($CDCl_3$, 125.03 MHz): δ (ppm) 169.60 (s, PdC), 144.38 (s, CNO_2), 137.06 (s, *ortho* CH, major isomer), 136.78 (s, *ortho* CH, minor isomer), 120.81 (s, *meta* CH, minor isomer), 120.65 (s, *meta* CH, major isomer), 35.56 (d, PCH, major isomer, $^1J_{PC}$= 22.9 Hz), 35.14 (d, PCH, minor isomer, $^1J_{PC}$= 22.9 Hz), 30.11 (s, cyclohexyl CH_2), 27.41 (d, cyclohexyl CH_2, $^3J_{PC}$= 11.0 Hz), 26.16 (s,

cyclohexyl CH_2). Signals were attributed on the basis of gs-NOESY and gs-HSQC experiments (appendix 3).

$^{31}P\{^1H\}$ NMR ($CDCl_3$, 202.46 MHz, 298 K): δ (ppm) 34.23 (s, major isomer), 31.43 (s, minor isomer).

Anal calcd. For $C_{48}H_{74}N_2O_4P_2Pd_2I_2$ (MW= 1271.71): C, 45.33; H, 5.87; N, 2.20; P, 4.87. Found: C, 45.06; H, 5.87; N, 2.11; P, 4.89.

No X-ray data were obtained.

4.4.3.2 Synthesis of *trans* iodo-4-nitrophenyl(tricyclohexylphosphine) dimethylimidazol-2-ylidenepalladium (II) 47

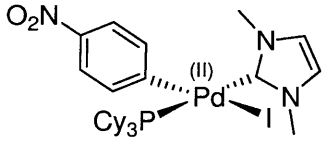

47

Bis(iodo-4-nitrophenyl(tricyclohexylphosphine)palladium(II)) (220 mg, 0.173 mmol, 1 eq) and the silver carbene transfer agent di(*bis*(dimethylimidazol-2-ylidenesilver(I)) hexaiodotetraargentate (155 mg, 0.173 mmol, 1eq) were strirred at room temperature in DCM under argon. The reaction mixture gradually faded from bright red to pale yellow. The solution was filtered through Celite®, evaporated, and the residue was triturated with Et_2O to afford a pale yellow powder. The collected mass was 147 mg (58 %) and the batch number was AN/533/B.

^1H NMR (CD_2Cl_2, 500.13 MHz): δ (ppm) 7.64 (dt, 2H, *meta* aromatic CH, $^3J_{HH}$= 8.7 Hz, $^5J_{PH}$= 1.9 Hz), 7.54 (dt, 2H, *meta* aromatic CH, $^3J_{HH}$= 8.7 Hz, $^4J_{PH}$= 2.1 Hz), 6.70 (s, 1H, dmiy CH), 6.68 (s, 1H, dmiy CH), 3.82 (s, 6H, dmiy CH_3), 1.80-1.87 (m, 9H, PCy_3 CH overlapping with PCy_3 CH_2), 1.61-1.69 (m, 6H, PCy_3 CH_2), 1.47-1.60 (m, 9H, two overlapping PCy_3 CH_2), 1.08-1.22 (m, 3H, PCy_3 CH_2), 0.88-1.01 (m, 6H, PCy_3 CH_2).

^{13}C NMR ($CDCl_3$, 125.03 MHz): δ (ppm) 176.23 (s, dmiy PdC), 175.07 (m, $PhNO_2$ PdC), 144.37 (s, $PhNO_2$ CNO_2), 137.43 (d, $PhNO_2$ *ortho* CH, $^3J_{PC}$= 2.3 Hz), 122.37 (s, dmiy CH), 122.34 (s, dmiy CH), 120.46 (s, $PhNO_2$ meta CH), 38.00 (s, NCH_3), 34.89 (d, PCy_3 CH, $^1J_{PC}$= 19.2 Hz), 30.77 (s, PCy_3 CH_2), 28.08 (d, PCy_3 CH_2, J_{PC}= 10.5 Hz), 27.01 (d, PCy_3 CH_2, J_{PC}= 1.4 Hz).

$^{31}P\{^1H\}$ NMR (CD_2Cl_2, 202.46 MHz, 298 K): δ (ppm) 30.39

High resolution ESI_{pos}-MS (MeCN): $[M-I]^+$ found 604.2291 (calc. 604.2287, dev: 1.2 ppm)

This compound slowly decomposes at room temperature, precluding the use of elemental analysis to determine its purity. Despite repeated attempts, it was not possible to grow crystals suitable for X-ray diffraction, but gs-HSQC and gs-NOESY experiments (see appendix 3) indicated the *trans* geometry.

4.4.3.3 Synthesis of *trans* iodo-4-nitrophenyl *bis*(tricyclohexylphosphine)palladium(II) 46

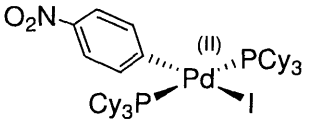

46

Tricyclohexylphosphine (281 mg, 1 mmol, 1 eq) and $Pd(dba)_2$ (288 mg, 0.5 mmol, 0.5 eq) were stirred in THF under argon at room temperature. After 5 min, 4-iodo-nitrobenzene (128 mg, 0.51 mmol, 0.51 eq) was added in one portion to the clear orange-red solution. The reaction mixture turned golden brown within 1 min, and was left stirring at room temperature for 30 min. The solution was then evaporated to dryness, and the residue was triturated with acetone, to wash the remaining dibenzylideneacetone. The resulting powder was dissolved in DCM, filtered through Celite®, and evaporated. The residue was triturated with Et_2O to afford a pale beige powder. The collected mass was 246 mg (54 %) and the batch number was AN/577/A

^{1}H NMR (CD_2Cl_2, 500.13 MHz): δ (ppm) 7.72 (d, 2H, *ortho* aromatic CH, $^{3}J_{HH}$= 8.6 Hz), 7.60 (d, 2H, *meta* aromatic CH, $^{3}J_{HH}$= 8.6 Hz), 1.96-2.10 (bs, 3H, PCy_3 CH), 1.79 (d, 6H, PCy_3 CH_2, $^{3}J_{HH}$= 11.7 Hz), 1.63 (d, 6H, PCy_3 CH_2, $^{3}J_{HH}$= 12.4 Hz), 1.51 (m, 9H, PCy_3 CH_2), 1.04-1.14 (m, 3H, PCy_3 CH_2), 0.86-1.01 (m, 6H, PCy_3 CH_2).

^{13}C NMR (CD_2Cl_2, 125.03 MHz): δ (ppm) 174.64 (bs, PdC), 143.85 (s, CNO_2), 138.12 (m, *ortho* CH), 120.04 (s, *meta* CH), 35.18 (m, PCy_3 CH), 30.28 (s, PCy_3 CH_2), 27.55 (m, PCy_3 CH_2), 26.41 (s, PCy_3 CH_2).

^{31}P{^{1}H} NMR (CD_2Cl_2, 202.46 MHz, 298 K): δ (ppm) 19.74.

Anal calcd. For $C_{42}H_{70}NO_2P_2PdI$ (MW= 916.28): C, 55.05; H, 7.70; N, 1.53. Found: C, 55.04; H, 7.76; N, 1.51.

No X-ray data were obtained.

4.5 Bibliography and notes

1. Fairlamb, I. J. S., *Tetrahedron* **2005,** 61, 9661-9662.
2. K. C. Nicolaou, P. G. B. D. S., *Angew. Chem. Int. Ed.* **2005,** 44, 4442-4489.
3. Mizoroki, T.; Mori, K.; Ozaki, A., *Bull. Chem. Soc. Jap* **1971,** 44, 581.
4. Heck, R. F.; Nolley, J. P., *J. Org. Chem.* **1972,** 37, 2320-2322.
5. Beletskaya, I. P.; Cheprakov, A. V., *Chem. Rev.* **2000,** 100, 3009-3066.
6. Farina, V., *Adv. Synth. Cat.* **2004,** 346, 1519-1521.
7. Davis, M. F.; Clarke, M.; Levason, W.; Reid, G.; Webster, M., *Eur. J. Inorg. Chem.* **2006,** 2773-2782.
8. Suzuki, A., *Chem. Commun.* **2005,** 4759-4763.
9. Chinchilla, R.; Najera, C., *Chem. Rev.* **2007,** 874-922.
10. Guram, A. S.; Rennels, R. A.; Buchwald, S. L., *Angew. Chem. Int. Ed.* **1995,** 34, 1348-1350.
11. Louie, J.; Hartwig, J. F., *Tetrahedron Lett.* **1995,** 36, 3609-3612.
12. Anderson, K. W.; Tundel, R. E.; Ikawa, T.; Altman, R. A.; Buchwald, S. L., *Angew. Chem. Int. Ed.* **2006,** 45, 6523-6527.
13. Heaton, B., *Mechanisms in homogeneous catalysis.* 1st ed.; Wiley-VCH: Weinheim, 2005.
14. Amatore, C.; Genin, E.; Jutand, A.; Mensah, L., *Organometallics* **2007,** 26, 1875-1880.
15. Amatore, C.; Jutand, A., *J. Organomet. Chem.* **1999,** 576, 254-278.
16. Amatore, C.; Jutand, A.; Khalil, F.; M'Barki, M. A.; Mottier, L., *Organometallics* **1993,** 12, 3168-3178.
17. Brown, J. M., *J. Organomet. Chem.* **2004,** 689, 4006-4015.
18. Cantat, T.; Agenet, N.; Jutand, A.; Pleixats, R.; Moreno-Mañas, M., *Eur. J. Org. Chem.* **2005,** 4277-4286.
19. Knowles, J. P.; Whiting, A., *Org. Biomol. Chem.* **2007,** 5, 31-44.
20. Vicent, C.; Viciano, M.; Mas-Marzá, E.; Sanaú, M.; Peris, E., *Organometallics* **2006,** 25, 3713-3720.
21. Lewis, A. K. de K.; Caddick, S.; Cloke, F. G. N.; Billingham, N. C.; Hitchcock, P. B.; Leonard, J., *J. Am. Chem. Soc.* **2003,** 125, 10066-10073.
22. Christmann, U.; Vilar, R., *Angew. Chem. Int. Ed.* **2005,** 44, 366-374.
23. Andraos, J., *Org. Proc. Res. Dev.* **2005,** 9, 404-431.
24. Ahlquist, M.; Norrby, P.-O., *Organometallics* **2007,** 26, 550-553.
25. Kantchev, E. A. B.; O'Brien, C. J.; Organ, M.G., *Angew. Chem. Int. Ed.* **2007,** 46, 2768-2813.
26. by monoligated, one means that there is only one ancillary ligand (phosphine, NHC) per Pd atom. Coordination of a solvent molecule, for example, or halide anions, is still possible. See ref 24.
27. Marion, N.; Díez-González, S.; Nolan, S. P., *Angew. Chem. Int. Ed.* **2007,** 46, 2988-3000.
28. Kackstell, R.; Harkal, S.; Jiao, H.; Spannenberg, A.; Borgmann, C.; Röttger, D.; Nierlich, F.; Elliot, M.; Niven, S.; Cavell, K. J.; Navarro, O.; Viciu, M. S.; Nolan, S. P.; Beller, M., *Chem. Eur. J.* **2004,** 10, 4661-4670.
29. Navarro, O.; Kelly, R. A.; Nolan, S. P., *J. Am. Chem. Soc.* **2003,** 125, 16194-16195.
30. Viciu, M. S.; Germaneau, R. F.; Navarro-Fernandez, O.; Stevens, E. D.; Nolan, S. P., *Organometallics* **2002,** 21, 5470-5472.
31. Andreu, M. G.; Zapf, A.; Beller, M., *Chem. Commun.* **2000,** 2475-2476.
32. Selvakumar, K.; Zapf, A.; Spannenberg, A.; Beller, M., *Chem.Eur.J.* **2002,** 8, 3901-3906.

33. Frisch, A. C.; Zapf, A.; Briel, O.; Kayser, B.; Shaikh, N.; Beller, M., *Journal of Molecular Catalysis A: Chemical* **2004,** 214, 231-239.
34. Kackstell, R.; Harkal, S.; Jiao, H.; Spannenberg, A.; Borgmann, C.; Röttger, D.; Nierlich, F.; Elliot, M.; Niven, S.; Cavell, K. J.; Navarro, O.; Viciu, M. S.; Nolan, S. P.; Beller, M., *Chem.Eur.J.* **2004,** 10, 3891-3900.
35. Hartwig, J. F.; Paul, F., *J. Am. Chem. Soc.* **1995,** 117, 5373-5374.
36. Braunstein, P.; Matt, D.; Nobel, D., *J. Am. Chem. Soc.* **1988,** 110, 3207-3212.
37. Ahlquist, M.; Fristrup, P.; Tanner, D.; Norrby, P.-O., *Organometallics* **2006,** 25, 2066-2073.
38. Schlummer, B.; Scholz, U., *Adv. Synth. Cat.* **2004,** 346, 1599-1626.
39. Trost, B. M., *Angew. Chem. Int. Ed.* **1995,** 34, 259-281.
40. Dogula, K.; Sames, D., *Science* **2006,** 312, 67-72.
41. Kakiuchi, F.; Murai, S., *Acc. Chem. Res.* **2002,** 35, 826-834.
42. Ritleng, V.; Sirlin, C.; Pfeffer, M., *J. Am. Chem. Soc.* **2002,** 102, 1731-1770.
43. Campeau, L.-C.; Parisien, M.; Jean, A.; Fagnou, K., *J. Am. Chem. Soc.* **2006,** 128, 581-590.
44. Campeau, L.-C.; Rousseaux, S.; Fagnou, K., *J. Am. Chem. Soc.* **2005,** 127, 18020-18021.
45. Bedford, R. B.; Betham, M., *J. Org. Chem.* **2006,** 71, 9403-9410.
46. Parisien, M.; Valette, D.; Fagnou, K., *J. Org. Chem.* **2005,** 70, 7578-7584.
47. Garcia-Cuadrado, D.; Braga, A. A. C.; Maseras, F.; Echavarren, A. M., *J. Am. Chem. Soc.* **2006,** 128, 1066-1067.
48. Garcia-Cuadrado, D.; deMendoza, P.; Braga, A. A. C.; Maseras, F.; Echavarren, A. M., *J. Am. Chem. Soc.* **2007,** 129, 6880-6886.
49. Davies, D. L.; Donald, S. M. A.; Macgregor, S. A., *J. Am. Chem. Soc.* **2005,** 127, 13754-13755.
50. Bellina, F.; Cauteruccio, S.; Rossi, R., *Eur. J. Org. Chem.* **2006,** 1379-1382.
51. Lewis, J. C.; Bergman, R. G.; Ellman, J. A., *J. Am. Chem. Soc.* **2007,** 129, 5332-5333.
52. Wilson, R. M.; Thalji, R. K.; Bergman, R. G.; Ellman, J. A., *Org. Lett.* **2006,** 8, 1745-1747.
53. Wiedemann, S. H.; Lewis, J. C.; Ellman, J. A.; Bergman, R. G., *J. Am. Chem. Soc.* **2006,** 128, 2452-2462.
54. Wiedemann, S. H.; Ellman, J. A.; Bergman, R. G., *J. Org. Chem.* **2006,** 71, 1969-1976.
55. Lewis, J. C.; Wu, J. Y.; Bergman, R. G.; Ellman, J. A., *Angew. Chem. Int. Ed.* **2006,** 45, 1589-1591.
56. Colby, D. A.; Bergman, R. G.; Ellman, J. A., *J. Am. Chem. Soc.* **2006,** 128, 5604-5605.
57. Thalji, R. K.; Ahrendt, K. A.; Bergman, R. G.; Ellman, J. A., *J. Org. Chem.* **2005,** 70, 6775-6781.
58. Wiedemann, S. H.; Bergman, R. G.; Ellman, J. A., *Org. Lett.* **2004,** 6, 1685-1687.
59. Tan, K. L.; Ellman, J. A.; Bergman, R. G., *J. Org. Chem.* **2004,** 69, 7329-7335.
60. Lewis, J. C.; Wiedemann, S. H.; Bergman, R. G.; Ellman, J. A., *Org. Lett.* **2004,** 6, 35-38.
61. Tan, K. L.; Vasudevan, A.; Bergman, R. G.; Ellman, J. A.; Souers, A. J., *Org. Lett.* **2003,** 5, 2131-2134.
62. Tan, K. L.; Bergman, R. G.; Ellman, J. A., *J. Am. Chem. Soc.* **2002,** 124, 3202-3203.
63. Tan, K. L.; Bergman, R. G.; Ellman, J. A., *J. Am. Chem. Soc.* **2002,** 124, 13964-13965.
64. Billingsley, K.; Buchwald, S. L., *J. Am. Chem. Soc.* **2007,** 129, 3358-3366.
65. Navarro, O.; Marion, N.; Mei, J.; Nolan, S. P., *Chem. Eur. J.* **2006,** 12, 5142-5148.
66. Kudo, N.; Perseghini, M.; Fu, G. C., *Angew. Chem. Int. Ed.* **2006,** 45, 1282-1284.
67. Billingsley, K. L.; Anderson, K. W.; Buchwald, S. L., *Angew. Chem. Int. Ed.* **2006,** 45, 3484-3488.
68. Deprez, N. R.; Sanford, M. S., *Inorg. Chem.* **2007,** 46, 1924-1935.
69. Deprez, N. R.; Kalyani, D.; Krause, A.; Sanford, M. S., *J. Am. Chem. Soc.* **2006,** 128, 4972-4973.
70. Wang, X.; Gribkov, D. V.; Sames, D., *J. Org. Chem.* **2007,** 72, 1476-1479.

71. Touré, B. B.; Lane, B. S.; Sames, D., *Org. Lett.* **2006,** 8, 1979-1982.
72. Wang, X.; Lane, B. S.; Sames, D., *J. Am. Chem. Soc.* **2005,** 127, 4996-4997.
73. Sezen, B.; Sames, D., *J. Am. Chem. Soc.* **2005,** 127, 5284-5285.
74. lane, B. S.; Brown, M. A.; Sames, D., *J. Am. Chem. Soc.* **2005,** 127, 8050-8057.
75. Sezen, B.; Sames, D., *J. Am. Chem. Soc.* **2003,** 125, 5274-5275.
76. Sezen, B.; Sames, D., *J. Am. Chem. Soc.* **2003,** 125, 10580-10585.
77. Sezen, B.; Sames, D., *J. Am. Chem. Soc.* **2004,** 126, 13244-13246.
78. Sezen, B.; Sames, D., *Org. Lett.* **2003,** 5, 3607-3610.
79. Bellina, F.; Calandri, C.; Cauteruccio, S.; Rossi, R., *Tetrahedron* **2007,** 63, 1970-1980.
80. Yokooji, A.; Okazawa, T.; Satoh, t.; Miura, M.; Nomura, M., *Tetrahedron* **2003,** 59, 5685-5689.
81. Mori, A.; Sekiguchi, A.; Masui, K.; Shimada, T.; Horie, M.; Osakada, K.; Kawamoto, M.; Ikeda, T., *J. Am. Chem. Soc.* **2003,** 125, 1700-1701.
82. Dick, A. R.; Kampf, J. W.; Sanford, M. S., *J. Am. Chem. Soc.* **2005,** 127, 12790-12791.
83. Canty, A. J., *Acc. Chem. Res.* **1992,** 25, 83-90.
84. Uson, R.; Fornies, J.; Navarro, R. J., *J. Organomet. Chem.* **1975,** 96, 307-309.
85. Byers, P. K.; Canty, A. J.; Skelton, B. W.; White, A. H., *J. Chem. Soc. Chem. Commun.* **1986**, 1722-1723.
86. Guo, R.; Portscheller, J. L.; Day, V. W.; Malinakova, H. C., *Organometallics* **2007,** 26, 3874-3883.
87. Kalyani, D.; Sanford, M. S., *Org. Lett.* **2005,** 7, 4149-4152.
88. Dick, A. R.; Kampf, J. W.; Sanford, M. S., *Organometallics* **2005,** 24, 482-485.
89. Van Leeuwen, P. W. N. M., *Homogeneous catalysis*. Kluwer Academic Publishers: Dortrecht, 2004.
90. Crabtree, R. H., *The organometallic chemistry of the transition metals*. 3rd ed.; Wiley: New York, 2000.
91. Herrmann, W. A.; Brossmer, C.; Öfele, K.; Reisinger, C.-P.; Priermeier, T.; Beller, M.; Fischer, H., *Angew. Chem. Int. Ed.* **1995,** 34, 1844-1848.
92. Beletskaya, I. P.; Cheprakov, A. V., *J. Organomet.Chem.* **2004,** 689, 4055-4082.
93. Ozawa, F.; Fujimori, M.; Yamamoto, T.; Yamamoto, A., *Organometallics* **1986,** 5, 2144-2149.
94. Ozawa, F.; Hidaka, T.; Yamamoto, T.; Yamamoto, A., *J. Organomet. Chem.* **1987,** 330, 253-263.
95. McGuinness, D. S.; Cavell, K. J.; Skelton, B. W.; White, A. H., *Organometallics* **1999,** 18, 1596-1605.
96. Marshall, W. J.; Grushin, V. V., *Organometallics* **2003,** 22, 1591-1593.
97. Magill, A. M.; Yates, B. F.; Cavell, K. J.; Skelton, B. W.; White, A. H., *Dalton Transactions* **2007**, 3398-3406.
98. Dyker, G., *Angew. Chem. Int. Ed.* **1992,** 31, 1023-1025.
99. Cardenas, D. J.; Martin-Matute, B.; Echavarren, A. M., *J. Am. Chem. Soc.* **2006,** 128, 5033-5040.
100. Carturan, G.; Biasiolo, M.; Daniele, S.; Mazzocchin, G. A.; Ugo, P., *Inorg. Chim. Acta* **1986,** 119, 19-24.
101. Galardon, E.; Ramdeehul, S.; Brown, J. M.; Cowley, A.; Hii, K. K.; Jutand, A., *Angew. Chem. Int. Ed.* **2002,** 41, 1760-1763.
102. García-Iglesias, M.; Buñuel, E.; Cárdenas, D. J., *Organometallics* **2006,** 25, 3611-3618.
103. Normand, A. T.; Hawkes, K. J.; Clement, N. D.; Cavell, K. J.; Yates, B. F., *in press, Organometallics*.
104. attempts at preparing **A** independently from tmiy and allyl bromide failed due to a side reaction of tmiy with **A**.

105. Stambuli, J. P.; Incarvito, C. D.; Buhl, M.; Hartwig, J. F., *J. Am. Chem. Soc.* **2004,** 126, 1184-1194.
106. Lousame, M.; Fernández, A.; López-Torres, M.; Vázquez-García, D.; Vila, José M.; Suárez, A.; Ortigueira, Juan M.; Fernández, Jesús J., *Eur. J. Inorg. Chem.* **2000**, 2055-2062.
107. Grim, S. O.; McFarlane, W.; Davidoff, E. F.; Marks, T. J., *J. Phys. Chem.* **1966,** 70, 581-584.
108. Shekhar, S.; Hartwig, J. F., *J. Am. Chem. Soc.* **2004,** 126, 13016-13027.
109. both these compounds are commercially available. Source: 2006-2007 STREM chemicals catalogue.
110. No particular geometry is intended in the Pd(IV) structure in Scheme 25.
111. Milet, A.; Dedieu, A.; Kapteijn, G.; Koten, G. V., *Inorg. Chem.* **1997,** 36, 3223-3231.
112. no particular geometry of **C** or **E** is intended.
113. Grushin, V. V., *Organometallics* **2000,** 19, 1888-1900.
114. oxidative addition is expected to be faster with **45** than with aryl iodides however it is unlikely that this step would be the rate determining one in this case.
115. the major isomer could not be identified.
116. significant decomposition occurred due to the stoichiometric generation of Pd(0).
117. Bacciu, D.; Cavell, K. J.; Fallis, I. A.; Ooi, L.-l., *Angew. Chem. Int. Ed.* **2005,** 44, 5282-5284.

5 Appendices

5.1 Appendix 1: publications from this thesis

A. T. Normand, K. J. Hawkes, N. D. Clement, K. J. Cavell*, Brian F. Yates*, *Organometallics, in press.* "Atom efficient catalytic coupling of imidazolium salts with ethylene involving Ni-NHC complexes as intermediates: a combined experimental and DFT study"

5.2 Appendix 2: ^{1}H NMR spectra of Z and E-1-(2-butenyl)-3-methylimidazolium bromide

3.824
0.491
9.146
3.374
4.487
6.275
0.820
0.739
5.875
41.489
1.216
1.256
18.695
2.314
DMF
DMSO

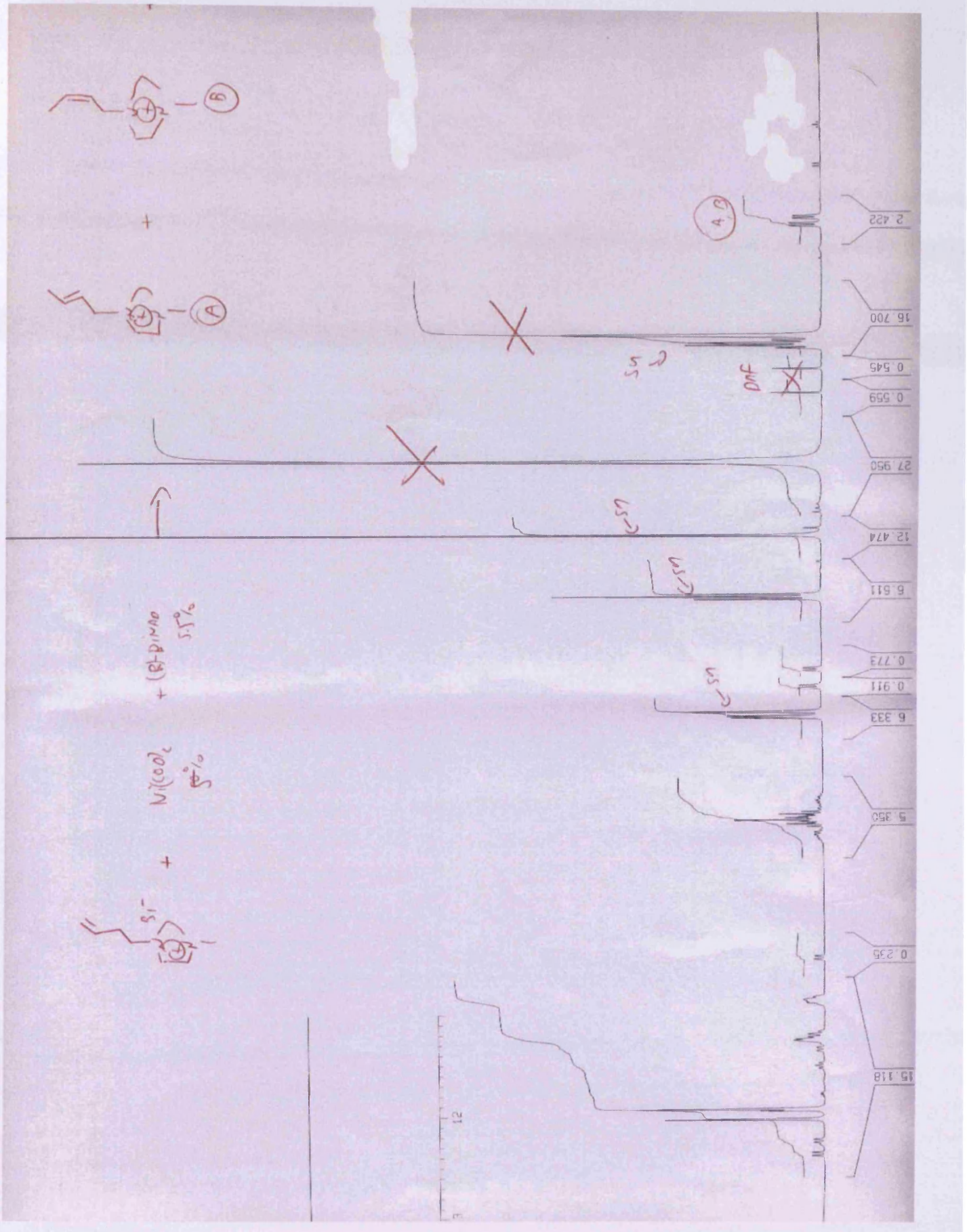
(R)-BINAP
5.2%
Ni(COD)2
5%
DMF
2.422
16.700
0.545
0.559
27.950
12.474
5.611
0.773
0.911
6.333
5.350
0.235
15.118

5.3 Appendix 3: gs-NOESY and gs-HSQC spectra

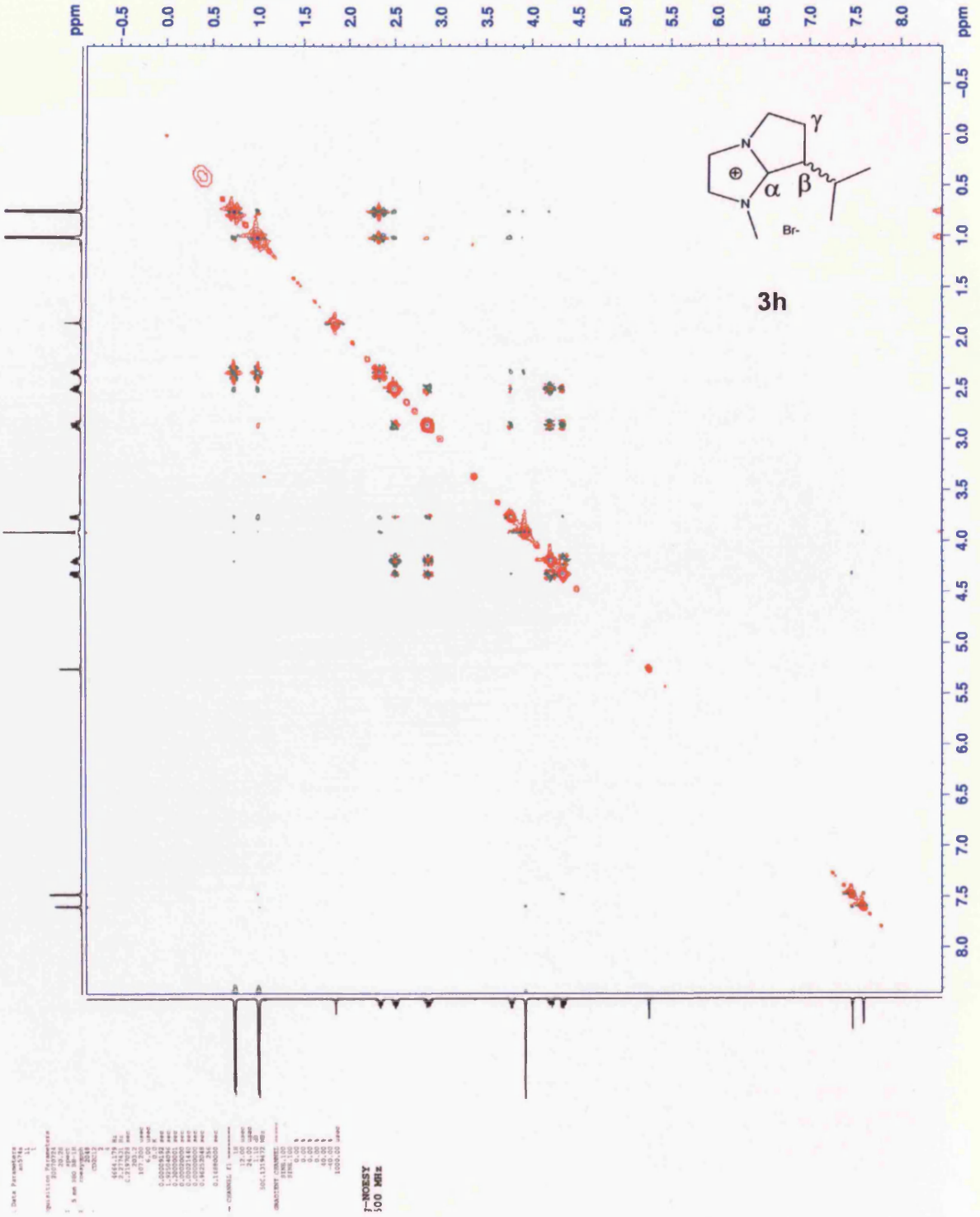
ppm
−0.5
0.0
0.5
1.0
1.5
2.0
2.5
3.0
3.5
4.0
4.5
5.0
5.5
6.0
6.5
7.0
7.5
8.0
γ
α
β
Br-
3h

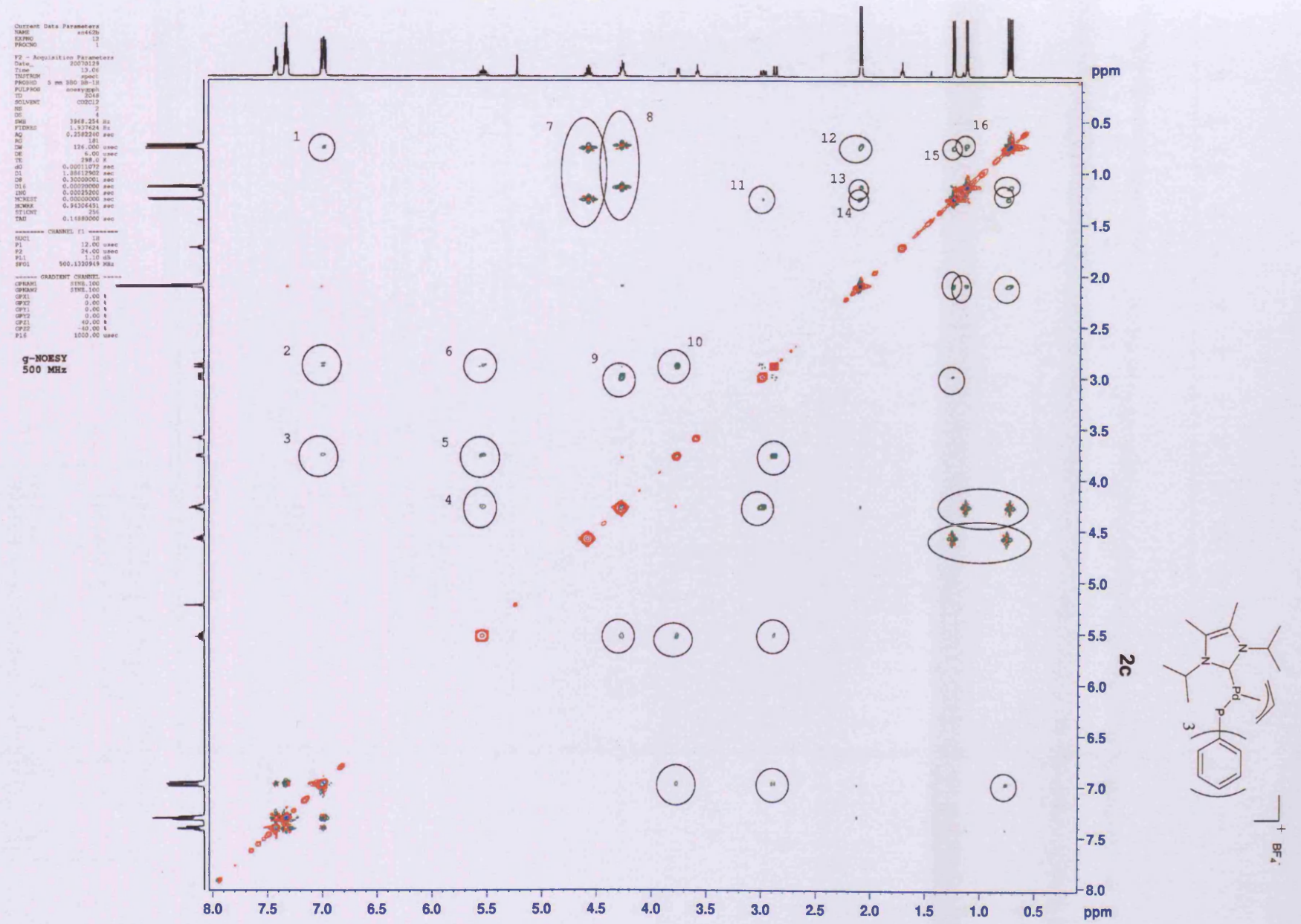
g-NOESY
500 MHz
ppm
2c
BF4-

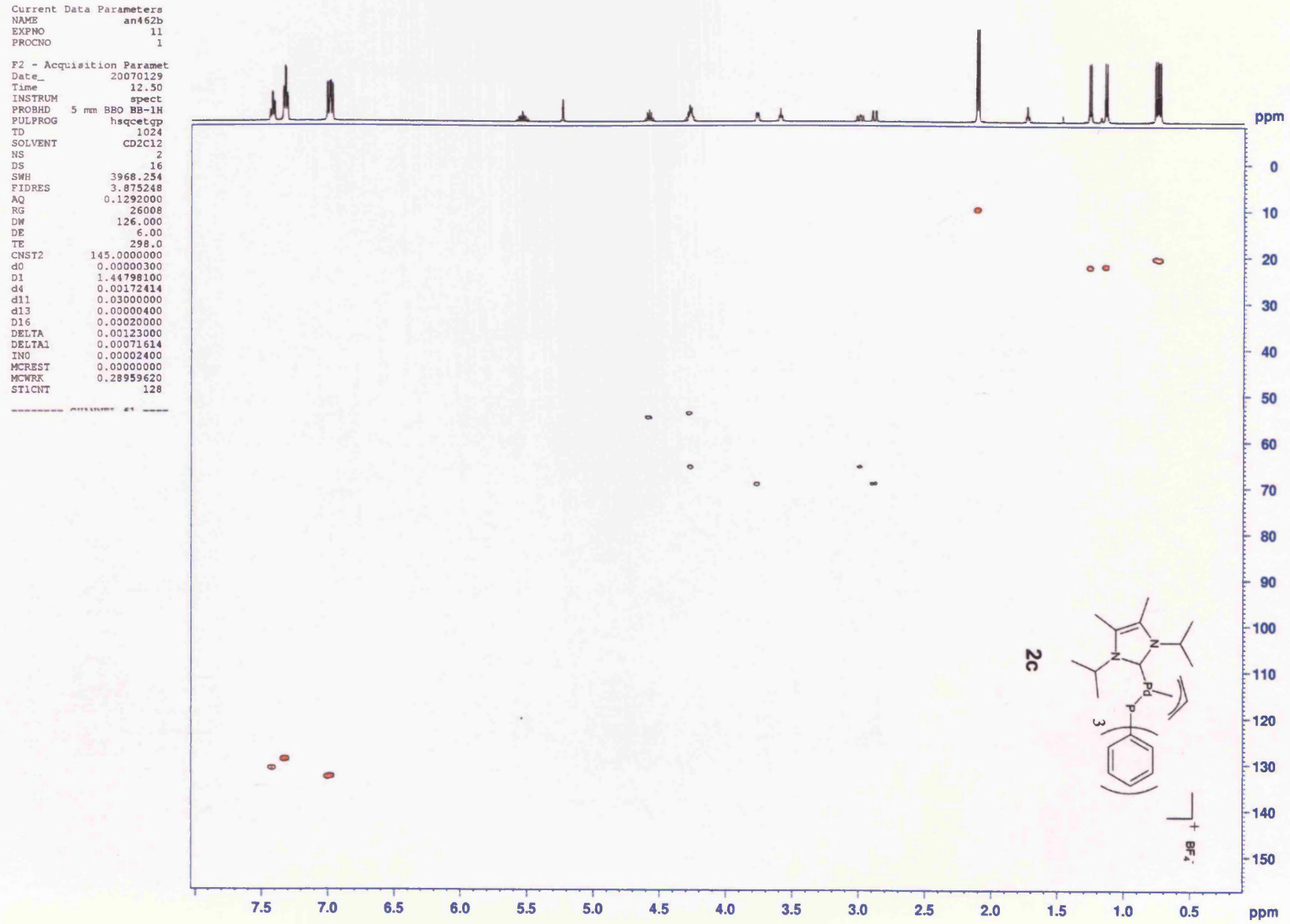
Current Data Parameters
NAME an462b
EXPNO 11
PROCNO 1
F2 - Acquisition Paramet
Date_ 20070129
Time 12.50
INSTRUM spect
PROBHD 5 mm BBO BB-1H
PULPROG hsqcetgp
TD 1024
SOLVENT CD2C12
NS 2
DS 16
SWH 3968.254
FIDRES 3.875248
AQ 0.1292000
RG 26008
DW 126.000
DE 6.00
TE 298.0
CNST2 145.0000000
d0 0.00000300
D1 1.44798100
d4 0.00172414
d11 0.03000000
d13 0.00000400
D16 0.00020000
DELTA 0.00123000
DELTA1 0.00071614
IN0 0.00002400
MCREST 0.00000000
MCWRK 0.28959620
ST1CNT 128
ppm
0
10
20
30
40
50
60
70
80
90
100
110
120
130
140
150
7.5
7.0
6.5
6.0
5.5
5.0
4.5
4.0
3.5
3.0
2.5
2.0
1.5
1.0
0.5
ppm
2c
N
N
Pd
P
3
+
BF4-

g-NOESY
500 MHz
2d
ppm
7.5 7.0 6.5 6.0 5.5 5.0 4.5 4.0 3.5 3.0 2.5 2.0 1.5 1.0 0.5 0.0
1 2 3 4 5 6 7 8 9 10 11 12 13 14 15 16 17 18
OMe
BF4-

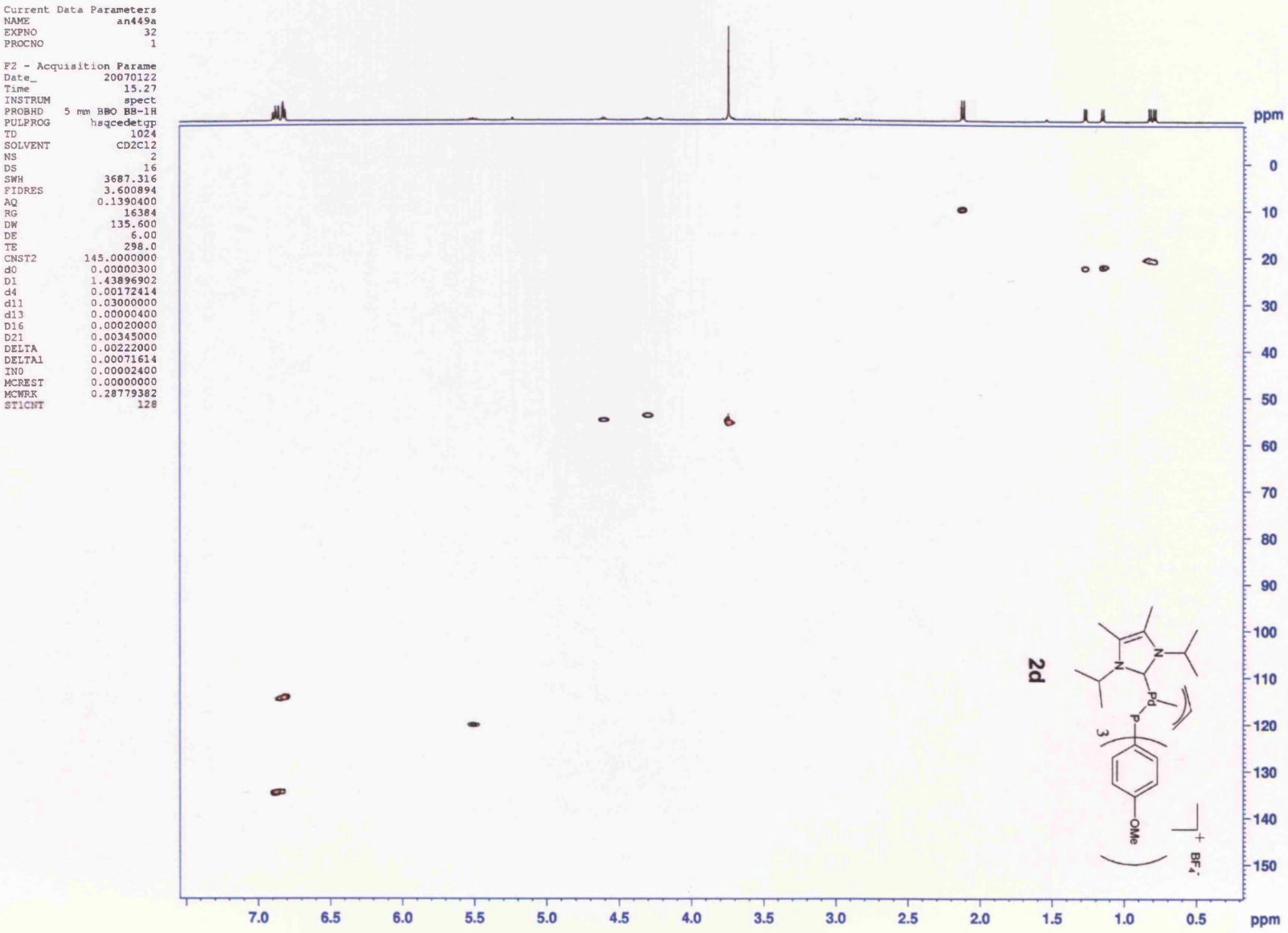
Current Data Parameters
NAME an449a
EXPNO 32
PROCNO 1
F2 - Acquisition Parame
Date_ 20070122
Time 15.27
INSTRUM spect
PROBHD 5 mm BBO BB-1H
PULPROG hsqcedetgp
TD 1024
SOLVENT CD2C12
NS 2
DS 16
SWH 3687.316
FIDRES 3.600894
AQ 0.1390400
RG 16384
DW 135.600
DE 6.00
TE 298.0
CNST2 145.0000000
d0 0.00000300
D1 1.43896902
d4 0.00172414
d11 0.03000000
d13 0.00000400
D16 0.00020000
D21 0.00345000
DELTA 0.00222000
DELTA1 0.00071614
IN0 0.00002400
MCREST 0.00000000
MCWRK 0.28779382
ST1CNT 128
ppm
0
10
20
30
40
50
60
70
80
90
100
110
120
130
140
150
7.0
6.5
6.0
5.5
5.0
4.5
4.0
3.5
3.0
2.5
2.0
1.5
1.0
0.5
ppm
2d
N
N
Pd
P
3
OMe
+
BF4-

3c
OMe
Pd
BF4
ppm

```
Current Data Parameters
NAME                  an452b
EXPNO                     41
PROCNO                     1

F2 - Acquisition Paramet
Date_               20070124
Time                    9.35
INSTRUM                spect
PROBHD    5 mm BBO BB-1H
PULPROG        hsqcedetgp
TD                      1024
SOLVENT             CD2C12
NS                         2
DS                        16
SWH                 3968.254
FIDRES              3.875248
AQ                 0.1292000
RG                     16384
DW                     126.000
DE                        6.00
TE                       298.0
CNST2             145.0000000
d0                  0.00000300
D1                  1.44818497
d4                  0.00172414
d11                 0.03000000
d13                 0.00000400
D16                 0.00020000
D21                 0.00345000
DELTA               0.00222000
DELTA1              0.00071614
IN0                 0.00002400
MCREST              0.00000000
MCWRK               0.28963700
ST1CNT                    128
```

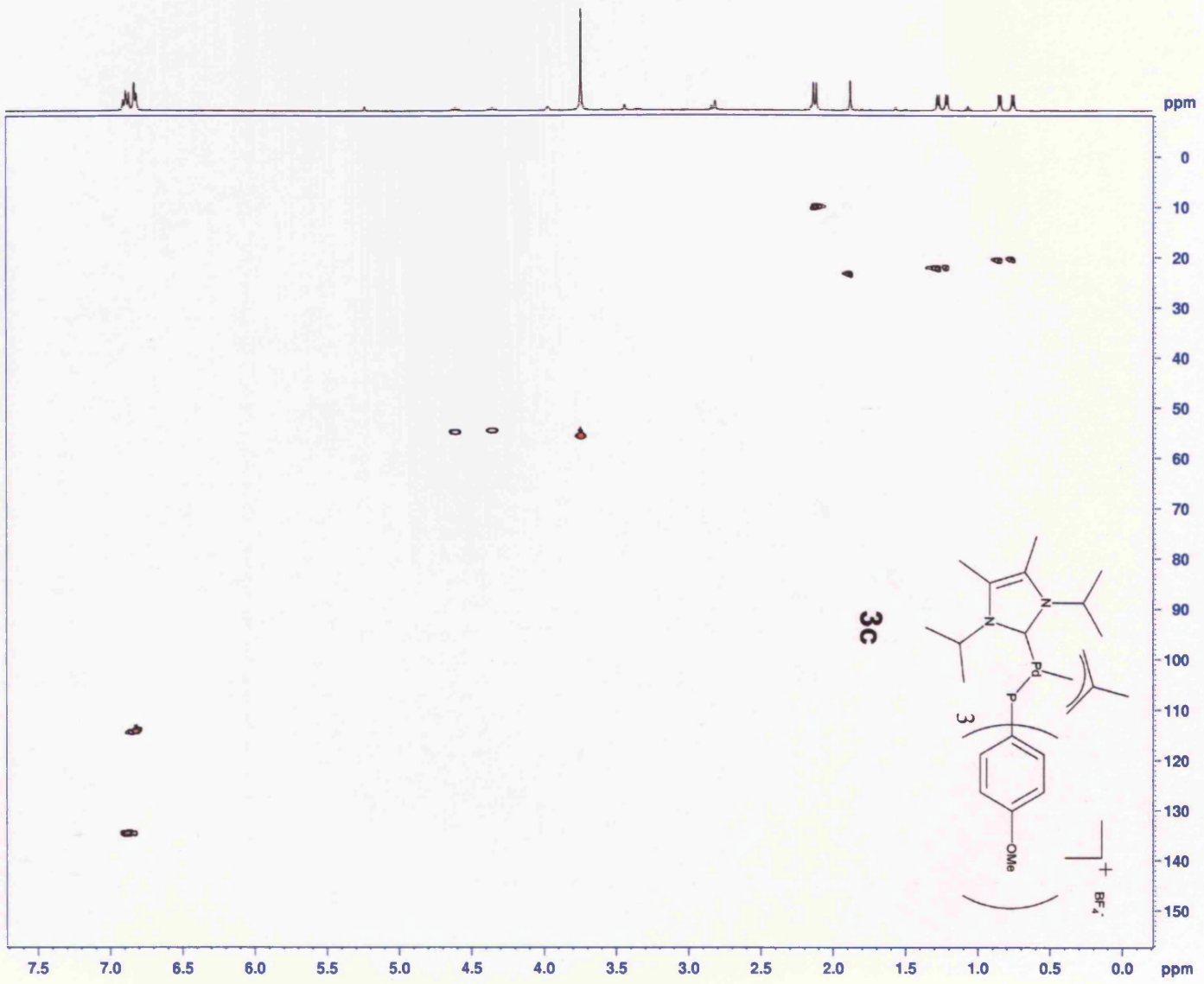

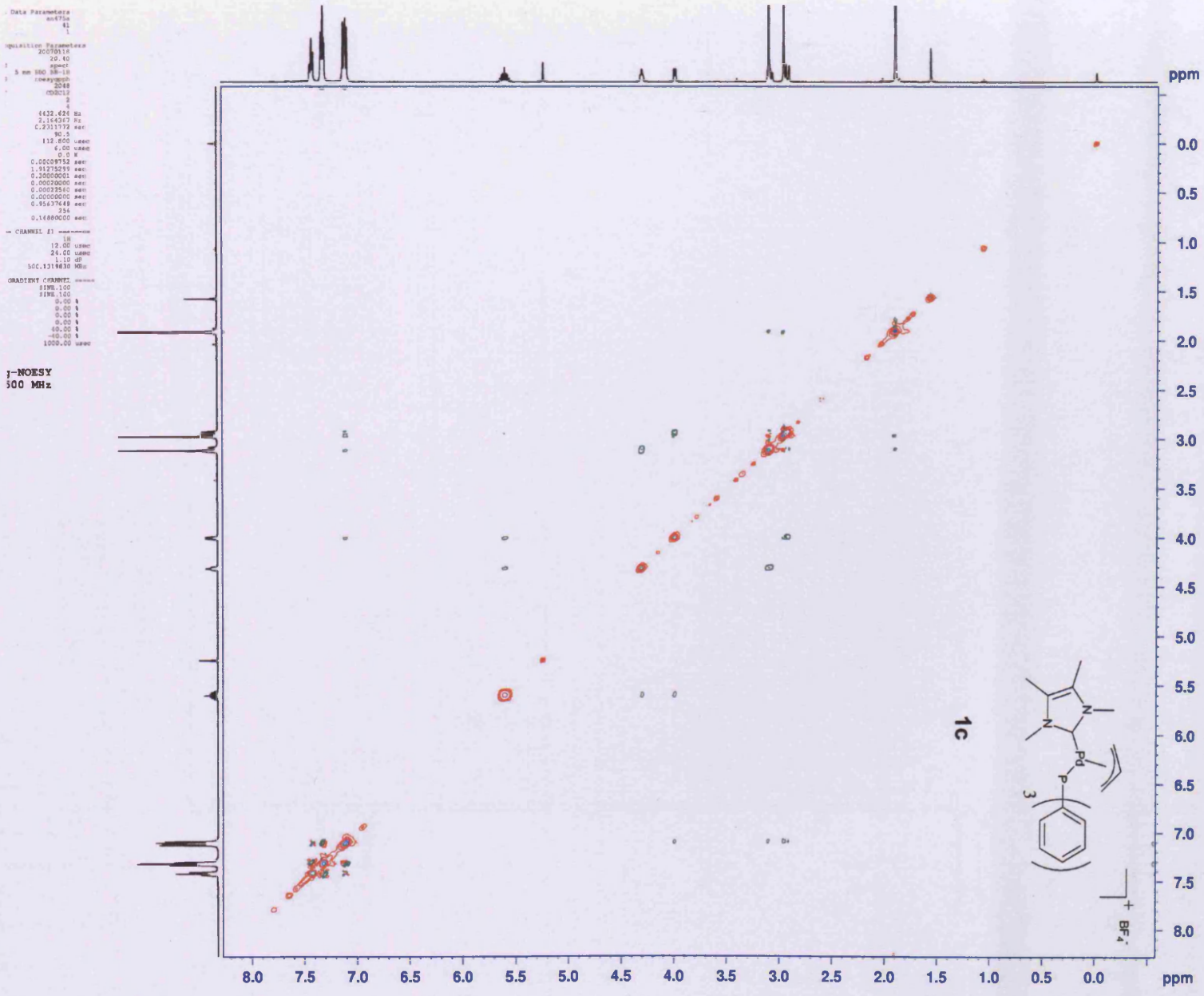
ppm
0.0
0.5
1.0
1.5
2.0
2.5
3.0
3.5
4.0
4.5
5.0
5.5
6.0
6.5
7.0
7.5
8.0
8.0 7.5 7.0 6.5 6.0 5.5 5.0 4.5 4.0 3.5 3.0 2.5 2.0 1.5 1.0 0.5 0.0
ppm
1c
Pd
P
3
BF4-

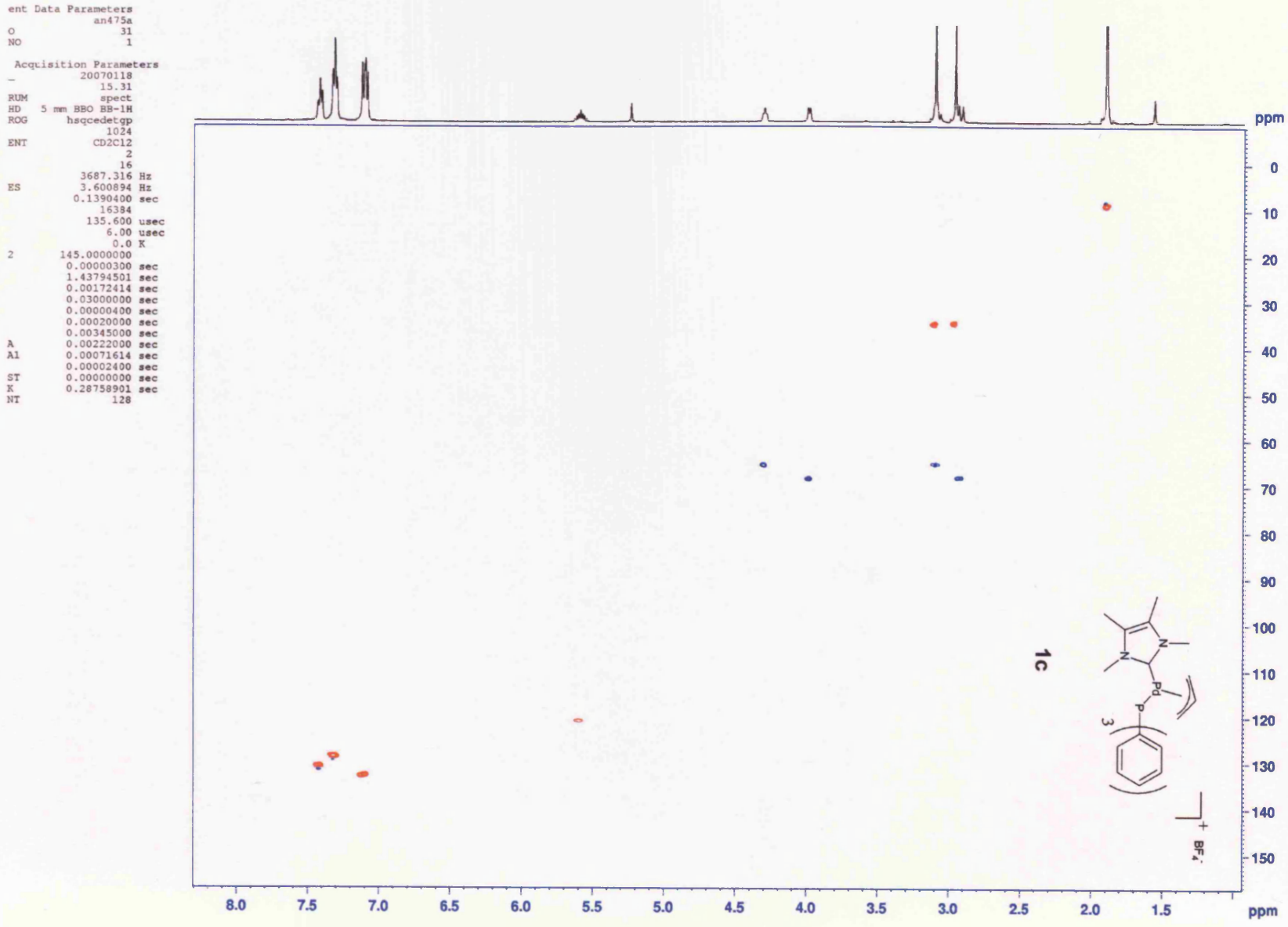
ent Data Parameters
an475a
O 31
NO 1
Acquisition Parameters
20070118
15.31
RUM spect
HD 5 mm BBO BB-1H
ROG hsqcedetgp
1024
ENT CD2Cl2
2
16
3687.316 Hz
ES 3.600894 Hz
0.1390400 sec
16384
135.600 usec
6.00 usec
0.0 K
2 145.0000000
0.00000300 sec
1.43794501 sec
0.00172414 sec
0.03000000 sec
0.00000400 sec
0.00020000 sec
0.00345000 sec
A 0.00222000 sec
A1 0.00071614 sec
0.00002400 sec
ST 0.00000000 sec
K 0.28758901 sec
NT 128
ppm
0
10
20
30
40
50
60
70
80
90
100
110
120
130
140
150
8.0
7.5
7.0
6.5
6.0
5.5
5.0
4.5
4.0
3.5
3.0
2.5
2.0
1.5
ppm
1c
N
N
Pd
P
3
+
BF4-

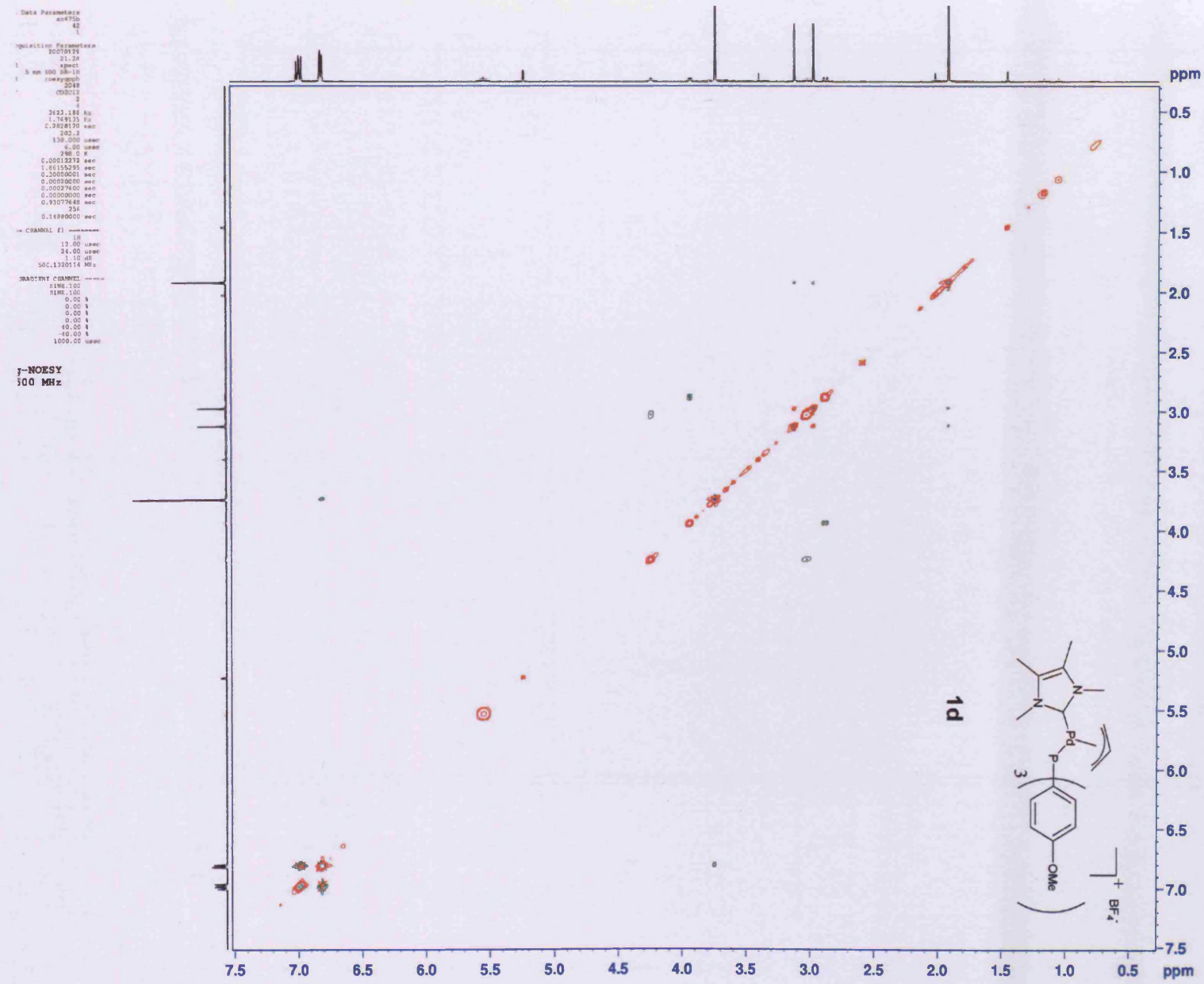
ppm
7.5
7.0
6.5
6.0
5.5
5.0
4.5
4.0
3.5
3.0
2.5
2.0
1.5
1.0
0.5
1d
OMe
BF4-

1d
OMe
BF4-
Pd
P
N
N
3
ppm

Data Parameters
an473c
32
1
Acquisition Parameters
20070129
20.18
aspect
5 mm BBO BB-1H
1 cmaxygpph
2048
CD2Cl2
2
1
3832.630 Hz
1.866518 Hz
0.2680592 sec
703.2
130.800 usec
6.00 usec
298.0 K
0.00011552 sec
1.87588894 sec
0.30000001 sec
0.00020000 sec
0.00026160 sec
0.00000000 sec
0.93784447 sec
256
0.14880000 sec
CHANNEL f1
10
12.00 usec
24.00 usec
1.10 dB
500.1320995 MHz
GRADIENT CHANNEL
51MH.100
51MH.100
0.00 %
0.00 %
0.00 %
0.00 %
40.00 %
-40.00 %
1000.00 usec
j-NOESY
500 MHz
ppm
0.5
1.0
1.5
2.0
2.5
3.0
3.5
4.0
4.5
5.0
5.5
6.0
6.5
7.0
7.5
7.5 7.0 6.5 6.0 5.5 5.0 4.5 4.0 3.5 3.0 2.5 2.0 1.5 1.0 0.5 ppm
1e
N
N
Pd
P
3
+
BF4-

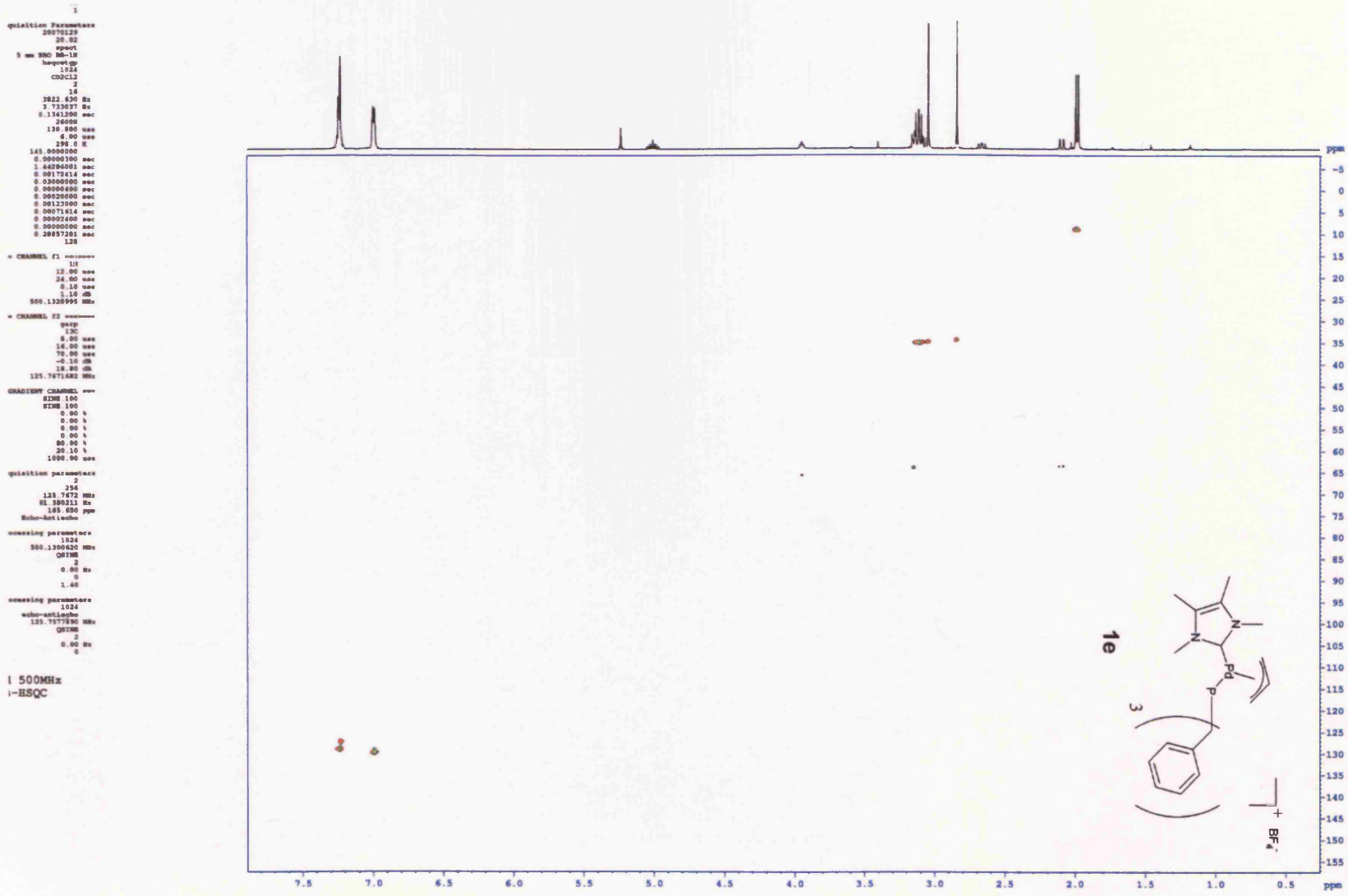
1
quisition Parameters
20070129
20.02
spect
5 mm BBO BB-1H
hsqcetgp
1024
CH2Cl2
2
16
3822.636 Hz
3.733037 Hz
0.1341200 sec
26000
130.880 usec
6.00 usec
298.0 K
145.0000000
0.00000100 sec
1.44296401 sec
0.00172414 sec
0.03000000 sec
0.00000400 sec
0.00020000 sec
0.00123000 sec
0.00071614 sec
0.00002400 sec
0.00000000 sec
0.20857201 sec
128
= CHANNEL f1 ======
1H
12.00 usec
24.00 usec
0.10 usec
1.10 dB
500.1320995 MHz
= CHANNEL f2 ======
garp
13C
8.00 usec
16.00 usec
70.00 usec
-0.10 dB
18.80 dB
125.7671682 MHz
GRADIENT CHANNEL ===
SINE.100
SINE.100
0.00 %
0.00 %
0.00 %
0.00 %
80.00 %
20.10 %
1000.00 usec
quisition parameters
2
256
125.7672 MHz
81.380311 Hz
165.630 ppm
Echo-Antiecho
ocessing parameters
1024
500.1300620 MHz
QSINE
2
0.00 Hz
0
1.40
ocessing parameters
1024
echo-antiecho
125.7577890 MHz
QSINE
2
0.00 Hz
0
1 500MHz
i-HSQC
1e
3
P
Pd
N
N
BF4-
ppm
7.5
7.0
6.5
6.0
5.5
5.0
4.5
4.0
3.5
3.0
2.5
2.0
1.5
1.0
0.5
ppm
-5
0
5
10
15
20
25
30
35
40
45
50
55
60
65
70
75
80
85
90
95
100
105
110
115
120
125
130
135
140
145
150
155

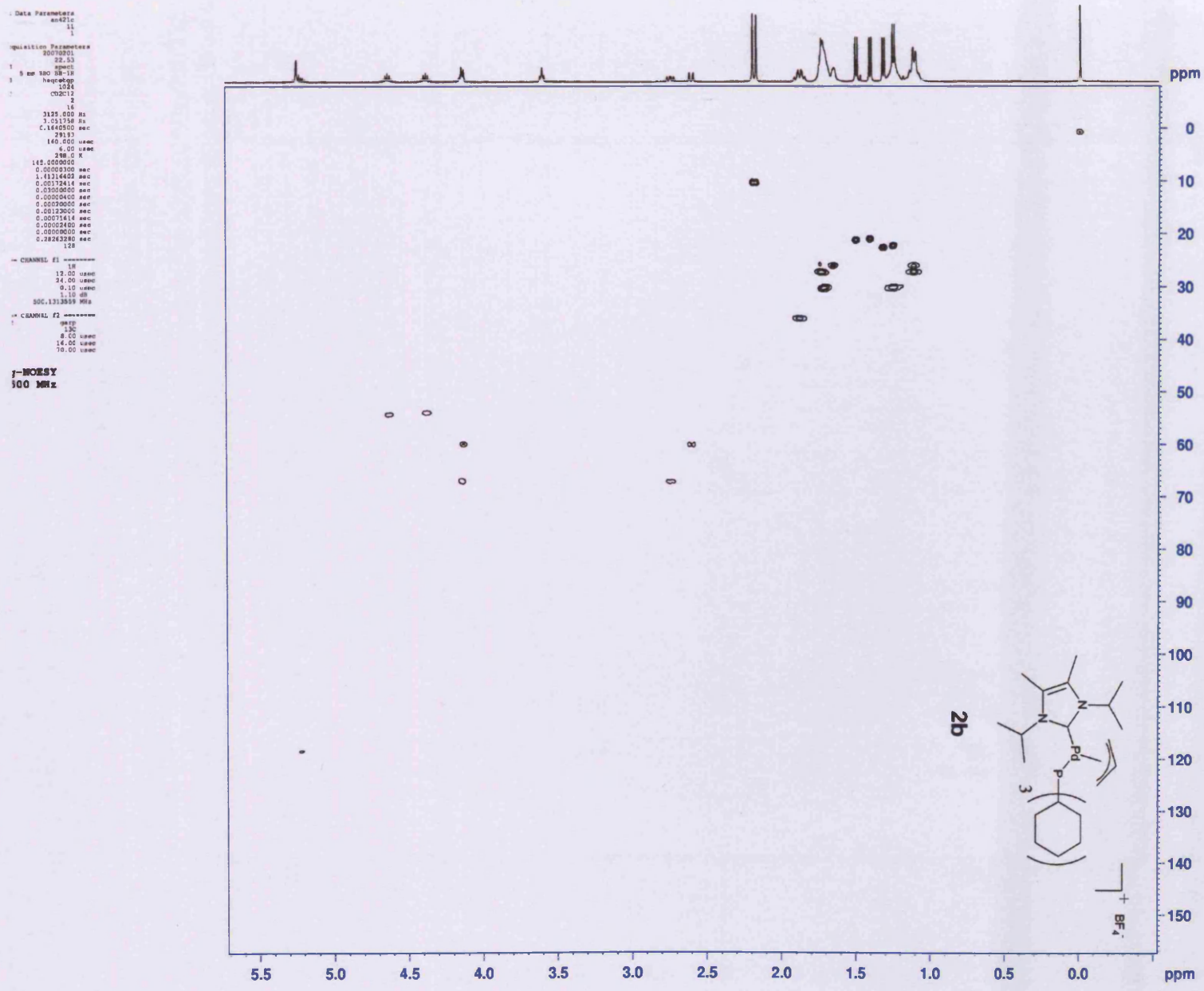
ppm
0
10
20
30
40
50
60
70
80
90
100
110
120
130
140
150
5.5
5.0
4.5
4.0
3.5
3.0
2.5
2.0
1.5
1.0
0.5
0.0
ppm
2b
Pd
P
3
N
N
BF4

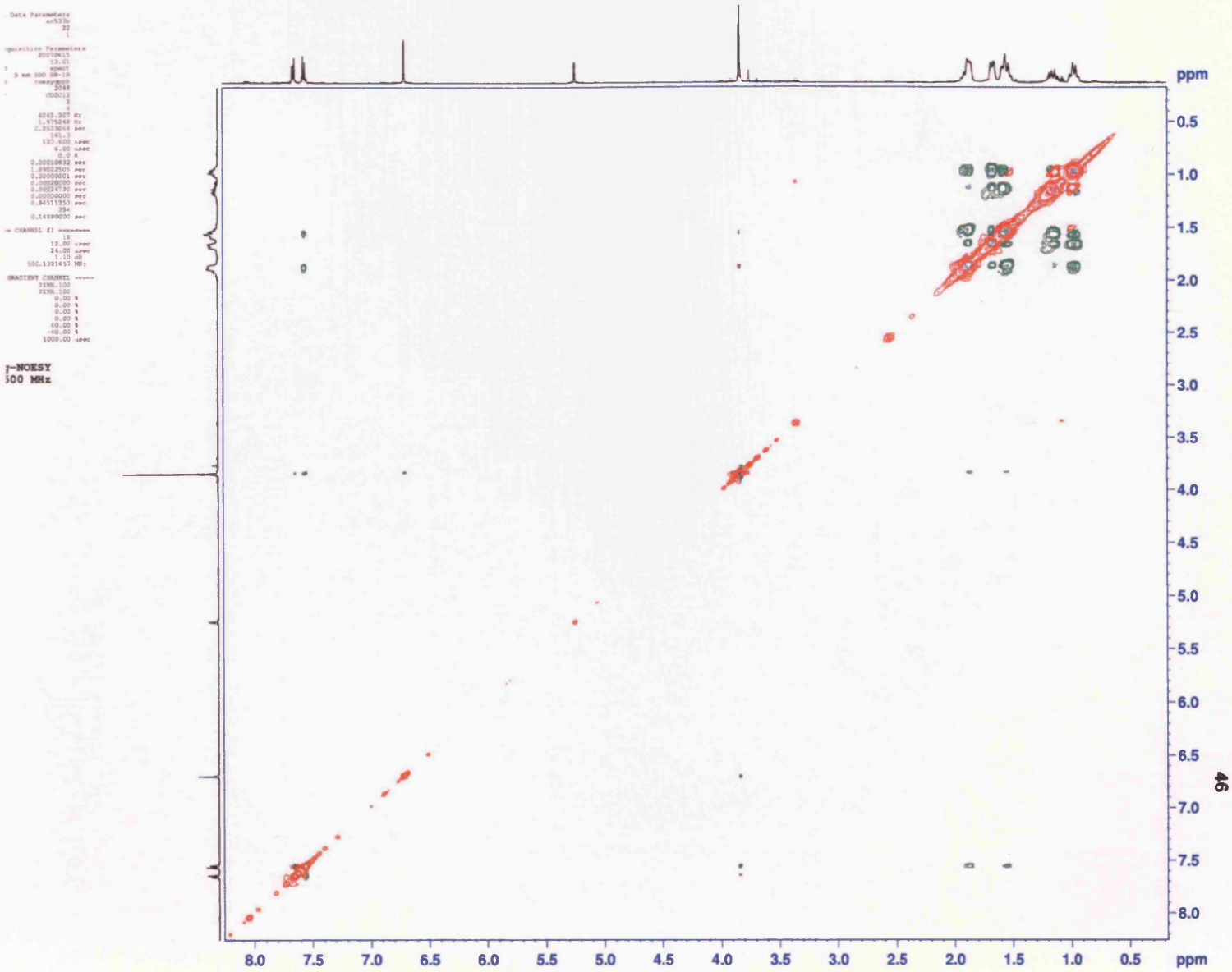
Data Parameters
an533b
22
1
Acquisition Parameters
20070615
13.01
spect
5 mm BBO BB-1H
cmaygs600
2048
CDCl3
2
1
6045.307 Hz
1.975248 Hz
0.25538044 sec
161.3
123.600 usec
6.00 usec
0.0 K
0.00010832 sec
1.89022505 sec
0.30000001 sec
0.00020000 sec
0.00024120 sec
0.00000000 sec
0.84511253 sec
256
0.14880000 sec
CHANNEL f1
1H
12.00 usec
24.00 usec
1.10 dB
500.1321452 MHz
GRADIENT CHANNEL
SINE.100
SINE.100
0.00 %
0.00 %
0.00 %
0.00 %
40.00 %
-40.00 %
1000.00 usec
J-NOESY
500 MHz
ppm
0.5
1.0
1.5
2.0
2.5
3.0
3.5
4.0
4.5
5.0
5.5
6.0
6.5
7.0
7.5
8.0
8.0
7.5
7.0
6.5
6.0
5.5
5.0
4.5
4.0
3.5
3.0
2.5
2.0
1.5
1.0
0.5
ppm
46
O2N
Cy3P
Pd
I
N
N

```
ent Data Parameters
                an533a
O                   32
NO                   1

 Acquisition Parameters
-              20070613
                 21.01
RUM                spect
HD    5 mm BBO BB-1H
ROG         hsqcedetgp
                  1024
ENT              CD2Cl2
                     2
                    16
               4166.667 Hz
ES             4.069010 Hz
            0.1230500 sec
              10321.3
               120.000 usec
                 6.00 usec
                  0.0 K
2          145.0000000
            0.00000300 sec
            1.45432901 sec
            0.00172414 sec
            0.03000000 sec
            0.00000400 sec
            0.00020000 sec
            0.00345000 sec
A           0.00222000 sec
A1          0.00071614 sec
            0.00002400 sec
ST          0.00000000 sec
K           0.29086581 sec
NT                 128
```

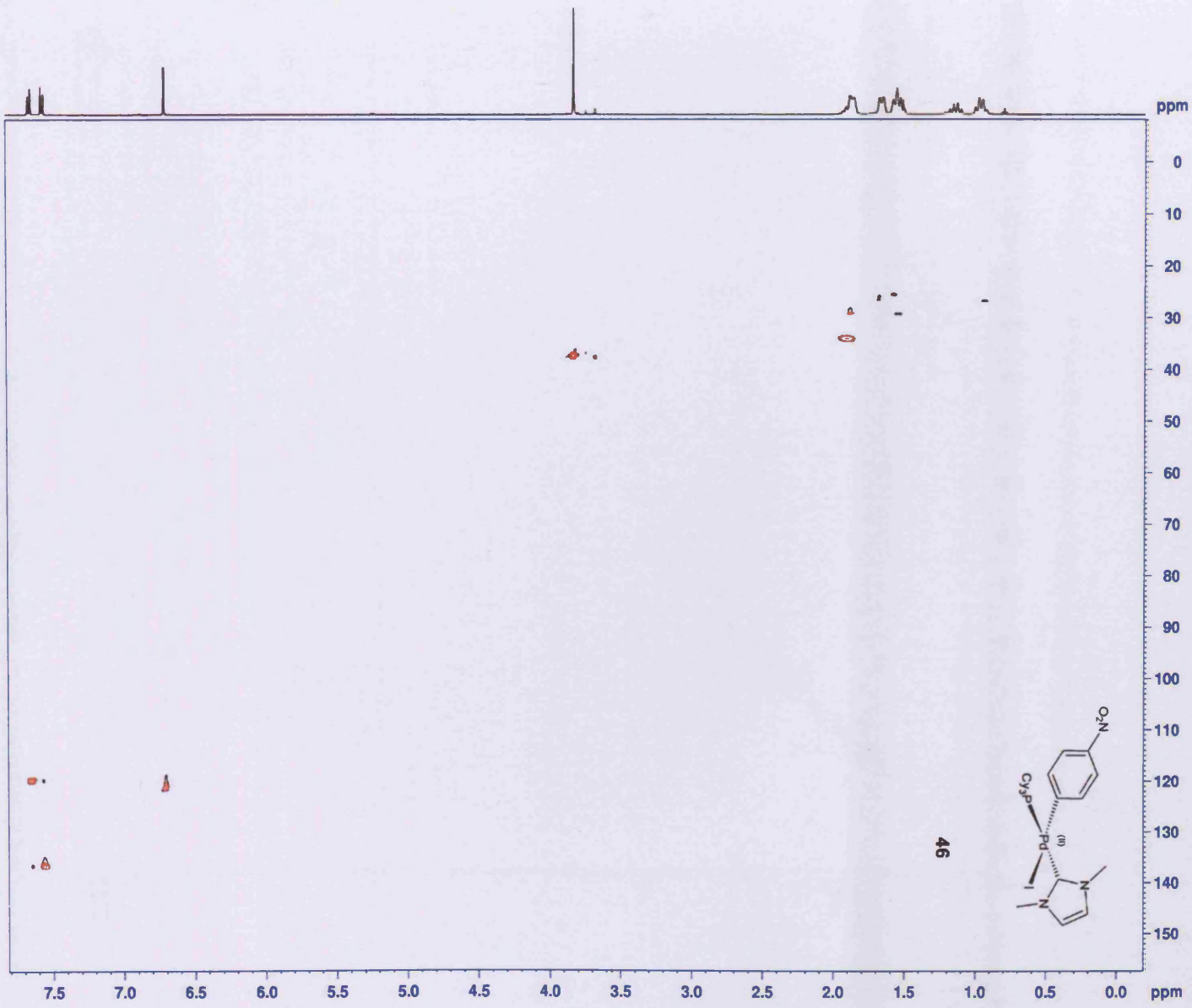

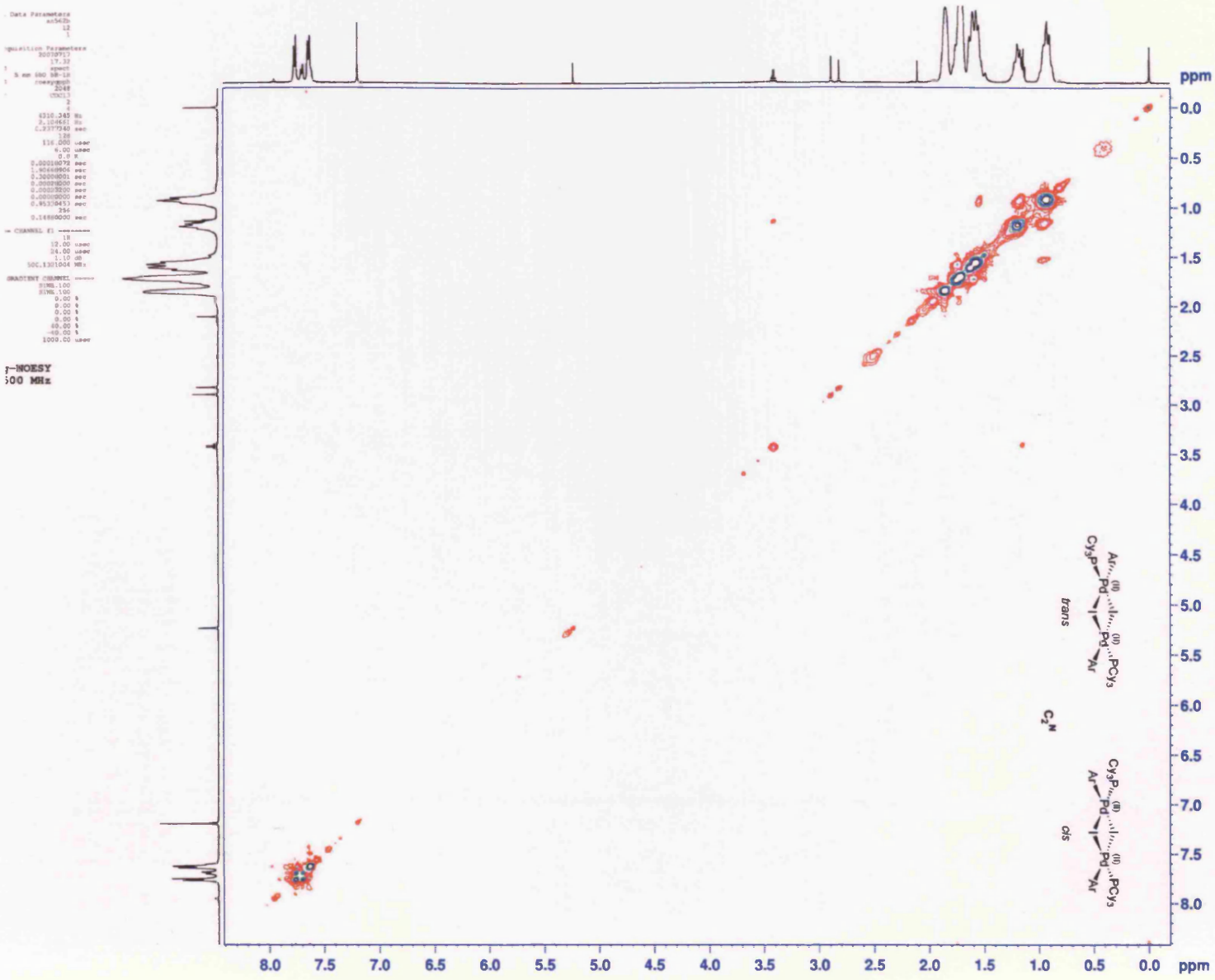
ppm
0.0
0.5
1.0
1.5
2.0
2.5
3.0
3.5
4.0
4.5
5.0
5.5
6.0
6.5
7.0
7.5
8.0
8.0 7.5 7.0 6.5 6.0 5.5 5.0 4.5 4.0 3.5 3.0 2.5 2.0 1.5 1.0 0.5 0.0 ppm
trans
cis
C_2H

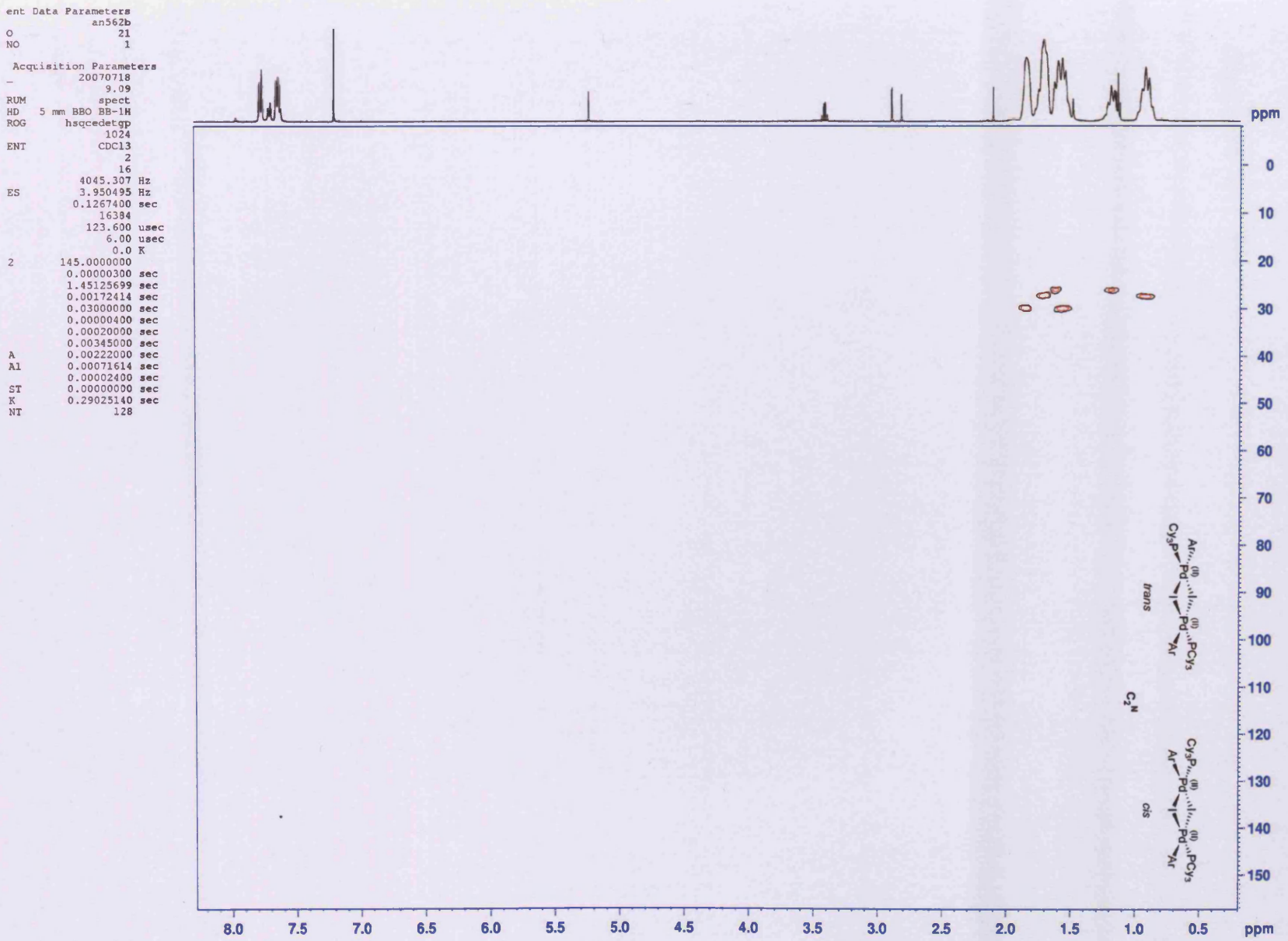
ent Data Parameters
an562b
O 21
NO 1
Acquisition Parameters
20070718
9.09
RUM spect
HD 5 mm BBO BB-1H
ROG hsqcedetgp
1024
ENT CDCl3
2
16
4045.307 Hz
ES 3.950495 Hz
0.1267400 sec
16384
123.600 usec
6.00 usec
0.0 K
2 145.0000000
0.00000300 sec
1.45125699 sec
0.00172414 sec
0.03000000 sec
0.00000400 sec
0.00020000 sec
0.00345000 sec
A 0.00222000 sec
A1 0.00071614 sec
0.00002400 sec
ST 0.00000000 sec
K 0.29025140 sec
NT 128
ppm
0
10
20
30
40
50
60
70
80
90
100
110
120
130
140
150
8.0
7.5
7.0
6.5
6.0
5.5
5.0
4.5
4.0
3.5
3.0
2.5
2.0
1.5
1.0
0.5
ppm
trans
cis
C2N

5.4 Appendix 4: ESI/MS and NMR spectra for the reactivity studies on 1b

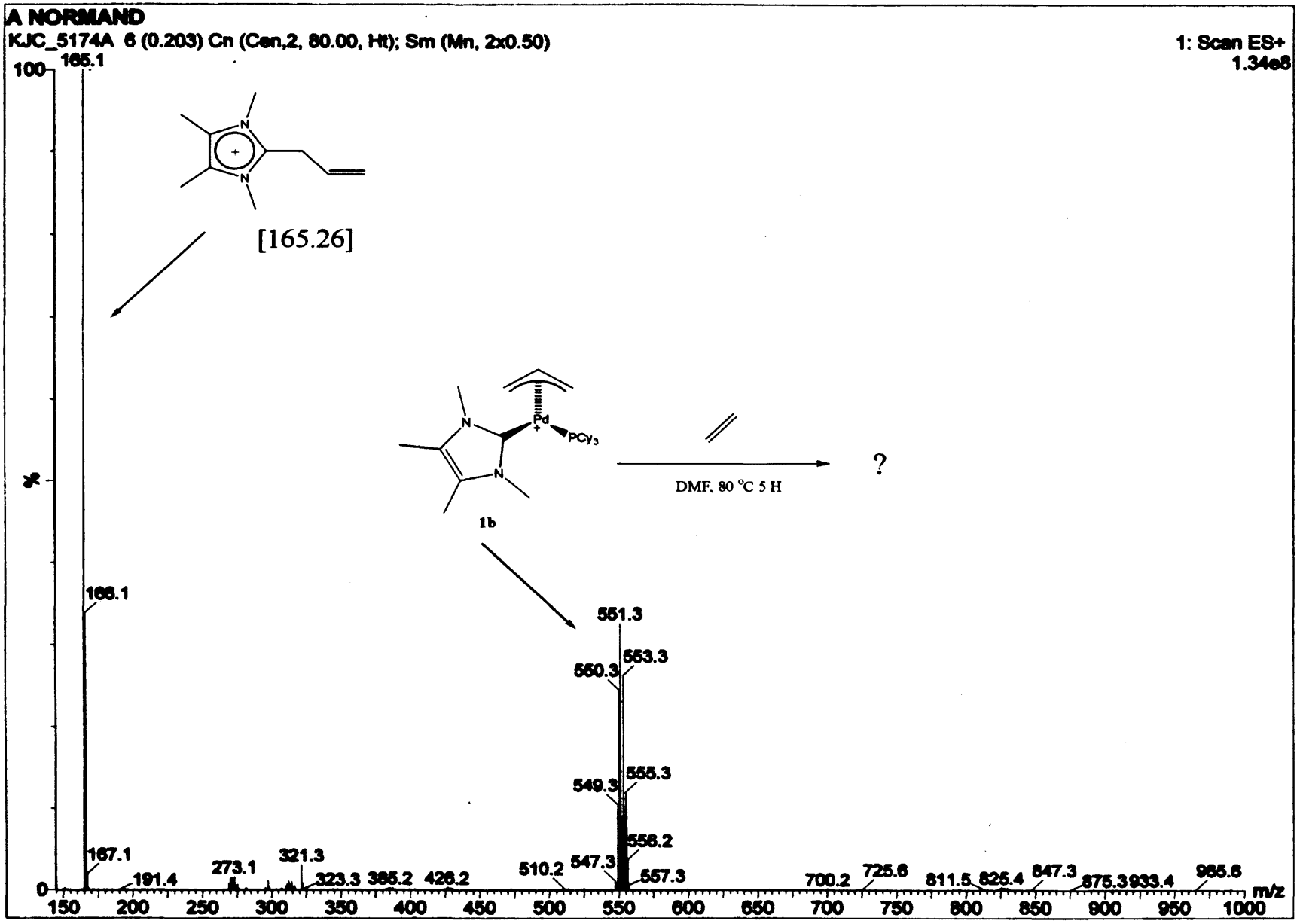
A NORMAND
KJC_5174A 6 (0.203) Cn (Cen,2, 80.00, Ht); Sm (Mn, 2x0.50)
1: Scan ES+
1.34e8
100
%
0
165.1
[165.26]
Pd
PCy3
1b
DMF, 80 °C 5 H
?
166.1
551.3
553.3
550.3
555.3
549.3
556.2
167.1
273.1
321.3
547.3
510.2
557.3
191.4
323.3
385.2
426.2
700.2
725.6
811.5
825.4
847.3
875.3
933.4
965.6
m/z
150
200
250
300
350
400
450
500
550
600
650
700
750
800
850
900
950
1000

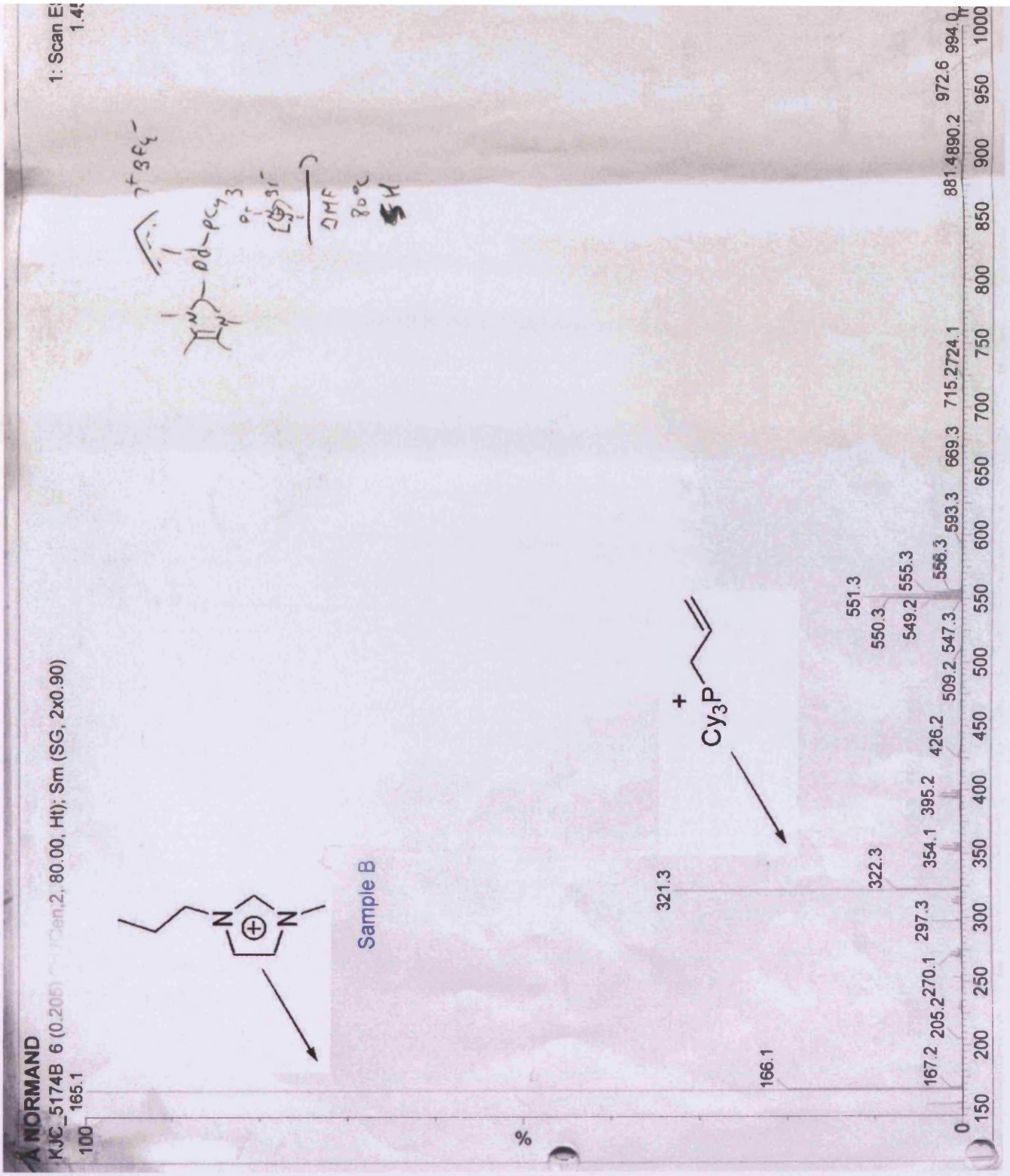

ESI/MS: Reaction of 1b with [pmim]Br

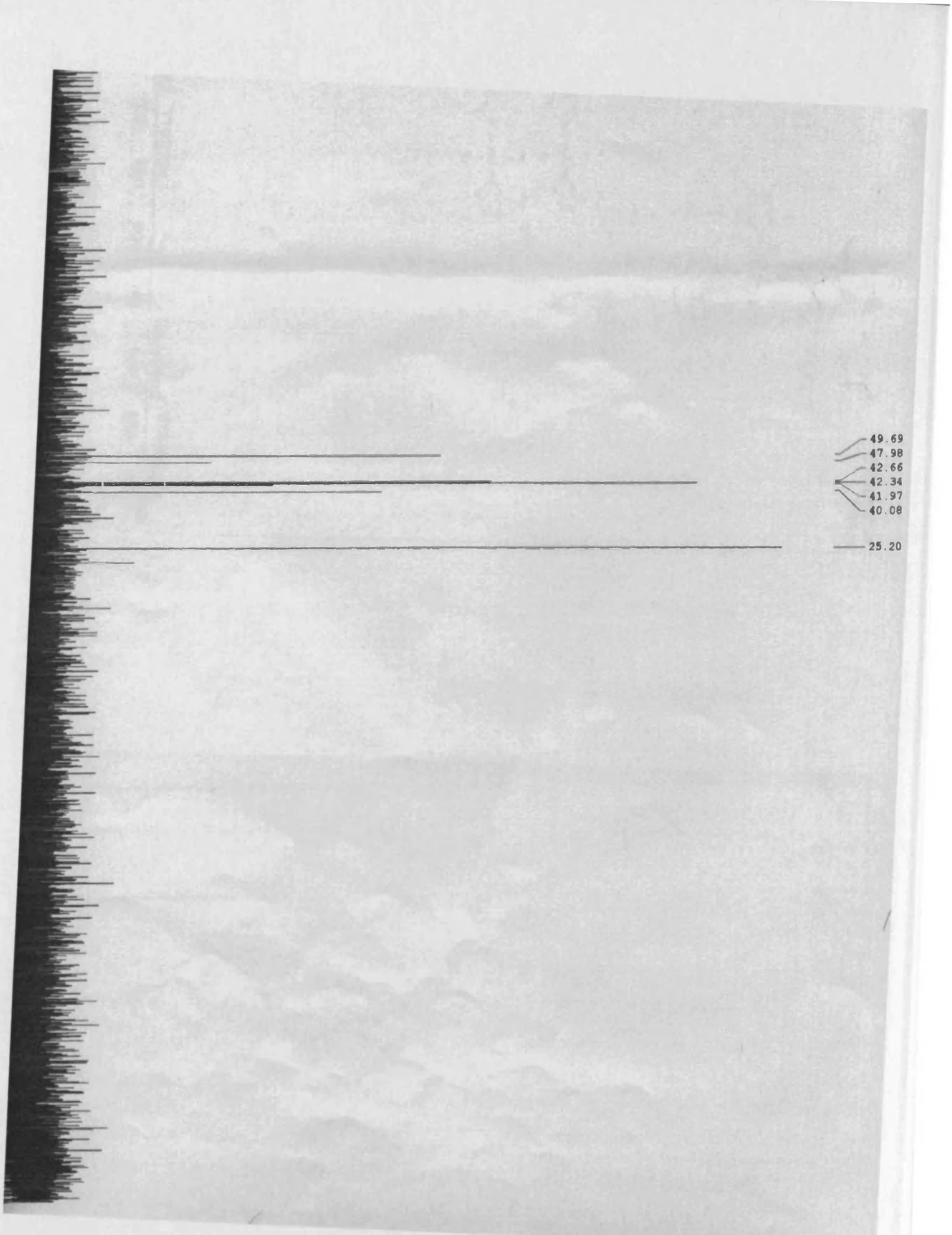

^{31}P NMR: Reaction of 1b with [pmim]Br

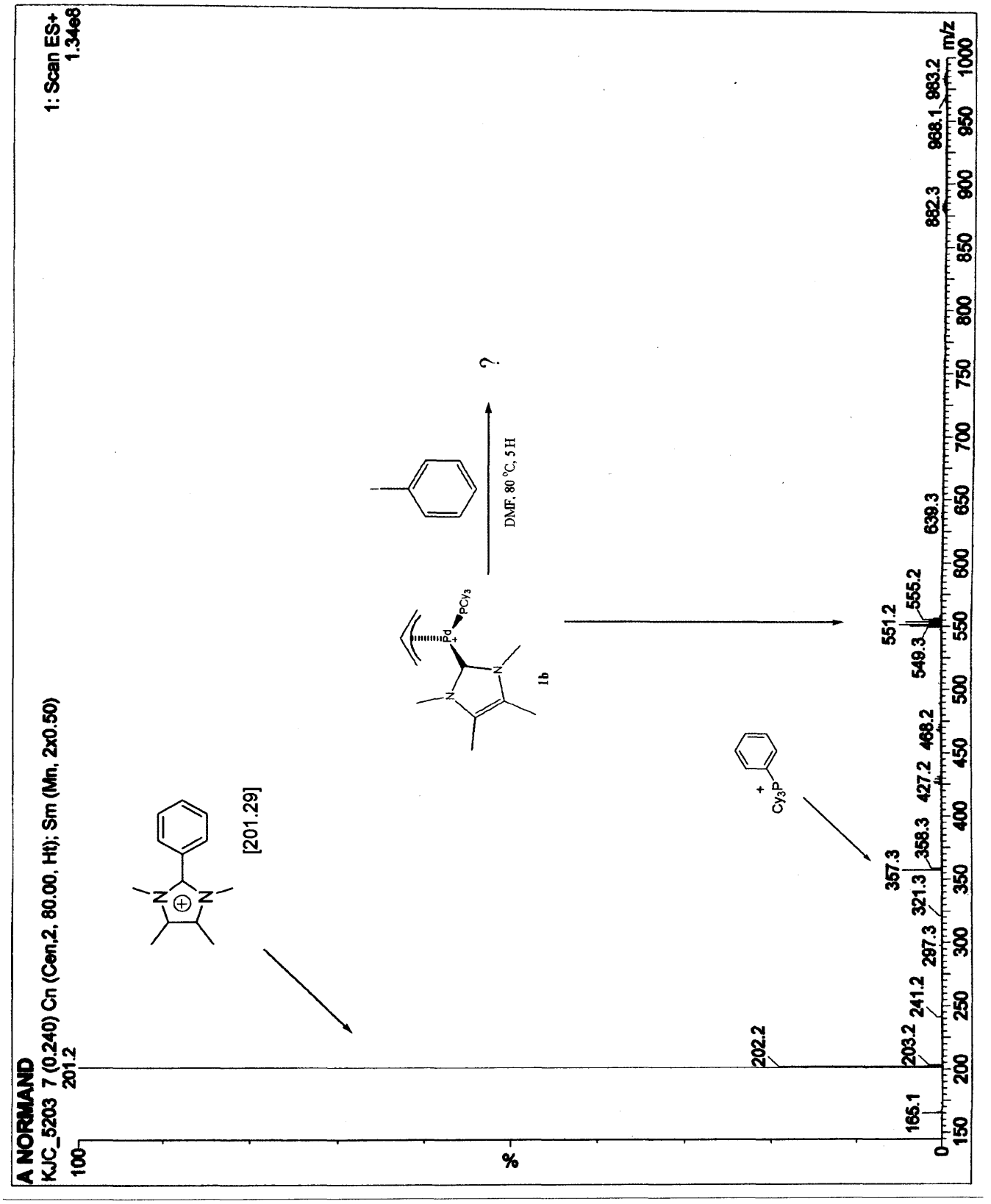

ESI/MS: reaction of 1b with PhI

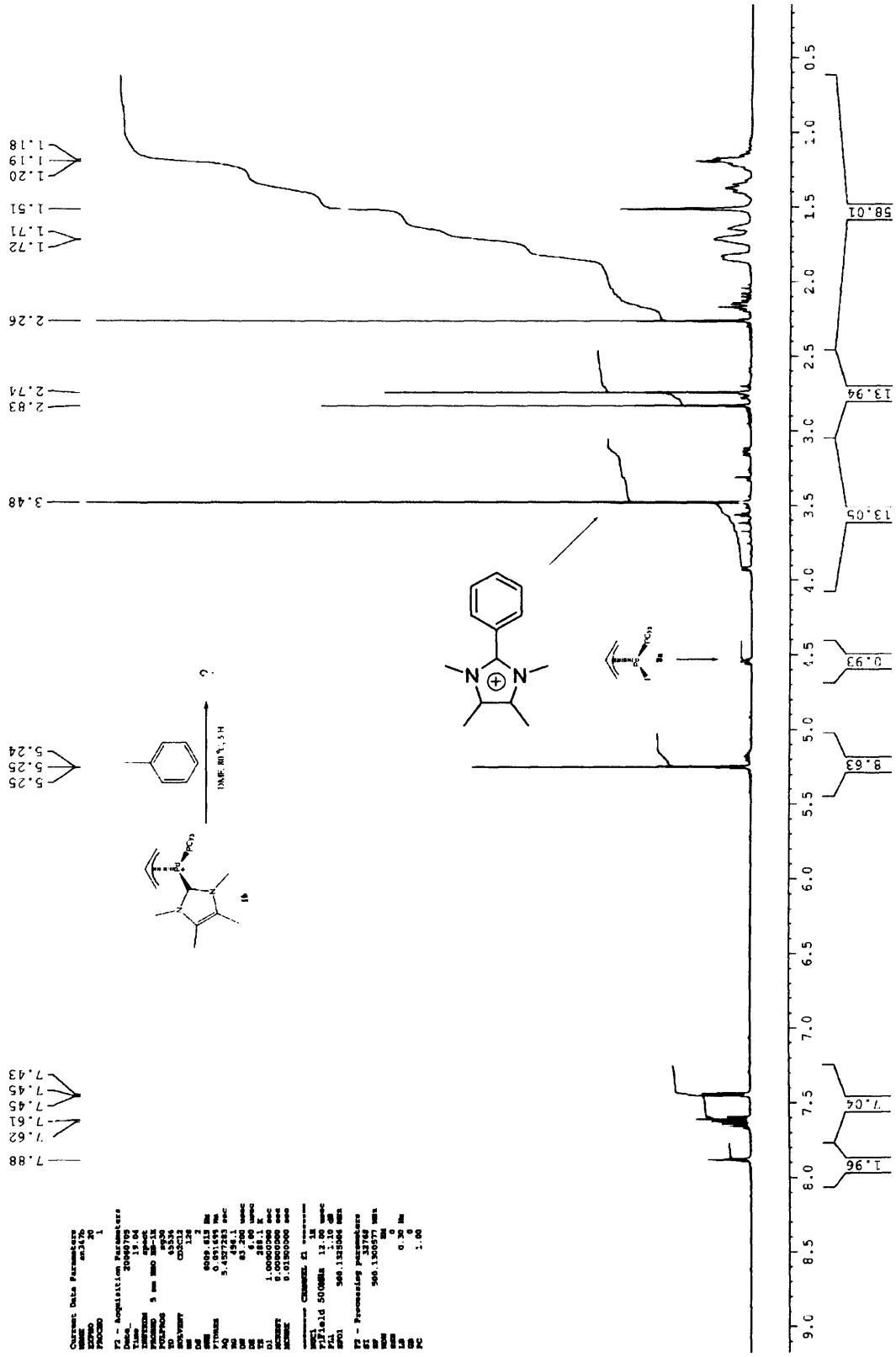

^{1}H NMR spectrum: reaction of 1b with PhI

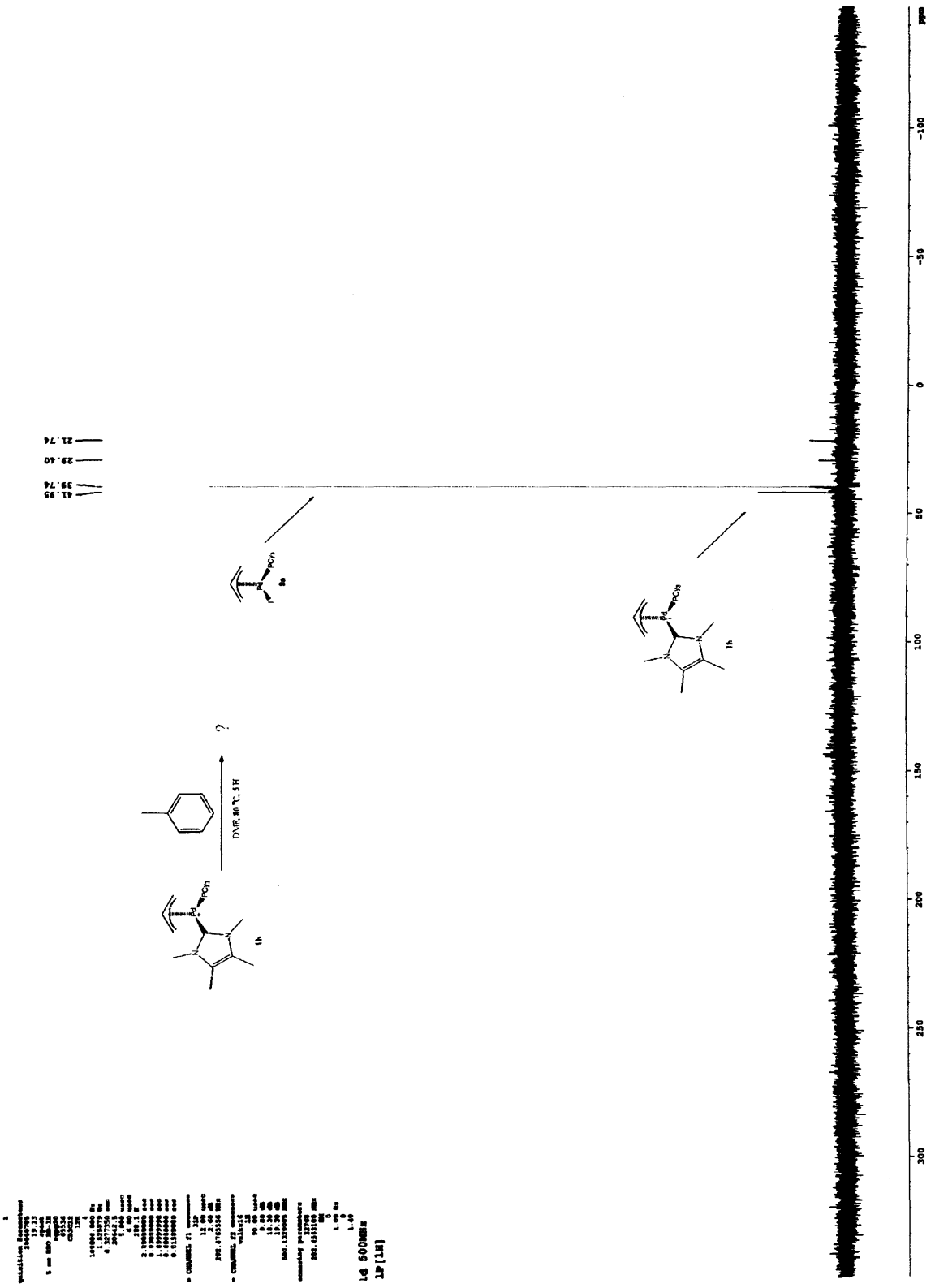

^{31}P NMR spectrum: reaction of 1b with PhI

ESI/MS: attempted direct arylation of dmim$^+$, no ligand.

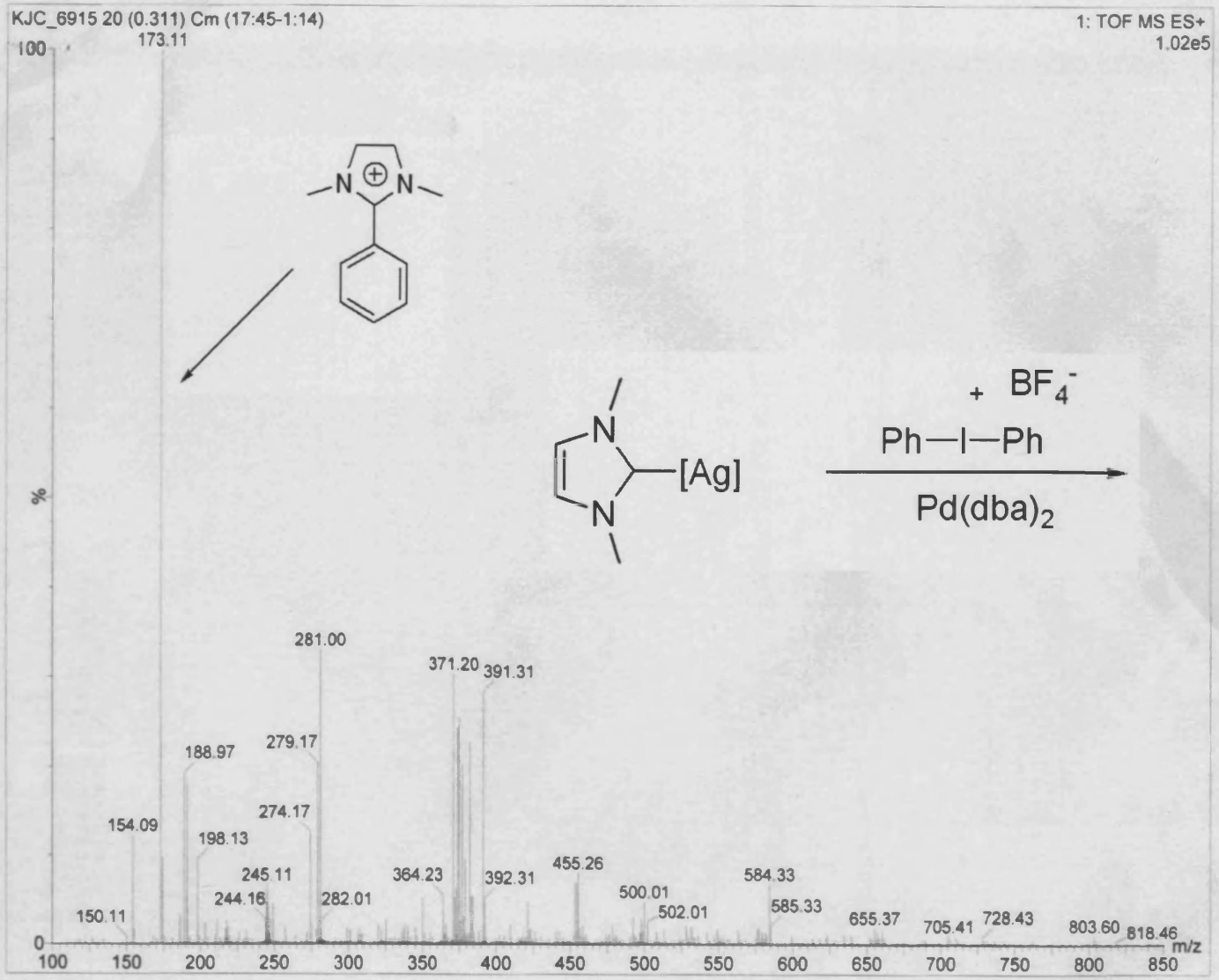

ESI/MS: attempted direct arylation of $dmim^+$, PPh_3.

ESI/MS: attempted direct arylation of dmim$^+$, PCy_3.

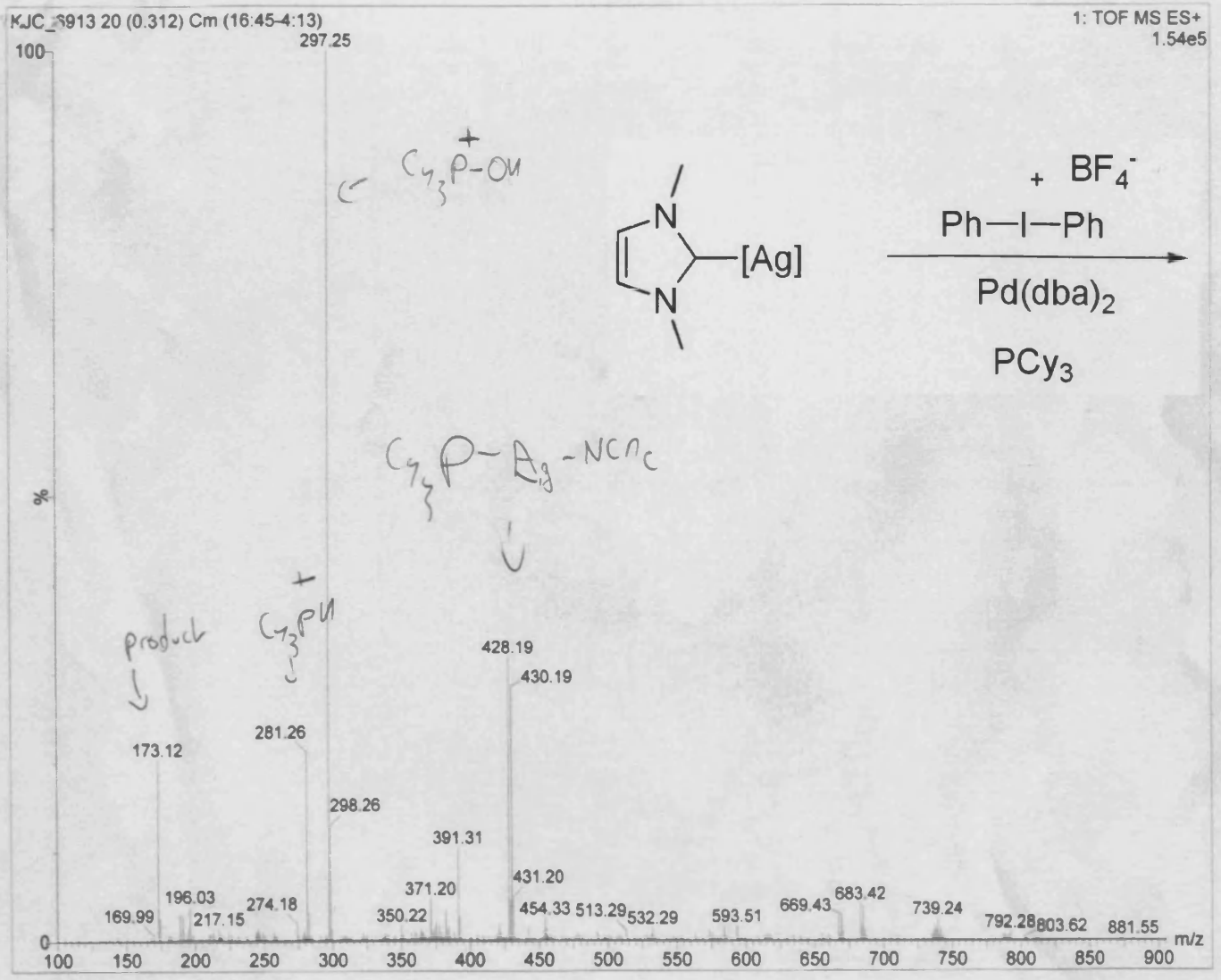

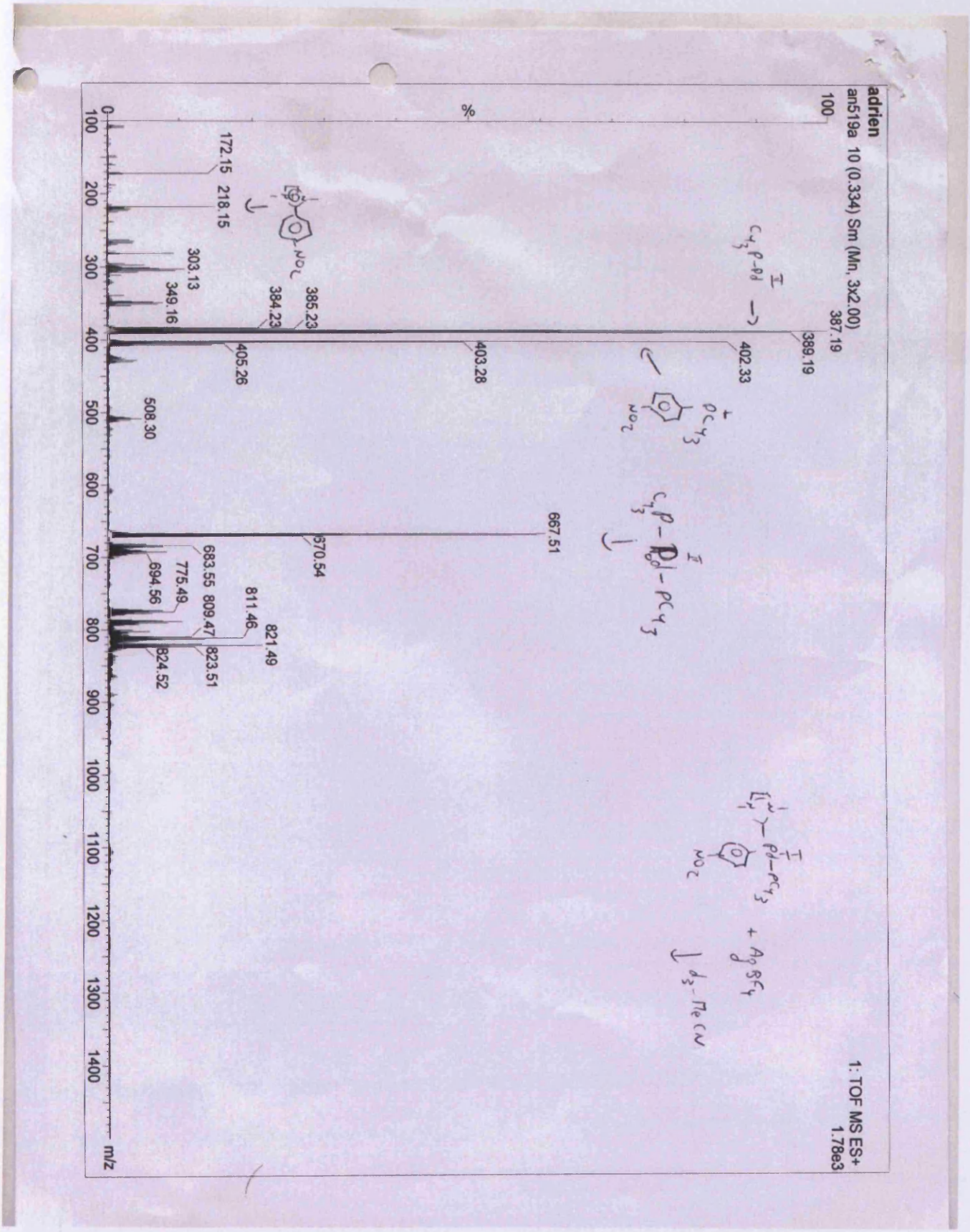

ESI/MS: decomposition of 48 in MeCN in the presence of $AgBF_4$

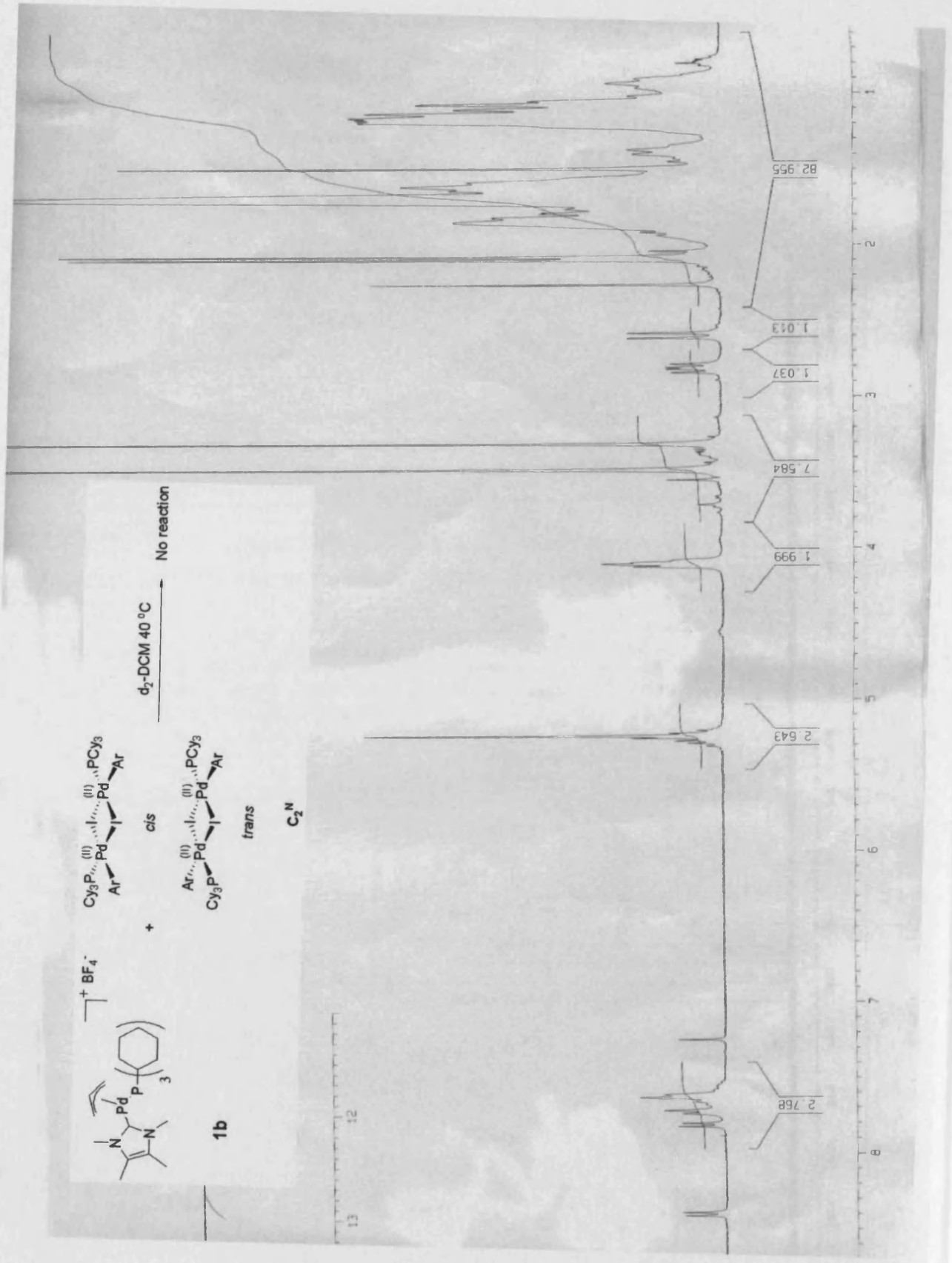

^{1}H NMR spectrum: reaction of 1b with C_2^N at 40 °C: no reaction

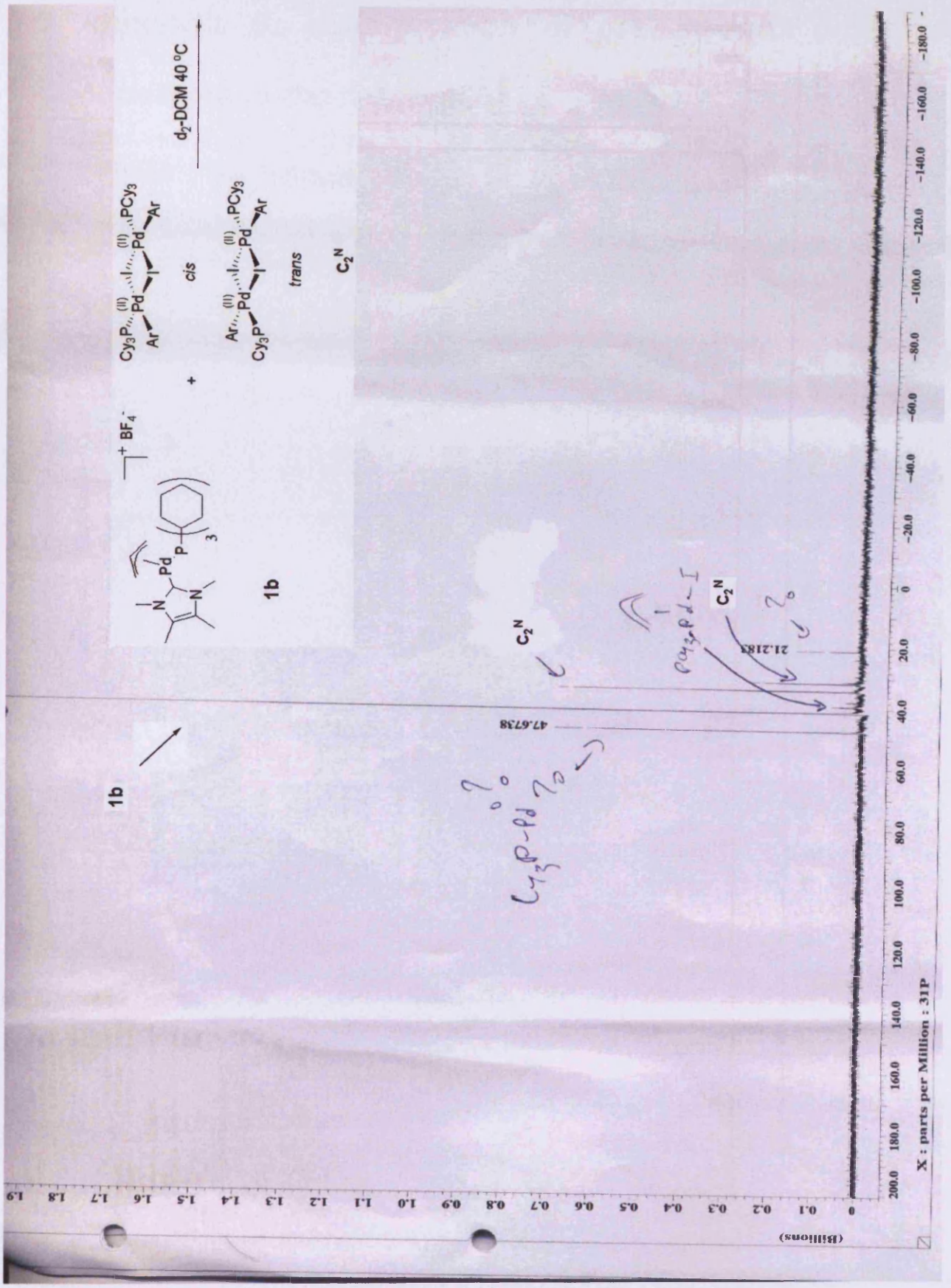

^{31}P NMR spectrum: reaction of 1b with C_2^N at 40 °C: no reaction

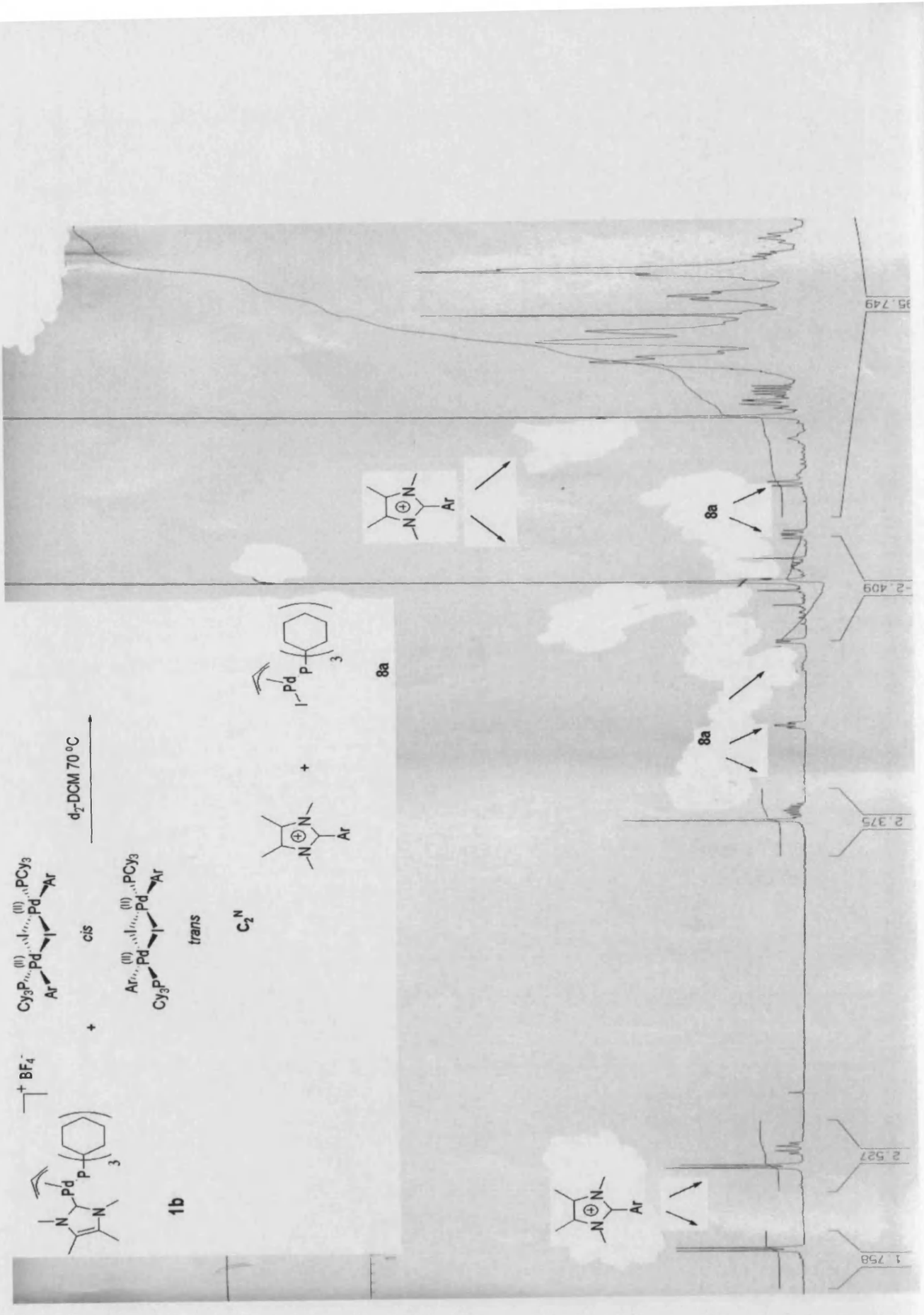

^{1}H NMR spectrum: reaction of 1b with C_2^N at 70 °C: 100 % conv.

5.5 Appendix 5: determination of pseudo-zero order rate constants in the reaction of 1b with ArI